# UC Santa Cruz
## UC Santa Cruz Electronic Theses and Dissertations

**Title**

An examination of the marine nitrogen cycle: insights from novel stable nitrogen isotopic approaches

**Permalink**

https://escholarship.org/uc/item/8dg807nm

**Author**

Batista, Fabian

**Publication Date**

2016

**Copyright Information**

Peer reviewed|Thesis/dissertation

UNIVERSITY OF CALIFORNIA
SANTA CRUZ


**AN EXAMINATION OF THE MARINE NITROGEN CYCLE: INSIGHTS
FROM NOVEL STABLE NITROGEN ISOTOPIC APPROACHES**


A dissertation submitted in partial satisfaction
of the requirements for the degree of

DOCTOR OF PHILOSOPHY

in

OCEAN SCIENCES

by

**Fabian C. Batista**

September 2016


The Dissertation of Fabian C. Batista
is approved:

_____
Professor Matthew D. McCarthy, chair


_____
Professor Ana Christina Ravelo


_____
Nancy Prouty, Ph.D.



_____
Tyrus Miller
Vice Provost and Dean of Graduate Studies

# Table of Contents

# List of Figures

# List of Tables

# Abstract

An examination of the marine nitrogen cycle: insights from novel stable nitrogen isotopic approaches

by

Fabian C. Batista

Paleoceanographic studies typically employ stable nitrogen isotopic measurements of total combustible N ($\delta^{15}N_{TN}$) in marine sediments to infer temporal changes in surface ocean marine N dynamics. However, $\delta^{15}N_{TN}$ is a highly non-specific measurement, susceptible to confounding issues including non-marine N sources, and offers little, if any, information regarding degradation and/or alteration of primary $\delta^{15}N$ signals. Recent development of novel biomarker and microfossil based proxies provide new analytical capabilities to circumvent issues with $\delta^{15}N_{TN}$.

Here, I explore the utility of compound specific nitrogen isotopic analysis of individual amino acids measurements ($\delta^{15}N_{AA}$) of proteinaceous material isolated from marine sediments and deep-sea coral. With these data I infer past changes in nitrate $\delta^{15}N$ fueling primary production at the base of the food web, ecosystem structure, and the extent of heterotrophic resynthesis influencing sedimentary and coral-skeletal $\delta^{15}N_{TN}$ records. Within sediments and corals, I demonstrate that $\delta^{15}N_{AA}$ based parameters reflect that of sinking particles and surface collected planktonic biomass and thus serve as a robust, albeit complex proxy to infer ecosystem and nutrient dynamic changes for at least the last few hundred years on the California Margin. In sediments I find an unexpected $\delta^{15}N$ offset in major operational fractions and molecular compound classes. This result (1) challenges a major assumption

organic nitrogen in sediments is dominated by amide functionality (i.e., proteinaceous N) and (2) highlights possible issues with standard protein hydrolysis techniques.

Lastly, I analyze the $\delta^{15}N$ composition of foraminifera-bound N (FB-$\delta^{15}N$) to assess the Plio-Pleistocene history of whole ocean nitrogen dynamics from the oligotrophic North Pacific for the last 5 million years. This region contains calcareous nannofossil rich sediments, ideal for preserved FB-$\delta^{15}N$ records. These new FB-$\delta^{15}N$ records support an expansion of suboxic regions, consistent with previous evidence, but also indicate that the whole ocean $\delta^{15}N$ budget was stable throughout the Plio-Pleistocene. This latter result implies that kinetic isotopic fractionations of marine N transformations and the ratio of pelagic to benthic denitrification, must not have changed during Plio-Pleistocene transition, despite included drastic global scale changes in sea level, shelf area, and volume of the major oxygen deficient zones.

# Acknowledgements

denitrifier method, both of which were essential to generate data for Chapter 3.

Thank you to Tessa Hill for offering access to an excellent bamboo coral collection

and to Tom Guilderson for offering beam time on the accelerator at LLNL to generate

$^{14}$C based age control for the coral time series records summarized in the Appendix.

The text of this dissertation includes material from the following previously

published material:

Embedding the aforementioned publication, an Elsevier Subscription Article, in

this dissertation as Chapter 1 falls under the Article Sharing and Personal Use policies

for this Published Journal Article (PJA) established by Elsevier which reads: "Theses

and dissertations which contain embedded PJAs as part of the formal submission can

be posted publicly by the awarding institution with DOI links back to the formal

publications on ScienceDirect".  The article can be found with the Digital Object

Identifier (DOI) in the full citation in an appropriate database, alternatively with the

following url: http://dx.doi.org/10.1016/j.gca.2014.08.002.  The online accessible

supplementary material, Electronic Annex, was also integrated into Chapter 1.  The

work was original research by Fabian C. Batista, the co-authors, A. C. Ravelo and M.

D. McCarthy, listed in this publication directed and supervised the research, while co-

authors J. Crusius and M. A. Casso contributed radiometric analyses to generate the

age model.  I am indebted to several funding agencies for financial support of this

dissertation including the National Science Foundation, the Consortium of Ocean Leadership, Friends of Long Marine Lab, and the Myers Trust.

I am grateful beyond words for the army of friends and supporters that have crossed my path, particularly in my time here at UCSC, but none other than my family could have made this long academic journey possible. Thank you Mom and Dad for your bottomless support, love and encouragement, particularly over the last half year, during the final push. Sabrina, my dear sister, thank you for being my tireless advocate. Susan and Jairo, thank you for your love, encouragement and support, especially in the last few months, as Megan, myself and the little ones invaded your home and your pantry; and thank you to all of our family members for your patience while Megan and I missed yet another holiday because we were stuck across the across the country or behind the redwood curtain.

Last but not least, thank you to my dear wife and co-pilot, Megan for being my rock. I am ever grateful that we took on parenthood (now twice!); your patience, encouragement and ever lasting love and support were essential for me to remain determined through the entirety of this epic academic journey, on which we embarked so long, long ago.


***


*I love deadlines. I like the whooshing sound they make as they fly by.*
-Douglas Adams

# Dedication

To Mom, the most industrious person that I know; I only hope that I emulate your work ethics, and will pass that on to my own progeny.

To Dad, you embarked on your journey to California from São Paulo at the chipper age of 28, the same age when I began this here journey; I suspect this made as much sense to you as your trip to the US did to your parents, thank you for your unconditional support.

To Lillian and Isaac, I love watching you both grow.  It only remains for me to pass the academic baton, for which I encourage you to heed this warning: should you fancy science, be an engineer; if is art that inspires you, be an architect.

To Megan, somehow I hope that closure on these following chapters does not mean that we have to become adults; what a journey we embarked on 16 years ago, hoping from one college town to the next, but I suppose we should lay down roots somewhere for the sake of our young family.

***

*If I have seen further it is by standing on the shoulders of giants.*
- Isaac Newton

*Perpetual devotion to what a man calls his business is only to be sustained by perpetual neglect of many other things.*
- Robert Louis Stevenson

# Epigraph

*There are several viewpoints from which the chemist can approach the ocean. He can consider the oceans as:*

*A dynamic mixing system, in which composition changes take place partly from internal processes and partly as a result of the circulation and mixing of water masses*

*A reservoir that is intermediate between the runoff of components from the continents and exchange reactions with the sediments*

*A biological system in which virtually all the biochemical changes associated with living organisms take place*

*A grand septic tank in which organic materials are decomposed mostly in the near-surface water or at the bottom*

*A vast chemical system, in which interactions. occur among an enormous number of components, both organic and inorganic, ranging in concentration through 12 orders of magnitude*

*An environment that is being invaded by man through his social, agricultural, and industrial activities*

*The key to interpreting the past history of the earth and as the custodian of its relics.*

- Alfred C. Redfield

# Introduction

**Importance of the marine nitrogen cycle**

In the marine environment, bioavailable N or fixed N, excluding $N_2$, mainly in the form of nitrate, is an essential macronutrient required by all marine primary producers. The marine N cycle is comprised of complex biogeochemical transformations between the various forms of fixed N (e.g., nitrate, nitrite, ammonia, and nitrogen oxides), most of them mediated by microorganisms, including the major source and sink processes of fixed nitrogen, biological nitrogen fixation and denitrification, respectively. At present, the global N cycle is being perturbed through the addition of artificial fertilizers, i.e., fixed N, that can result in cascading effects and unintended consequences on the biogeochemical cycling of other closely coupled elements, particularly that of carbon (Gruber and Galloway, 2008). Establishing new robust tools to evaluate past and present perturbations in the marine N cycle is essential for projecting the potential feedbacks in marine N biogeochemistry in the context of such drastic current global environmental change.

**Stable nitrogen isotopes: a proxy for the past and present marine nitrogen cycle**

The stable nitrogen isotopic ($\delta^{15}N$) composition of nitrate in the marine environment provides a measure of the relative importance of the primary source and sink processes of fixed oceanic N. Utility of present day nitrate $\delta^{15}N$ measurements rely on pelagic $N_2$ fixation, benthic and pelagic denitrification*, and N assimilation by phytoplankton, which impart distinct imprints on the $\delta^{15}N$ composition of $NO_3^-$

with unique isotopic preference of $^{14}N$ over $^{15}N$ (Cline and Kaplan, 1975; Sigman and Casciotti, 2001b)

In the modern ocean, nitrate is the most abundant form of fixed N and deep oceanic nitrate has a remarkably homogenous $\delta^{15}N$ value of 5±0.5‰ (Sigman et al., 2000; Sigman and Casciotti, 2001a, b; Galbraith et al., 2008). Pelagic $N_2$ fixation adds fixed N with a $\delta^{15}N$ close to that of atmospheric $N_2$, ca. -2 to 0‰, with its negligible isotopic effect ($\varepsilon$) (Wada and Hattori, 1976), which acts to decrease the local thermocline nitrate $\delta^{15}N$ (Dore et al., 2002; Knapp et al., 2005; Casciotti et al., 2008). In contrast, denitrification enriches the $\delta^{15}N$ of residual nitrate, but the degree of isotopic enrichment is dependent upon the fraction of unreacted local fixed N (Mariotti et al., 1981). Benthic denitrification removes fixed N from sedimentary pore-waters to near if not completion, resulting in a minor N isotopic effect with an $\varepsilon_{BD}$ value of ca. ~0 to 3‰ (Lehmann et al., 2004; Brandes et al., 2007), but recent estimates suggest that $\varepsilon_{BD}$ values are slightly higher at 4 to 8‰ (Lehmann et al., 2007; Granger et al., 2011; Alkhatib et al., 2012; Somes et al., 2013). Pelagic denitrification exhibits a $\varepsilon_{PD}$ value on the order of 20 to 30‰ (Somes et al., 2013). At steady state, the fixed N source and sink terms are balanced, so the relative ratio of pelagic to benthic denitrification, with their accompanying $\varepsilon$ values, sets the global $\delta^{15}N$ of whole ocean fixed N (Brandes and Devol, 2002; Altabet 2006).

These N cycle processes that remove or add nitrate (e.g., denitrification and $N_2$ fixation, respectively) impart $\delta^{15}N$ signals on the global mean surface nitrate reservoir. These $\delta^{15}N$ signatures are then assimilated by phytoplankton biomass,

enter the marine food web and integrated into sinking particulate N (PN). Equipped with this information, total sedimentary N isotopic ($\delta^{15}N_{TN}$) records have been used readily in paleoceanographic studies of the nitrogen cycle as a proxy for the $\delta^{15}N$ of exported PN and by extension the $\delta^{15}N$ of dissolved inorganic N (DIN; e.g., nitrate) (e.g., Altabet et al., 1999). However, in any given location, $\delta^{15}N_{TN}$ values inherently reflect local, regional and global processes including (1) changes in the $\delta^{15}N$ of preformed nitrate, (2) regional nitrate $\delta^{15}N$ enrichment (e.g., denitrification) or depletion (e.g., $N_2$ fixation) relative to the whole ocean, (3) and relative changes in the extent of nitrate consumption by marine autotrophs during primary production (Altabet 2006; Galbraith et al., 2008).

Ideally, the fidelity of $\delta^{15}N_{TN}$ records faithfully record past temporal variations in primary signals, i.e., the $\delta^{15}N$ of sinking PN. However, the global average offset between surface sedimentary $\delta^{15}N_{TN}$ and $\delta^{15}N$ values of sinking PN an offset, with $\delta^{15}N_{TN}$ higher than $\delta^{15}N$ of PN by approximately 2‰ or 3‰, particularly in the deep ocean relative to coastal settings (Robinson et al., 2012). The mechanism behind this broadly observed increase in sedimentary $\delta^{15}N_{TN}$ relative to $\delta^{15}N$ in sinking PN is likely due to pre- and post- depositional diagenetic effects during transfer to the sedimentary record. Typically, depositional environments in shallow waters, with high accumulation rates of organic matter and low bottom water oxygen content tend to exhibit highly preserved primary $\delta^{15}N_{TN}$ signals relative to sinking PN, in contrast to open ocean records of $\delta^{15}N_{TN}$. However, laboratory experiments studying oxic versus anoxic control on diagenetic isotope effects on $\delta^{15}N$ of PN remain equivocal,

with the $\delta^{15}N$ of remaining organic matter either increase or decrease (Lehmann et al., 2002). Other confounding issues of sedimentary $\delta^{15}N_{TN}$ measurements include mixtures of multiple N sources, particularly in continental margins, where temporal changes in the ratio of terrestrial to marine derived N may drive $\delta^{15}N_{TN}$ excursions.

**On the development and application of novel paleoceanographic proxies for the nitrogen cycle**

The overarching goal of this dissertation is to contribute to proxy development and validation of novel compound specific nitrogen isotopic analyses of amino acids ($\delta^{15}N_{AA}$) to circumvent the aforementioned issues with traditional paleoceanographic reconstructions of the marine nitrogen cycle with sedimentary $\delta^{15}N_{TN}$ records. Seminal work by McClelland and co-authors (2002, 2003) showed that two groups of protein AA are differentiated based on their $\delta^{15}N$ behavior during trophic transfer. During each trophic step, the $\delta^{15}N$ of source AA (Src; $\delta^{15}N_{Src}$) remain essentially unaltered while the $\delta^{15}N$ of trophic AA (Tr; $\delta^{15}N_{Tr}$) are enriched relative to the mean baseline $\delta^{15}N$ of dissolved inorganic nitrogen (DIN). Recent work has corroborated this characteristic $\delta^{15}N$ offset of Src and Tr AA in individual autotrophic and heterotrophic organisms (e.g., Schmidt et al., 2004; McCarthy et al., 2007; Chikaraishi et al., 2007, 2009; McCarthy et al., 2013; Decima et al., 2013). Ecological applications have employed this characteristic offset in one or more Src and Tr AA pairings to estimate the trophic position (TP) of individual organisms (Chikaraishi et al., 2007; Chikaraishi et al., 2009; Hannides et al., 2009; Hannides et al., 2013). Consequently, the $\delta^{15}N_{AA}$ pattern in an sample appears to simultaneously

provide: (i) an internally normalized estimate for trophic position, unaffected by matrix or any additional non-AA N source, and (ii) an estimate of the $\delta^{15}N$ of nitrogen sources (e.g., nitrate) at the base of the food web. While these parameters have been used extensively to investigate trophic relationships in individual organisms, sinking particulate organic matter (POM) and deep-sea coral, but little work has been done to apply these tools to the paleoceanographic sedimentary record.

Chapter 1 is a proof of concept where I present the first examination of $\delta^{15}N_{AA}$ measurements in marine sedimentary organic matter from Santa Barbara Basin (SBB), a California borderland basin. I demonstrate that in a depositional environment such as SBB, with excellent organic matter preservation, sedimentary $\delta^{15}N_{AA}$ based parameters reflect that of sinking particles and surface collected planktonic biomass which indicates that in such a depositional environment, $\delta^{15}N_{AA}$ data may contribute to paleoenvironmental reconstructions of ecosystem and nutrient dynamics. In my exploration of this novel data set, I found a significant $\delta^{15}N$ offset between sedimentary $\delta^{15}N_{TN}$ value and the reconstructed $\delta^{15}N$ value of total hydrolysable amino acids ($\delta^{15}N_{THAA}$); a stark inconsistency given that all sedimentary organic N should be comprised of proteinaceous N.

Chapter 2 is a follow up study, where I explore this contradictory finding from Chapter 1 regarding this $\delta^{15}N$ significant offset in $\delta^{15}N_{TN}$ and $\delta^{15}N_{THAA}$ measurements in plankton, sinking POM and sediments. To examine this $\delta^{15}N$ offset, I generate a $\delta^{13}C$ and $\delta^{15}N$ budget for SBB samples used in Chapter 1, by isolating fractions based on standard molecular level separations of organic matter. A significant diversity in

$\delta^{15}N$ values of sedimentary ON fractions was observed, suggesting substantial diversity in either biochemical makeup, and/or partitioning, of sedimentary nitrogenous compounds. The quantitative distribution of N containing fractions and associated $\delta^{15}N$ results suggest that total sedimentary organic N $\delta^{15}N$ values are likely strongly dependent on the relative contributions of acid-soluble and acid-insoluble operational fractions, which may have different water column sources of proteinaceous vs. non-proteinaceous nitrogenous compounds.

In Chapter 3, I shift gears and apply a recently developed novel analytical tool based on the $\delta^{15}N$ of planktonic foraminifera-bound N (FB-$\delta^{15}N$) to open ocean records in the western tropical and subtropical Pacific Ocean. The primary goal for this chapter was to examine and validate the broadly observed increase in denitrification throughout the low latitude eastern boundary upwelling regions the marine N cycle at ca. 2 Ma (Robinson et al., 2014), but also to evaluate the response in nitrogen fixation to the expansion in denitrification over long-time scales.

Finally, in Appendix A, I briefly revisit $\delta^{15}N_{AA}$ proxies as a potential tool for generating novel $\delta^{15}N$ records from proteinaceous skeletons of several deep-sea octocorals (Family Isididae). The coral specimens for this project were live-collected from the California Margin at the Monterey Canyon and Pioneer Seamount and were used to evaluate interannual and interdecadal variability of regional nutrient and ecosystem dynamics for the northern sector of the California Current System. Together, these novel $\delta^{15}N$ data coupled with bulk stable $\delta^{13}C$ isotopic records reveal

long-term, multi-decadal to multi-century stability in regional nutrient availability and

ecosystem productivity, despite minor interannual variations in $\delta^{13}C$ and $\delta^{15}N$ values.

**References**

Alkhatib, M., Lehmann, M.F. and del Giorgio, P.A. (2012) The nitrogen isotope effect of benthic remineralization-nitrification-denitrification coupling in an estuarine environment. Biogeosciences 9, 1633-1646.

Altabet, M. (2006a) Constraints on oceanic N balance/imbalance from sedimentary 15 N records. Biogeosciences Discussions 3, 1121-1155.

Altabet, M., Pilskaln, C., Thunell, R., Pride, C., Sigman, D., Chavez, F. and Francois, R. (1999) The nitrogen isotope biogeochemistry of sinking particles from the margin of the Eastern North Pacific. Deep-Sea Research Part I-Oceanographic Research Papers, 655-679.

Altabet, M.A. (2006b) Isotopic tracers of the marine nitrogen cycle: Present and past, Marine organic matter: biomarkers, isotopes and DNA. Springer, pp. 251-293.

Brandes, J.A., Devol, A.H. and Deutsch, C. (2007) New developments in the marine nitrogen cycle. Chemical Reviews 107, 577-589.

Casciotti, K.L., Trull, T.W., Glover, D.M. and Davies, D. (2008) Constraints on nitrogen cycling at the subtropical North Pacific Station ALOHA from isotopic measurements of nitrate and particulate nitrogen. Deep-Sea Research Part Ii-Topical Studies in Oceanography 55, 1661-1672.

Chikaraishi, Y., Kashiyamal, Y., Ogawa, N.O., Kitazato, H. and Ohkouchi, N. (2007) Metabolic control of nitrogen isotope composition of amino acids in macroalgae and gastropods: implications for aquatic food web studies. Marine Ecology-Progress Series 342, 85-90.

Chikaraishi, Y., Ogawa, N., Kashiyama, Y., Takano, Y., Suga, H., Tomitani, A., Miyashita, H., Kitazato, H. and Ohkouchi, N. (2009) Determination of aquatic food-web structure based on compound-specific nitrogen isotopic composition of amino acids. LIMNOLOGY AND OCEANOGRAPHY-METHODS, 740-750.

Cline, J.D. and Kaplan, I.R. (1975) Isotopic fractionation of dissolved nitrate during denitrification in the eastern tropical north pacific ocean. Marine Chemistry 3, 271-299.

Decima, M., Landry, M.R. and Popp, B.N. (2013) Environmental perturbation effects on baseline delta N-15 values and zooplankton trophic flexibility in the southern California Current Ecosystem. Limnology and Oceanography 58, 624-634.

Dore, J.E., Brum, J.R., Tupas, L.M. and Karl, D.M. (2002) Seasonal and interannual variability in sources of nitrogen supporting export in the oligotrophic subtropical North Pacific Ocean. Limnology and Oceanography 47, 1595-1607.

Galbraith, E.D., Sigman, D.M., Robinson, R.S. and Pedersen, T.F. (2008) Nitrogen in past marine environments.

Granger, J., Prokopenko, M.G., Sigman, D.M., Mordy, C.W., Morse, Z.M., Morales, L.V., Sambrotto, R.N. and Plessen, B. (2011) Coupled nitrification-denitrification in sediment of the eastern Bering Sea shelf leads to N-15 enrichment of fixed N in shelf waters. Journal of Geophysical Research-Oceans 116.

Gruber, N. and Galloway, J.N. (2008) An Earth-system perspective of the global nitrogen cycle. Nature 451, 293-296.

Hannides, C.C., Popp, B.N., Choy, C.A. and Drazen, J.C. (2013) Midwater zooplankton and suspended particle dynamics in the North Pacific Subtropical Gyre: A stable isotope perspective. Limnol. Oceanogr 58, 1931-1946.

Hannides, C.C.S., Popp, B.N., Landry, M.R. and Graham, B.S. (2009) Quantification of zooplankton trophic position in the North Pacific Subtropical Gyre using stable nitrogen isotopes. Limnology and Oceanography 54, 50-61.

Knapp, A.N., Sigman, D.M. and Lipschultz, F. (2005) N isotopic composition of dissolved organic nitrogen and nitrate at the Bermuda Atlantic time-series study site. Global Biogeochemical Cycles 19.

Lehmann, M.F., Sigman, D.M. and Berelson, W.M. (2004) Coupling the N-15/N-14 and O-18/O-16 of nitrate as a constraint on benthic nitrogen cycling. Marine Chemistry 88, 1-20.

Lehmann, M.F., Sigman, D.M., McCorkle, D.C., Granger, J., Hoffmann, S., Cane, G. and Brunelle, B.G. (2007) The distribution of nitrate N-15/N-14 in marine sediments and the impact of benthic nitrogen loss on the isotopic composition of oceanic nitrate. Geochimica Et Cosmochimica Acta 71, 5384-5404.

Mariotti, A., Germon, J.C., Hubert, P., Kaiser, P., Letolle, R., Tardieux, A. and Tardieux, P. (1981) EXPERIMENTAL-DETERMINATION OF NITROGEN KINETIC ISOTOPE FRACTIONATION - SOME PRINCIPLES - ILLUSTRATION FOR THE DENITRIFICATION AND NITRIFICATION PROCESSES. Plant and Soil 62, 413-430.

McCarthy, M.D., Lehman, J. and Kudela, R. (2013) Compound-specific amino acid delta N-15 patterns in marine algae: Tracer potential for cyanobacterial vs. eukaryotic organic nitrogen sources in the ocean. Geochimica Et Cosmochimica Acta 103, 104-120.

McClelland, J.W., Holl, C.M. and Montoya, J.P. (2003) Relating low delta N-15 values of zooplankton to N-2-fixation in the tropical North Atlantic: insights provided by stable isotope ratios of amino acids. Deep-Sea Research Part I-Oceanographic Research Papers 50, 849-861.

McClelland, J.W. and Montoya, J.P. (2002) Trophic relationships and the nitrogen isotopic composition of amino acids in plankton. Ecology 83, 2173-2180.

Robinson, R.S., Etourneau, J., Martinez, P.M. and Schneider, R. (2014) Expansion of pelagic denitrification during early Pleistocene cooling. Earth Planet. Sci. Lett. 389, 52-61.

Schmidt, K., McClelland, J.W., Mente, E., Montoya, J.P., Atkinson, A. and Voss, M. (2004) Trophic-level interpretation based on delta N-15 values: implications of tissue-specific fractionation and amino acid composition. Marine Ecology-Progress Series 266, 43-58.

Sigman, D.M., Altabet, M.A., McCorkle, D.C., Francois, R. and Fischer, G. (2000) The delta N-15 of nitrate in the Southern Ocean: Nitrogen cycling and circulation in the ocean interior. Journal of Geophysical Research-Oceans 105, 19599-19614.

Sigman, D.M. and Casciotti, K.L. (2001a) Nitrogen Isotopes in the Ocean, in: John, H.S. (Ed.), Encyclopedia of Ocean Sciences. Academic Press, Oxford, pp. 1884-1894.

Sigman, D.M. and Casciotti, K.L. (2001b) Ocean Process Tracers: Nitrogen Isotopes in the Ocean, in: John, H.S. (Ed.), Encyclopedia of Ocean Sciences. Academic Press, Oxford, pp. 1884-1894.

Somes, C.J., Oschlies, A. and Schmittner, A. (2013) Isotopic constraints on the pre-industrial oceanic nitrogen budget. Biogeosciences 10, 5889-5910.

Wada, E. and Hattori, A. (1976) NATURAL ABUNDANCE OF N-15 IN PARTICULATE ORGANIC-MATTER IN NORTH PACIFIC OCEAN. Geochimica Et Cosmochimica Acta 40, 249-251.

CHAPTER ONE

# Compound specific amino acid $\delta^{15}N$ in marine sediments: A new approach for studies of the marine nitrogen cycle

Fabian C. Batista[1], A. Christina Ravelo[1], John Crusius[2], Michael A. Casso[3], Matthew D. McCarthy[1]

[1] Ocean Sciences Department, University of California, Santa Cruz

[2] U.S. Geological Survey, University of Washington, School of Oceanography

[3] U.S. Geological Survey, Woods Hole Science Center

*Chemical reactions in the ocean... are largely determined by phenomena which occur at interfaces... seawater is bounded by two of the most extensive interfaces on earth—the one where it meets the air above, the other where it mingles with the sediment below.*

– Fritz Koczy

ABSTRACT

The nitrogen (N) isotopic composition ($\delta^{15}N$) of bulk sedimentary N ($\delta^{15}N_{bulk}$) is a common tool for studying past biogeochemical cycling in the paleoceanographic record. Empirical evidence suggests that natural fluctuations in the $\delta^{15}N$ of surface nutrient N are reflected in the $\delta^{15}N$ of exported planktonic biomass and in sedimentary $\delta^{15}N_{bulk}$. However, $\delta^{15}N_{bulk}$ is an analysis of total combustible sedimentary N, and therefore also includes mixtures of N sources and/or selective removal or preservation of N-containing compounds. Compound-specific nitrogen isotope analyses of individual amino acids ($\delta^{15}N_{AA}$) are novel measurements with the potential to decouple $\delta^{15}N$ changes in nutrient N from trophic effects, two main processes that can influence $\delta^{15}N_{bulk}$ records. As a proof of concept study to examine how $\delta^{15}N_{AA}$ can be applied in marine sedimentary systems, we compare the $\delta^{15}N_{AA}$ signatures of surface and sinking POM sources with shallow surface sediments from the Santa Barbara Basin, a sub-oxic depositional environmental that exhibits excellent preservation of sedimentary organic matter. Our results demonstrate that $\delta^{15}N_{AA}$ signatures of both planktonic biomass and sinking POM are well preserved in such surface sediments. However, we also observed an unexpected inverse correlation between $\delta^{15}N$ value of phenylalanine ($\delta^{15}N_{Phe}$; the best AA proxy for N isotopic value at the base of the food web) and calculated trophic position. We used a simple N isotope mass balance model to confirm that over long time scales, $\delta^{15}N_{Phe}$ values should in fact be directly dependent on shifts in ecosystem trophic position. While this result may appear incongruent with current applications of $\delta^{15}N_{AA}$ in food webs,

it is consistent with expectations that paleoarchives will integrate N dynamics over much longer timescales. We therefore propose that for paleoceanographic applications, key $\delta^{15}N_{AA}$ parameters are ecosystem trophic position, which determines relative partitioning of $^{15}N$ into source AA versus trophic AA pools, and the integrated $\delta^{15}N_{AA}$ of all common protein AA ($\delta^{15}N_{THAA}$), which serves as a proxy for the $\delta^{15}N$ of nutrient N. Together, we suggest that these can provide a coupled picture of regime shifts in planktonic ecosystem structure, $\delta^{15}N$ at the base of food webs, and possibly additional information about nutrient dynamics.

**Introduction**

Paleoceanographic studies of the nitrogen (N) cycle have employed the stable N isotopic composition of total N ($\delta^{15}N_{bulk}$) in marine sediments as a proxy for $\delta^{15}N$ of the sinking flux of organic matter (OM) (Altabet et al., 1999). By extension, past $\delta^{15}N_{bulk}$ fluctuations have often been interpreted as a change in photoautotrophic utilization of the surface dissolved inorganic nitrogen (DIN) reservoir. However, in HNLC regions (Altabet and Francois, 1994) and in regions that exhibit complete utilization DIN sources, the $\delta^{15}N_{bulk}$ is often taken to reflect the $\delta^{15}N$ value of sub-euphotic zone DIN (Altabet et al., 1999; Liu et al., 2008).

However, mixtures of sedimentary N sources, as well as pre- and post-depositional $\delta^{15}N$ alteration, can confound accurate paleoceanographic interpretations of marine sedimentary $\delta^{15}N_{bulk}$ records. First, $\delta^{15}N_{bulk}$ records are susceptible to time varying changes in the contribution of marine and terrestrial N or inorganic and organic N (e.g., Kienast et al., 2005). Further, alteration of bulk organic matter (e.g.,

selective removal or addition of specific N containing compounds) can variably alter

the sedimentary $\delta^{15}N_{bulk}$ in open-ocean sedimentary environments during early

diagenesis (Robinson et al., 2012), analogous to similar changes in $\delta^{15}N_{bulk}$ widely

documented for suspended particulate organic matter (POM) in the water column

(Altabet, 1988; Altabet, 1996; Hannides et al., 2013). Such changes are thought to be

microbially mediated (Macko and Estep, 1984), although exact mechanisms are not

well understood, and $\delta^{15}N$ changes associated with sedimentary organic matter

(SOM) degradation have also been shown to variable (Lehmann et al., 2002). Various

approaches have attempted to circumvent these issues, with the goal of developing

proxies that might directly reflect $\delta^{15}N_{bulk}$ of exported surface production. These

include measuring microfossil-bound organic N (Robinson et al., 2004; Ren et al.,

2009), or specific $\delta^{15}N$ values of well-preserved biomarkers such as chlorins and

porphyrins (Sachs and Repeta, 1999; Higgins et al., 2010).  However, such

approaches typically directly reflect the $\delta^{15}N$ value for only a very minor fraction of

total sedimentary organic N (SON).

Compound-specific nitrogen isotope analyses of individual amino acids ($\delta^{15}N_{AA}$)

are novel measurements that have the potential to simultaneously provide information

regarding the $\delta^{15}N$ of sub-euphotic zone DIN and trophic transfer, potentially

circumventing other issues that may directly impact $\delta^{15}N_{bulk}$ measurements, such as

$\delta^{15}N$ alteration in deep, remote, organic-poor depositional settings (e.g., Altabet,

2005) or in coastal settings that are susceptible to contamination by terrestrial N

sources (e.g., Kienast et al., 2005). Early work by McClelland and co-authors (2002,

2003) showed that two groups of protein AA are differentiated based on their N isotopic behavior during trophic transfer; $\delta^{15}N$ of source AA (Src) group remain essentially unaltered, while $\delta^{15}N$ of trophic AA (Tr) become isotopically enriched with each trophic step. Recent work has corroborated the differential enrichment of these groups in multiple organisms (Chikaraishi et al., 2007), and in many recent studies the offsets in $\delta^{15}N$ between characteristic Src (e.g., phenylalanine) and Tr (e.g., glutamic acid) AA have been used to estimate the trophic position (TP) of individual organisms (e.g., Chikaraishi et al., 2007, 2009; Popp et al., 2007; Hannides et al., 2009) and of suspended and sinking POM (e.g., McCarthy et al., 2007). Further, diagnostic changes in $\delta^{15}N_{AA}$ patterns also accompany bacterial degradation and AA resynthesis (McCarthy et al., 2007; Calleja et al., 2013). Because the large majority of particulate organic N (ON) is composed of amino acids, this suggests that $\delta^{15}N_{AA}$ parameters may be able to directly reveal the extent of microbial alteration to the major ON constituent of sediments, and at the same time provide a molecular-level view of potential effects of degradation on $\delta^{15}N_{bulk}$ values.

$\delta^{15}N_{AA}$ measurements may have great potential in paleobiogeochemical reconstructions of the marine N cycle. $\delta^{15}N_{AA}$ measurements of oceanic sinking particles indicate that $\delta^{15}N$ values of Src AA from surface planktonic sources are preserved in deep ocean sediment traps, and also that planktonic trophic structure information is maintained in diagnostic $\delta^{15}N$ offsets between the Tr and Src AA group (McCarthy et al., 2007). Further, analyses of deep-sea proteinaceous coral skeletons have confirmed that specific $\delta^{15}N_{AA}$ proxies can directly record $\delta^{15}N$ values of

surface nitrate and long term records of change in planktonic trophic structure in some regions (Sherwood et al., 2011; Sherwood et al., 2014). Together, early work has suggested that $\delta^{15}N_{AA}$ measurements in paleoarchives may be able to simultaneously monitor baseline excursions in surface nutrient dynamics, record the mean planktonic ecosystem structure, and constrain the degree to which microbial degradation has shifted $\delta^{15}N_{bulk}$ values. Carstens and co-authors (2013) demonstrated that lacustrine sedimentary $\delta^{15}N_{AA}$ patterns are similar to those observed for plankton in several alpine lakes where $\delta^{15}N_{AA}$ patterns and specific $\delta^{15}N_{AA}$–based indices (e.g., $\Sigma V$ and trophic or "transformation" level) appear well preserved relative to sinking POM. However, to our knowledge there are no previously published reports examining $\delta^{15}N_{AA}$ in the marine sedimentary record. $\delta^{15}N_{AA}$ measurements in sediments offer major opportunities, as well as potential challenges. Marine sedimentary measurements of $\delta^{15}N_{AA}$–based indices would greatly extend the time horizon beyond the relatively short time periods recorded by deep-sea proteinaceous corals (Sherwood et al., 2011, 2014), allowing for a new way to examine N cycle changes over millennial time scales, and potentially longer. However, sedimentary N is a complicated matrix, and much more susceptible to post depositional alteration. Therefore, the first step for $\delta^{15}N_{AA}$ applications is to evaluate preservation of $\delta^{15}N_{AA}$ signatures, as well as existing $\delta^{15}N_{AA}$ parameters in a well-characterized sedimentary system.

We present here a first investigation of marine sedimentary $\delta^{15}N_{AA}$ patterns, coupling $\delta^{15}N_{AA}$ measurements from shallow marine sediments with both sediment

trap and mixed plankton tow data from the overlying water column. Santa Barbara

Basin (SBB) was selected as a study site because it is a well-characterized region of

high primary production and sedimentation rates, with suboxic bottom waters and

thus excellent sedimentary organic matter (SOM) preservation. The main objectives

of this study were first to examine the extent to which $\delta^{15}N_{AA}$ of fresh marine algal

biomass and sinking POM is reflected in SOM in a high accumulation, low oxygen

depositional setting. To do this, we analyzed selected water column samples to

confirm the expected universal $\delta^{15}N_{AA}$ patterns for fresh algal-based sources, and then

compared these with $\delta^{15}N_{AA}$ patterns preserved in sediments. Second, we assessed

paleo-biomarker potential for existing $\delta^{15}N_{AA}$ parameters in a marine sedimentary

system. Specifically, our goal was to evaluate the potential for $\delta^{15}N$ of Src AA as a

potential paleoproxy for relative changes in DIN $\delta^{15}N$, not influenced by sources of

terrestrial particulate organic and inorganic N in coastal settings like SBB. Also we

examined $\delta^{15}N_{AA}$-based estimates of trophic position, TP (e.g., Chikaraishi et al.,

2009), as a new tool to reconstruct planktonic ecosystem changes, as reflected in

primary production. Finally, these AA-based parameters in the SBB surface

sedimentary record were evaluated in the context of regional ecosystem data.

   Overall, our goal in choosing the SBB system was to evaluate current assumptions

regarding CSI-AA parameters in a setting with strong OM preservation, reducing the

potential that diagenetic change could not complicate basic interpretations. Our

results indicate excellent preservation of $\delta^{15}N_{AA}$ patterns in SOM. However our

results, together with a $\delta^{15}N$-based isotope mass balance model, also strongly suggest

that a new paradigm will be required for applications of $\delta^{15}N_{AA}$ in paleoarchives, in which the constraints of long-term N mass balance create interdependence of common CSI-AA proxies.

**Materials and Methods**

**Study Site**

All samples were collected within the Santa Barbara Basin (SBB), a borderland basin on the California Margin, bounded to the north by the California coastline and to the south by the Northern Channel Islands. The SBB is a superb location for high-resolution paleoceanographic records in part because of high rates of marine primary production and rapid accumulation rates dominated by marine OM (~0.5 cm/yr), although episodic precipitation events during fall and winter storms also can contribute terrestrial input (Thunell et al., 1995). High sedimentation rates and limited flushing of SBB below its sill depth (475 m), combined with a regionally intense oxygen minimum zone, produce a suboxic depositional environment, which results in annually varved sediments. These attributes have made the SBB the focus of numerous high-resolution Holocene paleoclimate studies (Barron et al., 2010 and references therein).

**Water column and sedimentary OM samples**

The mixed plankton tow (>35 μm) from 30 m and a 40 cm multicore from 588 m were collected in SBB (34°14' N, 120°02' W) in June 2008. The multicore was immediately sectioned into 1 cm intervals after core recovery, and samples were then stored frozen until freeze-dried for further processing. The sediment trap sample is a

one-year nitrogen-flux weighted composite of twelve individual one-month collections from April 1999 to March 2000 in the SBB (34°14' N, 120°02' W) at a water depth of 450 m. Roland et al. (2008) provides a thorough description of sample preservation and the sediment-trap time-series methodology for these samples.

## Age Model: unsupported $^{210}$Pb

The age model for the multicore was constructed using $^{210}$Pb dating. Between 2 and 4 grams of dried, disaggregated sediment was sealed in counting vials and stored for at least 21 days to allow for the in-growth of $^{222}$Ra and $^{214}$Pb to approximate equilibrium values. Samples were counted for 2-5 d using a Princeton Gamma-Tech Ge well detector (Princeton, NJ), detecting the 46.3 keV $^{210}$Pb peak. Detector efficiencies were determined by counting standards filled to the same vial height as the samples using EPA standard pitchblend ore. Supported $^{210}$Pb activities were determined from the total $^{210}$Pb activity at the base of the core, whereas excess $^{210}$Pb was calculated by subtracting the supported $^{210}$Pb from the total $^{210}$Pb activity. Sediment ages were inferred using the constant rate of supply (CRS) model (Appleby and Oldfield, 1978) down to 32 cm, and an average linear sedimentation rate (0.18 cm/yr) from 20-30 cm was applied for intervals below 32 cm.

## Bulk stable isotopic analysis

All isotopic analysis were performed at the UCSC Light Stable Isotope Facility (http://es.ucsc.edu/~silab) using a Carlo Erba CHNO-S 1108 interfaced with a Finnigan Conflo II to a Thermo-Finnigan Delta Plus XP isotope ratio mass spectrometer. Bulk carbon ($\delta^{13}$C) and nitrogen ($\delta^{15}$N) isotopic values were measured

on lyophilized and homogenized material, pelletized in tin capsules. The $\delta^{13}$C

analyses of organic carbon ($\delta^{13}C_{OC}$) was measured on samples pretreated with 10%

HCl to remove carbonates (Hedges and Stern, 1984), followed by several rinses with

Milli-Q grade water, and then oven-dried overnight at 50° C.  Measurements were

performed in duplicate. Acetanilide from Indiana University

(http://mypage.iu.edu/~aschimme/compounds.html) was used as a laboratory

standard, with a typical analytical precision of 0.2‰ (±1 s.d.), for calibration of both

$\delta^{15}$N and $\delta^{13}$C.  Bulk isotope values are reported in standard per mil (‰) notation,

relative to VPDB and air for $\delta^{13}$C and $\delta^{15}$N respectively.

**Amino acid hydrolysis, purification and derivatization for CSIA**

Approximately 6 mg of lyophilized mixed plankton tow (~0.5 to 1 mg OC), ~180

mg lyophilized of sediment trap material (~7 mg OC) or ~500 mg of sediment (~11

mg OC) were used for CSIA-AA.  Individual amino acids were liberated using

standard acid hydrolysis conditions (110º C, 20hr; e.g., Lee and Cronin, 1982),

followed by purification with cation-exchange chromatography (Fabian et al., 1991;

Veuger et al., 2005; Takano et al., 2010), and finally conversion to

trifluoroacetyl/isopropyl ester (TFAA) derivatives, as detailed in previously published

procedures (Silfer et al., 1991; McCarthy et al., 2007; Calleja et al., 2013; McCarthy

et al., 2013).  The AA mole percent (mol%$_{AA}$) compositions were quantified

independently on the same TFAA derivatives using a GC-MS (Agilent 7890 GC

coupled to a 5975 MSD).  The N isotopic composition of individual AA ($\delta^{15}N_{AA}$) was

determined by gas chromatography / continuous flow isotope ratio mass spectrometry

(GC-C-IRMS) using previously described chromatographic conditions (Sherwood et al., 2014) and standard corrections (McCarthy et al, 2013). Under our analytical conditions, we were typically able to determine the $\delta^{15}N$ values for 13 AA: alanine (Ala), glycine (Gly), serine (Ser), valine (Val), threonine (Thr), and leucine (Leu), isoleuceine (Ile), proline (Pro), phenylalanine (Phe), tyrosine (Tyr), lysine (Lys), glutamine + glutamic acid (Glx) and aspartamine + aspartic acid + (Asx). We note that during acid hydrolysis, glutamine (Gln) is quantitatively converted to glutamic acid (Glu), and aspartamine (Asn) to aspartic acid (Asp), thus isotopic results for these combined AA are by convention reported as Glx and Asx, respectively. More detailed explanations of both CSI-AA protocols and Mol% calculations can be found in the Electronic Annex.

## $\delta^{15}N_{AA}$ nomenclature, groupings, and parameter definitions

Protein AA are divided into two main groupings, based on current literature conventions (e.g., Popp et al., 2007; McCarthy et al., 2007). The trophic AA (Tr AA; Ala, Asx, Glx, Ile, Leu, Pro, Val) are those generally exhibiting more enriched $\delta^{15}N$ values, du to assumed larger $^{15}N$ enrichment with trophic transfer. The source AA (Src AA; Gly, Lys, Phe, Ser, Tyr) are those with typically lower $\delta^{15}N$ values, based on the assumption of little to no $\delta^{15}N$ change with trophic transfer. We note that Thr was originally grouped with source AA (McClelland and Montoya, 2002; Chikaraishi et al, 2009), however has now been shown to in fact have "inverse" N isotopic fractionation with trophic transfer that is unique among commonly measured AA (Germain et al., 2013). Following the convention of previous authors (e.g., McCarthy

21

et al., 2013) $\delta^{15}N_{AA}$ data are organized for SBB samples by Tr and Src AA groupings, and then in alphabetical order.

The $\delta^{15}N$ value of total hydrolysable amino acids ($\delta^{15}N_{THAA}$) is employed as a proxy for total proteinaceous $\delta^{15}N$ value. $\delta^{15}N_{THAA}$ is calculated as the mole percent weighted sum of $\delta^{15}N_{AA}$ values following McCarthy et al. (2013):

[1]  $\delta^{15}N_{THAA} = \Sigma(\delta^{15}N_{AA} \cdot mol\%_{AA})$

where $\delta^{15}N_{AA}$ is the $\delta^{15}N$ value of individual AA determined by GC-IRMS and mol%$_{AA}$ is the molar contribution of each AA quantified with GC-MS.

Individual $\delta^{15}N_{AA}$ values were also normalized to $\delta^{15}N_{THAA}$ (see equation 1). The result, $\Delta\delta^{15}N_{AA-THAA}$, offers an internally consistent way to compare $\delta^{15}N_{AA}$ patterns between samples by removing the influence of potential variations in inorganic N source isotopic value (McCarthy et al., 2013), for example in this region variation in the $\delta^{15}N$ of sub-euphotic zone DIN through time.

Trophic positions were calculated from $\delta^{15}N_{AA}$ values of Glx and Phe, following the most widely applied current formulation from Chikaraishi et al. (2009). This approach is based on a calibrated difference in $\delta^{15}N_{Glx}$ and $\delta^{15}N_{Phe}$ defined as:

[2]  $TP = \dfrac{(\delta^{15}N_{Glx} - \delta^{15}N_{Phe} - 3.4‰)}{7.6‰} + 1$

where 3.4‰ is the empirical difference between $\delta^{15}N_{Glx}$ and $\delta^{15}N_{Phe}$ in aquatic marine autotrophs and 7.6‰ is the N isotopic trophic enrichment factor (TEF) of $\delta^{15}N_{Glx}$ relative to $\delta^{15}N_{Phe}$ per trophic transfer.

Analogous measures of relative trophic position were calculated from the difference in the mean $\delta^{15}N$ of Tr AA ($\delta^{15}N_{Tr}$) and Src AA ($\delta^{15}N_{Src}$) groups, $\delta^{15}N_{Tr-Src}$ after Sherwood et al. (2011).

**Diagenetic indicators**

Three independent metrics were used to assess early diagenetic alteration, based on AA changes in proteinaceous SOM. The degradation index (DI) (Dauwe and Middelburg, 1998; Dauwe et al., 1999) is based on multivariate analysis of protein amino acid composition, and was calculated after Dauwe et al. (1999):

[3]   $DI=\sum_i \left[ \frac{var_i - AVG_i}{STD_i} \right] \times fac.\,coef_i$

where $var_i$ is the mole percentage of AA i in our data set and the $AVG_i$ and $STD_i$ are the mean and standard deviation of AA i in the reference data set used by Dauwe et al. (1999), and fac.coef$_i$ is the factor coefficient for AA i based on the first principal component factor from Table 1 in Dauwe et al. (1999). The reactivity index (RI) (Jennerjahn and Ittekkot, 1997) is an independent quantitative metric proposed for the "quality" of OM, based on the ratio of aromatic AA (Tyr and Phe) to two non-protein AA (β-ala and γ-aba),

[4]   $RI=\frac{Tyr+Phe}{\beta ala + \gamma aba}$.

Finally, the $\Sigma V$ parameter is a proxy for total heterotrophic AA resynthesis, originally proposed by McCarthy et al. (2007), and is based on the average deviation of individual $\delta^{15}N$ values of Tr AA (Ala, Val, Leu, Ile, Pro, Asx, Glx) from the $\delta^{15}N_{Tr}$ (the mean $\delta^{15}N$ of Tr AA). The $\Sigma V$ value essentially expresses relative "scatter"

around the mean in the $\delta^{15}N_{AA}$ pattern, and so is by definition internally normalized, eliminating the influence of inter-sample variation in bulk $\delta^{15}N$ values. We calculated $\Sigma V$:

[5] $\quad \Sigma V = \frac{1}{n} \Sigma |\chi_i|$

where $\chi_i$, is the offset in $\delta^{15}N$ of each AA from the average $= [\delta^{15}N_i - AVG\ \delta^{15}N_i]$, and n is the number of AA used in the calculation.

**Results and Discussion**

**$\delta^{15}N_{AA}$ patterns in water column vs. sedimentary organic matter**

To explore whether $\delta^{15}N_{AA}$ in sediments reflects expected patterns for exported primary production, we compared $\delta^{15}N_{AA}$ patterns in SOM with a local mixed plankton tow, and also a one-year flux-weighted composite of monthly SBB sediment trap samples (Fig. 1-1). The $\delta^{15}N$ distribution of Tr AA and Src AA values in all samples had similar patterns (Fig. 1-1a, Table EA 1-1). Mixed plankton tow and sediment trap $\delta^{15}N$ values of Tr AA ranged from 10.4 to 17.1‰ (mean: 13.9 ± 2.2‰) and 10.0 to 15.5‰ (mean: 13.0 ± 2.0‰), respectively. The $\delta^{15}N$ values of Src AA for the tow and trap ranged from 6.1 to 12.1‰ (mean: 9.2 ± 2.3‰) and 3.9 to 10.2‰ (mean: 7.1 ± 2.3‰), respectively (Table EA 1-2). The general $\delta^{15}N$ offsets of Tr and Src AA in all of our sample types (plankton, POM, and SOM) are consistent with expectations mixed planktonic source material. This is further supported by the $\delta^{15}N_{AA}$ based TP estimates, which ranged from 0.6 to 1.6 in all samples (see Section 3.3.2), very similar to the range in trophic positions in POM from the Pacific (1.0 to

2.4; McCarthy et al., 2007), consistent with a mixture of primary and secondary production. The general $\delta^{15}N_{AA}$ pattern evident in all three sample types (Fig. 1-1b) is also consistent with expected $\delta^{15}N_{AA}$ patterns from autotrophs, as first observed by Macko and co-authors (Macko et al., 1987). Other authors (c.f., McClelland et al., 2002, 2003; McCarthy et al., 2007, 2013; Chikaraishi et al., 2007, 2009) have since confirmed that $\delta^{15}N_{AA}$ patterns in both natural and cultured photoautotrophs are largely universal, regardless of taxonomic group or N source. The $\delta^{15}N_{AA}$ patterns preserved in SOM here are therefore very similar not only to algae, but also to those in ocean sinking POM previously measured in the equatorial Pacific (McCarthy et al., 2007, 2013). We note that based on the essentially "universal" $\delta^{15}N_{AA}$ patterns expected in fresh marine algal sources (e.g., McCarthy et al, 2013), these findings for our selected water column samples serve primarily to verify the expected AA isotope patterns in the main sources to SBB sediments.

There are, however, also several finer scale differences in $\delta^{15}N$ values of specific AA between the tow and trap samples evident in Figure 1-1a. Trap $\delta^{15}N_{AA}$ values of Ala, Glx, Gly, Phe, Ser and Thr are all significantly different from plankton tow values (Student's $t$-test, $n \geq 3$, $p<0.05$), with each of these AA depleted by 1.7 to 6.9 ‰ (Table EA-1). These differences cannot be attributed to AA molar compositional changes, which remain similar across samples (see Section 3.2). It is more likely differences are related to the different time scales represented by the plankton tow versus the yearly-integrated trap sample. As noted above, the general photoautotrophic *pattern* is very similar, however specific $\delta^{15}N$ values would be

expected to vary seasonally. Further, different algae species can also express different $\delta^{15}N_{AA}$ fractionations for some specific AA, particularly for Gly and Ser, both within and among taxa (c.f., Chikaraishi et al., 2009).

Because the plankton tow in this study represents a single time point, we hypothesize that the $\Delta\delta^{15}N_{tow-trap}$ for specific AA may reflect a difference in the relative mix of planktonic sources for a single sampling versus the annual integration represented by the composite trap sample. The AA Thr, as noted above, is unique, not falling within either Source or Trophic AA groups in terms of its $\delta^{15}N$ values observed in ecosystems. Thr typically shows an inverse isotopic effect with trophic transfer, and so may have potential utility as an indicator of metabolic differences (Germain et al., 2013). We hypothesize that the apparent offset in Thr $\delta^{15}N$ values between trap and tow samples could reflect temporal changes in planktonic community structure, however because the systematics of Thr $\delta^{15}N$ values are very poorly understood, changes are difficult to interpret. Overall, however, the similarity in the broader $\delta^{15}N_{AA}$ pattern for the trap versus tow samples (see also discussion of normalized data below) suggests that water column OM sources to sedimentary ON in the SBB have similar $\delta^{15}N_{AA}$ patterns, as would be expected. This is consistent with relatively little change in $\delta^{15}N_{AA}$ patterns previously observed in sinking POM (McCarthy et al, 2007) and in oligotrophic and eutrophic lacustrine sedimentary environments (Carstens et al., 2013). Together, this implies that $\delta^{15}N_{AA}$ patterns in both trap and tow are likely representative of long-term POM sources to SBB SOM.

The $\delta^{15}N_{AA}$ patterns in SOM of multicore intervals (fluff layer to 39 cm; Fig. 1-1b) also generally resemble those of the mixed tow and sediment trap. Average $\delta^{15}N_{Tr}$ and $\delta^{15}N_{Src}$ for all multicore intervals range from 3.1 to 17.6‰ (mean: 11.4±2.6‰) and 4.7 to 12.4‰ (mean: 8.8±1.7‰), respectively (see Table EA-2). The mean $\delta^{15}N_{Tr}$ in the mixed tow, sediment trap and average sediment intervals are 13.2‰, 12.5‰, and 11.4‰, respectively. In each multicore interval, $\delta^{15}N_{Glx}$ is the most enriched "trophic" AA and $\delta^{15}N_{Thr}$ the most depleted AA, as in both water column sample types. Overall, $\delta^{15}N_{AA}$ compositions of averaged multicore intervals are significantly correlated to both sediment trap (Pearson's r=0.86, p«0.01, n=13) and mixed tow (Pearson's r=0.95, p«0.01, n=13) $\delta^{15}N_{AA}$ signatures.

Normalizing $\delta^{15}N_{AA}$ to $\delta^{15}N$ of total hydrolysable proteinaceous material ($\Delta\delta^{15}N_{AA-THAA}$, *see Section 2.6*) offers an internally consistent way to specifically compare $\delta^{15}N_{AA}$ *patterns*, by removing potential variation in the $\delta^{15}N$ of baseline inorganic N sources through time. The striking uniformity in $\Delta\delta^{15}N_{AA-THAA}$ patterns of the mixed tow, sediment trap and averaged sediment core data (Fig. 1-1c) confirms similar offsets between $\delta^{15}N_{Tr}$ and $\delta^{15}N_{Src}$ in all three sample types, and in fact even extends to the level of individual AA variations within each group. The similarity of both water column and sedimentary $\Delta\delta^{15}N_{AA-THAA}$ patterns again is consistent with the conclusion that $\delta^{15}N_{AA}$ compositions in SOM in SBB are a well-preserved archive of primary production $\delta^{15}N_{AA}$ patterns. This result is also consistent with conclusions from a recent study in alpine lacustrine environments (Carstens et al., 2013). Together this suggests that at least in similar suboxic depositional regimes, $\delta^{15}N_{AA}$ derived

proxies are likely faithfully preserved, and so have substantial potential as paleoceanographic tools.

**AA content and indicators of diagenetic alteration**

The degree of diagenetic alteration of accumulated sedimentary OM provides the fundamental context for understanding downcore trends in $\delta^{15}N_{AA}$, including potential paleoenvironmental interpretations discussed below (*Section 3.3*). Because AA are one of the most labile of compound classes (Cowie and Hedges, 1994; McCarthy and Bronk, 2008), a number of different AA-based proxies for relative degradation state have been developed. These include proxies based on relative AA yields (e.g., THAA), others related to relative changes in molar % of individual AA (the DI and RI indices), and a newly defined compound-specific isotopic metric proposed to specifically indicate microbial AA resynthesis ($\Sigma V$). Because these proxies and $\delta^{15}N_{AA}$ data all derive from the same pool of hydrolysable AA, we would expect that the behavior of diagenetic proxies should directly indicate the relative alteration of the OM pool, and ultimately be consistent with $\delta^{15}N_{AA}$ changes we observe.

The contribution of THAA normalized to organic carbon (OC) content of the mixed tow and sediment trap composite is 180 and 48 mg THAA (per 100 mg OC), respectively (following the reporting convention of Cowie and Hedges, 1992) (Fig. 2a). This represents a 73% loss of THAA between fresh plankton and sinking trap material, and is consistent with the large decrease in exported POM relative to surface plankton OM, and also rapid degradation with depth in the upper water column

28

(Cowie and Hedges, 1992, 1994; Cowie et al., 1995; Wakeham et al., 1997; Lee et al., 2000; Hedges et al., 2001). Rapid remineralization of THAA in sinking POM in the upper water column has been attributed to multiple factors, including animal heterotrophy in the euphotic zone, loss of protein-rich intracellular material through autotrophic cell lysis (Cowie and Hedges, 1992, 1994; Cowie et al., 1995; Wakeham et al., 1997; Lee et al., 2000; Hedges et al., 2001).

In surface sediments OC-normalized THAA content further decreased in the top 3 cm from a mean of $40 \pm 7$ to $10 \pm 3$ mg THAA (per 100 mg OC) below 3 cm (Fig. 1-2a), representing an additional 75% loss of sedimentary THAA. This loss of THAA during sedimentary burial, and the percent of OC comprised by THAA-C that can be recovered with the hydrolysis techniques applied here, are well within ranges observed in sediments from multiple oceanic regions (2-30%; e.g., Moore et al., 2012 and references therein). The overall loss of THAA in SBB sediments is similar to observations in other coastal sediments (Cowie et al., 1994, 1995; Burdige and Martens, 1988), and the relative magnitude of THAA lost in SBB *surface* sediments is remarkably consistent with similar quantitative comparisons of THAA loss. For example, in observations from Dabob Bay, WA ~80% of the measured amino acid flux through midwater depths was lost and apparently remineralized at the sediment-water interface (Cowie and Hedges, 1992).

However, despite the overall 94% decrease in OC-normalized THAA from the mixed tow to SOM intervals (deeper than 3 cm), the AA mol% composition in all water column and sediment samples are the same within error (Fig. 1-3). This implies

that minimal changes in the AA composition of OM have occurred between water column and sedimentary samples. This further implies that, at least on the bulk compositional level, the primary processes underlying large THAA losses are removal and remineralization, not degradation or diagenetic alteration of overall AA composition. Put another way, the relative mol% composition data suggests that despite the remineralization of >90% of AA, removal of AA was not selective, and the OM which has survived burial is molecularly similar to water column sources and therefore "fresh" or "unaltered". A caveat to this interpretation is that photosynthetic and heterotrophic sources of proteinaceous material can have similar bulk AA compositions (e.g., Cowie et al., 1992). However, in coastal, high-productivity and low oxygen environments such as SBB, sinking POM are expected to be the dominant source of SOM. Prior CSI-AA observations in both shallow and deep sediment traps (McCarthy et al., 2007; 2009; Hannides et al., 2013), was well as solid state NMR- based explorations of sinking POM composition observations (Hedges et al., 2001) strongly support the idea that remnant algal material dominates sinking flux to the sediments. Finally, the minimal contribution of non-protein AA in all samples from this study (<1.5 mol% of THAA), lends further support the idea that heterotrophic or bacterial sources are not major components of proteinaceous material in sinking POM.

Despite the fact that AA mole compositions of various marine sources are all generally similar (Cowie et al., 1992), fine scale AA mole compositional changes can provide a more sensitive metric to assess OM alteration. Several widely used

degradation parameters have been shown to provide more quantitative and sensitive assessments of OM preservation compared to qualitative mol%$_{AA}$ comparisons. The DI is a multivariate metric commonly used to assess OM preservation, and is based on the relative changes in multiple AA compositions with degradation (see Section 3.7; Dauwe et al., 1998; 1999). The exact suite of AA we used to calculate DI differs slightly from those proposed by Dauwe and co-authors (1999), since Methionine, Arginine, and Histidine were either not abundant or are not detected in our GC-based protocol. For this reason, the exact DI values calculated here are not directly comparable to those reported in the original papers. However, variable AA groupings are now commonly used to calculate DI, and it is relative shifts in DI values (using the same AA suite) that are most diagnostic (e.g., McCarthy, et al., 2007).

The DI values for all sample types measured here are positive, ranging from 1.1 to 2.8 (Fig. 1-2b). Specifically, the mixed tow and sediment trap composite have DI values of 2.1 and 1.8, respectively; the top three cm of SOM have DI values between 2.5 and 2.8, declining to an average of 1.4 ± 0.3 with a weak downcore trend (Pearson's $r$ = -0.02). Downcore DI values were also significantly correlated to OC-normalized THAA (Pearson's $r$ = 0.89, $p$ = 0.0021). Lower DI values indicate a higher degree of OM alteration, with typical plankton DI values greater than 1, sinking POM often in the range -1 to 1, and marine sediments generally less than 0. Overall, DI values in average SOM samples of 1.4 are similar to water column values of ~2.0, which suggests that compositional changes relative to sinking POM with planktonic biomass are minimal. This is consistent with algal biomass as the primary

31

component of sinking POM preserved in SOM of high productivity, rapid accumulation in coastal suboxic depositional settings as present in SBB.

RI is an independent quantitative metric proposed for the "quality" of OM, based on the ratio of aromatic AA (Tyr and Phe) to two main non-protein AA ($\beta$-ala and $\gamma$-aba), see section 3.7 (Jennerjahn and Ittekkot, 1997). The basis for RI is that aromatic AA (Tyr and Phe) are concentrated in cell plasma, and thus are sensitive indicators of cell lysis and/or decay processes (Mobius et al., 2011), while the non-protein AA $\beta$-ala and $\gamma$-aba are microbial degradation products. Consistent with this expectation, $\beta$-ala and $\gamma$-aba were only quantified in downcore sediments intervals ($\geq$3 cm). Combined, these non-protein AA make up less than 1.5 mol%, with no significant downcore trend, similar to observations by Cowie and Hedges (1994) in WA margin coastal sediments. As originally defined, RI values near 0 indicative extensive OM degradation, while living marine plankton have RI values between 4 and 6 (Jennerjahn and Ittekkot, 1997). Our multicore intervals below 3 cm exhibited RI values between 2.5 and 3.8, without any significant downcore trend (Fig. 1-3c), also consistent with DI, which also indicates excellent preservation of remaining algal sourced OM.

Finally, we also explored a new parameter based specifically on relative changes in CSI-AA values. The $\Sigma$V index is based on the average deviation of a subset of AA ($\delta^{15}N_{Tr}$ values; see section 3.7) and has been proposed to indicate total heterotrophic *resynthesis* of proteinaceous material (e.g, McCarthy et al., 2007; 2013). The $\Sigma$V tracks separate processes compared to the indicators discussed above, as it

fundamentally indicates whether the AA pool has been isotopically altered by microbial uptake and resynthesis, irrespective of any appreciable change having occurred in AA mol% composition. As such, this parameter is perhaps most germane to the preservation of source information in $\delta^{15}N_{AA}$ isotopic patterns. Water column POM samples have $\Sigma V$ values ranging from 1.5‰ to 2.1‰ for the plankton tow and sediment trap composite respectively (Fig. 1-3c). These values are consistent with increased heterotrophic contributions to biomass in sinking POM (McCarthy et al., 2007). Most downcore $\Sigma V$ values are also similar to water column sources, ranging from 1.3 to 1.8‰. The only slightly higher $\Sigma V$ values observed (2.2 – 3.3‰) are in fact at the sediment-water interface. It would seem unexpected that surficial sediments would be more microbially altered than the layers lying below. One possible explanation is provided by Prokopenko et al. (2006) and references therein, noting that thick mats of *Beggiatoa* spp. in this region are not buried, but occur commonly at the surface to upper few cm of sediments in the anoxic SBB. Although visual evidence of these mats were not noted, it is possible that the elevated surficial $\Sigma V$ values might indicate some incidental direct sampling of microbial mat biomass at this location.

Taken together, however, all diagenetic parameters tell a similar story of well-preserved proteinaceous material. In spite of the marked decline in recoverable THAA in the SBB sample suite, all molecular-level AA proxies (DI, RI, $\Sigma V$) consistently indicate very minimal AA alteration in these SBB SOM samples relative to surface and sinking POM. This strongly supports the hypothesis that SOM $\delta^{15}N_{AA}$

data, at least in suboxic to anoxic and high OM depositional environments like SBB, and likely faithfully reflect planktonic source $\delta^{15}N_{AA}$ patterns, and so have strong potential for ecological and environmental reconstruction.

**Paleo-environmental and -oceanographic implications**

**$\delta^{15}N_{bulk}$ and $\delta^{15}N_{THAA}$ as complementary proxies for sedimentary N studies**

Because planktonic $\delta^{15}N_{AA}$ patterns appear well preserved in SBB SOM, we expect that $\delta^{15}N$ value of total proteinaceous OM ($\delta^{15}N_{THAA}$; see Equation 1 in Section 3.6) is also well preserved.  For paleoceanographic applications, sedimentary $\delta^{15}N_{THAA}$ values provide new kinds of information beyond what can be gleaned from $\delta^{15}N_{bulk}$ measurements alone. First, in part because of generally high AA liability, terrestrial AA in riverine sediment sources are rapidly replaced with marine-derived AA (e.g., Keil and Fogel, 2001), therefore SOM THAA likely represents almost uniquely marine sources (Keil and Fogel, 2001).  Since $\delta^{15}N_{bulk}$ in continental margin sediments are often influenced by temporally varying amounts of terrestrial N ($N_{terr}$), $\delta^{15}N_{THAA}$ therefore likely provides a better measure than $\delta^{15}N_{bulk}$ of changes in the $\delta^{15}N$ of marine $N_{org}$. Second, because $\delta^{15}N_{THAA}$ derives from a dominant compound class of particulate organic N, $\delta^{15}N_{THAA}$ eliminates potential confounding influences of other N-bearing compound classes (e.g., chlorophylls, nucleic acids, carbohydrates), each with their own unique $\delta^{15}N$ signatures (Werner & Schmidt, 2002; Sachs et al. 1999; Higgins et al., 2011).

$\delta^{15}N_{THAA}$ and $\delta^{15}N_{bulk}$ were therefore directly compared in each sample of our three sample types. The values of $\delta^{15}N_{THAA}$ in the mixed tow (11.8 ± 0.7‰), sediment

trap composite ($10.6 \pm 0.7$‰) and average multicore intervals ($9.9 \pm 0.7$‰) are all

*enriched* relative to $\delta^{15}N_{bulk}$ (by +4.6‰, +3.9‰ and +2.9‰, respectively; Fig. 1-4,

Table 1-1). We note that while the water column samples are not extensive in this

study, there nevertheless seems to be a progressive trend in the offset between the

$\delta^{15}N$ value of the total hydrolysable proteinaceous pool, $\delta^{15}N_{THAA}$, and the $\delta^{15}N$ value

of the total N in our samples, $\delta^{15}N_{bulk}$. For brevity, we define this offset as

$\Delta\delta^{15}N_{THAA–bulk}$.  The $\Delta\delta^{15}N_{THAA–bulk}$ is greatest in the freshest samples, and then

appears to narrow progressively from sediment trap samples into buried sediments.

There are several possibilities for the uniform enrichment of $\delta^{15}N_{THAA}$ relative to

total N (e.g., *positive* values of $\Delta\delta^{15}N_{THAA—bulk}$) in all samples. One might be the

admixture of terrestrial material. The $\delta^{15}N$ of $N_{terr}$ can vary, but typically has an

approximate $\delta^{15}N$ range of approximately 0 to 3‰ (e.g., Sigman et al., 2001),

depleted primarily due to anthropogenic fixed N introduced as synthetic fertilizers.

Therefore, the $\Delta\delta^{15}N_{THAA–bulk}$ offset might be hypothesized to be due to a mixture of

isotopically distinct $N_{terr}$. Direct estimates of $\delta^{15}N_{terr}$ values for our study region

support lower values for $\delta^{15}N_{terr}$.  For example, Sweeney and Kaplan (1980) estimated

$\delta^{15}N_{terr}$ to be 2.8‰ from terrestrial runoff at the eastern end of the Southern California

Bight southeast of the SBB, and recent measurements of $\delta^{15}N_{bulk}$ of POM reported

values of $2.9 \pm 1.5$‰ (n=5) in 8 coastal streams along the Santa Barbara Channel

(Page et al., 2008). Therefore, neither the inter-sample comparison, nor the uniformly

positive $\Delta\delta^{15}N_{THAA—bulk}$ support terrestrial N as the explanation. Further, the

generally similar $\delta^{15}N_{bulk}$ values between the mixed tow (6.8‰), sediment trap

composite (7.2‰) and all multicore intervals (6.6 to 7.5‰; mean=6.9 ± 0.3‰; Fig. 1-4) also do not support $N_{terr}$ inputs, which would by definition be essentially absent in fresh plankton tow, and should increase (not decrease) in trap and sediment samples. We also note that the $\delta^{15}N_{bulk}$ values of tow, sediment and sediment trap samples are all consistent with previous results of suspended POM of 6.8 ±0.8‰ (Page et al., 2008), sinking POM of (Thunell, 1998) and SOM (Prokopenko et al., 2006) from SBB. Finally, the fact that plankton tow sample (presumably devoid of $N_{terr}$) exhibits the *greatest* $\Delta\delta^{15}N_{THAA-bulk}$ offset, while sediments on average had the *smallest* offset, is also contradictory to what would be expected from an increasing contribution of $^{15}N$-depleted $N_{terr}$ in traps and sediments.

To further test this inference, we estimated the $N_{terr}$ versus $N_{mar}$ contribution to total N in all samples based on simple stable isotopic end-member mixing. First, stable carbon isotope values, $\delta^{13}C_{org}$, were used to estimate the terrigenous OC contribution, $OC_{terr}$. Applying terrestrial end-member, $\delta^{13}C_{terr}$ of -28.0‰ (Thunell et al., 1998), and a marine end-member, $\delta^{13}C_{mar}$ of -21.0‰ (this study and Roland et al., 2008), yields an $OC_{terr}$ contribution of 8-19%. This range is also consistent with $OC_{terr}$ estimates by Prokopenko and co-authors (2006) for SBB sediments, and also the relatively small $OC_{terr}$ contribution to SBB sediment trap material based on compound-class $\delta^{13}C$ and $\Delta^{14}C$ values (Roland et al., 2008). A similar bulk isotope approach yields a $N_{terr}$ contribution of 15-21%, based on $\delta^{15}N_{bulk}$ end-member values for $\delta^{15}N_{mar}$ of 8.0‰ from subsurface nitrate $\delta^{15}N$ (Sigman et al., 2003) and for $\delta^{15}N_{terr}$ of 2.9±0.8‰ from riverine suspended POM (Page et al., 2008).

We can then use these estimates of $N_{terr}$ to consider the potential influence of terrestrial input on on the $\Delta\delta^{15}N_{THAA—bulk}$. The *highest* $N_{terr}$ contribution estimate (21%) would correspond to a change in $\delta^{15}N_{bulk}$ of ~1‰. This could therefore explain less than a third of the observed $\Delta\delta^{15}N_{THAA—bulk}$ offsets. We note that it is not possible from $\delta^{15}N_{AA}$ data alone to assess the effect of a given contribution of $N_{terr}$ on the $\delta^{15}N_{THAA}$ values, because this would require knowing what fraction of AA are ultimately derived from terrestrial sources. However, as noted above, prior literature would suggest that terrestrial derived AA contributions in these samples is likely very small. An additional approach to assess the same question would be to consider the implication of possible terrestrial derived AA on AA-based trophic position (TP) estimates of SBB samples. Because characteristic AA offsets in primary producers are very different in terrestrial systems (Chikaraishi et al., 2011), AA-based TP estimates would likely be altered in samples with any substantial terrestrial AA contributions. TP estimates from these sediments are discussed in more detail below (*Section 3.3*), however the fact that TP estimates for all sample types closely match expectations for purely marine particles (~1.5) (McCarthy et al., 2007), together with excellent preservation noted by degradation indices above, further supports the conclusion that $N_{terr}$ is not a major contributor to $\delta^{15}N_{THAA}$.

Instead, we hypothesize that the observed magnitude of $\Delta\delta^{15}N_{THAA—bulk}$ in SBB samples is more likely linked to variation in the biochemical composition of marine OM. Estimates of $\Delta\delta^{15}N_{THAA—bulk}$ with existing $\delta^{15}N_{AA}$ and $\delta^{15}N_{bulk}$ data from laboratory cultures and natural samples, for both autotrophs and bacteria (McCarthy

et al., 2007; Pan et al., 2007; McCarthy et al., 2013), strongly support this hypothesis (see Electronic Annex for explanation of $\Delta\delta^{15}N_{THAA-bulk}$ estimates).  Average $\Delta\delta^{15}N_{THAA-bulk}$ values in autotrophic and bacterial biomass from published datasets (Table EA 1-1) range from +2.3 to +3.5‰, similar to the range observed in all SBB sample types, +2.9 to +4.6‰.  Further, linear regressions of $\delta^{15}N_{bulk}$ versus $\delta^{15}N_{THAA}$ of these data (Table 1-1, Fig. EA 1-1) offers an approximation of the mean $\Delta\delta^{15}N_{THAA-bulk}$ in cultured and natural biomass. The y-intercept of these regressions predict a range of $\Delta\delta^{15}N_{THAA-bulk}$ from +1.7 to 3.5‰ derived from culture studies for which CSI-AA data exists. This offset in pure cells *must* be related to offsets in the average $\delta^{15}N$ values between protein and other nitrogenous compound classes (e.g., nucleic acids, carbohydrates, chlorophylls, lipids) each with unique ranges of biosynthetic N fractionation (Hayes, 2001; Werner and Schmidt, 2002). While $\delta^{15}N_{THAA}$ data are not yet extensive, this literature comparison (Table 1-1, Fig. EA 1-1) strongly suggests that while $\Delta\delta^{15}N_{THAA-bulk}$ values in fresh biomass fall in a generally similar range, there could also be variations between specific groups of algae microorganisms.

Overall, however, the culture data suggests that $\Delta\delta^{15}N_{THAA-bulk}$ in both tow, trap, and sediments are mostly related to a relative mixture of nitrogenous organic compound classes, as opposed to terrigenous or other inputs. That $\Delta\delta^{15}N_{THAA-bulk}$ values in all sample types are similar to ranges in pure cultures (Table 1-1, Fig. EA 1-1) supports this conclusion, and also strongly supports the inference of excellent $N_{org}$ preservation discussed above. We hypothesize that the differences in the magnitude

of $\Delta\delta^{15}N_{THAA—bulk}$ between the mixed tow and trap samples could be associated with planktonic community composition, especially considering different time scales of the specific samples that were available for this study (i.e., annual integration for traps versus a single sampling for the mixed plankton tow). Alternatively, it is also possible that preferential loss of different nitrogenous compound classes during water column remineralization and sediment burial could explain the apparent trend in decreasing $\Delta\delta^{15}N_{THAA—bulk}$; indeed, the fact that this offset is lowest in sediments is also consistent with extensive NMR data suggesting that proteinaceous material dominates sedimentary $N_{org}$ preserved in recently deposited sediments (Knicker et al., 1996; Knicker and Hatcher, 1997; Nguyen and Harvey, 1997, 1998; Knicker and Hatcher, 2001; Knicker et al., 2002).

Overall, we therefore hypothesize that sedimentary $\delta^{15}N_{THAA}$ will therefore reflect $\delta^{15}N$ of integrated *proteinaceous* material exported from the surface ocean. If a consistent average relationship exists between $\delta^{15}N_{THAA}$ and $\delta^{15}N_{bulk}$ in primary production (as has been indicated both by our comparison here, and also in earlier literature; e.g., McCarthy et al., 2013) then an appropriate calibration factor should be able to reconstruct $\delta^{15}N$ values of bulk exported primary production from $\delta^{15}N_{THAA}$ measured in sediments. Characterizing the range in $\Delta\delta^{15}N_{THAA–bulk}$ values of fresh marine OM and comparing $\Delta\delta^{15}N_{THAA–bulk}$ of sinking and sedimentary OM in various depositional settings will therefore be important for developing $\delta^{15}N_{THAA}$ as a potential paleoproxy. In any environmental application, we also suggest that $\Sigma V$

values will be useful to evaluate if microbial resynthesis may have altered initial relationships.

**Interrelationship of Source and Trophic AA values in sedimentary archives: dependence of individual values of $\delta^{15}N_{AA}$ on trophic position**

As noted above, the most important applications of $\delta^{15}N$ CSI-AA to date have been based on the ability to decouple primary production $\delta^{15}N$ signatures from the effects of trophic transfer, and so simultaneously indicate baseline $\delta^{15}N$ values together with precise values for trophic position (TP; *methods*). Among the source AA, $\delta^{15}N_{Phe}$ in particular has been shown to be the best proxy for integrated $\delta^{15}N$ values at the base of the marine food webs. This conclusion has come primarily from measurements in individual marine organisms, both in culturing and feedings studies (e.g., Chikaraishi et al. 2009; Germain et al., 2013), and in environmental studies of specific organisms or mixed plankton samples (e.g., Schmidt et al., 2004; McCarthy et al., 2007; Popp et al., 2007; Chikaraishi et al., 2009; Hannides et al., 2009, 2013). Recently, the same conclusion has also been strongly supported by paleoceanographic work with deep-sea corals (Sherwood et al., 2011; Sherwood et al., 2014). Together, past work therefore suggests that $\delta^{15}N_{Phe}$ in marine sediments could represent a direct proxy for integrated $\delta^{15}N$ value of baseline nitrogen sources. Sedimentary $\delta^{15}N_{Phe}$ values in multicore intervals are ~10‰ at the core top, declining to ~8‰ in the upper half (<20 cm), and increasing again toward 10‰ at the bottom of the core (Fig. 1-5a). The range of sedimentary $\delta^{15}N_{Phe}$ values, 8.1 to 12.4‰ (mean=10.0‰) span $\delta^{15}N_{Phe}$ in the mixed tow (10.6‰) and sediment trap composite (8.6 ‰) samples (Fig. 1-5a,

Table EA-1). If sedimentary $\delta^{15}N_{Phe}$ values directly track baseline values, as hypothesized, then these trends might indicate regional excursions in the $\delta^{15}N$ of exported primary production.

The TP record shows a similar pattern of change over most of the downcore profile, except the deepest 3 intervals (Fig. 1-5b). Most TP values in all three sample types fall in the range of 1 to 1.5, consistent with prior sinking POM results (McCarthy et al., 2007); the overall average TP of sediment intervals (1.2±0.2) is slightly lower than the mixed plankton tow and sediment trap composite samples (both 1.4 TP, within error). The TP values of these sample types should represent the average TP of a mixture of marine OM sources in the (McCarthy et al., 2007). However, what is most striking in the data is that TP values appear to mirror $\delta^{15}N_{Phe}$ throughout most of the core (0 to ~ 30cm). In the upper depths (with the best resolution), this inverse relationship is strongest, with TP values progressively increasing from ~1.0 at the core top, to ~1.5 at 16 cm depth, coincident with a *decrease* in $\delta^{15}N_{Phe}$. However, in the deepest few samples (≥28 cm; 3 out of 15 samples) this relationship is not observed, with TP and $\delta^{15}N_{Phe}$ values trending in the same direction (both increasing with depth). Overall, however, variations of TP and $\delta^{15}N_{Phe}$ over both water column and multicore samples exhibit a significant inverse correlation between TP and $\delta^{15}N_{Phe}$ (Pearson's $r$=-0.56, $p$=0.029, n=15). Assuming the $\delta^{15}N_{THAA}$ is well preserved (as the data discussed above clearly indicate) this relationship suggests *interdependence* exists between $\delta^{15}N_{Phe}$ and TP values. Such a conclusion would run directly counter to current $\delta^{15}N_{AA}$ theory and common

applications in animals, which assumes these qualities are fundamentally independent.

The most likely explanation for this apparent contradiction may lie in the long time scales of sedimentary accumulation, as opposed to more discrete temporal $\delta^{15}N_{AA}$ measurements in organisms. Over long time scales, $\delta^{15}N$ values in a system must be constrained by N isotopic and mass balance. We hypothesize that this constraint should in fact create an intrinsic interdependence between TP (i.e., related to the isotopic separation between source and trophic AA groups) and the $\delta^{15}N$ values of all AA. To test this idea we constructed a simple isotope mass balance model to examine TP dependence on $\delta^{15}N$ values of source AA ($\delta^{15}N_{Src}$), and trophic AA ($\delta^{15}N_{Tr}$).

Figure 1-6 is a schematic of the main assumptions underlying the isotope mass balance model, showing the partitioning of $\delta^{15}N$ between trophic and source AA groups, as well as trophic enrichment factors (TEF) during trophic transfer. Our model assumes a steady state isotope mass balance for a fixed $\delta^{15}N$ composition of the proteinaceous pool, $\delta^{15}N_{THAA}$, and also a constant ratio of trophic AA, $f_{Tr}$, and source AA, $f_{Src}$ (e.g., mole fraction of each AA group) which comprise the total THAA pool, $f_{THAA}$ (Eqn. 6):

[6] $f_{THAA} \cdot \delta^{15}N_{THAA} = f_{Src} \cdot \delta^{15}N_{Src} + f_{Tr} \cdot \delta^{15}N_{Tr}$

The $\delta^{15}N_{Tr}$ and $\delta^{15}N_{Src}$ values in Equation 6, as well as the average $\delta^{15}N$ offset *between* the two groups, $\beta_{Tr/Src}$, are determined by three factors: (1) the baseline $\delta^{15}N$ of primary production and fractionation for both AA groups, trophic, $\alpha_{Tr}$, and

source, $\alpha_{Src}$, relative to $\delta^{15}N_{THAA}$, (2) trophic enrichment factors (TEF) for trophic

AA, $TEF_{Tr}$, and source AA, $TEF_{Src}$, groups, and (3) the value of TP (Fig. 1-6, Eqn.

7):

[7] $\delta^{15}N_{Tr} - \delta^{15}N_{Src} = \alpha_{Src} + (TEF_{Src} \cdot TP) + \alpha_{Tr} + (TEF_{Tr} \cdot TP)$

Combining equations (6) and (7):

[8] $\delta^{15}N_{Src} = \dfrac{f_{THAA} \cdot \delta^{15}N_{THAA} - f_{Tr}[\alpha_{Src} + (TEF_{Src} \cdot TP) + \alpha_{Tr} + (TEF_{Tr} \cdot TP)]}{f_{Src} + f_{Ttr}}$

A specific $\delta^{15}N_{Phe}$ value can than be calculated with the following:

[9] $f_{Src} \cdot \delta^{15}N_{Src} = \sum_{i=1}^{n} f_{Src_i} \cdot \left(\delta^{15}N_{Phe} + \varepsilon_{Src_i - Phe}\right)$

where, $fsrc$, is the mole fraction of each source AA, and $\varepsilon_{Src_i - Phe}$ is the offset

between the $\delta^{15}N$ of each source AA and $\delta^{15}N_{Phe}$. See Table EA 1-3 for values of

model parameters.

The model output for $\delta^{15}N_{Tr}$ and $\delta^{15}N_{Src}$, driven by values of TP over the range

observed in our sediment samples, clearly demonstrates the dependence of both

$\delta^{15}N_{Tr}$ and $\delta^{15}N_{Src}$ on the systems TP, given the model assumptions (Fig. 1-7). The

offset between $\delta^{15}N_{Tr}$ and $\delta^{15}N_{Src}$ increases linearly with increasing TP, as it must.

Therefore, this simple model demonstrates that *under the constraint of isotopic mass*

*balance, values of both $\delta^{15}N_{Src}$ and $\delta^{15}N_{Tr}$ become necessarily dependent on TP*. This

is because any individual $\delta^{15}N_{AA}$ value fundamentally results from the partitioning of

a fixed source pool of AA (with a fixed $^{15}N/^{14}N$ ratio) between the Tr and Src AA

groups.

Further, we then examined if this simple model could also reproduce measured variation in $\delta^{15}N_{Phe}$ in SBB sediments. To apply the model to examine actual SBB data, we used the measured TP of each sediment interval, and then we used the model to calculate $\delta^{15}N_{Phe}$ from Eqn. 9. The mole fraction of each Src AA, $f_{Src_i}$, was based on the measured mol% of the SBB plankton tow (Fig. 1-3), and N isotopic offsets of source AA relative to Phe, $\varepsilon_{Src_i-Phe}$, were derived from averages of field and culture data for autotrophic organisms (Table EA 1-3) (McClelland and Montoya, 2002; McClelland et al., 2003; Chikaraishi et al., 2007; McCarthy et al., 2007; Chikaraishi et al., 2009; McCarthy et al., 2013). The magnitude of the measured SBB isotope changes, as well as overall shape of the observed $\delta^{15}N_{Phe}$ records, are clearly captured by the model output (Fig. 1-8). Modeled and observed sedimentary $\delta^{15}N_{Phe}$ values are significantly positively correlated (Pearson's $r=+0.58$, $p=0.036$, n=13) when $\delta^{15}N_{THAA}$ values are set to 8‰ (i.e., the approximate average of sub-euphotic zone nitrate $\delta^{15}N$ from water column data in Sigman et al., 2005).

Overall, these results strongly support our hypothesis that long-term isotope mass balance underlies the observed inverse relationship between TP and $\delta^{15}N_{Phe}$. However, our simple model also clearly cannot capture all environmental factors that could impact $\delta^{15}N_{Phe}$, and we suggest this is why exact observed $\delta^{15}N_{Phe}$ values (as opposed to the *trends*) are not identical to model output values. Some potential factors not captured by our model include time-varying changes of nutrient $\delta^{15}N$, (and also $\delta^{15}N_{THAA}$), any variation in percentage of N-utilization, the mole fraction of Tr and Src groups, variability in individual values of $\alpha_{Src_i-Phe}$, or differences in either

$\alpha_{Tr}$ or $\alpha_{Src}$. We note that AA preservation changes do not seem to be relevant here (see discussion above in *Section 3.2*), however, plankton composition changes might influence the mole fraction of Tr and Src groups, and so $\varepsilon_{Src_i-Phe}$ offsets (see Table EA 1.3). Further, if periods occur where basic model assumptions (e.g., complete N utilization, and a "closed system" with a constant N isotope mass balance) no longer apply, then the inverse relationship between $\delta^{15}N_{Phe}$ and TP would also no longer be predicted. It is tempting to speculate that such factors could underlie the deepest several data points in the record (below 28 cm), where $\delta^{15}N_{Phe}$ and TP appears to have a positive – not an inverse relationship (Fig. 1.5). However, below 28 cm, there are very few data, and interpretation of such finer details of this core is therefore beyond the scope of our current data set. Overall, what seems most striking is that a very simple mass balance model can recreate not only the observed overall interrelationship between TP and $\delta^{15}N_{Phe}$, but can also capture the relative magnitude of changes observed in a natural system.

Together, our model and the SBB data suggest that a fundamentally different paradigm may be required for CSI-AA temporal reconstructions in paleoarchives. Specifically, in contrast to past studies of samples collected in the water column, our sedimentary analyses and simple model indicate that over long time scales (given the assumption of steady state N balance), measured individual $\delta^{15}N_{AA}$ values must become directly dependent on TP change. This suggests that two key parameters, TP and $\delta^{15}N_{THAA}$ (the total proteinaceous pool $\delta^{15}N$ value), are in fact the master variables. Dependence of AA $\delta^{15}N$ value on TP change also should of course extend

to each individual AA, not just to $\delta^{15}N_{Phe}$ or the average $\delta^{15}N_{Tr}$ or $\delta^{15}N_{Src}$ groups.

However, the strength of the TP dependence for any specific AA in turn depends on

its relative mol% and its TEF value (the very different slopes of $\delta^{15}N_{Tr}$ versus $\delta^{15}N_{Src}$

shown in Fig. 1.7 illustrate both these effects). Finally, however, it is also very

important to note that in cases where TP in a record is *unchanging* (i.e., as in both

case studies for deep sea corals so far published; Sherwood et al., 2011, 2014), then

TP variation by definition has no effect, and $\delta^{15}N_{Phe}$ (or $\delta^{15}N_{Src}$) values should again

directly reflect baseline $\delta^{15}N$ values. However, in cases where TP varies, then

$\delta^{15}N_{THAA}$ should become the only direct proxy for baseline $\delta^{15}N$ values.

**Regional interpretation of TP and $\delta^{15}N_{THAA}$ records**

We have hypothesized that sedimentary profiles of $\delta^{15}N_{THAA}$, coupled with TP and

$\delta^{15}N_{Tr–Src}$ (a broader proxy for TP, *see Section 2.6*), may be used to differentiate

temporal changes in baseline $\delta^{15}N$ values from changes in ecosystem trophic

structure. Our downcore records from the SBB offers a unique opportunity to

evaluate these AA-based parameters as potential paleoceanographic indicators of

regional physical and ecosystem changes in the Southern California Bight (SCB).

[210]Pb-based chronology determined that the deepest sediment interval in the

multicore is ca.1870 and that the average sedimentation rate is 0.29 cm yr$^{-1}$. This

sedimentation rate is consistent with previous estimates of 0.12 to 0.5 cm yr$^{-1}$ for SBB

(Barron et al., 2010). CSI-AA data were analyzed at 13 intervals throughout the

sediment core at low temporal resolution, particularly prior to ca. 1980 (Fig. 1.9).

Because of the low resolution of the record prior to ca. 1980, the lack of trends in all

46

three CSI-AA parameters could simply be a result of aliasing of high frequency variations. However, $\delta^{15}N_{THAA}$, TP and $\delta^{15}N_{Tr-Src}$ decrease markedly after 1980. $\delta^{15}N_{THAA}$ decreases from 10.6 to 9.3‰, TP decreases from 1.6 to 0.6, and $\delta^{15}N_{Tr-Src}$ decreases from 5.0 to 2.0‰. These parameters are now briefly considered in the context of regional oceanography.

Assuming complete nitrate utilization for the system and that $\delta^{15}N_{THAA}$ reflects changes in the DIN $\delta^{15}N$ of source water to the region, then a $\delta^{15}N_{THAA}$ decrease of ca. 1.3‰ would imply a decrease in DIN $\delta^{15}N$ also of ~1.3‰ in SBB since 1980. The annual mean subsurface DIN $\delta^{15}N$ in SBB today is ~8‰ (Sigman et al., 2003; 2005). This value is likely set by the relative ratio of the dominant surface and subsurface sources throughout SBB, which include the equatorward CA Current (CC), poleward Southern CA Countercurrent (SCCC) and the poleward CA Undercurrent (CUC) (Hickey and Royer, 2001). The sub-euphotic zone nitrate $\delta^{15}N$ in the CUC (at ca. 300 m) near Baja California exhibits values up to 15-16‰, but decreases northward along the CA margin from 8-10‰ in the SBB (Sigman et al., 2003; Sigman et al., 2005) to deep-ocean $\delta^{15}N$ values (ca. 6‰) off the coast of Washington (Kienast et al., 2002). One way to change the average $\delta^{15}N$ of DIN of sub-euphotic water in SBB could simply be a change in the admixture of source waters to SBB. Assuming the DIN $\delta^{15}N$ values of CUC and CC end-members have not changed since 1980, then the decreasing $\delta^{15}N_{THAA}$ values could imply a greater proportion of $\delta^{15}N$-depleted nitrate from the northerly CC relative to the $\delta^{15}N$-enriched CUC in the admixture of these currents to SBB. This is broadly consistent with documented physical oceanographic

changes occurring throughout the CCS during this period, and also expected changes in the relative ratio of CCS source waters to the SBB (e.g., Palacios et al. 2004; Rykaczewski et al. 2010).

Contemporaneous with the declining trend in $\delta^{15}N_{THAA}$ are declining trends in TP and $\delta^{15}N_{Tr–Src}$ parameters since ca. 1980. These trends indicate that the average TP of the export flux has decreased in the SBB over this time period. This observation also seems consistent with documented CCS-wide ecosystem changes. Specifically, declining zooplankton biomass since ca. 1950 (Lavaniegos and Ohman, 2003, 2007), as well as nutricline shoaling and increases in *Chl a* since ~1980 (Rykaczewski et al. 2010), are thought to represent a more productive and likely less complex marine food-web, having fewer trophic transfers (Rykaczewski and Checkley, 2008; Aksnes et al., 2009). Such a shift would be consistent with declining average planktonic TP values, as reflected in $\delta^{15}N_{Tr–Src}$ values. This would imply that since 1980, the average TP of the export flux has decreased in the SBB.

Taken together, records of $\delta^{15}N_{THAA}$, TP and $\delta^{15}N_{Tr–Src}$ since ca. 1980 provide a first attempt to use these CSI-AA parameters as proxies of regional physical and ecosystem change. Broad trends in these new data since 1980 are consistent with general ecosystem changes throughout the CCS. Based on the observations and discussion above, we hypothesize that CSI-AA data, in organic-rich, anoxic or sub-oxic environments such as the SBB, may be a useful addition to the toolkit used to study paleoceanographic N biogeochemical cycling and ecosystem and baseline DIN changes.

**Summary and Conclusions**

Similar planktonic patterns of $\delta^{15}N_{AA}$ values were found in sedimentary organic matter (SOM) and water column POM sources from the Santa Barbara Basin. Together with molecular-level indicators of preservation (e.g., DI, RI, etc.), this supports our basic hypothesis that SOM $\delta^{15}N_{AA}$ data preserve $\delta^{15}N_{AA}$ patterns of local planktonic sources. We conclude that at least in similar environments having excellent OM preservation, $\delta^{15}N_{AA}$ derived proxies have great potential in paleoceanographic studies to track variations in the marine N cycle. Specifically, they can provide a record of both baseline $\delta^{15}N$ values and also trophic structure of exported primary production.

However, our data also suggest that a fundamentally new conceptual framework is likely required for CSI-AA proxies in paleoceanographic applications. The SBB multicore data showed an inverse relationship between TP values and individual $\delta^{15}N_{Phe}$ values through most of the record. A simple isotope mass balance model confirms that in fact an interdependence of individual $\delta^{15}N_{AA}$ values on TP is expected for any record which integrates exported production over long temporal scales, and thus is constrained by long term $\delta^{15}N$ mass balance (i.e., typical for most paleoceanographic archives). This idea represents a significant departure from current assumptions about the independence of source AA $\delta^{15}N$ values (e.g., $\delta^{15}N_{Phe}$) and TP estimates, at least as these apply in modern, short time frame, ecosystem studies. However, it is also important to note that in cases where TP is *unchanging* throughout a record, such dependence is by definition removed, and the direct linkage between

49

source AA and baseline $\delta^{15}N$ values should again comply with utility in modern ecosystems. For example, several recent studies have demonstrated deep-sea proteinaceous coral records with essentially invariant TP (Sherwood et al., 2011; Prouty et al., 2014; Sherwood et al., 2014). When TP does not vary, the direct linkage between $\delta^{15}N_{Phe}$ (or $\delta^{15}N_{Src}$) and nitrate $\delta^{15}N$ indicated in these studies is fully consistent with our findings here.

We conclude that in sedimentary records, $\delta^{15}N_{AA}$ values will be strongly influenced by *both* changes in both TP and in $\delta^{15}N$ of the source inorganic nitrogen. This implies that in sediments changes in baseline $\delta^{15}N$ values are likely best reflected not by selected source AA (as is now assumed), but instead by $\delta^{15}N_{THAA}$ (the proxy for $\delta^{15}N$ value of total proteinaceous material). Our comparison of $\delta^{15}N_{THAA}$ in SBB water column sources and sediments also indicates that while trends in $\delta^{15}N_{THAA}$ likely track $\delta^{15}N$ of exported $N_{org}$, $\delta^{15}N_{THAA}$ *values* are also offset from bulk $\delta^{15}N$ values due to presence of other nitrogenous organic compounds. Examination of literature CSI-AA data from algal cultures suggests a relatively constant correction factor, whose value is also consistent with our SBB observations. This suggests that applying an offset correction to sedimentary $\delta^{15}N_{THAA}$ is necessary to reconstruct $\delta^{15}N$ of marine ON sources.

Taken together, these results suggest that in regions with complete nitrate utilization, $\delta^{15}N_{THAA}$ may represent the best new proxy for the $\delta^{15}N$ of nitrate, and (unlike $\delta^{15}N_{bulk}$) one that is independent of potentially confounding inorganic N sources. However, more work is now needed to more precisely determine the offset

50

between $\delta^{15}N_{THAA}$ and $\delta^{15}N$ of bulk algal $N_{org}$, and we suggest this is one of the most important areas of future research for application of CSI-AA proxies in paleoarchives. Overall, our results imply that in paleoceanographic contexts TP together with $\delta^{15}N_{THAA}$ represent the central CSI-AA parameters, and that these must always be assessed together. We suggest that, at least in sedimentary environments where AA are well preserved, TP and $\delta^{15}N_{THAA}$ should provide a coupled picture of regime shifts in planktonic ecosystem structure, and also $\delta^{15}N$ at the base of food webs. Future work now needs to evaluate how well $\delta^{15}N_{AA}$ are preserved in other marine sedimentary environments, particularly those characterized by oxic and slow-depositional conditions. This work will be critical to assess the potential of $\delta^{15}N_{AA}$ proxies in deep, open-ocean sediments.

**Acknowledgements**

## References

Aksnes D. L. and Ohman M. D. (2009) Multi-decadal shoaling of the euphotic zone in the southern sector of the California Current System. Limnology and Oceanography 54(4): 1272-1281.

Altabet M. (1996) Nitrogen and carbon isotopic tracers of the source and transformations of particles in the deep-sea. In Particle Flux in the Ocean. (eds. V. S. P. H. S. D. P. J. Ittekkot), John Wiley & Son Ltd. 57.

Altabet M. and Francois R. (1994) Sedimentary nitrogen isotopic ratio as a recorder for surface ocean nitrate utilization. Global Biogeochemical Cycles 8(1): 103-116.

Altabet M., Pilskaln C., Thunell R., Pride C., Sigman D., Chavez F. and Francois R. (1999) The nitrogen isotope biogeochemistry of sinking particles from the margin of the Eastern North Pacific. Deep-Sea Research Part I 46: 655-679.

Altabet M. A. (1988) Varitiations in nitrogen isotopic composition between sinking and suspended particles - implications for nitrogen cycling and particle transformation in the open ocean. Deep-Sea Research Part I 35(4): 535-554.

Appleby P. and Oldfield F. (1978) The calculation of lead-210 dates assuming a constant rate of supply of unsupported$^{210}$ Pb to the sediment. Catena 5(1): 1-8.

Barron J. A., Bukry D. and Field D. (2010) Santa Barbara Basin diatom and silicoflagellate response to global climate anomalies during the past 2200 years. Quaternary International 215(1-2): 34-44.

Burdige D. J. and Martens C. S. (1988) Biogeochemical cycling in an organic-rich coastal marine basin: 10. The role of amino-acids in sedimentary carbon and nitrogen cycling. Geochimica Et Cosmochimica Acta 52(6).

Calleja M. L., Batista F., Peacock M., Kudela R. and McCarthy M. D. (2013) Changes in compound specific delta N-15 amino acid signatures and D/L ratios in marine dissolved organic matter induced by heterotrophic bacterial reworking. Marine Chemistry 149: 32-44.

Chikaraishi Y., Kashiyama Y., Ogawa N. O., Kitazato H. and Ohkouchi N. (2007) Metabolic control of nitrogen isotope composition of amino acids in macroalgae

and gastropods: implications for aquatic food web studies. Marine Ecology Progress Series 342: 85-90.

Chikaraishi Y., Ogawa N., Kashiyama Y., Takano Y., Suga H., Tomitani A., Miyashita H., Kitazato H. and Ohkouchi N. (2009) Determination of aquatic food-web structure based on compound-specific nitrogen isotopic composition of amino acids. LIMNOLOGY AND OCEANOGRAPHY-METHODS: 740-750.

Cowie G. L. and Hedges J. I. (1992) Sources and reactivities of amino-acids in a coastal marine environment. Limnology and Oceanography 37(4).

Cowie G. L. and Hedges J. I. (1994) Biochemical indicators of diagenetic alteration in natural organic-matter mixtures. Nature 369(6478).

Cowie G. L., Hedges J. I., Prahl F. G. and Delange G. J. (1995) Elemental and major biochemical-changes across an oxidatino front in a relict turbidite - an oxygen effect. Geochimica Et Cosmochimica Acta 59(1): 33-46.

Dauwe B. and Middelburg J. J. (1998) Amino acids and hexosamines as indicators of organic matter degradation state in North Sea sediments. Limnology and Oceanography 43(5).

Dauwe B., Middelburg J. J., Herman P. M. J. and Heip C. H. R. (1999) Linking diagenetic alteration of amino acids and bulk organic matter reactivity. Limnology and Oceanography 44(7).

Fabian V., Morvai M., Pinterszakacs M. and Molnarperl I. (1991) Standarization of cation-exchange cleanup prior to gas-chromatography of amino-acids. Journal of Chromatography 553(1-2): 87-92.

Germain L. R., Koch P. L., Harvey J. and McCarthy M. D. (2013) Nitrogen isotope fractionation in amino acids from harbor seals: implications for compound-specific trophic position calculations. Marine Ecology Progress Series 482: 265-+.

Hannides C. C., Popp B. N., Choy C. A. and Drazen J. C. (2013) Midwater zooplankton and suspended particle dynamics in the North Pacific Subtropical Gyre: A stable isotope perspective. Limnol. Oceanogr 58(6): 1931-1946.

Hannides C. C. S., Popp B. N., Landry M. R. and Graham B. S. (2009) Quantification of zooplankton trophic position in the North Pacific Subtropical Gyre using stable nitrogen isotopes. Limnology and Oceanography 54(1): 50-61.

Hayes J. M. (2001) Fractionation of carbon and hydrogen isotopes in biosynthetic processes. Stable Isotope Geochemistry 43: 225-277.

Hedges J. I., Baldock J. A., Gelinas Y., Lee C., Peterson M. and Wakeham S. G. (2001) Evidence for non-selective preservation of organic matter in sinking marine particles. Nature 409(6822): 801-804.

Hedges J. I. and Stern J. H. (1984) Carbon and Nitrogen Determinations of Carbonate-Containing Solids. Limnology and Oceanography 29(3): 657-663.

Hickey B. M. and Royer T. C. (2001) California and Alaska Currents. In Encyclopedia of Ocean Sciences (Second Edition). (eds. J. H. Steele). Oxford, Academic Press: 455-466.

Higgins M. B., Robinson R. S., Carter S. J. and Pearson A. (2010) Evidence from chlorin nitrogen isotopes for alternating nutrient regimes in the Eastern Mediterranean Sea. Earth and Planetary Science Letters 290(1-2): 102-107.

Jennerjahn T. C. and Ittekkot V. (1997) Organic matter in sediments in the mangrove areas and adjacent continental margins of Brazil .1. Amino acids and hexosamines. Oceanologica Acta 20(2).

Keil R. G. and Fogel M. L. (2001) Reworking of amino acid in marine sediments: Stable carbon isotopic composition of amino acids in sediments along the Washington coast. Limnology and Oceanography 46(1): 14-23.

Kienast S. S., Calvert S. E. and Pedersen T. F. (2002) Nitrogen isotope and productivity variations along the northeast Pacific margin over the last 120 kyr: Surface and subsurface paleoceanography. Paleoceanography 17(4).

Knicker H. and Hatcher P. G. (1997) Survival of protein in an organic-rich sediment: Possible protection by encapsulation in organic matter. Naturwissenschaften 84(6): 231-234.

Knicker H. and Hatcher P. G. (2001) Sequestration of organic nitrogen in the sapropel from Mangrove Lake, Bermuda. Organic Geochemistry 32(5): 733-744.

Knicker H., Hatcher P. G. and Gonzalez-Vila F. J. (2002) Formation of heteroaromatic nitrogen after prolonged humification of vascular plant remains as revealed by nuclear resonance spectroscopy. Journal of Environmental Quality 31(2): 444-449.

Knicker H., Scaroni A. W. and Hatcher P. G. (1996) C-13 and N-15 NMR spectroscopic investigation on the formation of fossil algal residues. Organic Geochemistry 24(6-7): 661-669.

Lavaniegos B. E. and Ohman M. D. (2003) Long-term changes in pelagic tunicates of the California Current. Deep-Sea Research Part Ii-Topical Studies in Oceanography 50(14-16): 2473-2498.

Lavaniegos B. E. and Ohman M. D. (2007) Coherence of long-term variations of zooplankton in two sectors of the California Current System. Progress in Oceanography 75(1): 42-69.

Lee C., Wakeham S. G. and Hedges J. I. (2000) Composition and flux of particulate amino acids and chloropigments in equatorial Pacific seawater and sediments. Deep-Sea Research Part I-Oceanographic Research Papers 47(8): 1535-1568.

Lehmann M. F., Bernasconi S. M., Barbieri A. and McKenzie J. A. (2002) Preservation of organic matter and alteration of its carbon and nitrogen isotope composition during simulated and in situ early sedimentary diagenesis. Geochimica Et Cosmochimica Acta 66(20): 3573-3584.

Liu Z. H., Altabet M. A. and Herbert T. D. (2008) Plio-Pleistocene denitrification in the eastern tropical North Pacific: Intensification at 2.1 Ma. Geochemistry Geophysics Geosystems 9.

Macko S. A. and Estep M. L. (1984) Microbial alteration of stable nitrogen and carbon isotopic compositions of organic matter. Organic Geochemistry 6: 787-790.

Macko S. A., Fogel M. L., Hare P. E. and Hoering T. C. (1987) Isotopic fractionation of nitrogen and carbon in the synthesis of amino-acids by microorganisms. Chemical Geology 65(1): 79-92.

McCarthy M. D., Benner R., Lee C. and Fogel M. L. (2007) Amino acid nitrogen isotopic fractionation patterns as indicators of heterotrophy in plankton, particulate, and dissolved organic matter. Geochimica Et Cosmochimica Acta 71(19): 4727-4744.

McCarthy M. D. and Bronk D. A. (2008) ANALYTICAL METHODS FOR THE STUDY OF NITROGEN. Nitrogen in the Marine Environment, 2nd Edition: 1219-1275.

McCarthy M. D., Lehman J. and Kudela R. (2013) Compound-specific amino acid delta N-15 patterns in marine algae: Tracer potential for cyanobacterial vs. eukaryotic organic nitrogen sources in the ocean. Geochimica Et Cosmochimica Acta 103: 104-120.

McClelland J. W., Holl C. M. and Montoya J. P. (2003) Relating low delta N-15 values of zooplankton to N-2-fixation in the tropical North Atlantic: insights provided by stable isotope ratios of amino acids. Deep-Sea Research Part I-Oceanographic Research Papers 50(7): 849-861.

McClelland J. W. and Montoya J. P. (2002) Trophic relationships and the nitrogen isotopic composition of amino acids in plankton. Ecology 83(8): 2173-2180.

Mobius J., Gaye B., Lahajnar N., Bahlmann E. and Emeis K. C. (2011) Influence of diagenesis on sedimentary delta N-15 in the Arabian Sea over the last 130 kyr. Marine Geology 284(1-4): 127-138.

Nguyen R. T. and Harvey H. R. (1997) Protein preservation during early diagenesis in marine waters and sediments. Abstracts of Papers of the American Chemical Society 214: 66-GEOC.

Nguyen R. T. and Harvey H. R. (1998) Protein preservation during early diagenesis in marine waters and sediments. In Nitrogen-Containing Macromolecules in the Bio- and Geosphere. (eds. B. A. Stankiewicz and P. F. VanBergen). 707: 88-112.

Page H. M., Reed D. C., Brzezinski M. A., Melack J. M. and Dugan J. E. (2008) Assessing the importance of land and marine sources of organic matter to kelp forest food webs. Marine Ecology Progress Series 360: 47-62.

Palacios D. M., Bograd S. J., Mendelssohn R. and Schwing F. B. (2004) Long-term and seasonal trends in stratification in the California Current, 1950-1993. Journal of Geophysical Research-Oceans 109(C10).

Pan B. S., Wolyniak C. J. and Brenna J. T. (2007) The intramolecular delta N-15 of lysine responds to respiratory status in Paracoccus denitrificans. Amino Acids 33(4): 631-638.

Prokopenko M. G., Hammond D. E., Berelson W. M., Bernhard J. M., Stott L. and Douglas R. (2006) Nitrogen cycling in the sediments of Santa Barbara basin and Eastern Subtropical North Pacific: Nitrogen isotopes, diagenesis and possible

chemosymbiosis between two lithotrophs (Thioploca and Anammox) "riding on a glider". Earth Planet. Sci. Lett. 242(1-2): 186-204.

Prouty N. G., Roark E. B., Koenig A. E., Demopoulos A. W. J., Batista, F. C.,, Kocar B. D., Selby D., McCarthy M. D. and Mienis F. (2014) Deep-sea coral record of human impact on watershed quality in the Mississippi River Basin. Global Biogeochemical Cycles.

Ren H., Sigman D. M., Meckler A. N., Plessen B., Robinson R. S., Rosenthal Y. and Haug G. H. (2009) Foraminiferal Isotope Evidence of Reduced Nitrogen Fixation in the Ice Age Atlantic Ocean. Science 323(5911): 244-248.

Robinson R. S., Brunelle B. G. and Sigman D. M. (2004) Revisiting nutrient utilization in the glacial Antarctic: Evidence from a new method for diatom-bound N isotopic analysis. Paleoceanography 19(3).

Robinson R. S., Kienast M., Albuquerque A. L., Altabet M., Contreras S., Holz R. D., Dubois N., Francois R., Galbraith E., Hsu T. C., Ivanochko T., Jaccard S., Kao S. J., Kiefer T., Kienast S., Lehmann M., Martinez P., McCarthy M., Mobius J., Pedersen T., Quan T. M., Ryabenko E., Schmittner A., Schneider R., Schneider-Mor A., Shigemitsu M., Sinclair D., Somes C., Studer A., Thunell R. and Yang J. Y. (2012) A review of nitrogen isotopic alteration in marine sediments. Paleoceanography 27: 13.

Roland L. A., McCarthy M. D. and Guilderson T. (2008) Sources of molecularly uncharacterized organic carbon in sinking particles from three ocean basins: A coupled Delta C-14 and delta C-13 approach. Marine Chemistry 111(3-4): 199-213.

Rykaczewski R. R. and Dunne J. P. (2010) Enhanced nutrient supply to the California Current Ecosystem with global warming and increased stratification in an earth system model. Geophysical Research Letters 37.

Sachs J. P. and Repeta D. J. (1999) Oligotrophy and nitrogen fixation during eastern Mediterranean sapropel events. Science 286(5449): 2485-2488.

Schmidt K., McClelland J. W., Mente E., Montoya J. P., Atkinson A. and Voss M. (2004) Trophic-level interpretation based on delta N-15 values: implications of tissue-specific fractionation and amino acid composition. Marine Ecology-Progress Series 266: 43-58.

Sherwood O. A., Guilderson T. P., Batista F. C., Schiff J. T. and McCarthy M. D. (2014) Increasing subtropical North Pacific Ocean nitrogen fixation since the Little Ice Age. Nature 505(7481): 78-+.

Sherwood O. A., Lehmann M. F., Schubert C. J., Scott D. B. and McCarthy M. D. (2011) Nutrient regime shift in the western North Atlantic indicated by compound-specific delta N-15 of deep-sea gorgonian corals. Proceedings of the National Academy of Sciences of the United States of America 108(3): 1011-1015.

Sigman D. M., Granger J., DiFiore P. J., Lehmann M. M., Ho R., Cane G. and van Geen A. (2005) Coupled nitrogen and oxygen isotope measurements of nitrate along the eastern North Pacific margin. Global Biogeochemical Cycles 19(4).

Sigman D. M., Robinson R., Knapp A. N., van Geen A., McCorkle D. C., Brandes J. A. and Thunell R. C. (2003) Distinguishing between water column and sedimentary denitrification in the Santa Barbara Basin using the stable isotopes of nitrate. Geochemistry Geophysics Geosystems 4.

Silfer J. A., Engel M. H., Macko S. A. and Jumeau E. J. (1991) Stable carbon isotope analysis of amino-acid enantiomers by conventional isotope ratio mass-spectrometry and combined gas-chromatography isotope ratio mass-spectrometry. Analytical Chemistry 63(4): 370-374.

Takano Y., Kashiyama Y., Ogawa N. O., Chikaraishi Y. and Ohkouchi N. (2010) Isolation and desalting with cation-exchange chromatography for compound-specific nitrogen isotope analysis of amino acids: application to biogeochemical samples. Rapid Communications in Mass Spectrometry 24(16): 2317-2323.

Thunell R. C. (1998) Particle fluxes in a coastal upwelling zone: sediment trap results from Santa Barbara Basin, California. Deep-Sea Research Part Ii-Topical Studies in Oceanography 45(8-9): 1863-1884.

Thunell R. C., Tappa E. and Anderson D. M. (1995) Sediment fluxes and varve fomation in Santa Barbara Basin, offshore California. Geology 23(12): 1083-1086.

Veuger B., Middelburg J. J., Boschker H. T. S. and Houtekamer M. (2005) Analysis of N-15 incorporation into D-alanine: A new method for tracing nitrogen uptake by bacteria. Limnology and Oceanography-Methods 3: 230-240.

Wakeham S. G., Lee C., Hedges J. I., Hernes P. J. and Peterson M. L. (1997) Molecular indicators of diagenetic status in marine organic matter. Geochimica Et Cosmochimica Acta 61(24).

Werner R. A. and Schmidt H. L. (2002) The in vivo nitrogen isotope discrimination among organic plant compounds. Phytochemistry 61(5): 465-484.

**Figure 1.1 $\delta^{15}N_{AA}$ values in water column (plankton tow vs. sinking POM) vs. sedimentary OM from SBB.**

As noted in text, AA are arranged by "Source" (Ala to Val), "Trophic" (Gly to Tyr), and "Metabolic" (Thr) groupings now common in the literature. (a) Water column OM: a single mixed tow (>30μm, 30m) (circles) and 1-year N flux-weighted sediment trap composite (diamonds); (b) values from 13 sediment intervals of 40 cm multicore; and (c) normalized comparison of all three sample types. $\delta^{15}N_{THAA}$ values are normalized to total hydrolysable amino acids (THAA; $\Delta\delta^{15}N_{AA-THAA}$) to allow direct comparison of relative $\delta^{15}N_{AA}$ patterns. Vertical bars in (a) represent mixed tow and trap sample standard deviations of replicate $\delta^{15}N$ analyses (n ≥ 3). In (b) specific analytical errors are not shown for clarity, however standard deviation for individual AA measurements averaged 1.1‰ (see Electronic Annex Table EA 1.1). In (c) vertical bars indicate propagated analytical errors from replicate analysis of individual $\delta^{15}N_{AA}$ and $\delta^{15}N_{THAA}$ for the mixed tow and trap sample, and represent the average propagated analytical error for all sediment samples.
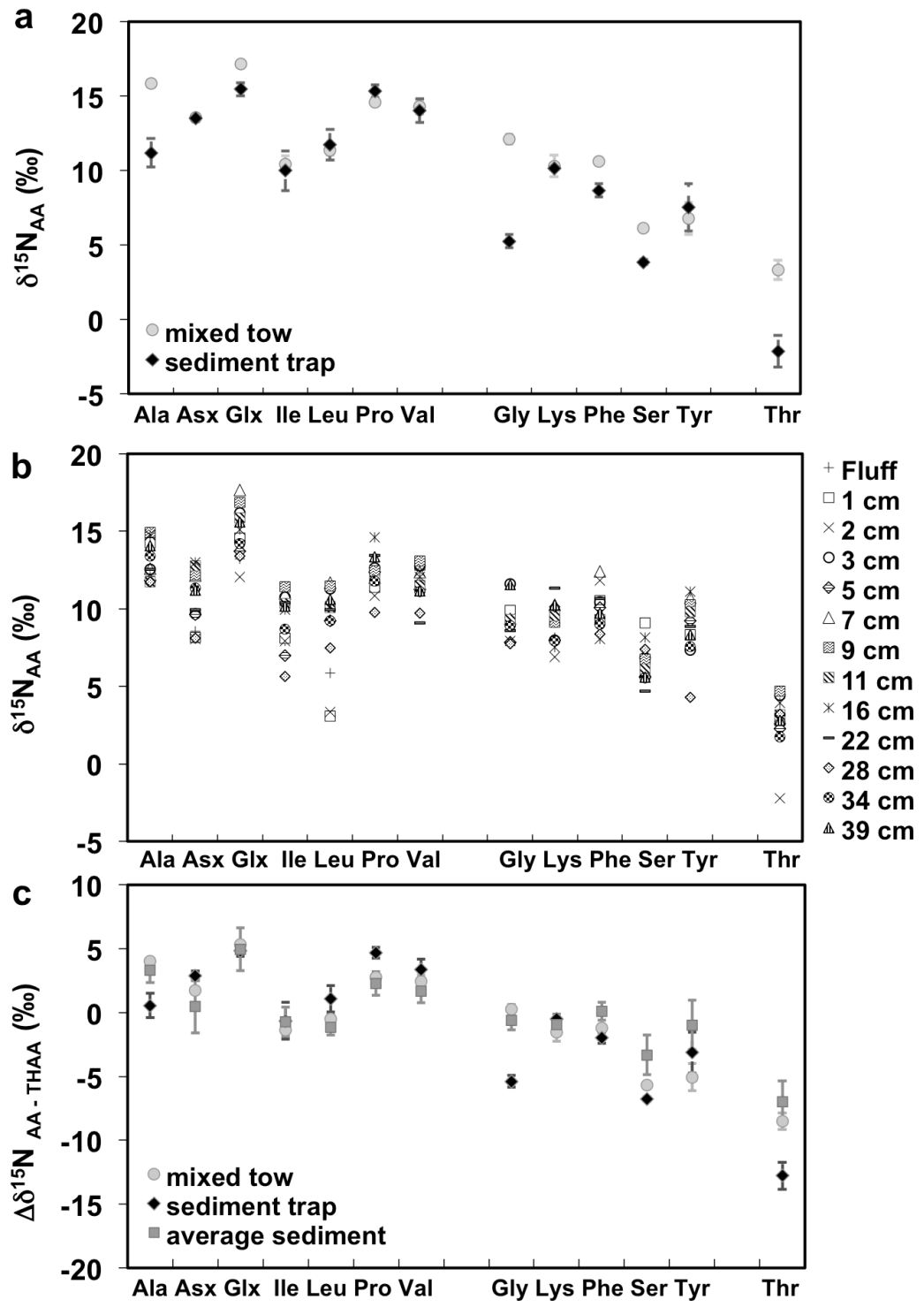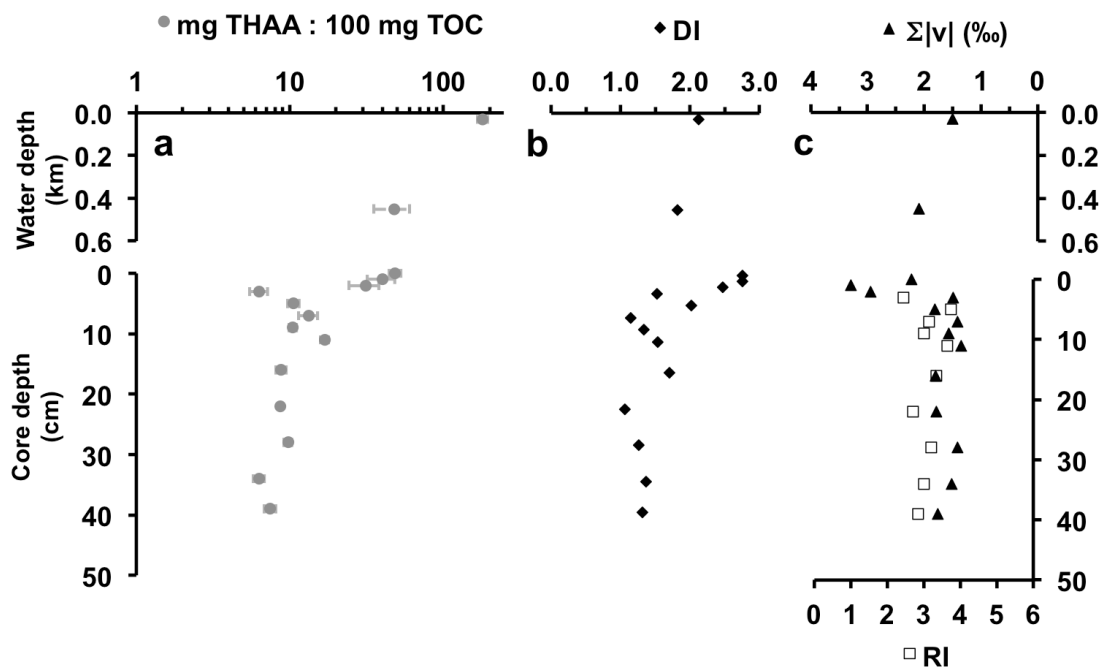
**Figure 1.2 Amino acid diagenetic indicators in water column and sediments.**
Water column samples are shown on upper axis, and multicore sediment values are
shown on lower axis for (a) total hydrolyzable amino acids (THAA), expressed as mg
THAA per 100 mg OC (after Cowie and Hedges, 1994); (b) the degradation index
(DI) (e.g., Dauwe et al., 1999); (c) the reactivity index (RI) (e.g., Jennerjahn and
Ittekkot, 1997) and ΣV (McCarthy et al., 2007; as defined in Materials and Methods).
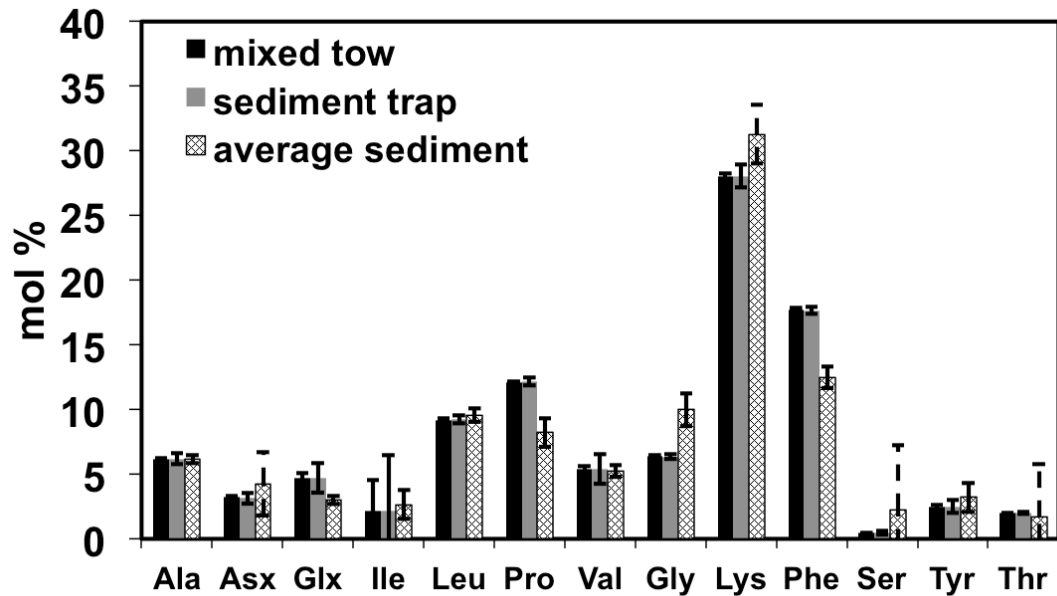
**Figure 1.3 Average amino acid composition for plankton, sediment trap, and sediment samples.**
For plankton, error bars indicate standard deviation of replicate analyses for a single tow; for traps, error bars indicate standard deviation of replicate analyses for a single 1 yr flux-weighted composite sample; for sediments error bars represent standard deviation of all multicore intervals analyzed (n=13).
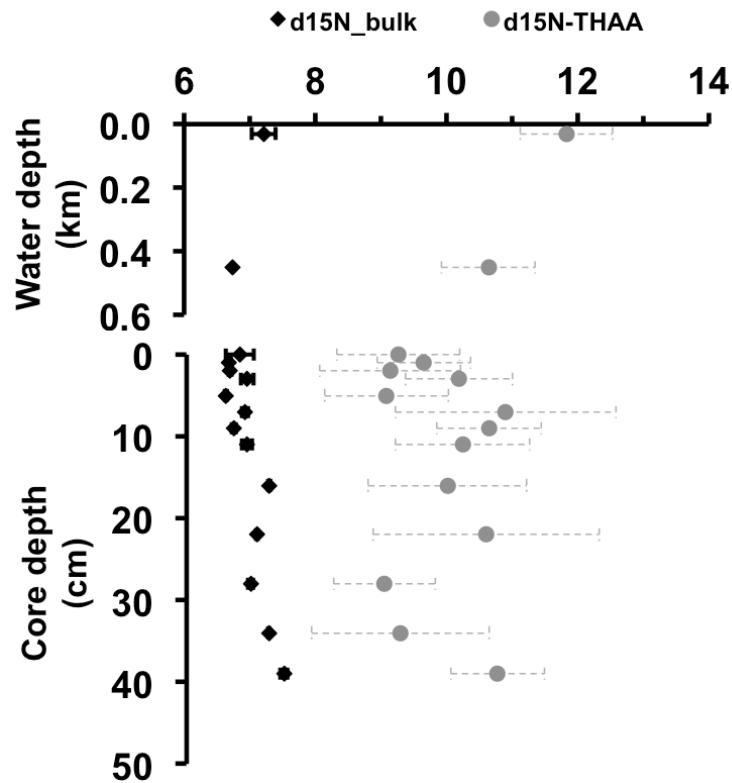
**Figure 1.4 $\delta^{15}N_{bulk}$ and $\delta^{15}N_{THAA}$ in water column and sedimentary samples.** Top axis: plankton tow and sinking POM, bottom axis: multicore sediment intervals. As defined in text (*methods*), $\delta^{15}N_{bulk}$ represents $\delta^{15}N$ measurement on total N in sample, while $\delta^{15}N_{THAA}$ is a proxy for $\delta^{15}N$ value of the total hydrolyzable amino acid pool.
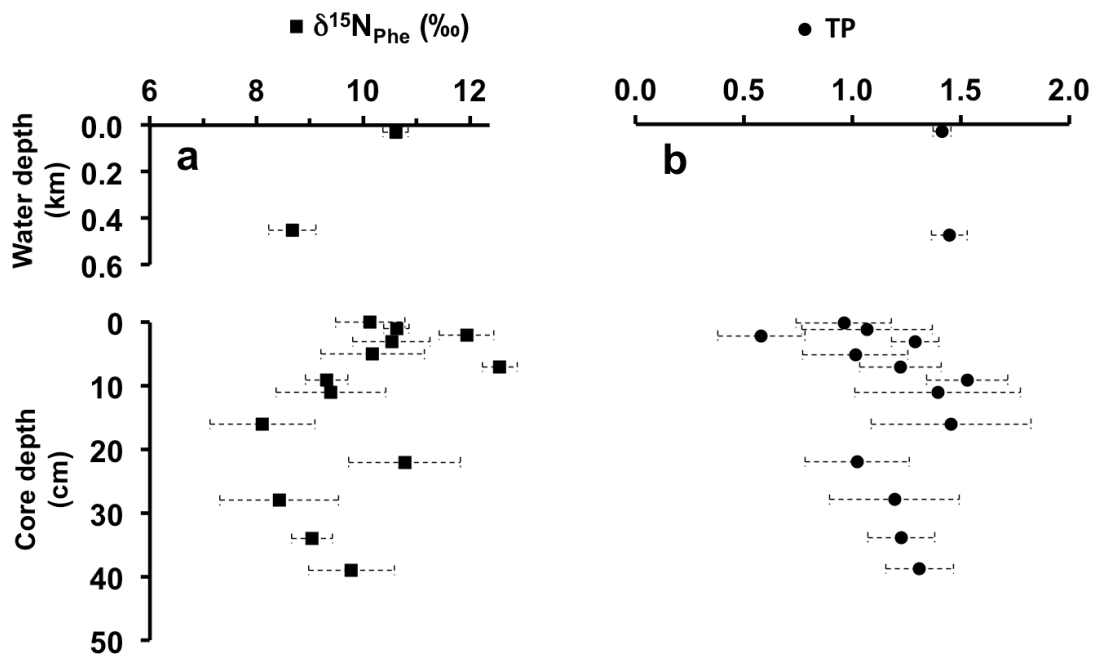
**Figure 1.5 Comparison of $\delta^{15}N_{Phe}$ and trophic position (TP) in water column POM and multicore sediment samples.**

An inverse relationship of TP vs. $\delta^{15}N_{Phe}$ is significant at the 95% confidence interval (Pearson's $r$=-0.56, $p$=0.029, n=15). This suggests interdependence between $\delta^{15}N_{Phe}$ values and planktonic ecosystem TP over timescales of sedimentary accumulation.
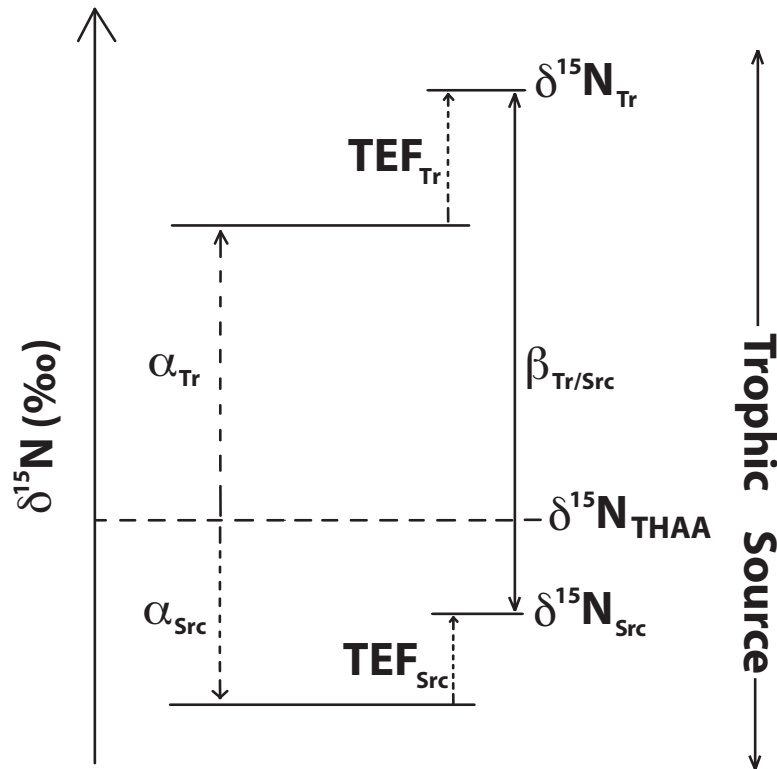
**Figure 1.6 Conceptual diagram showing main assumptions underlying the isotope mass balance model of amino acid $\delta^{15}N$ values and trophic position.** Y-axis is the relative $\delta^{15}N$ value, referenced to $\delta^{15}N$ value of total AA pool ($\delta^{15}N_{THAA}$; dashed horizontal line). Trophic AA (Tr) by definition have $\delta^{15}N$ values above this line, while Source AA (Src) have $\delta^{15}N$ values below. $\delta^{15}N$ offsets of average Tr AA ($\delta^{15}N_{Tr}$) and average Src AA ($\delta^{15}N_{Src}$) values from the total AA pool (i.e., $\delta^{15}N_{THAA}$) in autotrophs are indicated by $\alpha$ values (see Equations 6-9, Section 3.3.2). The changing offset between $\delta^{15}N_{Tr}$ and $\delta^{15}N_{Src}$ (or $\beta_{Tr/Src}$, connected by a solid double arrow line) then reflects the combined effects of the original offsets in primary producers, $\alpha$, combined with a relative $\delta^{15}N$ change of AA groups with each progressive trophic transfer (trophic enrichment factor; TEF). At steady state, if $\delta^{15}N_{THAA}$ is assumed to be constant, than both $\delta^{15}N_{Tr}$ and $\delta^{15}N_{Src}$ values are inherently dependent on the degree of trophic transfer (or trophic position).
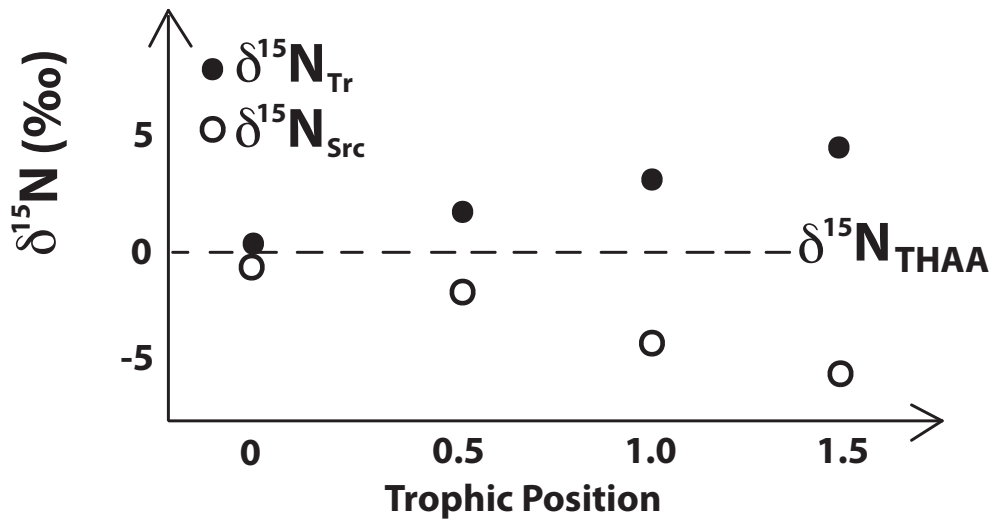
**Figure 1.7 Isotope mass balance model output showing $\delta^{15}N_{Tr}$ and $\delta^{15}N_{Src}$ values as a function of trophic position.**
Y-axis indicates relative $\delta^{15}N$ values ($\delta^{15}N$ value for the total THAA pool, $\delta^{15}N_{THAA}$, is arbitrarily set at zero). Trophic positions (0.5 to 1.5) span total range observed in SBB sediments. The slopes of the $\delta^{15}N_{Tr}$ and $\delta^{15}N_{Src}$ output are the average TEF values for each AA group.
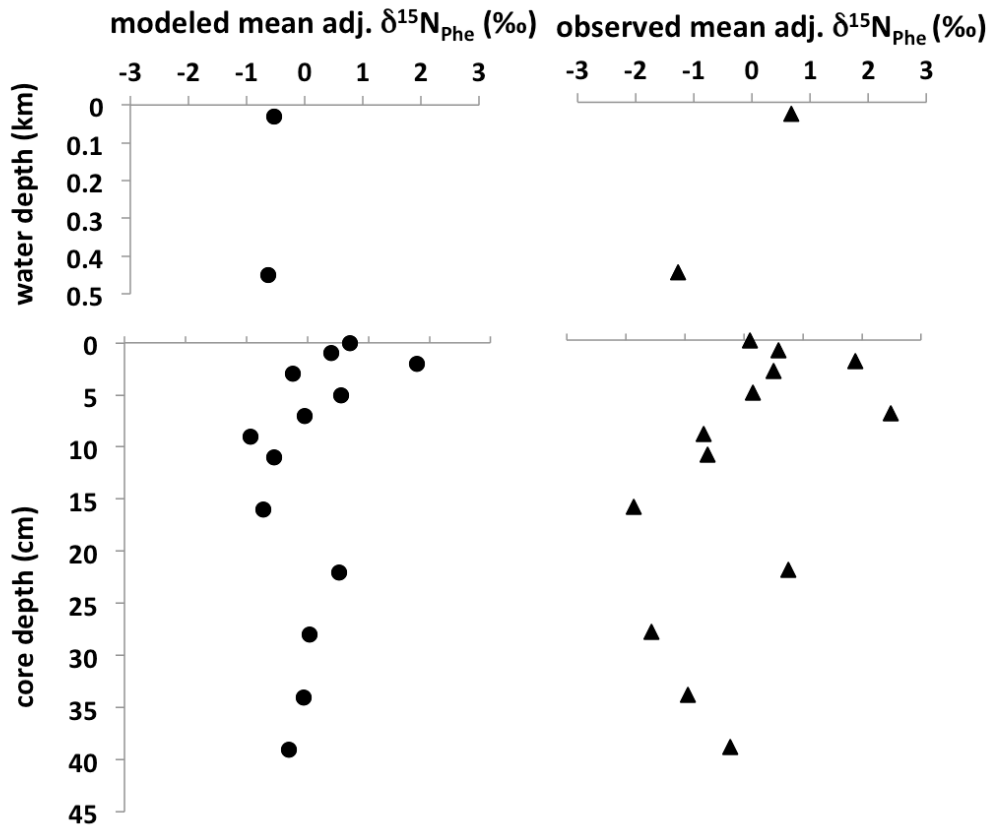
**Figure 1.8 Comparison of measured $\delta^{15}N_{Phe}$ values with isotope mass balance model predicted $\delta^{15}N_{Phe}$.**
Water column (top panels) and downcore (bottom panels) values of the mean adjusted $\delta^{15}N_{Phe}$ values from model output (left side), are compared with SBB sedimentary measurements (right). As detailed in text (*Section* 3.3.2), modeled $\delta^{15}N_{Phe}$ values are a function of trophic position.
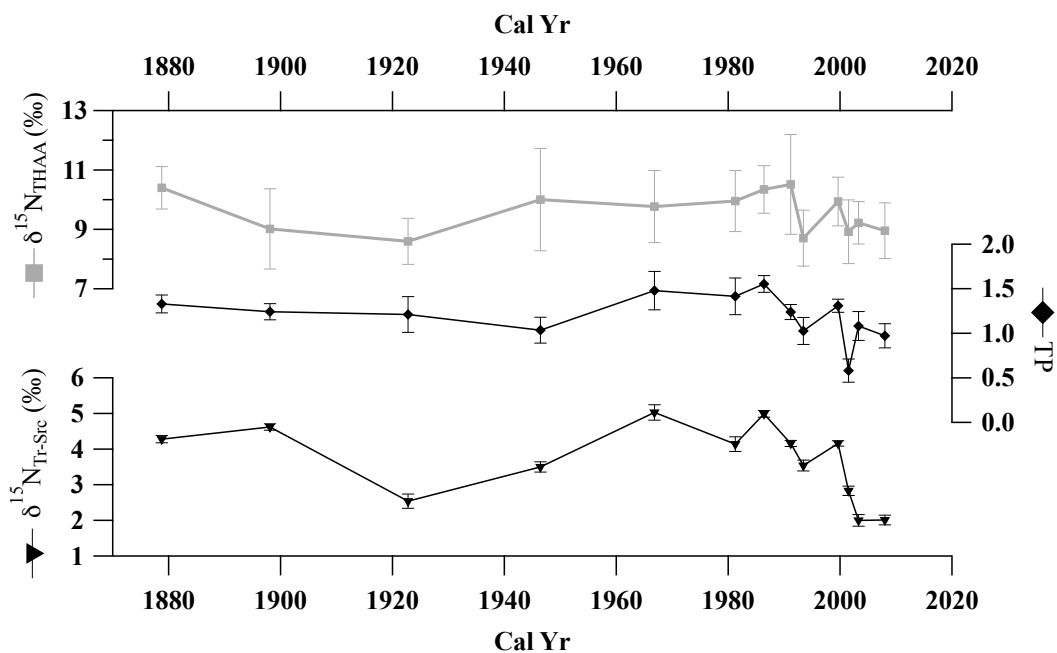
**Figure 1.9 The sedimentary record of CSI-AA parameters in SBB since ca. 1880.**
$\delta^{15}N_{THAA}$ (the $\delta^{15}N$ value of total proteinaceous material), trophic position ($TP_{Glu/Phe}$)
explicitly estimated after Chikaraishi et al. (2009) and $\delta^{15}N_{Tr-Src}$ (the offset between
$\delta^{15}N_{Tr}$ and $\delta^{15}N_{Src}$, an analogous measure of trophic enrichment) are as defined in text
(*Methods; Section 2.6*). Vertical bars for $\delta^{15}N_{THAA}$, TP, and $\delta^{15}N_{Tr-Src}$ represent
propagated analytical error for calculated parameters.

**Table 1.1 Mean $\Delta\delta^{15}N_{THAA-bulk}$ values and regression statistics for $\delta^{15}N_{AA}$ vs $\delta^{15}N_{bulk}$ for published data sets.**

| Sample type | n | $\Delta\delta^{15}N_{THAA-bulk}$ (‰) | slope | y-int | $r^2$ | p | Reference |
|---|---|---|---|---|---|---|---|
| autotrophs, bacteria | 6 | $3.5 \pm 0.3$ | 1.0 | 3.5 | 1.0 | 1.2E-06 | Macko et al., 1987 |
| bacteria | 2 | $2.3 \pm 0.9$ | 1.3 | 3.3 | 1.0 | 0.24 | Pan et al., 2008 |
| autotrophs, bacteria | 7 | $2.5 \pm 3.0$ | 0.9 | 1.7 | 0.9 | 0.09 | McCarthy et al., 2013 |
| mixed tow | 1 | 4.6 | | | | | this study |
| sediment trap | 1 | 3.9 | | | | | this study |
| sediment | 13 | $2.9 \pm 0.6$ | 0.9 | 3.4 | 0.1 | 1.5E-09 | this study |

**Electronic Annex**

**Description of amino acid hydrolysis, purification and derivatization for CSIA**

Samples were acid hydrolyzed using 6 N HCl for 20 hr at 110 °C, then hydrolysates were diluted to ~1 N HCl and filtered to remove particulates. The AA fraction was purified from filtered hydrolysates by cation-exchange chromatography using Dowex 50W-X8 resin (100-200 mesh, proton form). Resin was conditioned by sequentially rinsing with 2 to 3 times the resin bed volume of $NH_4OH$ (2 N), Milli-Q, and HCl (2 N). Hydrolysates (adjusted to ca. 1 N HCl) were loaded onto columns three times, while salts and other organic contaminants are not retained. Following three rinses with Milli-Q grade water (5 mL), AA were eluted with three rinses of 2 N $NH_4OH$ (5 mL), and evaporated to dryness under a stream of $N_2$. Purified AA were redissolved in 0.1 N HCl (1 mL) and protonated by heating in a 60° C water bath (5 mins), then evaporated to dryness under a stream of $N_2$ in preparation for derivatization to TFA isopropyl esters (IPA-TFAA) based on the protocol by Silfer et al. (1991). Detailed descriptions of derivative protocols have been previously described (McCarthy et al., 2007; Calleja et al., 2013; McCarthy et al., 2013).

The N isotopic composition of individual AA ($\delta^{15}N_{AA}$) by gas chromatography continuous flow isotope ratio mass spectrometry (GC-IRMS) and associated chromatographic conditions were previously published (Sherwood et al., 2014). Briefly, a 1 µL aliquot of each sample was injected and analyzed for $\delta^{15}N_{AA}$ in quadruplicate, with an associated average standard deviation for $\delta^{15}N$ analyses of

each AA of 1.1‰, ranging from 0.1‰ to 4.7‰ (mean and standard deviations of $\delta^{15}N_{AA}$ given in Table EA-1).

The AA mole percent (mol%$_{AA}$) composition of samples was analyzed with an Agilent 7890A GC coupled to a 7683B MSD based on external AA stds. The chromatography column and chromatographic conditions were identical to those used for $\delta^{15}N_{AA}$ analysis, described by Sherwood et al. (2013). We verified the linearity of response factors (area/nMol on column) for characteristic ions of the IPA-TFAA derivative for each AA of our external standard mixture of 16 AA, from repeated injections (n ≥ 3). Response factors for each AA were found to be strongly linear at four different concentrations over 3 orders of magnitude (nM to μM), well beyond the range of our sample concentrations. Further, AA recoveries from the column cleanup and extraction steps were independently tested during method development, and found to be essentially quantitative (average AA recovery >95%). Finally, we verified that laboratory internal reference materials (Cyanobacteria and Monterey Bay surface sediment) yield identical mol% values within error when analyzed independently by a previously published HPLC protocol (Broek et al., 2013).
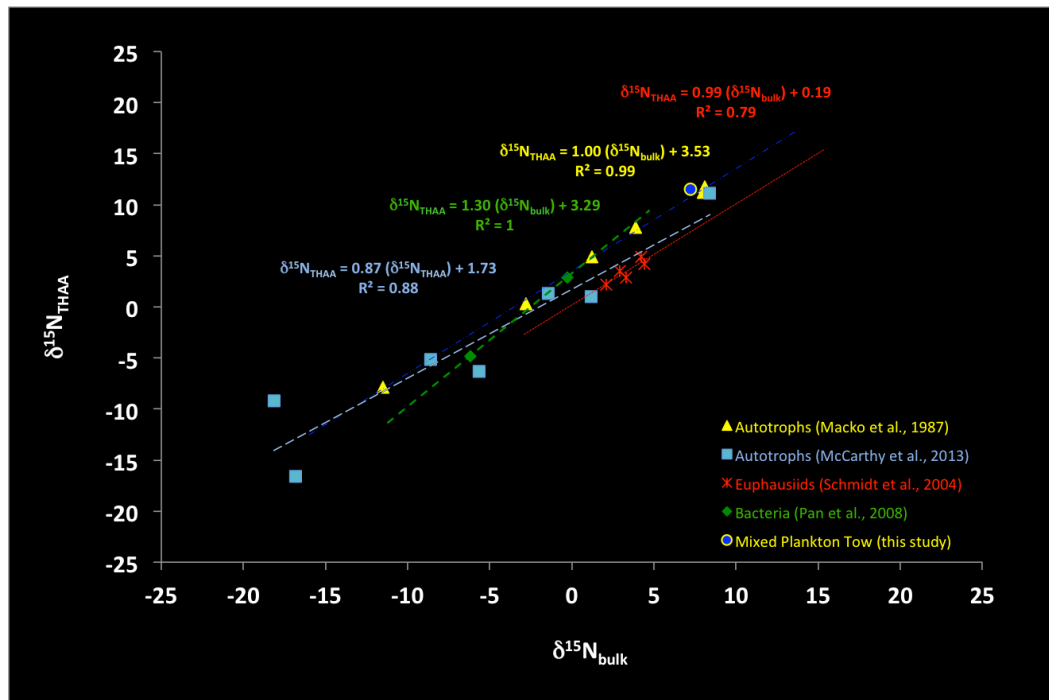
**Figure EA-1-1. Regressions of $\delta^{15}N_{bulk}$ vs. $\delta^{15}N_{THAA}$ for autotrophs and zooplankton compiled from published data and the SBB mixed tow.**
The y-intercept from these regressions ($\Delta\delta^{15}N_{THAA-bulk}$) for autotrophs bracket the $\Delta\delta^{15}N_{THAA-bulk}$ for all SBB samples (see text, Ch. 1, section 3.3.1).

**Table EA-1-1. Individual $\delta^{15}N_{AA}$ values and standard deviations for replicate analyses (n$\geq$3) for each sample.**

| Sample | Depth | ALA | ASP | GLU | ILE | LEU | PRO | VAL | GLY | LYS | PHE | SER | TYR | THR | THAA |
|---|---|---|---|---|---|---|---|---|---|---|---|---|---|---|---|
| mixed tow | 30 m | 15.8±0.2 | 13.6±0.2 | 17.1±0.2 | 10.4±0.5 | 11.3±0.3 | 14.6±0.2 | 14.3±0.5 | 12.1±0.3 | 10.3±0.7 | 10.6±0.2 | 6.1±0.1 | 6.8±1.1 | 3.3±0.6 | 11.9±0.7 |
| sediment trap | 450 m | 11.2±1 | 13.5±0.2 | 15.5±0.4 | 10±1.3 | 11.7±1 | 15.3±0.4 | 14±0.8 | 5.2±0.4 | 10.2±0.1 | 8.7±0.4 | 3.9±0.2 | 7.5±1.6 | -2.1±1.1 | 10.3±0.7 |
| multicore | 0 cm | 12.1±1.9 | 8.6±2.6 | 13.2±1.6 | 7.9±1.8 | 5.8±0.3 | 11.7±1 | 11.1±1.5 | 8.9±0.6 | 8.1±0.8 | 10±0.6 | 6.8±2.9 | 9.8±1.7 | 4.6±1.4 | 9±0.9 |
| | 1 cm | 14.2±0.7 | 8.1±1.2 | 14.6±2.3 | 8.1±1 | 3.1±0.4 | 11.4±0.7 | 12.8±0.3 | 9.9±0.3 | 9.3±0.6 | 10.5±0.2 | 9.1±0.6 | 8.3±1.5 | 2.9±0.4 | 9.2±0.7 |
| | 2 cm | 14.8±1.1 | 8±2.8 | 12±1.5 | 7.9±2.1 | 3.4±0.6 | 10.8±1.4 | 12.4±0.5 | 9.4±0.4 | 6.9±1.3 | 11.8±0.5 | 6.6±1.4 | 10±1.5 | -2.2±0.9 | 8.9±1.1 |
| | 3 cm | 12.6±0.5 | 9.7±4.7 | 16.2±0.5 | 10.7±1.1 | 11.3±1 | 12.6±1 | 12.8±0.7 | 11.6±0.4 | 8±0.5 | 10.4±0.7 | 6.8±1.2 | 7.4±3 | 4.4±1.5 | 9.9±0.8 |
| | 5 cm | 11.8±1.4 | 9.6±3.9 | 13.7±1.6 | 7±1.1 | 9.2±0.3 | 12.4±1.3 | 11.2±0.4 | 7.8±0.8 | 8±0.7 | 10.1±1 | 5.6±1.4 | 9.2±2 | 2.3±1 | 8.7±0.9 |
| | 7 cm | 12.6±0.8 | 12.1±2.7 | 17.6±1.4 | 11±0.7 | 11.7±0.6 | 12±0.9 | 12.4±1.2 | 9.4±1.5 | 10.2±0.8 | 12.4±0.3 | 6±0.6 | 10.7±0.6 | 2.9±1.1 | 10.5±1.7 |
| | 9 cm | 14.9±0.5 | 12.2±2.1 | 16.9±1.4 | 11.4±0.5 | 11.5±0.6 | 12.4±0.3 | 13.1±0.3 | 9.2±0.5 | 9.2±0.6 | 9.3±0.4 | 6.8±0.6 | 10.3±2.8 | 4.7±1.4 | 10.3±0.8 |
| | 11 cm | 11.7±0.4 | 12.8±0.7 | 15.9±2.8 | 10.3±1.1 | 10.1±0.7 | 11.8±0.3 | 11.5±0.7 | 9.3±0.5 | 9.5±0.8 | 9.3±1 | 6.1±1.3 | 9.8±0.8 | 3.2±2.4 | 10±1 |
| | 16 cm | 14.8±1 | 13±0.9 | 15.1±2.7 | 9.9±1.2 | 10.2±0.9 | 14.6±0.8 | 12.1±1.6 | 7.9±1.1 | 7.5±1.4 | 8.1±1 | 8.1±2.8 | 11.1±4.1 | 3.9±0.9 | 9.8±1.2 |
| | 22 cm | 12.6±1.4 | 9.9±0.7 | 14.3±1.6 | 10.4±0.9 | 9.9±0.7 | 13.5±0.8 | 9.1±0.2 | 8.6±0.9 | 11.3±1.1 | 10.7±1 | 4.7±3.3 | 8.9±1.9 | 3.2±1.9 | 10±1.7 |
| | 28 cm | 11.7±1.1 | 8.1±2.2 | 13.4±2 | 5.6±0.7 | 7.5±0.9 | 9.8±1.9 | 9.7±1.7 | 7.7±0.6 | 10.1±0.3 | 8.4±1.1 | 7.4±1.4 | 4.3±1.6 | 3.2±1.8 | 8.6±0.8 |
| | 34 cm | 13.4±0.8 | 11.3±1.6 | 14.2±1.1 | 8.7±1.1 | 9.2±0.3 | 11.8±0.7 | 11.1±1.2 | 8.9±1.3 | 7.9±1.4 | 9±0.4 | 5.6±1 | 7.6±2.1 | 1.7±2.4 | 9±1.4 |
| | 39 cm | 14.1±0.7 | 11.2±0.8 | 15.6±0.9 | 10.2±1.3 | 10.6±0.7 | 13.4±1.1 | 11.1±1.6 | 11.5±0.2 | 10.2±0.4 | 9.7±0.8 | 5.6±1.4 | 8.3±1.3 | 2.8±1.8 | 10.4±0.7 |

**Table EA-1-2.  Minimum, maximum, mean, median and $\sigma^{*}$ for $\delta^{15}N_{AA}$ of all AA, source and trophic AA grouped by sample type.**

| | min (‰) | max (‰) | mean (‰) | median (‰) | σ (‰) |
|---|---|---|---|---|---|
| All $\delta^{15}N_{AA}$ | | | | | |
| Mixed tow | 3.3 | 17.1 | 11.3 | 15.2 | 3.9 |
| Sediment trap | -2.1 | 15.5 | 9.6 | 12.8 | 4.8 |
| Multicore | -2.2 | 17.6 | 9.7 | 10.6 | 3.3 |
| $\delta^{15}N_{Src}$ | | | | | |
| Mixed tow | 6.1 | 12.1 | 9.2 | 10.3 | 2.3 |
| Sediment trap | 3.9 | 10.2 | 7.1 | 10.3 | 2.3 |
| Multicore | 4.3 | 12.4 | 8.7 | 10.8 | 1.8 |
| $\delta^{15}N_{Tr}$ | | | | | |
| Mixed tow | 10.4 | 17.1 | 13.9 | 11.3 | 2.2 |
| Sediment trap | 10.0 | 15.5 | 13.0 | 13.0 | 2.0 |
| Multicore | 3.1 | 17.6 | 11.4 | 12.0 | 2.6 |

[*]$\sigma$ here represents a measure of the distribution of measured $\delta^{15}N_{AA}$ within each category.

**Table EA-1-3. Parameters applied in the amino acid N isotope mass balance model based on Equations 6 to 9.**

| Parameter | Value |
|-----------|-------|
| $f_{THAA}$ | 1 |
| $f_{Tr}{}^{a}$ | 0.54 |
| $f_{Src}{}^{a}$ | 0.46 |
| $\alpha_{Src}{}^{b}$ | -2.7 ± 1.6‰ |
| $\alpha_{Tr}{}^{b}$ | 1.3 ± 1.7‰ |
| $TEF_{Src}{}^{c}$ | 0.37 ± 0.28‰ |
| $TEF_{Tr}{}^{c}$ | 4.42 ± 0.06‰ |
| $\varepsilon_{Gly-Phe}{}^{d}$ | 1.4 ± 0.6‰ |
| $\varepsilon_{Lys-Phe}{}^{d}$ | 3.1 ± 1.4‰ |
| $\varepsilon_{Met-Phe}{}^{d}$ | -2.07 ± 0.06‰ |
| $\varepsilon_{Ser-Phe}{}^{d}$ | -2.9 ± 0.6‰ |
| $\varepsilon_{Tyr-Phe}{}^{d}$ | 1.0 ± 1.7‰ |
| $f_{Gly}{}^{e}$ | 0.28 |
| $f_{Lys}{}^{e}$ | 0.45 |
| $f_{Met}{}^{e}$ | 0.03 |
| $f_{Phe}{}^{e}$ | 0.13 |
| $f_{Ser}{}^{e}$ | 0.03 |
| $f_{Tyr}{}^{e}$ | 0.08 |

a. Ratio of mol% of Tr and Src AA groups based on seven Tr (Ala, Asx, Glx, Ile, Leu, Pro, Val) and six (Gly, Lys, Met, Phe, Ser, Tyr) Src AA from the SBB mixed plankton tow sample.
b. The average $\delta^{15}N$ offsets of Tr and Src AA groups from literature data (McClelland et al., 2002, 2003; McCarthy et al., 2013; Chikaraishi et al., 2007, 2009) relative to estimated values of $\delta^{15}N_{THAA}$ (equation 1) using average mol% AA values from Cowie and Hedges (1992).
c. The average trophic enrichment factor (TEF) based on the mean $\delta^{15}N$ offsets of all Tr ($TEF_{Tr}$) or Src ($TEF_{Src}$) AA between consumer and diet in literature data from feeding studies (McClelland et al., 2002, 2003; Chikaraishi et al., 2007, 2009).
d. The average $\delta^{15}N$ offset of each Src AA (e.g., Gly, Lys, Met, Ser, Tyr) from Phe in autotrophic organisms from literature data (McClelland et al., 2002, 2003; McCarthy et al., 2013; Chikaraishi et al., 2007, 2009).
e. Mole fraction of Src AA (e.g., Gly, Lys, Met, Ser, Tyr, Phe) from SBB mixed plankton tow in this work.

CHAPTER TWO

---

# Sources of labile vs. refractory organic nitrogen in marine sediments: A coupled elemental and stable isotopic perspective from Santa Barbara Basin

Fabian C. Batista[1], A. Christina Ravelo[1], Carsten J. Schubert[2], Matthew D. McCarthy[1]

[1] Ocean Sciences Department, University of California, Santa Cruz

[2]Eawag, Swiss Federal Institute of Aquatic Science and Technology

*In all affairs it's a healthy thing now and then to hang a question mark on the things you have long taken for granted.*
— Bertrand Russell

*We are trying to prove ourselves wrong as quickly as possible, because only in that way can we find progress.*
— Richard Feynman

ABSTRACT

Understanding the formation and molecular composition of marine sedimentary organic matter is challenged by the transformations of surface-derived organic matter during its transit to the seafloor. These transformations, as revealed by standard wet-chemical techniques, include an increase of a molecular uncharacterized component (MUC) at the expense of identifiable biochemicals. Recent work coupling wet-chemical hydrolytic-based separations of refractory and labile components of organic matter with stable and radioisotope analysis of organic carbon, has confirmed the acid-insoluble (AI) fraction to be a direct proxy for MUC, while the acid-soluble (AS) fraction mostly represents the sum of labile biochemical classes. Therefore, isotopic measurement on these fractions represents a powerful way to investigate sources of MUC in the absence of molecular level data. To our knowledge, this approach has never focused on organic nitrogen (ON).

Past spectroscopic analysis of hydrolytic separations of recently buried sedimentary organic matter indicated proteinaceous material dominates ON in bulk, AS and AI fractions; suggesting that the $\delta^{15}N$ value of total hydrolysable proteinaceous material should provide a good proxy for the $\delta^{15}N$ value of total sedimentary ON. However, this framework has been called into question with the first marine $\delta^{15}N$ measurements on individual amino acids from highly preserved marine sediments, which showed strong offsets in $\delta^{15}N$ between total hydrolysable amino acids (THAA) and total nitrogen (TN), $\Delta\delta^{15}N_{THAA-TN} \sim 3\text{-}5\text{‰}$ (Batista et al., 2014). Here is a first attempt to combine quantitative N yields and $\delta^{15}N$

78

measurements of major fractions from highly preserved, organic matter-rich marine sediments, including AS, AI, THAA, lipid and clay-bound components, with an overarching goal to constrain sources, molecular character and relative $\delta^{15}N$ values of these sedimentary N pools.

A significant diversity in $\delta^{15}N$ values of sedimentary ON fractions was observed, suggesting substantial diversity in either biochemical makeup, and/or partitioning, of sedimentary nitrogenous compounds. $\delta^{15}N$ values of THAA were higher than AS by 2-4‰ and 5-7‰ higher than AI, suggesting that non-proteinaceous compounds are important components of both AS and AI fractions. Consistent $\delta^{15}N$ offsets observed between fractions in the water column and sediments, strongly suggests that preservation of non-proteinaceous like ON, likely originates from primary production. These findings are contrary to existing nitrogen based spectroscopic evidence. Our data for the AI fraction is consistent with this material representing the most refractory ON in sediments, and so is perhaps of most interest for understanding what controls the long-term removal of organic nitrogen from the oceans. Our results suggest that total sedimentary ON $\delta^{15}N$ values are likely strongly dependent on the relative contributions of AS and AI operational fractions, which may have different water column sources of proteinaceous vs. non-proteinaceous nitrogenous compounds. We suggest that a main goal for future work should be to devise approaches which can reveal the nature of non-proteinaceous ON, in particular in the refractory (AI) fraction.

**Introduction**

A major longstanding problem in marine organic geochemistry is to understand the formation and molecular composition of organic matter (OM) preserved in sediments. Sinking particulate organic matter (POM) is the main source for organic carbon and nitrogen delivered to the sea floor, however globally only approximately 10 % of export production reaches the sediment-water interface, and less than 1% is ultimately preserved during long-term burial (e.g., Hedges, 1992). This enormous attenuation of OM between algal source and sedimentary preservation leaves enormous latitude for compositional change. Understanding the processes which control molecular transformation of specific sources to ultimate burial is therefore essential to a mechanistic understanding of the global biogeochemical cycles of carbon (C) and nitrogen (N), as well as for interpreting the sedimentary record. However, the details of such organic compositional changes and their mechanistic underpinning remain elusive.

A main challenge is that, once surface-derived OM transits the mesopelagic "twilight zone", very little organic material can be identified at the molecular level (e.g., Lee, 2004). The biochemical composition of marine OM, as revealed by standard wet-chemical techniques, has repeatedly shown a progressive decrease in identifiable biochemicals with depth and increasing degradation (Wakeham et al., 1997), and a concomitant increase in the "molecularly uncharacterized component" (MUC). MUC is an operational concept, broadly defined as all organic material that remains after major biochemical classes have been accounted for. These major

biochemicals are typically comprised of total hydrolysable amino acids (THAA), total

carbohydrates (TCHO), and total extractable lipids and pigments (Hedges 2000;

Hedges et al., 2001). By this definition, MUC in plankton is generally small (~15%

of organic carbon), however in deep sinking POM and surface sediments it accounts

for almost all (~75% - 80%) of the organic matter (c.f., Hedges, 1992; Wakeham et

al., 1997; Hedges, 2000). Put another way, less than 20% of organic carbon

preserved in sediments can typically be identified with standard molecular-level

techniques.

Because MUC in sediments is outside the analytical window of molecular-level

analyses, spectroscopic and isotopic approaches have provided most information

about source, transformation, and functional group composition. Solid-state nuclear

magnetic resonance (NMR) spectroscopy, for example, has proven to be a powerful

tool for the characterization of organic matter in soils and sediments, indicating

overall functional group composition (e.g., Schmidt et al., 1997; Knicker and

Hatcher, 2001; Hwang et al., 2006). A more recent approach has been to couple acid

hydrolysis with stable ($\delta^{13}$C) and radioisotope ($\Delta^{14}$C) analysis of carbon. Work in

both sinking particles and sediments has shown that susceptibility to acid hydrolysis

can provide a simple but effective filter to isolate labile biochemical classes from

more refractory material (Wang et al., 1996; Wang et al., 1998; Wang and Druffel,

2001; Hwang and Druffel, 2003; Hwang et al., 2005; Hwang and Druffel, 2006; Chen

et al., 2008; Roland et al., 2008). Such work has shown that the "acid insoluble" (AI)

fraction can be typically used as a direct proxy for MUC, while the "acid soluble"

(AS) fraction mostly represents the sum of more labile biochemical classes. Isotopic measurement on these fractions, coupled with quantitative yields, therefore represents a powerful new way to investigate sources of MUC in the absence of molecular level data. To our knowledge, however, this approach has never focused on organic nitrogen (ON).

As with the broader OM pool, most ON in sediments cannot be identified at the molecular level; THAA accounts for the vast majority of ON recoverable at the molecular level, however yields nevertheless are typically 30-40% of total sedimentary ON (e.g., Cowie and Hedges, 1994). At the same time, solid-state cross polarization magic angle spinning (CPMAS) NMR studies have also universally indicated that amide N accounts for essentially all ON functionality in recent sediments (Knicker et al., 1996; Knicker and Hatcher, 1997; Knicker, 2000b; Knicker and Hatcher, 2001; Knicker, 2004). Together, these observations have strongly suggested that sedimentary ON is dominated by proteinaceous material, with low molecular-level yields likely due to either analytical matrix effects, and/or a variety of possible protection mechanisms linked to associations with minerals (i.e., Hedges et al., 2000; Keil and Mayer, 2014). Together, this suggests that the $\delta^{15}N$ value of hydrolysable proteinaceous material should provide a good proxy for the $\delta^{15}N$ value of total sedimentary ON.

Recent work, however, has called this framework into question. The first marine $\delta^{15}N$ measurements on individual AA from marine sediments demonstrated consistent offsets in $\delta^{15}N$ values of THAA and total nitrogen (TN) ($\Delta\delta^{15}N_{THAA-TN}$; Batista et al.,

2014). Batista and co-authors suggest that these $\delta^{15}N$ offsets ($\Delta\delta^{15}N$) were most consistent with distinct ON components of TN, likely preserved from primary production sources. This conclusion would dramatically change the basic assumptions about the identity of ON preserved in recently sediments, while presenting a quandary in terms of the possible molecular identity of a non-proteinaceous ON components. However, this prior work was done on bulk sediment, and as such was not able to address differences in N yield, $\delta^{15}N$ values, and likely composition between labile vs. more refractory ON pools. Further, such bulk analyses also cannot account for the potentially significant influence of inorganic nitrogen (IN) sources on sedimentary $\delta^{15}N$ values (e.g., Schubert and Calvert 2001; Freudenthal, 2001; Kienast et al. 2005; Shigemitsu et al., 2008).

Here we address these issues for the first time by examining bulk and compound-specific $\delta^{15}N$ data combined with $\delta^{15}N$ data for hydrolytic-based separations of refractory (AI) vs. labile (AS) fractions from marine sediment. Our overarching goal was to explore how coupling $\delta^{15}N$ measurements with targeted separations, for both ON and IN components, can be used to better understand sources and molecular character of refractory vs. labile ON components. Specifically, we explore using THAA $\delta^{15}N$ as a direct proxy for proteinaceous ON $\delta^{15}N$ values in all major sediment ON fractions. We measured the stable isotopic compositions $\delta^{15}N$ and $\delta^{13}C$), as well as relative contributions of C and N in bulk sediment, THAA (as a proxy for proteinaceous material), AS and AI fractions (as proxies for labile and refractory material, respectively), and finally clay-bound IN components from a sediment core

from the Santa Barbara Basin, on the California Margin, as well as these same

parameters in selected overlying plankton and sediment trap samples.

**Materials and Methods**

**Environmental setting**

Santa Barbara Basin (SBB), located in the Southern California bight, is in the mid

latitudes of the eastern Pacific margin's California Current system.  SBB is a semi-

enclosed, coastal basin, approximately 100 km long, 40 km wide and 590 m deep and

is bounded to the north by California coast and to the south by Northern Channel

Islands.  To the west, a 475 m deep sill separates the basin from the open ocean.  To

the east, the Anacapa Sill (~200 m), separates SBB from the Santa Monica Basin.

These sills restrict flow of subsurface waters into the basin, and thus limit its

ventilation.  Together with a regionally intense oxygen minimum zone, relatively

high marine productivity, POC flux ~0.1 g C * m$^{-2}$ * d$^{-1}$ (Thunell, 1998; Thunell et

al., 2007), and high sedimentation rates within SBB, ~4 mm * yr$^{-1}$ (Schimmellmann et

al., 1990), produce a suboxic depositional environment that precludes bioturbation by

benthic macrofauna and results in seasonally varying inputs of sediment as preserved

varves.

**Sample collection**

Surface sediments from SBB are the main sample, however the study also

encompasses some data on overlying planktonic biomass and sinking particles for

basic compositional context.  One mixed plankton biomass sample was collected in

June 2008 on the R/V R.G. Sproul at the center of the basin collected with a plankton

tow (35 μm mesh), towed at 30 m water depth for 30 minutes. A year-long composite

was prepared with discrete samples to represent the sinking particle flux from 1999 to

2000. The composite was based on normalized flux of sinking particulate nitrogen

from long-term trap collections at 450 m, approximately 10 m from the seafloor at the

center of SBB. Additional details on the sediment trap time-series methodology were

described previously (Thunell, 1998). Sediments were recovered in June 2008 on

R/V R.G. Sproul with a multicore from the center of the basin floor at a water depth

of 588 m. The recovered multicore used here was 40 cm long, with the sediment-

water interface intact. Immediately upon core recovery, it was sectioned in 1 cm

intervals. Plankton tow and multicore sediment samples were stored frozen within 2

h after recovery until ready for processing. Samples were lyophilized and

homogenized with a mortar and pestle prior to further sample pretreatment and

analysis.

**Extraction of operational fractions**

Total nitrogen (TN), total carbon (TC) and total organic carbon (TOC) were

analyzed on plankton, sinking particles and sediment. Bulk plankton, sinking

particles, and sediment were partitioned into several fractions of organic and

inorganic material using standard wet-chemical treatments (Fig. 2.1). Extractions

were chosen to target the major compositional forms of organic nitrogen (ON) and

inorganic nitrogen (IN), while providing ancillary data on organic carbon (OC).

Extractions included a lipid, acid-soluble (AS), total hydrolysable amino acids

(THAA), acid-insoluble (AI) and bound (Bound) fraction extracted from sinking

particles and sediments, while only the AS and THAA fraction were possible to examine in the plankton tow sample. Details of methods for each fractionation are given in following sections.

**Bulk Samples**

Lyophilized and homogenized plankton, sinking particles and sediments were used for "bulk" geochemical analyses of TC, TN and TOC. Approximately 50 mg of plankton, 100 mg sinking particles and 300 mg sediment (all total, lyophilized dry weight) were pretreated with 1 N HCl to remove IC, then rinsed to neutral pH with Milli-Q water and oven dried overnight at 50° C (Hedges and Stern, 1984). Dried samples were then used for elemental, isotopic, and other analyses as described below.

**Lipid extraction**

Lipids were extracted from untreated, lyophilized and homogenized sinking particles (~180 mg) and sediment (~1 g) with a 2:1 mixture of acetone and methanol (v:v) in 8 mL Pyrex vials with Teflon lined caps. Samples were sequentially vortexed, sonicated for 10 mins, and finally centrifuged for 10 mins at 3000 rpm. The supernatant was collected, and the process repeated four times. Total extract was combined to represent the "lipid" fraction (Fig. 2.1). The lipid-free residues were dried overnight at ~50° C and homogenized for AS extraction.

**Acid-soluble and acid-insoluble extraction**

The operational AS fraction was extracted using HCl hydrolysis, with the residual insoluble material (remaining solid phase post-hydrolysis) representing the AI

fraction. Approximately 29 mg of untreated lyophilized and homogenized plankton biomass, ~180-200 mg lipid-free, dried and homogenized sinking particles and sediments were weighed into 8 mL Pyrex vials with Teflon lined caps, and hydrolyzed with 6 N HCl under $N_2$ gas at 110° C (20 h) to extract the AS fraction (i.e., Wang et al., 1996). After hydrolysis, remaining solids were rinsed twice with Milli-Q water, vortexed, centrifuged. The supernatants were removed at each step, filtered through a GFF filter, and combined. The AS fraction was then dried with a Juoan (equipped with a foreline trap of liquid $N_2$ to protect the pump), and then re-dissolved in 0.02 N HCl. A small aliquot (calculated as equivalent to hydrolysis of ~2 mg plankton and ~20 mg of sinking particles and sediments), was pipetted into tin capsules, and dried overnight at 50° C for elemental and isotopic analysis. Further aliquots of the AS fraction, equivalent to ~6 mg plankton, ~100 mg sinking particles and sediment were retained for THAA extraction.

**THAA extraction**

The THAA fraction derived from aliquots of the AS fraction. Because AS by definition represents hydrolyzed combined AA cool, the free amino acids remaining after hydrolysis in the AS fraction were first purified by cation exchange chromatography (CEC), and then semi-stable, volatile trifluoroacetyl/isopropyl alcohol (TFA-IPA) ester derivatives were prepared for CSIA, as detailed previously as described previously (Batista et al., 2014). Briefly, the AS fraction, in dilute HCl (0.02 N HCl) was subjected to CEC with Dowex 50W-X8 resin (100-200 mesh, proton form; BioRad, USA), to isolate free amino acids (i.e., THAA fraction), from

salts and other organic contaminants not retained by the resin.  After eluting from the resin, the THAA fraction was evaporated to dryness under a stream of $N_2$ then dissolved in 0.02 N HCl (1 mL).  The THAA fraction was re-acidified in a 60° C water bath (5 mins), evaporated to dryness under a stream of $N_2$ then converted to TFA-IPA esters (Silfer et al., 1991), refer to Batista et al.s (2014) for complete details.

## Bound inorganic N extraction

The Bound fraction is operationally defined as material free from organic matter, isolated by aggressively oxidizing lyophilized, homogenized bulk sediment with a mixture of KOBr-KOH, to remove organic matter following previously described methods (Silva and Bremner, 1966; Schubert and Calvert, 2001).  Pre- and post-treatment masses of the Bound fraction were not tracked during the KOBr-KOH treatment; so reported yields of nitrogen and carbon in the Bound fraction are maximum values.

## Elemental and stable isotopic analysis

Elemental carbon and nitrogen content (per gram of untreated sample, not salt corrected) and stable isotopic compositions of carbon ($\delta^{13}C$) and nitrogen ($\delta^{15}N$) for fractions were determined at the University of California, Santa Cruz (UCSC) in the Light Stable Isotope Facility (www.es.ucsc.edu/~silab) and at Eawag: Swiss Federal Institute of Aquatic Sciences and Technology in Kastanienbaum, Switzerland (www.eawag.ch).

At UCSC, elemental compositions and $\delta^{13}C$ and $\delta^{15}N$ values for the TC, TN, TOC, AS, AI, and lipid fractions were determined on dried and homogenized material weighed into tin capsules (Costech Analytical Technologies, Inc., USA). Weight percent C and N for each fraction, except for the Bound fraction, was determined as a percent contribution to mass of material before pretreatment (i.e., carbonate removal), and are thus not biased towards higher wt% C or N values (Brodie et al., 2011a; Brodie et al., 2011b; Brodie et al., 2011c). Capsules were analyzed on a Carlo Erba EA1108 CHNS/O analyzer with a Costech zero-blank autosampler (Costech Analytical Technologies, Inc., USA) interfaced to a Thermo Finnigan Conflo II and Detla$^{Plus}$ XP isotope ratio mass spectrometer (Thermo Finnigan, USA). $\delta^{13}C$ and $\delta^{15}N$ measurements were analyzed with approximately 15% duplicates,to verify expected precision, and calibrated with both internal (gelatin) and international reference materials (acetanilide from Indiana University, (mypage.iu.edu/~aschimme/compounds.html); analytical reproducibility for both $\delta^{13}C$ and $\delta^{15}N$ measurements was ±0.2‰ (±1 s.d.).

The $\delta^{15}N$ composition of the THAA fraction, as well as the fraction of total N recoverable as individual AA, was determined by analysis of TFA-IPA esters of individual amino acids (AA), at UCSC. THAA nitrogen is defined as the sum of nitrogen yield for each of 16 individual AA (per gram of sample). The $\delta^{15}N$ of the THAA fraction is then calculated as the sum of individual AA $\delta^{15}N$ values, weighted by the mole % for each individual AA. Gas chromatography mass spectrometry (GC/MS) and continuous flow gas chromatography isotope ratio mass spectrometry

(GC/C/IRMS) conditions were as described previously (Batista et al., 2014) and are detailed in the electronic annex.

At Eawag, elemental compositions and $\delta^{13}C$ and $\delta^{15}N$ values of the Bound fraction were determined on dried, material weighed into tin capsules (Santis, Switzerland). Samples were analyzed on elemental analyze (Thermo quest, CE instruments, USA) interfaced to an on-line isotope ratio mass spectrometer (Isoprime, UK). $\delta^{15}N$ and $\delta^{13}C$ values were calibrated with the international reference materials, IAEA-N1 and VPDB, respectively, each with analytical reproducibility of ±0.2‰ (±1 s.d.).

## Results

### Relative recoveries of carbon and nitrogen

The relative contribution of total carbon and total nitrogen in the organic fractions (AS, AI, THAA and lipid) and the inorganic Bound fraction extracted from plankton, sinking particles and sediments are summarized in Table 2.1. Because there was negligible nitrogen in the lipid fraction, and so this did not contribute to the reported yields of ON. Fig. 2.2 shows relative abundance of components that comprise TOC and ON in all samples. For clarity the Bound fraction is not shown because it is operationally defined to be free of organic matter (c.f. Silva and Bremner, 1966).

The distribution of OC among the AI, AS, THAA, and lipid fractions in all samples is shown in Fig. 2.2a. In plankton the THAA fraction, a component of the AS fraction, accounted for 21% of TOC, within ranges noted by Cowie and Hedges (1994). Note that AS and lipid carbon were not determined for this sample, however the AS elemental and isotopic values discussed below suggest composition of AS is

90

as expected.  In sinking particles and sediments, AS, AI and lipid fractions together accounted for 95% and 100% of TOC, respectively.  AI carbon was the largest fractional contribution to OC in all samples, where it was determined, containing approximately twice the AS carbon and 20 times that of lipid carbon. There was also a notable shift in the relative contributions of each fraction from the water column to the sediments.  AS, THAA and lipid carbon decreased from 30%, 6% and 5%, respectively, in sinking particles; average sedimentary composition was 17%, 2% and 4%, respectively, similar to previous observations (e.g., Cowie and Hedges, 1994; Wang et al., 1996, 1998; Hwang and Druffel, 2003; Chen et al., 2008).  Meanwhile, AI carbon increased from 65% in sinking particles to an average of 83% in sediments. Within sediments intervals, there were also significant *negative* correlations between sediment depth and the OC content in the AS ($r$=-0.77, $p$<0.01), lipid ($r$=-0.57, $p$<0.05) and THAA ($r$=-0.65, $p$<0.05) fractions, and a significant *positive* correlation in AI carbon content ($r$=+0.77, $p$<0.01).  Overall, the relative distribution of AI and AS carbon for sinking particles and sediments in this study are similar to previous observations for sinking particles and sediments from the South China Sea (Chen et al., 2008), Northeast Pacific (Wang et al., 1996, 1998; Hwang and Druffel, 2003), and Santa Barbara Basin (Roland et al., 2008).

In terms of inorganics, there was no downcore trend in sedimentary Bound carbon or nitrogen (Table 1). Bound carbon, the operational carbonate containing fraction, averaged 27±5% of sedimentary TC downcore, and as noted above represents a maximum value (*see methods*).  Previous observations by Freudenthal et al. (2001)

also showed an IC-free Bound fraction contributes ca. 10% of sedimentary TC, while in SBB, IC contributions to TC were previously found to be ~8% of surface sediments (Mollenhauer and Eglinton, 2007). Inorganic N yields in the Bound fraction contributed an average of 13±1% sedimentary TN, similar to prior findings by Freudenthal and co-authors (2001) for Bound N. By mass balance, ~87% of sedimentary TN, after removing Bound IN (i.e., Schubert and Calvert, 2001), is therefore attributable to ON.

In contrast to OC data, fewer trends were apparent in relative ON contributions from AS and AI fractions, while THAA-N decreased from the water column into sediments (Fig. 2.2b). In sinking particles and sediments, AS and AI nitrogen together accounted for 100% of ON, with no measurable ON in the lipid fraction. The relative AS-N contribution to TN was 53% in sinking particles and 37±5% in sediments. As with OC, AI-N was the largest ON component in sediments and particles, representing 47% of TN in the composite sinking particle sample and 62±4% TN in sediments. We are unaware of any prior measurements for AI and AS nitrogen to which these results can be directly compared. The THAA-N decrease from the plankton to particles and sediments (32% in plankton; 11% in sinking particles, average 7±4% in sediments) is similar in both values and trends to data previously observed in other sediments (e.g., Cowie and Hedges, 1994).

**Weight percent carbon and nitrogen, and C/N ratios**

Comparisons of weight percent carbon (wt% C) and nitrogen (wt% N) represented by each organic fraction are shown in Fig. 2.3a and 2.3b, respectively. Specific

values for wt% C and wt% N for all fractions are also summarized in Table EA-1. As mentioned in *Methods and materials*, these wt% C and wt% N values for each fraction are determined as a percent of pretreatment mass of material (i.e., before carbonate removal), and are thus not biased towards higher wt% C or N values (i.e., Brodie et al., 2011a-c). However, the pre- and post-treatment mass of the Bound fraction was not tracked during the KOBr-KOH treatment. C/N ratios (weight ratios) for the TOC, AI and AS fractions are shown in Fig. 2.3c and reported in Table 2.2.

There was a general trend towards decreasing values of wt% C and wt% N from the plankton into sinking particles and then sediments, however there was no consistent trend within the sediment core. The AI fraction had the highest contributions to TC and TN, followed by the AS, THAA and lipid fractions. C/N values are highest in the AI fraction, followed by the TOC/TN and AS fractions.

The mixed plankton tow sample had 7.6 wt% TOC (without salt correction), lower than previously observed by Wang and co-authors (1998) for plankton from the region, 40 wt% TOC, with salt correction applied. However, the % TN for plankton (1.3%) was comparable to earlier observations (2.8%) by Wang and co-authors (1998) and the TOC/TN was 6.4, similar to Redfield ratio of 6-8 as expected (Redfield et al., 1958).

Sinking particles and sediments had a wt% TOC value of 3.7% for the composite sample, and an average value of 2.6±0.2% for sediments. These wt% TOC values are similar to previous observations for sinking particles reported from the region (Wang et al., 1996; Roland et al., 2008; Hwang et al., 2006). Wt% TN values for the

composite sinking particle sample was 0.53%, and sediments averaged 0.35±0.02%. These wt% N values were similar to values previously reported for sinking particles in SBB (Roland et al., 2008; Wang et al., 1998). The TOC/TN ratio for the composite trap sample was 8.1, similar to values previously determined for sinking particles in SBB (Roland et al., 2008; Thunell et al. 2007). Average sedimentary TOC/TN values were 9.4±0.3, again similar to the range for sediments previously observed at Station M (7.8 to 8.7; Wang et al., 1998; Hwang et al., 2006).

The AS fraction isolated from plankton had a C/N value of 4.3, however, as noted above the wt% C and N were not determined. In the composite sinking particles the AS fraction had 1.1 wt% C and 0.3 wt% N, and had a C/N value of 4.6. These C/N values are near the lower end of the range previously reported for AS in sinking particles from several high-productivity margin locations, including SBB (4.8 to 6.1; Roland et al., 2008). In sediments, AS wt% C and N values were 0.46±0.07% and 0.13±0.02%, respectively. AS material in sediments therefore had lower organic C and N contents than that from sinking particles, while its C/N value (4.1±0.1) was similar to particles (4.6).

The AI fraction isolated from sinking particles had lower wt% C and N values than AS, at 2.4% and 0.25%, respectively. This was, however, higher than AS values, which averaged wt% C and N values of 2.2±0.17 and 0.22±0.02, respectively. However, the C/N ratios in AI from the composite sinking particles and sediments were very similar, 11.2 and 11.7 respectively, both similar to previous observations for sinking particles from SBB (Roland et al., 2008).

The Bound fraction, isolated only from sediments, had average wt% C and N

values 1.09±0.25 and 0.1±0.0, respectively, and a C/N ratio of 27.6±6.5. These

bound wt% C values were an order of magnitude higher than has been observed in

surface sediments from other continental margin sediments (~0.1; Freudenthal et al.

2001). However, sediments were not decalcified in this study, in contrast to

Freudenthal and co-authors (2001). The Bound fraction had wt% N values that were

similar prior to observations of in both margin and Arctic Shelf sediments (0.05 to 0.1

wt% N; Freudenthal et al., 2001; Schubert and Calvert 2001). Likely due to the

presence of carbonates, the C/N value for the Bound fraction in this study (27.5±6.5)

was also larger than values (~ 3) observed by Freudenthal et al. (2001).

**Stable carbon and nitrogen compositions of isolated organic fractions**

The $\delta^{13}C$ and $\delta^{15}N$ values for organic and inorganic fractions are summarized in

Table 3. A comparison of $\delta^{13}C$ and $\delta^{15}N$ values for the isolated organic fractions is

shown in Fig. 2.4. The Bound fraction is not shown, because of its inorganic carbon

and nitrogen content, but bound values are summarized in Table 2.1 and Fig. EA 2-1.

Generally, the distribution of $\delta^{13}C$ and $\delta^{15}N$ values for organic fractions from the

water column and sediments follow a predictable progression of THAA > AS > TOC

(TN) > AI > lipid. The magnitudes of the $\delta^{13}C$ and $\delta^{15}N$ *offsets* for each fraction

(relative to TOC and TN) are also smaller in the water column relative to sediments.

However, $\delta^{15}N_{THAA}$ values were an exception, with the largest $\delta^{15}N$ offset between

THAA and TN (i.e., $\Delta\delta^{15}N_{THAA-TN}$) observed in plankton, and the smallest offsets

observed in sediments. In total sediments, there were no clear downcore variations in

either isotope value, however observed variations in both $\delta^{13}C_{TC}$ and $\delta^{15}N_{TN}$ around the mean value of ~1‰ to 1.5‰. These downcore $\delta^{13}C$ and $\delta^{15}N$ variations are also captured by each fraction. For instance, downcore variations in $\delta^{15}N_{TN}$ are observed in other $\delta^{15}N_{AS}$ and $\delta^{15}N_{AI}$, but are not discernible in $\delta^{15}N_{THAA}$ due to the magnitude of propagated error (ca. 1-3‰) linked to large number of individual isotope and molar percentage measurements required to quantify $\delta^{15}N_{THAA}$ (i.e., Batista et al., 2014).

The $\delta^{13}C$ values for each OC fraction are shown in Fig. 2.4a. For plankton, the $\delta^{13}C$ values for AS and TOC fractions were -18.7‰ and -19.2‰, respectively. Isolated fractions from the composite sinking particles were slightly depleted in $^{13}C$ relative to plankton, with $\delta^{13}C$ values for the AS, TOC, AI and lipid fractions that were -20.5‰, -21.6‰, -23.1‰, and -23.7‰, respectively. Sedimentary $\delta^{13}C$ values for each fraction were more similar to sinking particles with values for the AS, TOC, AI and lipid fractions that were -19.7±0.4‰, -22.0±0.4‰, -22.8±0.2‰, and -23.9±0.4‰, respectively. $\delta^{13}C$ results for each fraction fall within the range of previous $\delta^{13}C$ observations for sinking particles made in SBB by Roland et al. (2008) for the AS (-18.3 to -19.3‰), TOC (-21.3 to -22.1‰), AI (-22.7 to -24.2‰), and lipid (-23.4 to -24.1‰) fractions. These $\delta^{13}C$ results are also consistent with previous observations for plankton, sinking particles and sediments from Station M (Wang et al., 1996, 1998), and also the only other comparable sedimentary fractions from the South China Sea (Chen et al., 2008).

Bound sedimentary carbon had $\delta^{13}C$ values that ranged from -4.2‰ to -8.4‰, averaging -6.2±1.5‰ (Fig. EA 2-1). As noted above, Bound values in this study were

not decalcified, which likely explains the enrichment in $^{13}C$ and average sedimentary $\delta^{13}C$ value of -6.2‰ relative to the only other published data (carbonate free, $\delta^{13}C$ values ca. -23‰; Freudenthal et al., 2001).

The $\delta^{15}N$ compositions of isolated ON fractions are summarized in Fig. 4b. Plankton $\delta^{15}N$ values were 11.8‰ for THAA, 8.2‰ for AS, and 7.2‰ for TN. Sinking particles $\delta^{15}N$ values were 10.6‰ for THAA, 8.6‰ for AS, 6.8‰ for TN and 3.5‰ for AI. Similarly, average $\delta^{15}N$ values for sediment were 9.9‰±0.7‰ for THAA, 8.0±0.3‰ for AS, 6.9±0.3‰ for TN, and 5.5±0.3‰ for AI. In plankton, there was a $^{15}N$ enrichment in the THAA fraction relative to TN, resulting in a $\Delta\delta^{15}N_{THAA-TN}$ of 4.6‰. In sinking particles, THAA nitrogen was also enriched in $^{15}N$, with a $\delta^{15}N_{THAA}$ value of 10.6‰, relative to 6.8‰ for TN, resulting in a $\Delta\delta^{15}N_{THAA-TN}$ of 3.8‰. Similarly, sedimentary $\delta^{15}N_{THAA}$ values (9.9‰) were also higher than TN (7.0‰), but the $\Delta\delta^{15}N_{THAA-TN}$ in sediments (2.9‰) was lower by about 1‰ relative to water column samples. Zhang and Altabet (2008) also observed an enrichment in $^{15}N$ for amine-N groups isolated from sediments, relative to TN, leading to a $\Delta\delta^{15}N$ on the order of ~1.3‰. Though there are to our knowledge no other published $\delta^{15}N$ values for the AS and AI fractions to which these data can be compared, nevertheless we note that our $\delta^{15}N_{AS}$ values for our plankton (8.2‰), sinking particles (8.6‰) and average sediments (8.0‰) were similar, resulting in relatively consistent $\Delta\delta^{15}N_{AS-TN}$ values across all sample types. The $\delta^{15}N_{AI}$ values were only analyzed in sinking particles and sediments, but these data were also

consistently depleted in $^{15}$N, with $\Delta\delta^{15}N_{AI-TN}$ values ~2‰ for sinking particles and sediments.

The $\delta^{15}$N values for the Bound fraction were only determined in sediments, with $\delta^{15}$N values ranging from 4.4‰ to 6.0‰, and an average $\delta^{15}N_{Bound}$ value of 5.2±0.5‰ (Fig. EA 2-1).  The Bound fraction also had relatively consistent $\delta^{15}$N offsets vs. sedimentary TN, with average $\Delta\delta^{15}N_{Bound-TN}$ values of ~1.8‰.  The magnitude of this $\Delta\delta^{15}$N value is similar to observations in previously published data for the $\delta^{15}$N values of the bound fraction in marine sediments (Freudenthal et al., 2001; Schubert and Calvert, 2001; Kienast et al., 2005; Shigemitsu et al., 2008).

**Discussion**

**Nitrogen functional distribution: the assumption of sedimentary amide nitrogen**

As noted above, solid-state spectroscopic studies have provided invaluable data to constrain organic composition of material that cannot be identified at the molecular level (i.e., MUC).  Because much of our interpretation below can be constrained by such information, we briefly make the case for our underlying assumptions here. Solid-state $^{15}$N CPMAS NMR, and also nitrogen K-edge XANES, have provided remarkably consistent information about nitrogen functionality in across a variety of sediment types.  Both solid-state $^{15}$N CPMAS NMR and nitrogen K-edge XANES data have indicated that bulk ON in relatively modern sediments is dominated by amide nitrogen, similar to corresponding functional distributions in marine algal sources (Knicker and Ludemann, 1995; Knicker et al., 1996; Knicker, 2000b;

Vairavamurthy and Wang, 2002; Knicker, 2004). The same finding of amide-dominated detrital organics is also consistent with spectroscopic work in soils (Knicker et al., 1993; Schmidt et al., 1997; Knicker, 2000a; Knicker et al., 2000), marine sinking particles (Hedges et al., 2001; inferred from $^{13}$C-NMR data), and colloidal/dissolved organic matter at all ocean depths (McCarthy et al, 1997). To our knowledge, only a single study has so far directly examined marine sedimentary ON functionality with $^{15}$N-NMR in acid-separated fractions (Knicker and Hatcher, 1997, 2001); perhaps not surprisingly, the same amide N functionality was also found in both AS and AI sedimentary fractions.

Overall, amide-dominated ON is now a widely observed characteristic of detrital ON pools, crossing both terrestrial and marine environments. In the discussion that follows, we therefore base many of our interpretations on the working hypothesis that ON in our sediment fractions is also amide dominated. While we do not have direct spectroscopy-based nitrogen functional data for the samples in this study, we believe the essentially universal observation of amide ON in modern sediments makes this assumption well founded, especially given that these SBB samples represent recent deposition in a rapid burial, high preservation environment (Batista et al., 2014; Barron et al., 2010 and references therein). Finally, we also note that while spectroscopic functional data cannot distinguish between specific amide-containing molecules, the two major amide biochemical sources are amino acids and amino sugars (e.g., McCarthy et al., 1997), with amino acid by far dominant in fresh biomass (e.g., Hedges et al., 2001; Bianchi and Canuel, 2011).

**Carbon contributions and δ¹³C values in major sedimentary fractions**

The vertical trends in the relative yields of organic carbon in AS, AI, THAA and lipids isolated from our samples are consistent with the few other existing studies measuring these same fractions in sinking particles and sediments. As noted above, the relative organic carbon yields in AS, THAA and lipid fractions featured a strong decreasing trend from the water column to sediments. In our study, the AS operational fraction encompasses both TCHO and THAA biochemical classes, so it is not surprising that the decrease in AS from the water column into the sediments mirrors vertical trends in individual compound classes previously reported. For example, prior work has reported THAA, TCHO and lipid carbon yields in plankton at 24 - 44%, 21 - 48%, and 19 - 23%, respectively, decreasing to 20 - 43%, 5 - 19%, and 5 - 10%, respectively, in sinking particles, and to 2 - 20%, 3 - 19%, and 2 - 8%, respectively, in sediments (Wang et al., 1998; Hwang et al., 2003; Chen et al, 2008; Roland et al., 2008).

In terms of organic carbon represented by the AI fraction, the opposite (increasing) trend from the water column to sediments in our data is also consistent with expectations (Fig. 2.2). Previous studies have found AI carbon increased from 8-12% in plankton to 49-65% in sinking particles and 46-75% in sediments (Wakeham et al., 1997; Wang et al., 1998; Hwang et al., 2003, 2005; Chen et al., 2008; Roland et al., 2008). Overall, carbon yields in our data is therefore consistent with expected increases in the operational AI fraction, and conversely decreases in identifiable biochemical classes from water column to sediments (Wakeham et al., 1997; Wang et

al., 1998), consistent with the idea that progressive decrease in the lability of organic carbon occurs (Cowie and Hedges, 1994)

Our $\delta^{13}C$ results are further consistent with work that has suggested that at least AI carbon in sinking particles and sediments is dominated by lipid-like material. For example, characterization of AI in sinking particles and sediments from the CA margin using solid-state $^{13}C$-NMR found that alkyl and unsaturated/aromatic carbon were the dominant C forms, suggesting that AI was almost entirely lipid-like material (Hwang et al., 2006). Similarly, Hwang and co-authors (2003, 2005) compared the $\delta^{13}C$ and $\Delta^{14}C$ signatures of TCHO, THAA and lipid fractions and found the AI fraction to have essentially identical values as lipids. While we do not have solid-state $^{13}C$-NMR data, our $\delta^{13}C$ values for the AI fraction vs. other fractions are also consistent with these findings (Fig. 2.4), as well as with previously published $\Delta^{14}C$ for our sediment trap sample (Roland et al., 2008). Specifically, the fact that $\delta^{13}C$ values of our AI and lipid fractions were within ~1.0‰ of each other (at ~-23‰ and -23.8‰) strongly support this conclusion. In contrast, the heavier AS $\delta^{13}C$ signatures we observed are consistent with AS being a mixture dominated by TCHO and THAA, since both of these compound classes have a heavier $\delta^{13}C$ value relative to biomass TOC (Degens et al., 1968; DeNiro and Epstein 1977; Hayes, 2001). These relative AS $\delta^{13}C$ offsets from TOC are also similar to those reported in previous work (Wang et al., 1996, 1998; Hwang and Druffel 2003, 2005; Chen et al., 2008; Roland et al. 2008).

Average sedimentary $\delta^{13}C$ values for the Bound fraction confirm presence of inorganic carbon, consistent with this fraction not being treated to remove carbonates. However, in contrast, Freudenthal and co-authors (2001) have $\delta^{13}C$ values for a carbonate-free bound fraction, which indicates presence of residual OC. As a test for OC in the Bound fraction, isotopic mass balance for data in this study indicates that between 4% and 20% of Bound carbon is attributable to OC, assuming an end-member $\delta^{13}C_{OC}$ value of -22‰ with a $\delta^{13}C_{IC}$ value of -5‰ or -2, respectively.

**Nitrogen contributions to major sedimentary fractions**

In contrast with the OC results, the relative *similarity* in total nitrogen recoveries for the AS (i.e., labile) and AI (i.e., refractory) fractions between water column samples and sediments suggests relatively similar reactivity of TN. Only THAA showed major decreases in recovery (Fig. 2.2), an observation that is consistent with previous work showing that recovery of hydrolyzable amino acids decreases steadily with organic matter degradation (e.g., Cowie and Hedges 1994; Wakeham et al., 1997). However, the consistent offsets observed between AS and THAA N recovery is puzzling. While this suggests alternate sources of organic N may dominate both AS and AI, the specifics, as well as what alternate hypotheses may be reasonable, differ substantially between the two major fractions. We will therefore discuss each independently.

**Nitrogen in the AS fraction**

There is good similarity for AS-N yields in sinking particles and sediments in SBB, which is consistent with expectations for this high preservation regime (Batista

et al., 2014). C/N of the AS fraction is very low in both plankton (4.3), sinking

particles (4.6) and sediments (avg 4.1). This would suggest compositional similarity

between AS in the well-preserved SBB sediments and water column sources, and so

seems reasonable. Pure proteinaceous material would be expected to have a similar

C/N ratio (~3-4). Together with the spectral observations of amide nitrogen

functionality expected for both algal biomass and sediments (Section 4.1), the

comparison of yields and C/N ratios in AS vs. THAA fractions would seem consistent

with the assumption that mainly proteinaceous nitrogen (i.e., amino acids) dominates

the hydrolyzable ON pool in both sinking particles and sediments in this study.

Given this, the large divergence in AS-N versus THAA-N yields in both sinking

particles (64% AS-N and 11% THAA-N) and in sediments (~40% AS-N versus ~3 to

16% THAA-N; see Results and Fig. 2.2) are puzzling: these offsets alone would

instead suggest an opposite conclusion, that non-amino acid N dominates

hydrolyzable sedimentary nitrogenous material. Given prior data on amide

functionality noted above, such large offsets are particularly unexpected. Major non-

amino acid nitrogenous biochemicals in algal biomass include amino sugars and

pigments (e.g., Knicker 2004, McCarthy 2007). However, pigments, such as

chlorophyll and chlorophyll degradation products (i.e., chlorins), are removed as part

of the operational lipid isolation. Primary amines are an additional common ON

form, and novel polyamines have been reported to be a major N component in diatom

tests (Bridoux et al., 2011). However, these amines are associated with the opal

matrix, and it is unclear if they would be liberated by acid hydrolysis to the AS

fraction, without demineralization techniques (i.e., HF, Ingalls et al., 2010; Bridoux et al., 2011). Further, of all possibilities, only amino sugars would be consistent with dominant amide functionality universally observed in recent sediments (Section 4.1).

While there has been relatively little direct focus on sedimentary amino sugars, this possibility is supported by some studies, while contradicted by others. Large carbohydrate contributions to sedimentary AS has in fact been indicated by the only prior 13C-CPMAS NMR study to directly examine this AS fraction in extremely organic-rich sediments (Knicker and Hatcher, 2001). However, direct molecular-level analyses have indicated far lower concentrations. For example, Niggemann and Schubert (2006) isolated amino sugars and found them to be a negligible contribution (<2%) of TOC, thus they are not likely a dominant contribution to total sedimentary nitrogen. While it is common for molecular-level recoveries in geochemical samples to be far lower than more broad-based estimates from spectroscopy (e.g., McCarthy et al., 1997; Hedges et al., 2001), as noted above the low elemental ratios of the AS fraction (~3-4) also do not seem consistent with major contributions from relatively high C/N (~8) amino sugars. Overall, while amino sugars represent probably the most likely candidate for additional nitrogenous biochemicals in AS, it seems unlikely that they could explain the entire offsets in nitrogen contribution between AS and THAA fractions.

Inorganic nitrogen represents a second possible nitrogen source to AS, which may be able to at least partially explain the often contradictory aspects of the ON data. Clay-associated ammonium represents a major potential inorganic N source for

sediments (e.g., Silva and Bremner, 1966; Muller, 1977; Schubert and Calvert, 2001). In our samples clay-bound nitrogen (i.e., Bound N) represented ~13% of sedimentary TN, and while measured independently of AS (Fig. 2.1), they both showed no downcore trend (Table 1, Supplemental Table 1). If liberated ammonia was in fact recovered in the AS fraction, this could substantially reduce elemental ratios, with the IN source therefore potentially confounding a direct linkage between C/N ratios and organics composition. Ammonia can be liberated during acid hydrolysis from the degradation of amino acids, released from clay surfaces (i.e., exchangeable ammonia), and also possibly from the deamination of purines or pyrimidines (Sowden et al., 1977; Schulten et al., 1997; Knicker 2004). Under our analytical conditions, any ammonia liberated during hydrolysis would likely remain in the AS fraction as ammonium salts (C.S. Schubert, personal communication). At the same time, however, since our hydrolysis conditions were focused on amino acids, the complete liberation of clay bound N is uncertain, making it difficult to quantify a IN contribution to the AS fraction. Overall, because of the multiple possible contributing end-members, coupled with poorly constrained relative contributions, comparing δ15N signatures of these fractions, as we discussed below, may represent the best direct way to test this hypothesis.

**Nitrogen in the AI fraction**

The AI fraction represented the majority (~60%) of sedimentary TN (Table 2.1, Fig. 2.2), and had a strongly elevated C/N value (~16; Fig. 2.3). Such high C/N ratios are generally consistent with $\delta^{13}C$ values discussed above; together further supporting

the hypothesis that sedimentary AI is quantitatively dominated by hydrolysis resistant, lipid-like organic carbon (Hwang and Druffel, 2003; Hwang and Druffel, 2006). However, while our C/N values for the AI fraction are higher than other fractions, it is difficult to draw specific ON source inferences for such data; AI represents a mixture between nitrogenous-bearing and far more abundant non-nitrogen bearing organic compounds. This is a particularly problematic issue in a lipid-rich mixture. The operational lipid fraction was extracted from our samples prior to acid hydrolysis (Fig. 2.1), so at least the extractable N-containing lipids (such as chlorins) should not be present in the final AI fraction analyzed. While it is possible that some N-containing lipid material might still be present, measurements of total chlorin nitrogen (Sachs et al. 1999; Higgins et al. 2012), as well as previously discussed solid-state ^{15}N NMR data (Knicker and Hatcher, 2001) both suggest this contribution would be extremely small. We note that the only two previously determined C/N values for a sedimentary AI fraction have a considerable range: from somewhat lower than ours (9-10; Knicker and Hatcher, 2001), to substantially higher (~30; Hwang et al., 2006). However, again all these values are far more nitrogen-rich than would be expected for most typical total lipid extracts. Together, these considerations suggest that the large part of sedimentary N in the AI fraction is likely derived from different biochemical sources than the lipid-like material that appears to dominate AI organic carbon.

In terms of identifiable amino acids, the sedimentary AI fraction had the largest offset between nitrogen in AI vs. THAA nitrogen (~60% vs. 3 to 16%). If we assume

that inorganic ammonia has been quantitatively liberated by acid hydrolysis, than this observation, coupled with consideration of spectral data and alternate major biochemical ON sources above (4.3.1), strongly suggests either hydrolysis resistant amino acid and/or amino sugar as the main biochemical possibilities for AI material. While it might seem unexpected that such nominally labile biochemical classes would dominate nitrogen in a non-hydrolysable fraction, there is in fact abundant precedent for this across multiple environments.  For example, pyrolysis GC/MS characterization of the acid hydrolyzed residue (i.e., AI fraction) of soils and sediments has suggested the continued presence of proteinaceous material after hydrolysis (Schulten and Schnitzer, 1997; Leinweber  and Schulten, 2000; Knicker et al., 2001; Knicker 2004; Berwick et al., 2007).   Further, in marine colloidal OM, it has been clearly shown the most of the quantitatively dominant complex carbohydrates present (likely with a substantial amino sugar component) cannot be recovered by standard hydrolysis techniques (e.g., Benner et al., 1992; Repeta et al., 2002).

Multiple hypotheses have been proposed for the protection of biochemicals in sedimentary matrices (e.g., de Leeuw et al., 2006; Hedges and Keil, 1995; Gelin et al., 1999; Hedges et al., 2000; Knicker 2004; Mayer 2004; Keil and Mayer 2014), with yields of identifiable biochemical compound classes often invoked in an attempt to constrain specific sources and mechanisms.  However, perhaps analogous to high molecular weight DOM in the oceans (Repeta et al., 2002) the direct molecular-level yields of both sedimentary amino acid and amino sugars are typically low (i.e.,

107

Muller et al., 1986; Benner and Kaiser, 2003; Lomstein et al., 2006; Niggemann and Schubert, 2006), making information potential of such measurements limited. Our new $\delta^{15}N$ data on specific organic fractions therefore offers a new approach to evaluating non-hydrolysable ON preserved in sediments. Because amino acids are likely the main ON biochemical *source* in exported primary production, coupling compound-specific $\delta^{15}N$ values for directly measured hydrolysable amino acids together with $\delta^{15}N$ values for IN, and the operational AI and AS fractions, now provides a unique opportunity to evaluate sedimentary N biochemical identity, source and preservation.

### $\delta^{15}N$ values of labile sedimentary nitrogen fractions

The $\delta^{15}N$ signatures of all isolated fractions are consistently offset from $\delta^{15}N_{TN}$ values ($\Delta\delta^{15}N$), in both the water column and sediments, with essentially no vertical trend in the $\delta^{15}N$ values for most fractions from the water column to sediments, or within the sediment depths examined here (Fig. 2.4b). One exception may be THAA, which has a slightly larger $\Delta\delta^{15}N$ (i.e., $\Delta\delta^{15}N_{THAA—TN}$) in the water column than in sediments; however, this is in the range of error for these measurements (see *Materials and Methods*). Overall, the main observation is the large and generally constant $\Delta\delta^{15}N$ values for individual fractions (THAA, AS, AI, Bound; Fig. EA 2-1) relative to $\delta^{15}N_{TN}$. These large $\Delta\delta^{15}N$ values suggest that characteristically different nitrogen forms are represented in each operational fraction, but also that the distributions of different N forms remain relatively constant after deposition. $\Delta\delta^{15}N$

values for each fraction relative to $\delta^{15}N_{TN}$ therefore likely carries key information about specific sources and preservation of sedimentary nitrogen in each fraction.

**$\delta^{15}N$ of acid hydrolysable proteinaceous nitrogen**

The THAA fraction had the largest positive $\Delta\delta^{15}N$ values in every sample, with $\Delta\delta^{15}N_{THAA—TN}$ values of ~4‰ in plankton, and 2-4‰ in sinking particles and sediments. While there may be multiple processes operating, the general similarity of the $\Delta\delta^{15}N_{THAA – TN}$ offset in plankton, particles, and sediments strongly suggests the offsets are derived from original production sources, as opposed to degradation or post-depositional diagenetic effects. This interpretation is consistent with several lines of evidence. First, previous work using a range of analytical approaches has suggested that similar $\delta^{15}N$ offsets exist between THAA and TN (Fig. 2.5) for autotrophic cultures (Macko et al., 1986; Pan et al., 2007; McCarthy et al., 2013), as well as for zooplankton (Schmidt et al., 2004) and sediments (Carstens and Schubert, 2012). While the absolute $\Delta\delta^{15}N$ reported in pure biota is somewhat variable, isotopic offsets are always reported with a generally consistent direction and magnitude to those we observe in our data set. This strongly suggests that non-proteinaceous nitrogen biomolecules in water column sources have, on average, lower $\delta^{15}N$ values than THAA. The relative consistency of $\Delta\delta^{15}N$ in all ON fractions in our data therefore further suggests preservation of a similar mixture of these source nitrogenous biochemicals in at least recent sediments. This conclusion would be consistent with the well-preserved OM of SBB sedimentary regime (e.g., Reimers et al., 1990; Thunell, 1998; Huguet et al., 2007). Several authors have also

independently estimated the $\delta^{15}N$ of sedimentary ON, finding isotopic offsets also consistent with these findings. For example, Zhang and Altabet (2008) report higher $\delta^{15}N$ values for 'amine' nitrogen, which should represent a close proxy for THAA, from a range of sedimentary regimes.

## $\delta^{15}N$ of total hydrolysable material

The AS fraction represents total hydrolysable material, and as noted above, in principle should therefore comprise *both* THAA nitrogen, as well as hydrolysable sugars, but also may include ammonia liberated from clay (Sowden et al., 1977; Schulten et al., 1997). If interpretations of previous NMR data is correct (Knicker and Hatcher, 2001), such that proteinaceous material accounts for most hydrolysable sedimentary ON, than the $\delta^{15}N$ values of AS and THAA fractions would be expected to be very similar. However, the $\delta^{15}N$ values of AS and THAA fractions are again strongly offset from each other ($\delta^{15}N_{AS}$ ~2-4‰ lower than THAA in all samples; Fig. 2.4), suggesting differences in molecular composition and/or source(s). The $\Delta\delta^{15}N_{AS—TN}$ values were also consistently positive in both the water column and the sediments, however the offsets in the water column samples were much smaller ($\Delta\delta^{15}N_{AS—TN}$ ~+1‰; Fig. EA 2-2) than in sediments. Importantly, for the AS fraction, the yield of THAA-N should provide a direct constraint: hydrolysable proteinaceous material would, by definition, be measured as THAA. Together, the much lower $\delta^{15}N_{AS}$ values, coupled with relatively low contributions of THAA-N (18-32%) to AS-N must therefore indicate that the majority of AS-N is composed of non-proteinaceous sources.

To our knowledge, only a single prior study has directly coupled $^{15}N$ and $^{13}C$ CPMAS NMR data to examine the molecular composition of a marine sedimentary AS fraction. The same Knicker and Hatcher (2001) study noted above showed that AS-N from organic-rich sediment was dominated by amide functionality, similar to bulk sediment. However, the $^{13}C$ CPMAS NMR spectra of the same AS fraction were quite different: in contrast to the more complex bulk sediment spectra, it indicated AS was dominated by carbohydrate. In fact, the $^{13}C$-CPMAS spectra of the sedimentary AS fraction published in that study is remarkably similar to $^{13}C$ CPMAS spectra of complex carbohydrate-dominated colloidal material found in the upper ocean (Benner et al, 1992; McCarthy et al., 1993), which is now known to be quantitatively dominated by hydrolysis resistant complex heteropolysaccharide, containing a substantial amino sugar component (Aluwihare et al., 2008). Work on such complex sugars in the ocean water column has shown that despite their significant quantitative contribution to isolated material, they are extremely difficult to measure at the molecular level via standard hydrolytic techniques (Wakeham et al., 1997; Hedges et al., 2000; Hedges et al., 2001). While such comparisons are clearly circumstantial evidence only, together with our $\Delta\delta^{15}N_{AS-TN}$ data they are consistent in suggesting an unrecognized importance for amino sugar N in both the labile and resistant pools of ON in sediments. However, a major caveat remains that, at least for the AS fraction, possible IN could also represent a confounding variable.

## $\delta^{15}N$ of the inorganic nitrogen

The Bound N fraction is assumed to represent mostly IN, mainly in the form of ammonium, associated with clay minerals (Bremner et al., 1967; Schubert and Calvert 2001; Freudenthal et al., 2001; Shigemitsu et al., 2008; Li and Jia, 2011). Relative to TN, the lower $\delta^{15}N$ values for the sedimentary Bound fraction ($\Delta\delta^{15}N_{Bound—TN}$ of -2‰; Fig. EA 2-2) are consistent with clay-bound nitrogen derived from continents (Schubert and Calvert, 2001; Freudenthal et al., 2001; Shigemitsu et al., 2008; Li and Jia , 2011). It is possible that in-situ production of ammonium from organic matter degradation could also contribute, since this would also be expected to also have lower $\delta^{15}N$ value relative to total sedimentary ON (DeNiro and Epstein, 1981; Minagawa and Wada, 1984; Macko et al., 1986). The relatively low quantitative yield of Bound-N (maximum ~13% of sedimentary TN, see *Materials and methods*; Table 1), and the low $\delta^{15}N_{Bound}$ values for our samples are comparable to numerous studies from shallow surface sediments (e.g., Stevenson and Cheng, 1972; Muller et al., 1977; Freudenthal et al., 2001). Even if Bound N represents relatively small percentages of TN, the low $\delta^{15}N$ values means that this source can disproportionately influence total $\delta^{15}N$ values.

As noted above, it is known that exchangeable ammonium, bound to clay surfaces, can be released during acid-hydrolysis, whereas fixed ammonium is more strongly associated with clay minerals (Sowden et al., 1977; Schulten et al., 1997; Schulten and Schnitzer 1998). Unfortunately, our analyses cannot directly determine how much clay-bound ammonium may actually contribute to the AS and AI fractions. For

the AS fraction, it seems highly likely that bound N contributes to $\delta^{15}N_{AS}$ values we observe. After acid-hydrolysis, any ammonium that is not volatilized during drying of the AS fraction (*see Materials and methods*), would likely remain as ammonium salts (C.S. Schubert, *personal communication*). If bound IN was *quantitatively* transferred to the AS fraction, it would comprise ca. 38% of AS-N. Isotopic mass balance indicates can then be used to estimate the $\delta^{15}N$ of the AS-N ($\delta^{15}N_{AS\_est}$) that is *not* represented by ammonium. If the $\delta^{15}N_{Bound}$ value were taken to be 5‰, then the non-ammonium N (62% of AS-N) would have a $\delta^{15}N_{AS\_est}$ value of 9.8‰. This value is in fact very similar to the average sedimentary $\delta^{15}N_{THAA}$ of 9.9 ± 0.7‰. While clearly not tightly constrained, this close match in $\delta^{15}N$ values from a simple mass balance exercise suggests that ammonia does in fact remain in the AS fraction, as opposed to evaporating during hydrolysis and dry down. If inorganic bound ammonium in fact contribute to AS fraction, this would also help to explain the very low C/N values of the AS fraction noted above (section 4.3).

Finally, we acknowledge that a major caveat to this interpretation remains the uncertainty of partitioning of the bound IN between AS and AI pools: as noted above, it is also possible that bound N could influence the $\delta^{15}N_{AI}$ (discussed in the next section). If the entire clay-bound N reservoir resided in the AI fraction (and not AS fraction) after acid hydrolysis, then it would represent up to 22% of the AI-N. However, since the $\delta^{15}N_{Bound}$ value (~5‰) is essentially the *same* value as the $\delta^{15}N_{AI}$, isotopic mass balance unfortunately cannot place any direct constraint on contribution of bound N to AI.

## $\delta^{15}N$ of acid resistant material

The organic AI fraction is the largest reservoir of ON in our samples (ca. 60%) and also has the lowest $\delta^{15}N$ values (Fig. 2.4). This large AI N component has a $\Delta\delta^{15}N_{AI\text{—}TN}$ value of ca. -2‰, which as noted above, is very similar to $\Delta\delta^{15}N_{Bound\text{—}TN}$ for the Bound fraction (Fig. EA 2-2). The few previous sedimentary data sets used to directly examine the AI fraction have also found that this fraction represents the majority of sedimentary organic matter (Wang et al., 1996, 1998; Knicker et al., 1997; Wakeham et al., 1997; Hwang et al., 2003), consistent with our results. As noted above, previous work in both water column and sediments have also indicated that the AI fraction represents an older, and more refractory organic material (Wang et al., 1996, 1998, Wakeham et al., 1997; Hwang et al., 2003, 2006). Considering that our sample set from SBB is proximal to land, terrestrial material is a potential source of acid resistant, refractory carbon and nitrogen. However, $\delta^{13}C$ of TOC (Fig. 2-4 and Table 2.3) values indicate that the primary source of OM is marine-derived. Therefore, AI in this sediment likely represents the most direct proxy for marine derived ON that will be ultimately preserved in sedimentary archives.

To our knowledge no prior study that has used isotopic information to investigate the composition of ON within the AI fraction. The Knicker and Hatcher (2001) study referenced above showed that AI ON in a marine sapropel was dominated by amide functions, but most other work has focused only on carbon composition. Leinweber and Schulten (2000) and De La Rosa and co-authors (2008) showed that aliphatic and peptidic material both reside in the AI fraction. Previous work by Derenne and co-

authors (1993, 2003), and Nguyen and co-authors (2003), also indicated that some amide nitrogen derived from fresh and degraded plankton was non-hydrolysable. These first $\delta^{15}N_{AI}$ data therefore provide an opportunity to constrain not only biochemical sources and identity of this material, but also potentially the major mechanisms of ON preservation in the sedimentary record. Here we consider three possibilities that might explain the low $\delta^{15}N_{AI}$ values, in context of an assumed refractory organic fraction: partial hydrolysis during degradation, direct preservation of microbial remains or biosynthate, and finally selective preservation of proteinaceous vs. non-proteinaceous of algal or other nitrogen sources.

**Partial hydrolysis and deamination of proteinaceous-like material**

Several authors have shown that partial or incomplete hydrolysis of protein results in carbon and nitrogen isotopic fractionation of residual protein (Bada et al., 1989; Silfer et al., 1992). Therefore, at least for the proteinaceous fraction of AI, partial microbial degradation might represent one mechanism for changing relative $\delta^{15}N$ values. This effect has been hypothesized to account, at least in part, for more refractory dissolved organic nitrogen $\delta^{15}N$ values (Knapp et al., 2010; Knapp et al., 2011; Knapp et al., 2012), and more recently for major changes in $\delta^{15}N$ value of suspended ocean particulate organic matter (Hannides et al., 2013). The hypothesis is based on observations that partial hydrolysis of amide bonds preferentially remove the *light* isotope, leaving a residual (and presumed more refractory) material with *higher* $\delta^{15}N$ values. The degree of nitrogen isotopic fractionation during deamination has been estimated with fractionation factors, $\varepsilon$, which range from 2.5 to 5.5‰

115

(Macko et al., 1986; Bada et al., 1989; Silfer et al., 1992; Hannides et al., 2013), magnitudes that are generally similar to $\Delta\delta^{15}N_{AI-TN}$.

However, while these $\varepsilon$ values are similar in magnitude to the $\delta^{15}N$ offset of AI vs. total sedimentary ON, the *direction* of fractionation expected from partial hydrolysis is the opposite from our observations for the AI pool:  the AI material is presumed to be the residual, more refractory material, yet it has the *lower* $\delta^{15}N$ values, compared to all other ON fractions (Fig. 2.4).  Therefore, partial hydrolysis would seem highly unlikely as an explanation for isotopically light AI.

**Microbial sources**

A second general explanation for low $\delta^{15}N_{AI}$ might invoke preferential preservation of either multiple biochemical classes or proteinaceous nitrogen sources, each with characteristic offsets in their $\delta^{15}N$ values.  Microbial derived material (Rogers, 1974; McCarthy et al., 1997, 1998; Hedges et al., 2000), might represent one such possible source of isotopically distinct material. However, while microbial resynthesis in the water column or sediments is likely, several factors suggest that this is also an unlikely explanation for the overall low $\delta^{15}N_{AI}$ values. First, amino acid derived parameters for microbial degradation and resynthesis show little evidence of either process in these same sediments (Batista et al, 2014).  Further, while peptidoglycan has been suggested as an important, likely more refractory, nitrogen component "growing in" to sediments (Grutters et al., 2002), most nitrogen in peptidoglycan is derived from several interbridge amino acids in the $\delta^{15}N$-AA "Trophic" AA group (Ala, Glu, and Asp; e.g., Brock et al., 1994; McCarthy et al.,

1998; Hedges et al., 2000).  Based on typical $\delta^{15}$N-AA patterns (e.g., McCarthy et al., 2013), one would expect these AA, and so this source of N, to have *elevated* (as opposed lower) $\delta^{15}$N values, compared to the total THAA pool.

Finally, prior studies have suggested either no $\delta^{15}$N change linked to heterotrophic microbial resynthesis of ON, or else *increased* $\delta^{15}$N values (generally analogous to an additional trophic level; e.g., Macko et al 1986, McCarthy et al., 2007; Calleja et al, 2013).

Whiles these arguments together suggest microbial sources as unlikely explanations for low $\delta^{15}$N$_{AI}$ values, it is possible that microbial production supported by in-situ IN sources might lead to production of lower $\delta^{15}$N of organic material. Some microbial communities incorporate dissolved ammonia, for example, ammonia oxidizing bacteria (Keil and Kirchman, 1991).  If microbial production is reliant on bioavailable nitrogen from degradation of ON, microbial biomass would be expected to have lower $\delta^{15}$N values relative to bulk ON (Wada et al., 1980; Libes and Deuser, 1988; Lehmann et al., 2002; Mobius 2013).  Thus, this pathway might conceivably contribute to microbial biomass with lower $\delta^{15}$N values and in the AI fraction.

Finally, however, a basic problem underlying any direct bacterial-source explanation is that it would require that new bacterial biosynthate "growing in" to sediments would concentrated in the AI fraction: i.e., that arguably one of the "freshest" material pools in the sediment (recently produced bacterial biomass) would also be operationally the most resistant to analysis.  Numerous studies have indicated that live microbial biomass is not a significant fraction of sedimentary organic matter

(Kallmeyer and Pockalny, 2012; Carr et al., 2013), and as noted above THAA-based

degradation and bacterial resynthesis parameters in these same sediments indicate

little microbial contribution (Batista et al., 2014). Even if water column microbial

sources were preferentially preserved, such as in cell walls (Grutters et al., 2002;

Werner and Schmidt, 2002; Nguyen et al., 2003), this source therefore offers no

obvious explanation for *lower* $\delta^{15}N_{AI}$ values.

**Selective preservation of algal or terrestrial production**

Taken together, the previously discussed $\Delta\delta^{15}N$ offsets, and in particular the

observed similar $\Delta\delta^{15}N_{AS—TN}$ values for fresh autotrophic biomass, suggest selective

preservation of primary production sources (with more negative $\delta^{15}N$ values) as

perhaps the most plausible explanation for low $\delta^{15}N_{AI}$ values. However, we reiterate

that low $\delta^{15}N_{Bound}$ values also are an additional possible source of inorganic N that

might contribute to the low $\delta^{15}N_{AI}$ values, but as per our discussion above (Section

5.5) is difficult to precisely constrain. However, if we assume that AI nitrogen is

mainly organic, and is further dominated by amide functionality (as has been

discussed above in Section 4.1), and then this in turn suggests three basic possibilities

for AI N source.

The first is that non-proteinaceous material (such as amino sugar) might be far

more important component of AI, and so of total sedimentary ON, than is currently

unrecognized. We have also hypothesized this one possible explanation for the $\delta^{15}N$

values of the AS fraction (Section 4.4.1), and an overlap in composition for these

pools might be expected. However, the substantially lower $\delta^{15}N$ values for the AI

(vs. AS) fraction would seem to require non-proteinaceous material to make up a far greater proportion in AI. As discussed above for the AS fraction, the fact that complex heteropolysaccharide material exists in many sample types which cannot be quantified at the molecular level (Kaiser and Benner, 2008, 2009) is consistent with the idea of amino sugars as an AI component. Similarly, it has been shown that during hydrolysis and degradation of peptidoglycan, the polysaccharide moieties (amino sugar) preferentially remain, while the proteinaceous interbridge components are much more rapidly remineralized (Nagata et al, 2003). Protection by minerals, or other associations, clearly could also play a role (i.e., Keil et al., 1994; Lalonde et al., 2012; Keil and Mayer, 2014).

To our knowledge, there is no data that can clearly constrain this hypothesis for sediments. The two existing CPMAS $^{13}$C NMR spectral studies for sedimentary AI fractions suggest quite different results in different environments: in a well preserved, demineralized organic-rich sapropel, the CPMAS $^{13}$C NMR spectra of AI is complex (Knicker and Hatcher, 2001), with multiple functional groups consistent with a mixture of many biochemical classes, allowing for potentially important contributions by both amino sugar and proteinaceous nitrogen contributions. In contrast, CPMAS $^{13}$C NMR spectra for AI from demineralized sediments on a deeper California margin site are very different, showing dominance by only lipid-like material (Hwang et al., 2006). In this environment, any contribution of either carbohydrate or proteinaceous material would have to be relatively small, at least in terms of total carbon, so as to be obscured by the much larger aliphatic and aromatic

carbon resonances. However, we note that such carbon spectra probably provide only poor constraint for the much smaller nitrogenous AI component.

A second possibility consistent with assumed amide functionality is similar to that discussed above, e.g., that AI proteinaceous material had very different $\delta^{15}N$ values from AS proteinaceous material. As noted above in the discussion on microbial sources, one might hypothesize, for example, that some cellular fraction (e.g., cell walls) could be preferentially preserved in the refractory AI material, relative to more labile organic matter components (Macko et al., 1986; Grutters et al., 2002; Werner and Schmidt, 2002), with characteristic $\delta^{15}N$ offsets as well as different lability to acid hydrolysis. However, given that the available evidence (i.e., consistent $\Delta\delta^{15}N$ offsets in all fractions and samples) seems to point to a water column source (rather than direct microbial sources, or sedimentary diagenesis), we find this hypothesis unlikely. Further, there is no theoretical basis for this kind of partitioning of proteinaceous $\delta^{15}N$ values among algal intracellular components, based on current understanding of amino acid $\delta^{15}N$ fractionation patterns in algae (McCarthy et al., 2013).

Finally, terrestrial N sources are *generally* expected to have lower $\delta^{15}N$ compared with marine material (Sweeney and Kaplan, 1980; Schubert and Calvert, 2001; Keinast et al. 2005; Hatten et al., 2012). However, terrestrial plants also can have a very wide range of $\delta^{15}N$ from ~-5 to +18‰, with an average around 3‰ (Muller and Voss, 1999), limiting the use of generalized $\delta^{15}N$ endmembers as an indicator of OM sources in coastal settings. However, other bulk properties of terrestrial OM typically

are more predictable, such as lower $\delta^{13}C$ values and higher C/N values relative to marine OM (i.e., Prahl et al., 1994; Brodie et al., 2011a, 2011b, 2011c and references therein).  Based on these metrics, Batista et al. (2014) suggested that terrestrial input into total OM of these sediments is minor.

However, extensions of conclusions based on bulk sedimentary properties to the AI fraction are not necessarily clear-cut.  While the C/N values and $\delta^{13}C$ values of the AI fraction (ca. 16 and ca. -24‰, respectively) do not suggest pure terrestrial material, neither do they rule out terrestrial contribution (Fig. 2.3 and 2.5).  The only past study measuring compound-specific $\delta^{13}C$ amino acids ($\delta^{13}C$-AA) from riverine sources and marine sediments showed that $\delta^{13}C$-AA patterns are highly effective tracers for terrestrial AA (Keil and Fogel, 2001).  However, the same study also indicated that marine AA very rapidly replaced terrestrial AA, at least in the hydrolysable fraction: beyond direct riverine sediment deposit regions, terrestrial AA contributions rapidly became negligible.  Similar conclusions about rapid replacement of terrestrial with marine material in ocean shelf sediments have been reached in multiple studies using multiple tracers (e.g., Hedges, Keil, and Benner, 1997; Keil and Fogel, 2001; Careddu et al., 2015).  Together, such data suggests that a dominant terrestrial amide component in the AI fraction is unlikely.

Overall, of these three possibilities, while selective preservation of a low $\delta^{15}N_{AI}$ component derived from primary production seems the most likely explanation for $\delta^{15}N_{AI}$ values, we stress that current data cannot unambiguously constrain either the ultimate AI nitrogen source or its biochemical identity.  The potential for a currently

121

unappreciated hydrolysis-resistant carbohydrate component of AI, which might contribute to its low $\delta^{15}$N values vs. the proteinaceous pool, would need to be further investigated, possibly using coupled NMR and isotopic approaches. At the same time, we also cannot unambiguously rule out some terrestrial contribution (either organic or inorganic) to AI nitrogenous material. Unambiguously constraining any IN component directly in the AI fraction, as well as devising ways to target specifically terrestrially-derived ON functionality, would substantially narrow the field of potential AI nitrogen sources.

**Summary and Conclusions**

This study represents a first attempt to couple $\delta^{15}$N measurements with isolation of major labile vs. refractory organic matter fractions in marine sediments. Combined with both quantitative measurement and $\delta^{15}$N values of sedimentary proteinaceous material (THAA), extractable lipids, and inorganic sedimentary N, our overarching goal was to constrain both molecular character and relative $\delta^{15}$N values of major sedimentary ON pools. While past spectroscopic and molecular-level analyses have indicated proteinaceous material as likely dominating organic nitrogen in recent sediments, recently direct $\delta^{15}$N measurements on sedimentary proteinaceous material showed large and consistent offsets vs. total ON $\delta^{15}$N values. A main goal here was therefore to investigate the implications of this finding, by making direct $\delta^{15}$N measurements on multiple sedimentary organic N fractions, to constrain the relative contribution of proteinaceous N to both refractory and labile ON pools. We measured the relative abundance and stable isotopic ratios of four major operational

components of sedimentary organic matter: lipid, AS, AI, and THAA. We used these data to assess sources and composition of sedimentary ON which underlie bulk sediment $\delta^{15}$N values.

Relative carbon yields and $\delta^{13}$C values for the AS, AI, lipid and THAA fractions provided context directly comparable with past studies, and the similarity between our results and prior work suggests that fractions isolated from SBB sediments are broadly similar to those in other sediment systems. Specifically, our carbon data supports the conclusion that the AS fraction is dominated by labile major biochemicals (amino acids and carbohydrates; i.e., Hwang and Druffel, 2003), while AI values represent the more refractory material. The carbon isotope and recovery data also support lipid-like material as dominating the AI fraction (Hwang and Druffel, 2003), however our $\delta^{15}$N data on extractable lipids vs. AI suggests that refractory nitrogenous fraction is not lipid, and so likely has separate biochemical sources. Overall, however, the carbon data support the framework that AS represents more labile, fresher biochemicals, while AI represents more refractory, hydrolysis resistant sedimentary material (Hwang et al., 2006).

We observed significant diversity in $\delta^{15}$N values of sedimentary ON fractions, suggesting substantial diversity in either biochemical makeup, and/or partitioning, of sedimentary nitrogenous compounds. The AS fraction represents total hydrolysable material, and together with its low C/N ratio (~4) this suggested that "labile" AS nitrogen should be mostly hydrolysable AA. However, the large $\delta^{15}$N offsets between these fractions ($\Delta\delta^{15}$N$_{THAA-AS}$ of ~2 - 4‰) confirms that most nitrogen in

sedimentary AS must be non-proteinaceous. We have hypothesized that either amino sugars and/or inorganic N as the most likely alternate organic vs. inorganic N sources to AS. Because bound IN is liberated during hydrolysis, constitutes ~13% of TN in these sediments, and was found to have low $\delta^{15}N$ values (~5‰), we have hypothesized that IN may account for both low C/N ratios and low $\delta^{15}N$ values. If correct, this means that, in contrast to past work based on carbon, nitrogen content and isotopic ratios of the sedimentary AS fraction probably cannot be directly interpreted as representing labile organic N. However, further experiments to directly quantify IN source in AS would be required to verify this conclusion.

Our data for the AI fraction is consistent with this material representing the most refractory ON in sediments, and so is perhaps of most interest for understanding what controls the long-term removal of organic nitrogen from the oceans. AI was the largest ON fraction in our sediments, and was also the most constant in terms of both its contribution to TN and its $\delta^{15}N$ value. The large offsets we observed between $\delta^{15}N_{AI}$ and $\delta^{15}N_{THAA}$ values strongly suggest that non-proteinaceous organic dominates refractory sedimentary ON pool. This comparison therefore argues against some common hypotheses for ON preservation, such as protection of proteinaceous material (e.g., encapsulation), or minor structural modification of individual AA. While such mechanisms might influence yields, neither would be expected to strongly alter $\delta^{15}N$ values. Further, assuming that prior data indicating that sedimentary AI fraction (like bulk ON) is dominated by amide nitrogen is correct, then our new

isotopic data pose a conundrum: what accounts for the large $\delta^{15}N$ offset between sedimentary proteinaceous material, and the AI fraction?

While our data cannot unambiguously answer this question, comparison between our isolated fractions in water column vs. sediments strongly suggests the preservation of non-proteinaceous organic nitrogen, likely originating from primary production. This conclusion is supported by similar offsets observed between $\delta^{15}N_{THAA}$ and $\delta^{15}N_{AI}$ in both sediments and SBB yearly-integrated trap sample, but also by compiled past data from cultured plankton. Together, these observations suggest that at least for SON in this high preservation environment, selective preservation of nitrogenous biochemicals having characteristically lower $\delta^{15}N$ values (vs. proteinaceous material) is the most likely explanation for low $\delta^{15}N_{AI}$ values. We have hypothesized that hydrolysis-resistant amino sugars are the nitrogenous biochemical class most consistent with past NMR data, however at the same time this would conflict with low molecular level yields. While we cannot unambiguously rule out terrestrial contributions, $\delta^{13}C$ data suggests this explanation as unlikely to be the major one.

Taken together, our data clearly demonstrate the importance of independently considering the composition and cycling of labile vs. refractory organic nitrogen components. Specifically, our results suggest that total sedimentary ON $\delta^{15}N$ values are likely strongly dependent on the relative contributions of these two operational fractions (i.e., AS vs. AI), which in turn may be differently linked to water column sources of proteinaceous vs. non-proteinaceous nitrogenous compounds. We suggest

125

that a main goal for future work should be to devise approaches which can reveal the nature of non-proteinaceous ON, in particular in the refractory (AI) fraction. For example, coupled with isotopic measurements, linked carbon and nitrogen solid-state NMR might provide the most direct way to test ideas about AI composition, in particular to confirm or rule out potential contributions by amino sugars, or poly-amines. In addition, rapidly evolving compound-specific $\delta^{13}$C-AA fingerprinting approaches could directly test terrestrial (e.g., Larsen et al., 2012) vs. bacterial (e.g., Larsen et al., 2015) contributions, at least to the proteinaceous pool. We suggest that such approaches, coupled with hydrolytic separation into labile vs. refractory ON fractions, will represent a powerful new analytical approach toward both composition and stable nitrogen isotope values of total sedimentary nitrogen.

**Acknowledgements**

# References

Aluwihare, L.I. and Meador, T. (2008) CHEMICAL COMPOSITION OF MARINE DISSOLVED ORGANIC NITROGEN. Nitrogen in the Marine Environment, 2nd Edition, 95-140.

Bada, J.L., Schoeninger, M.J. and Schimmelmann, A. (1989) Isotopic Fractionation during Peptide-Bond Hydrolysis. Geochimica Et Cosmochimica Acta 53, 3337-3341.

Barron, J.A., Bukry, D. and Field, D. (2010) Santa Barbara Basin diatom and silicoflagellate response to global climate anomalies during the past 2200 years. Quaternary International 215, 34-44.

Batista, F.C., Ravelo, A.C., Crusius, J., Casso, M.A. and McCarthy, M.D. (2014) Compound specific amino acid delta N-15 in marine sediments: A new approach for studies of the marine nitrogen cycle. Geochimica Et Cosmochimica Acta 142, 553-569.

Benner, R. and Kaiser, K. (2003) Abundance of amino sugars and peptidoglycan in marine particulate and dissolved organic matter. Limnology and Oceanography 48.

Bianchi, T.S. and Canuel, E.A. (2011) Chemical Biomarkers in Aquatic Ecosystems. Chemical Biomarkers in Aquatic Ecosystems, 1-396.

Bridoux, M.C., Annenkov, V.V., Menzel, H., Keil, R.G. and Ingalls, A.E. (2011) A new liquid chromatography/electrospray ionization mass spectrometry method for the analysis of underivatized aliphatic long-chain polyamines: application to diatom-rich sediments. Rapid Communications in Mass Spectrometry 25, 877-888.

Brock, T.D., Madigan, M.T., Martinko, J.M., Parker, J., Brock, T.D., Madigan, M.T., Martinko, J.M. and Parker, J. (1994) Biology of microorganisms, Seventh edition. Biology of microorganisms, Seventh edition, xvii+909p-xvii+909p.

Brodie, C.R., Casford, J.S.L., Lloyd, J.M., Leng, M.J., Heaton, T.H.E., Kendrick, C.P. and Zong, Y.Q. (2011a) Evidence for bias in C/N, delta C-13 and delta N-15 values of bulk organic matter, and on environmental interpretation, from a lake sedimentary sequence by pre-analysis acid treatment methods. Quat. Sci. Rev. 30, 3076-3087.

Brodie, C.R., Heaton, T.H.E., Leng, M.J., Kendrick, C.P., Casford, J.S.L. and Lloyd, J.M. (2011b) Evidence for bias in measured delta N-15 values of terrestrial and aquatic organic materials due to pre-analysis acid treatment methods. Rapid Communications in Mass Spectrometry 25, 1089-1099.

Brodie, C.R., Leng, M.J., Casford, J.S.L., Kendrick, C.P., Lloyd, J.M., Zong, Y.Q. and Bird, M.I. (2011c) Evidence for bias in C and N concentrations and delta C-13 composition of terrestrial and aquatic organic materials due to pre-analysis acid preparation methods. Chem. Geol. 282, 67-83.

Calleja, M.L., Batista, F., Peacock, M., Kudela, R. and McCarthy, M.D. (2013) Changes in compound specific delta N-15 amino acid signatures and D/L ratios in marine dissolved organic matter induced by heterotrophic bacterial reworking. Marine Chemistry 149, 32-44.

Careddu, G., Costantini, M.L., Calizza, E., Carlino, P., Bentivoglio, F., Orlandi, L. and Rossi, L. (2015) Effects of terrestrial input on macrobenthic food webs of coastal sea are detected by stable isotope analysis in Gaeta Gulf. Estuarine Coastal and Shelf Science 154, 158-168.

Carr, S.A., Vogel, S.W., Dunbar, R.B., Brandes, J., Spear, J.R., Levy, R., Naish, T.R., Powell, R.D., Wakeham, S.G. and Mandernack, K.W. (2013) Bacterial abundance and composition in marine sediments beneath the Ross Ice Shelf, Antarctica. Geobiology 11, 377-395.

Carstens, D., Koellner, K.E., Buergmann, H., Wehrli, B. and Schubert, C.J. (2012) Contribution of bacterial cells to lacustrine organic matter based on amino sugars and D-amino acids. Geochimica Et Cosmochimica Acta 89.

Carstens, D. and Schubert, C.J. (2012) Amino acid and amino sugar transformation during sedimentation in lacustrine systems. Organic Geochemistry 50, 26-35.

Chen, F., Zhang, L., Yang, Y. and Zhang, D. (2008) Chemical and isotopic alteration of organic matter during early diagenesis: Evidence from the coastal area off-shore the Pearl River estuary, south China. Journal of Marine Systems 74, 372-380.

Cowie, G.L. and Hedges, J.I. (1994) Biochemical indicators of diagenetic alteration in natural organic-matter mixtures. Nature 369.

De La Rosa, J.M., Gonzalez-Perez, J.A., Hatcher, P.G., Knicker, H. and Gonzalez-Vila, F.J. (2008) Determination of refractory organic matter in marine sediments by chemical oxidation, analytical pyrolysis and solid-state (13)C nuclear magnetic resonance spectroscopy. European Journal of Soil Science 59, 430-438.

de Leeuw, J.W., Versteegh, G.J.M. and van Bergen, P.F. (2006) Biomacromolecules of algae and plants and their fossil analogues. Plant Ecology 182, 209-233.

Degens, E.T., Guillard, R.R., Sackett, W.M. and Hellebus.Ja (1968) METABOLIC FRACTIONATION OF CARBON ISOTOPES IN MARINE PLANKTON .I. TEMPERATURE AND RESPIRATION EXPERIMENTS. Deep-Sea Research 15, 1-&.

Deniro, M.J. and Epstein, S. (1977) MECHANISM OF CARBON ISOTOPE FRACTIONATION ASSOCIATED WITH LIPID-SYNTHESIS. Science 197, 261-263.

Derenne, S., Largeau, C. and Taulelle, F. (1993) Occurrence of Nonhydrolyzable Amides in the Macromolecular Constituent of Scenedesmus-Quadricauda Cell-Wall as Revealed by N-15 Nmr - Origin of N-Alkylnitriles in Pyrolysates of Ultralaminae-Containing Kerogens. Geochimica Et Cosmochimica Acta 57, 851-857.

Freudenthal, T., Wagner, T., Wenzhofer, F., Zabel, M. and Wefer, G. (2001) Early diagenesis of organic matter from sediments of the eastern subtropical Atlantic: Evidence from stable nitrogen and carbon isotopes. Geochimica Et Cosmochimica Acta 65, 1795-1808.

Gelin, F., Volkman, J.K., Largeau, C., Derenne, S., Damste, J.S.S. and De Leeuw, J.W. (1999) Distribution of aliphatic, nonhydrolyzable biopolymers in marine microalgae. Organic Geochemistry 30, 147-159.

Grutters, M., van Raaphorst, W., Epping, E., Helder, W., de Leeuw, J.W., Glavin, D.P. and Bada, J. (2002) Preservation of amino acids from in situ-produced bacterial cell wall peptidoglycans in northeastern Atlantic continental margin sediments. Limnology and Oceanography 47, 1521-1524.

Hannides, C.C., Popp, B.N., Choy, C.A. and Drazen, J.C. (2013) Midwater zooplankton and suspended particle dynamics in the North Pacific Subtropical Gyre: A stable isotope perspective. Limnol. Oceanogr 58, 1931-1946.

Hatten, J.A., Goni, M.A. and Wheatcroft, R.A. (2012) Chemical characteristics of particulate organic matter from a small, mountainous river system in the Oregon Coast Range, USA. Biogeochemistry 107, 43-66.

Hayes, J.M. (2001) Fractionation of carbon and hydrogen isotopes in biosynthetic processes. Stable Isotope Geochemistry 43, 225-277.

Hedges, J.I. (1992) GLOBAL BIOGEOCHEMICAL CYCLES - PROGRESS AND PROBLEMS. Marine Chemistry 39, 67-93.

Hedges, J.I., Baldock, J.A., Gelinas, Y., Lee, C., Peterson, M. and Wakeham, S.G. (2001) Evidence for non-selective preservation of organic matter in sinking marine particles. Nature 409, 801-804.

Hedges, J.I., Eglinton, G., Hatcher, P.G., Kirchman, D.L., Arnosti, C., Derenne, S., Evershed, R.P., Kogel-Knabner, I., de Leeuw, J.W., Littke, R., Michaelis, W. and Rullkotter, J. (2000) The molecularly-uncharacterized component of nonliving organic matter in natural environments. Organic Geochemistry 31, 945-958.

Hedges, J.I., Keil, R.G. and Benner, R. (1997) What happens to terrestrial organic matter in the ocean? Organic Geochemistry 27, 195-212.

Hedges, J.I. and Stern, J.H. (1984) Carbon and Nitrogen Determinations of Carbonate-Containing Solids. Limnology and Oceanography 29, 657-663.

Higgins, M.B., Robinson, R.S., Carter, S.J. and Pearson, A. (2010) Evidence from chlorin nitrogen isotopes for alternating nutrient regimes in the Eastern Mediterranean Sea. Earth Planet. Sci. Lett. 290, 102-107.

Huguet, C., Schimmelmann, A., Thunell, R., Lourens, L.J., Damste, J.S.S. and Schouten, S. (2007) A study of the TEX86 paleothermometer in the water column and sediments of the Santa Barbara Basin, California. Paleoceanography 22.

Hwang, J. and Druffel, E.R.M. (2006) Carbon isotope ratios of organic compound fractions in oceanic suspended particles. Geophys. Res. Lett. 33.

Hwang, J., Druffel, E.R.M., Eglinton, T.I. and Repeta, D.J. (2006) Source(s) and cycling of the nonhydrolyzable organic fraction of oceanic particles. Geochimica Et Cosmochimica Acta 70, 5162-5168.

Hwang, J., Druffel, E.R.M. and Komada, T. (2005) Transport of organic carbon from the California coast to the slope region: A study of Delta C-14 and delta C-13 signatures of organic compound classes. Global Biogeochemical Cycles 19.

Hwang, J.S. and Druffel, E.R.M. (2003) Lipid-like material as the source of the uncharacterized organic carbon in the ocean? Science 299, 881-884.

Ingalls, A.E., Whitehead, K. and Bridoux, M.C. (2010) Tinted windows: The presence of the UV absorbing compounds called mycosporine-like amino acids embedded in the frustules of marine diatoms. Geochimica Et Cosmochimica Acta 74, 104-115.

Kaiser, K. and Benner, R. (2008) Major bacterial contribution to the ocean reservoir of detrital organic carbon and nitrogen. Limnology and Oceanography 53.

Kaiser, K. and Benner, R. (2009) Biochemical composition and size distribution of organic matter at the Pacific and Atlantic time-series stations. Marine Chemistry 113.

Kallmeyer, J., Pockalny, R., Adhikari, R.R., Smith, D.C. and D'Hondt, S. (2012) Global distribution of microbial abundance and biomass in subseafloor sediment. Proc. Natl. Acad. Sci. U. S. A. 109, 16213-16216.

Keil, R.G. and Kirchman, D.L. (1991) CONTRIBUTION OF DISSOLVED FREE AMINO-ACIDS AND AMMONIUM TO THE NITROGEN REQUIREMENTS OF HETEROTROPHIC BACTERIOPLANKTON. Marine Ecology Progress Series 73, 1-10.

Keil, R.G., Mayer, L. M. (2014) Mineral Matrices and Organic Matter, in: Turekian, K.a.H., H. (Ed.), Treatise on Geochemistry, 2nd edition ed. Elsevier Ltd. , pp. 337-359.

Keil, R.G., Montlucon, D.B., Prahl, F.G. and Hedges, J.I. (1994) SORPTIVE PRESERVATION OF LABILE ORGANIC-MATTER IN MARINE-SEDIMENTS. Nature 370.

Kienast, M., Higginson, M.J., Mollenhauer, G., Eglinton, T.I., Chen, M.T. and Calvert, S.E. (2005) On the sedimentological origin of down-core variations of bulk sedimentary nitrogen isotope ratios. Paleoceanography 20, PA2009.

Knapp, A.N., Hastings, M.G., Sigman, D.M., Lipschultz, F. and Galloway, J.N. (2010) The flux and isotopic composition of reduced and total nitrogen in Bermuda rain. Marine Chemistry 120, 83-89.

Knapp, A.N., Sigman, D.M., Kustka, A.B., Sanudo-Wilhelmy, S.A. and Capone, D.G. (2012) The distinct nitrogen isotopic compositions of low and high molecular weight marine DON. Marine Chemistry 136, 24-33.

Knapp, A.N., Sigman, D.M., Lipschultz, F., Kustka, A.B. and Capone, D.G. (2011) Interbasin isotopic correspondence between upper-ocean bulk DON and subsurface nitrate and its implications for marine nitrogen cycling. Global Biogeochemical Cycles 25.

Knicker, H. (2000a) Biogenic nitrogen in soils as revealed by solid-state carbon-13 and nitrogen-15 nuclear magnetic resonance spectroscopy. Journal of Environmental Quality 29, 715-723.

Knicker, H. (2000b) Solid-state 2-D double cross polarization magic angle spinning N-15 C-13 NMR spectroscopy on degraded algal residues. Organic Geochemistry 31, 337-340.

Knicker, H. (2004) Stabilization of N-compounds in soil and organic-matter-rich sediments - what is the difference? Marine Chemistry 92, 167-195.

Knicker, H., Frund, R. and Ludemann, H.D. (1993) THE CHEMICAL NATURE OF NITROGEN IN NATIVE SOIL ORGANIC-MATTER. Naturwissenschaften 80, 219-221.

Knicker, H. and Hatcher, P.G. (1997) Survival of protein in an organic-rich sediment: Possible protection by encapsulation in organic matter. Naturwissenschaften 84, 231-234.

Knicker, H. and Hatcher, P.G. (2001) Sequestration of organic nitrogen in the sapropel from Mangrove Lake, Bermuda. Organic Geochemistry 32, 733-744.

Knicker, H. and Ludemann, H.D. (1995) N-15 AND C-13 CPMAS AND SOLUTION NMR-STUDIES OF N-15 ENRICHED PLANT-MATERIAL DURING 600 DAYS OF MICROBIAL-DEGRADATION. Organic Geochemistry 23, 329-341.

Knicker, H., Scaroni, A.W. and Hatcher, P.G. (1996) C-13 and N-15 NMR spectroscopic investigation on the formation of fossil algal residues. Organic Geochemistry 24, 661-669.

Knicker, H., Schmidt, M.W.I. and Kogel-Knabner, I. (2000) Nature of organic nitrogen in fine particle size separates of sandy soils of highly industrialized areas as revealed by NMR spectroscopy. Soil Biology & Biochemistry 32, 241-252.

Lalonde, K., Mucci, A., Ouellet, A. and Gelinas, Y. (2012) Preservation of organic matter in sediments promoted by iron. Nature 483, 198-200.

Lee, C. (2004) Transformations in the "Twilight Zone" and beyond. Marine Chemistry 92, 87-90.

Lehmann, M.F., Bernasconi, S.M., Barbieri, A. and McKenzie, J.A. (2002) Preservation of organic matter and alteration of its carbon and nitrogen isotope composition during simulated and in situ early sedimentary diagenesis. Geochimica Et Cosmochimica Acta 66, 3573-3584.

Leinweber, P. and Schulten, H.R. (2000) Nonhydrolyzable forms of soil organic nitrogen: Extractability and composition. Journal of Plant Nutrition and Soil Science-Zeitschrift Fur Pflanzenernahrung Und Bodenkunde 163, 433-439.

Li, Z. and Jia, G. (2011) Separation of total nitrogen from sediments into organic and inorganic forms for isotopic analysis. Organic Geochemistry 42, 296-299.

Libes, S.M. and Deuser, W.G. (1988) THE ISOTOPE GEOCHEMISTRY OF PARTICULATE NITROGEN IN THE PERU UPWELLING AREA AND THE GULF OF MAINE. Deep-Sea Research Part a-Oceanographic Research Papers 35, 517-533.

Lomstein, B.A., Jorgensen, B.B., Schubert, C.J. and Niggemann, J. (2006) Amino acid biogeo- and stereochemistry in coastal Chilean sediments. Geochimica Et Cosmochimica Acta 70.

Macko, S.A. and Estep, M.L. (1984) Microbial alteration of stable nitrogen and carbon isotopic compositions of organic matter. Organic Geochemistry 6, 787-790.

Macko, S.A., Estep, M.L.F., Engel, M.H. and Hare, P.E. (1986) KINETIC FRACTIONATION OF STABLE NITROGEN ISOTOPES DURING AMINO-ACID TRANSAMINATION. Geochimica Et Cosmochimica Acta 50, 2143-2146.

McCarthy, M., Pratum, T., Hedges, J. and Benner, R. (1997) Chemical composition of dissolved organic nitrogen in the ocean. Nature 390, 150-154.

McCarthy, M.D., Hedges, J.I. and Benner, R. (1998) Major bacterial contribution to marine dissolved organic nitrogen. Science 281, 231-234.

McCarthy, M.D., Lehman, J. and Kudela, R. (2013) Compound-specific amino acid delta N-15 patterns in marine algae: Tracer potential for cyanobacterial vs. eukaryotic organic nitrogen sources in the ocean. Geochimica Et Cosmochimica Acta 103, 104-120.

Minagawa, M. and Wada, E. (1984) STEPWISE ENRICHMENT OF N-15 ALONG FOOD-CHAINS - FURTHER EVIDENCE AND THE RELATION BETWEEN DELTA-N-15 AND ANIMAL AGE. Geochimica Et Cosmochimica Acta 48, 1135-1140.

Mobius, J. (2013) Isotope fractionation during nitrogen remineralization (ammonification): Implications for nitrogen isotope biogeochemistry. Geochimica Et Cosmochimica Acta 105, 422-432.

Mollenhauer, G. and Eglinton, T.I. (2007) Diagenetic and sedimentological controls on the composition of organic matter preserved in California Borderland Basin sediments. Limnology and Oceanography 52, 558-576.

Muller, A. and Voss, M. (1999) The palaeoenvironments of coastal lagoons in the southern Baltic Sea, - II. delta C-13 and delta N-15 ratios of organic matter - sources and sediments. Palaeogeography Palaeoclimatology Palaeoecology 145, 17-32.

Muller, P.J. (1977) C-N RATIOS IN PACIFIC DEEP-SEA SEDIMENTS - EFFECT OF INORGANIC AMMONIUM AND ORGANIC NITROGEN-COMPOUNDS SORBED BY CLAYS. Geochimica Et Cosmochimica Acta 41, 765-776.

Nagata, T., Meon, B. and Kirchman, D.L. (2003) Microbial degradation of peptidoglycan in seawater. Limnology and Oceanography 48, 745-754.

Nguyen, R.T., Harvey, H.R., Zang, X., van Heemst, J.D.H., Hetenyi, M. and Hatcher, P.G. (2003) Preservation of algaenan and proteinaceous material during the oxic decay of Botryococcus braunii as revealed by pyrolysis-gas chromatography/mass spectrometry and C-13 NMR spectroscopy. Organic Geochemistry 34, 483-497.

Niggemann, J. and Schubert, C.J. (2006) Sources and fate of amino sugars in coastal Peruvian sediments. Geochimica Et Cosmochimica Acta 70.

Pan, B.S., Wolyniak, C.J. and Brenna, J.T. (2007) The intramolecular delta N-15 of lysine responds to respiratory status in Paracoccus denitrificans. Amino Acids 33, 631-638.

Reimers, C.E., Lange, C.B., Tabak, M. and Bernhard, J.M. (1990) SEASONAL SPILLOVER AND VARVE FORMATION IN THE SANTA-BARBARA BASIN, CALIFORNIA. Limnology and Oceanography 35, 1577-1585.

Rogers, H.J. (1974) PEPTIDOGLYCANS (MUCOPEPTIDES) - STRUCTURE, FUNCTION, AND VARIATIONS. Annals of the New York Academy of Sciences 235, 29-51.

Roland, L.A., McCarthy, M.D. and Guilderson, T. (2008) Sources of molecularly uncharacterized organic carbon in sinking particles from three ocean basins: A coupled Delta C-14 and delta C-13 approach. Marine Chemistry 111, 199-213.

Sachs, J.P. and Repeta, D.J. (1999) Oligotrophy and nitrogen fixation during eastern Mediterranean sapropel events. Science 286, 2485-2488.

Schimmelmann, A., Lange, C.B. and Berger, W.H. (1990) CLIMATICALLY CONTROLLED MARKER LAYERS IN SANTA-BARBARA BASIN SEDIMENTS AND FINE-SCALE CORE-TO-CORE CORRELATION. Limnology and Oceanography 35, 165-173.

Schmidt, K., McClelland, J.W., Mente, E., Montoya, J.P., Atkinson, A. and Voss, M. (2004) Trophic-level interpretation based on delta N-15 values: implications of tissue-specific fractionation and amino acid composition. Marine Ecology-Progress Series 266, 43-58.

Schmidt, M.W.I., Knicker, H., Hatcher, P.G. and KogelKnabner, I. (1997) Improvement of C-13 and N-15 CPMAS NMR spectra of bulk soils, particle size fractions and organic material by treatment with 10% hydrofluoric acid. European Journal of Soil Science 48, 319-328.

Schubert, C.J. and Calvert, S.E. (2001) Nitrogen and carbon isotopic composition of marine and terrestrial organic matter in Arctic Ocean sediments: implications for nutrient utilization and organic matter composition. Deep-Sea Research Part I-Oceanographic Research Papers 48, 789-810.

Schulten, H.R. and Schnitzer, M. (1997) The chemistry of soil organic nitrogen: a review. Biology and Fertility of Soils 26, 1-15.

Schulten, H.R., SorgeLewin, C. and Schnitzer, M. (1997) Structure of "unknown" soil nitrogen investigated by analytical pyrolysis. Biology and Fertility of Soils 24, 249-254.

Sherwood, O.A., Guilderson, T.P., Batista, F.C., Schiff, J.T. and McCarthy, M.D. (2014) Increasing subtropical North Pacific Ocean nitrogen fixation since the Little Ice Age. Nature 505, 78-+.

Shigemitsu, M., Watanabe, Y.W. and Narita, H. (2008) Time variations of delta(15)N of organic nitrogen in deep western subarctic Pacific sediment over the last 145 ka. Geochem. Geophys. Geosyst. 9.

Silfer, J.A., Engel, M.H. and Macko, S.A. (1992) KINETIC FRACTIONATION OF STABLE CARBON AND NITROGEN ISOTOPES DURING PEPTIDE-BOND HYDROLYSIS - EXPERIMENTAL-EVIDENCE AND GEOCHEMICAL IMPLICATIONS. Chem. Geol. 101, 211-221.

Silfer, J.A., Engel, M.H., Macko, S.A. and Jumeau, E.J. (1991) Stable carbon isotope analysis of amino-acid enantiomers by conventional isotope ratio mass-spectrometry and combined gas-chromatography isotope ratio mass-spectrometry. Analytical Chemistry 63, 370-374.

Silva, J.A. and Bremner, J.M. (1966) DETERMINATION AND ISOTOPE-RATIO ANALYSIS OF DIFFERENT FORMS OF NITROGEN IN SOILS .5. FIXED AMMONIUM. Soil Science Society of America Proceedings 30, 587-&.

Sowden, F.J., Chen, Y. and Schnitzer, M. (1977) NITROGEN DISTRIBUTION IN SOILS FORMED UNDER WIDELY DIFFERING CLIMATIC CONDITIONS. Geochimica Et Cosmochimica Acta 41, 1524-1526.

Stevenson, F. and Cheng, C.N. (1972) ORGANIC GEOCHEMISTRY OF ARGENTINE BASIN SEDIMENTS - CARBON-NITROGEN

RELATIONSHIPS AND QUATERNARY CORRELATIONS. Geochimica Et Cosmochimica Acta 36, 653-&.

Sweeney, R.E. and Kaplan, I.R. (1980) NATURAL ABUNDANCES OF N-15 AS A SOURCE INDICATOR FOR NEAR-SHORE MARINE SEDIMENTARY AND DISSOLVED NITROGEN. Marine Chemistry 9, 81-94.

Thunell, R., Benitez-Nelson, C., Varela, R., Astor, Y. and Muller-Karger, F. (2007) Particulate organic carbon fluxes along upwelling-dominated continental margins: Rates and mechanisms. Global Biogeochemical Cycles 21.

Thunell, R.C. (1998) Particle fluxes in a coastal upwelling zone: sediment trap results from Santa Barbara Basin, California. Deep-Sea Research Part Ii-Topical Studies in Oceanography 45, 1863-1884.

Vairavamurthy, A. and Wang, S. (2002) Organic nitrogen in geomacromolecules: Insights on speciation and transformation with K-edge XANES spectroscopy. Environmental Science & Technology 36, 3050-3056.

Wakeham, S.G., Lee, C., Hedges, J.I., Hernes, P.J. and Peterson, M.L. (1997) Molecular indicators of diagenetic status in marine organic matter. Geochimica Et Cosmochimica Acta 61.

Walker, B.D. and McCarthy, M.D. (2012) Elemental and isotopic characterization of dissolved and particulate organic matter in a unique California upwelling system: Importance of size and composition in the export of labile material. Limnology and Oceanography 57, 1757-1774.

Wang, X.C. and Druffel, E.R.M. (2001) Radiocarbon and stable carbon isotope compositions of organic compound classes in sediments from the NE Pacific and Southern Oceans. Marine Chemistry 73, 65-81.

Wang, X.C., Druffel, E.R.M., Griffin, S., Lee, C. and Kashgarian, M. (1998) Radiocarbon studies of organic compound classes in plankton and sediment of the northeastern Pacific Ocean. Geochimica Et Cosmochimica Acta 62, 1365-1378.

Wang, X.C., Druffel, E.R.M. and Lee, C. (1996) Radiocarbon in organic compound classes in particulate organic matter and sediment in the deep northeast Pacific Ocean. Geophys. Res. Lett. 23, 3583-3586.

Werner, R.A. and Schmidt, H.L. (2002) The in vivo nitrogen isotope discrimination among organic plant compounds. Phytochemistry 61, 465-484.

White, H.K., Reddy, C.M. and Eglinton, T.I. (2007) Relationships between carbon isotopic composition and mode of binding of natural organic matter in selected marine sediments. Organic Geochemistry 38, 1824-1837.

Zhang, L. and Altabet, M. (2008) Amino-group-specific natural abundance nitrogen isotope ratio analysis in amino acids. RAPID COMMUNICATIONS IN MASS SPECTROMETRY, 559-566.
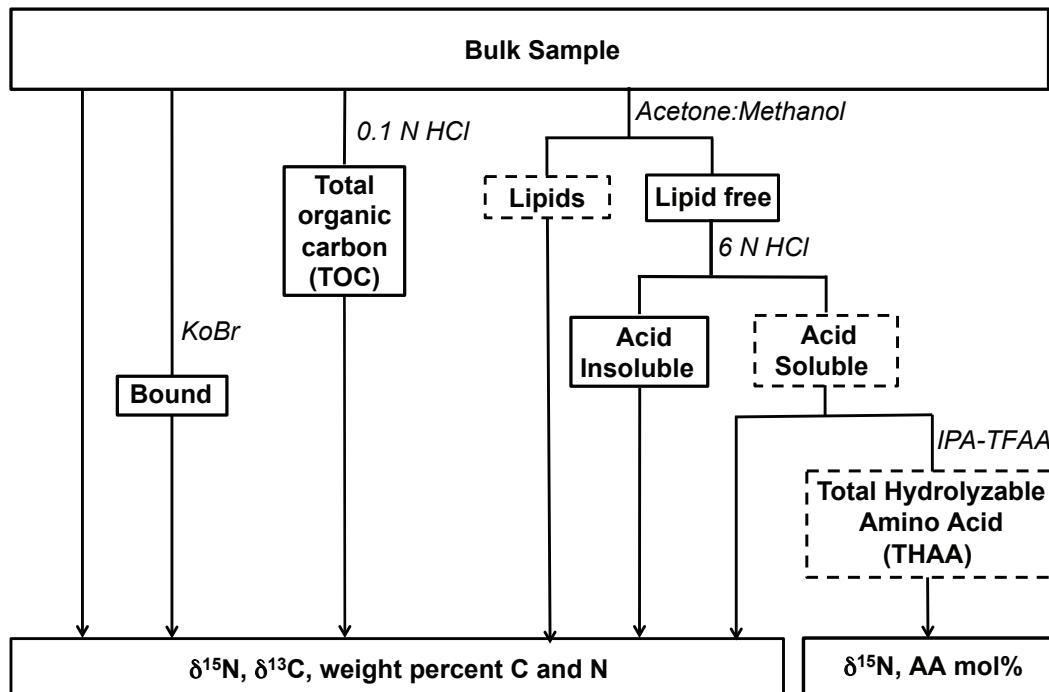
**Figure 2.1 Flow chart of the extraction procedure for isolating major operational fractions of carbon and nitrogen from the untreated, freeze-dried samples (bulk fraction).**
Total carbon and nitrogen content in all samples was accounted for by inorganic (Bound) and organic (Acid-insoluble, Acid Soluble, THAA and Lipid) operational fractions. Total carbon and nitrogen content was also determined on the bulk fraction. Analyses were performed on dried, homogenized aliquots of liquid extractions or solid residues.
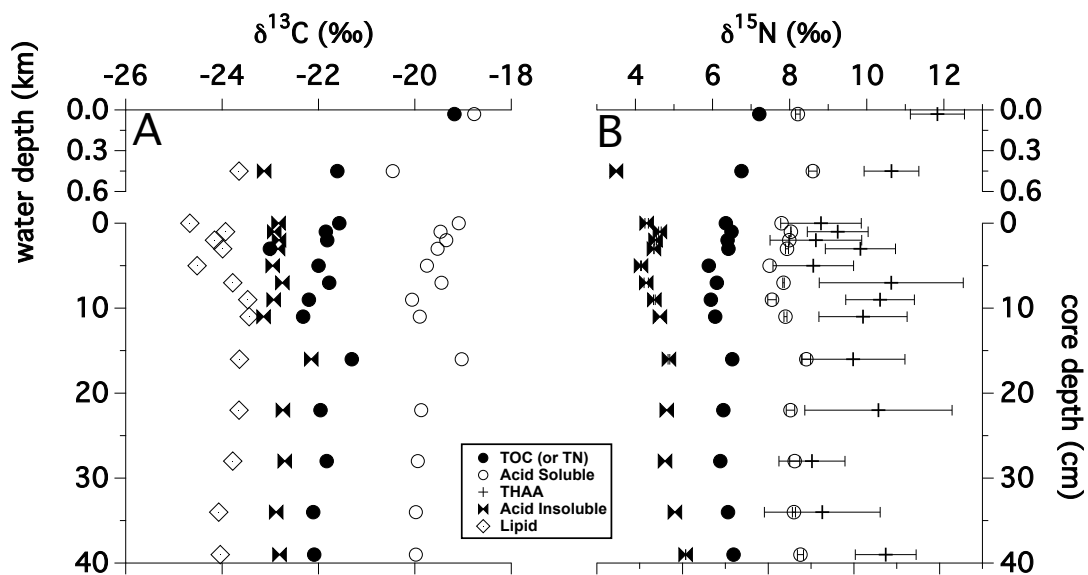
**Figure 2.2. Relative abundance of carbon and nitrogen in operational fractions of water column vs. sedimentary samples.**
Top vertical axis (water column depth): plankton tow and sinking POM; Bottom vertical axis (core depth): shallow sediment intervals. Fraction abbreviations as defined in text (methods) and Fig. 2.1. Sample fractions were analyzed for their relative contribution to sample TOC and TN (Table 3): acid-soluble (circle), acid-insoluble (double triangle), total hydrolysable amino acid (plus) and extractable lipid (diamond).
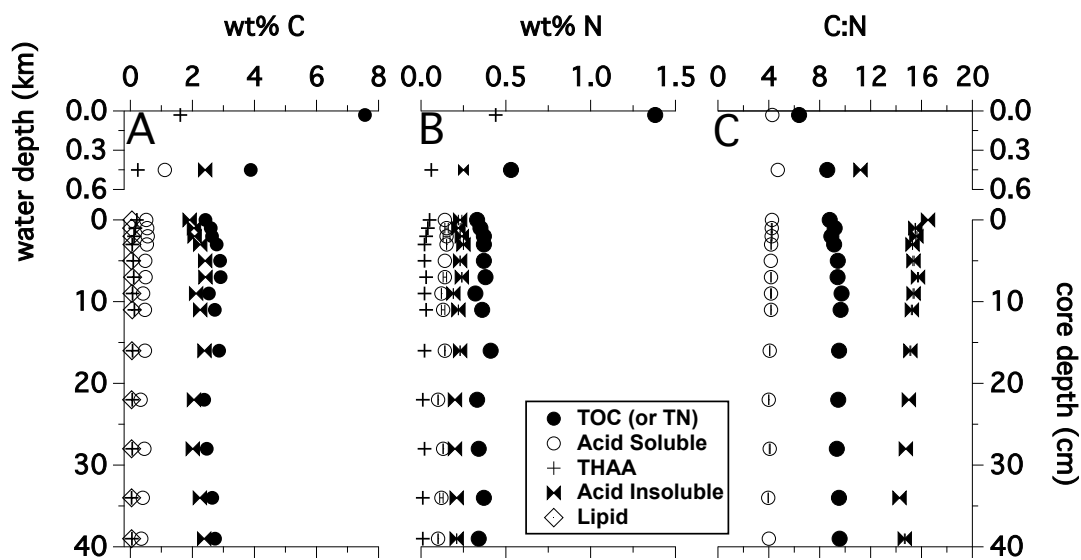
**Figure 2.3. Elemental composition represented by each operational organic fraction.**
Weight percent of carbon (A), nitrogen (B), and the measured C/N ratio (C) for organic fractions of water column (top vertical axis) and sediment (bottom vertical axis) samples. Abbreviations for each fraction are the same as in Materials and methods and Fig. 2.1. Weight percent carbon and nitrogen values indicate percentage of C and N represented by each measured organic class relative to the mass of untreated sample; specific values are also reported in Table EA 2.1, while C/N ratio values are summarized in Table 2.2.
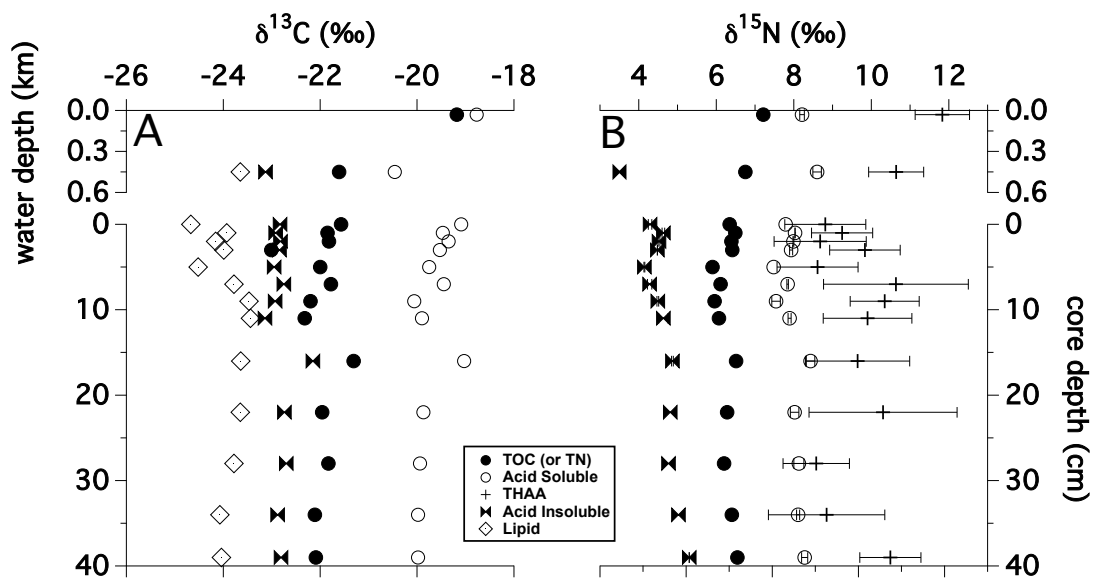
**Figure 2.4. δ¹³C and δ¹⁵N composition of water column and sedimentary organic matter.**
Stable carbon (left) and nitrogen (right) isotopic compositions for fractions of water column (top vertical axis) and sedimentary samples (bottom vertical axis). The δ¹³C and δ¹⁵N values for each fraction are given in Table 2.4.
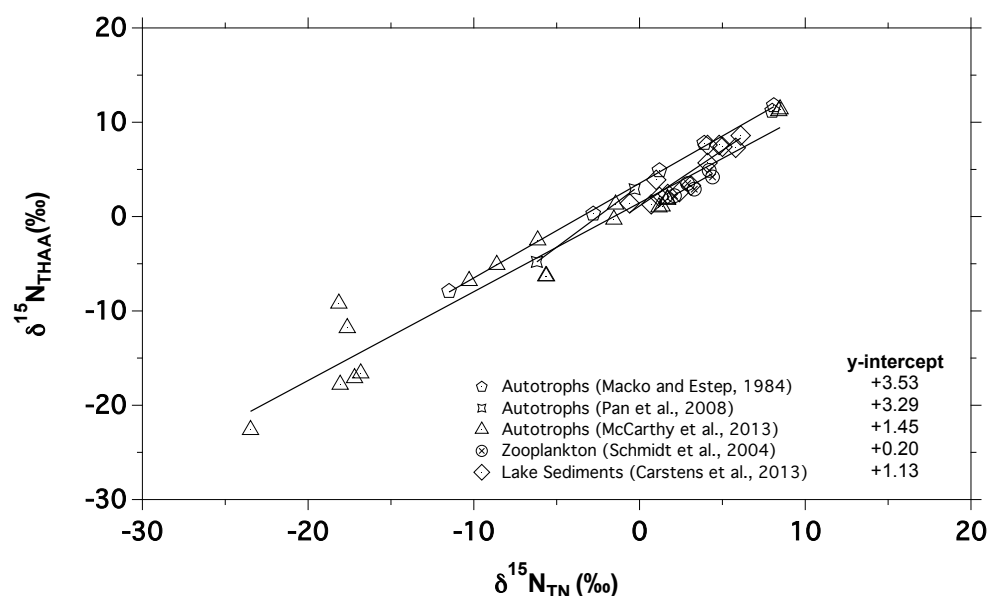
**Figure 2.5.** $\delta^{15}$N offset between THAA and TN in biomass of primary and secondary organisms and sedimentary organic matter.

A broadly observed $\delta^{15}$N offset ($\Delta\delta^{15}$N) of total N (TN) and the total hydrolysable amino acid (THAA) fraction in autotrophs, zooplankton, and lacustrine sediments. The y-intercept represents the relative mean $\delta^{15}$N offset of THAA over TN (i.e., $\Delta\delta^{15}N_{THAA—TN}$) in these samples.

**Electronic Annex**

**Nitrogen content and $\delta^{15}N$ composition of the THAA fraction**

The $\delta^{15}N$ composition of the THAA fraction, as well as the fraction of total N recoverable as individual AA, was determined by analysis of TFA-IPA esters of individual amino acids (AA), at UCSC. THAA nitrogen is defined as the sum of nitrogen yield for each of 16 individual AA (per gram of sample). The $\delta^{15}N$ of the THAA fraction is then calculated as the sum of individual AA $\delta^{15}N$ values, weighted by the mole % for each individual AA. Gas chromatography mass spectrometry (GC/MS) and continuous flow gas chromatography isotope ratio mass spectrometry (GC/C/IRMS) conditions were as described previously (Batista et al., 2014). Briefly aliquots of derivatized sample were injected on an Agilent 7890A/5977B GC/MS (Agilent Technologies, USA) for nitrogen content (and mole %), and injected on a Thermo Trace GC Ultra with GC PAL autosampler (CTC analytics) coupled to a Thermo Finnigan GC/C-III and Delta[Plus] XP isotope ratio mass spectrometer (Thermo Finnigan, USA) for $\delta^{15}N$ analysis.

Chromatographic conditions, details of AA nitrogen quantitation and isotopic standard corrections have also been described previously (Sherwood et al., 2014; McCarthy et al., 2013; Batista et al., 2014). Briefly, chromatographic conditions for analysis by GC/MS and GC/C/IRMS used 1 μL of sample injected onto a Forte BPX-5 capillary column (60 m x 0.32 mm x 1.0 μm film thickness) at an injector temperature of 250°C with constant helium flow rate. The GC oven was held at 70°C for 1 min, increased to 185°C at 10°C min^{-1}, held for 2 min, then increased at 2°C

min$^{-1}$ to 200°C and held for 10 min and finally increased to 300°C at 30°C min$^{-1}$, then held for 5 min.

An internal standard (nor-leucine) of known concentration and $\delta^{15}$N composition was added to each THAA fraction prior to conversion to TFA-IPA esters. The internal standard was used to track relative yield of nitrogen for individual AA from each sample and to confirm quality of the semi-stable ester during $\delta^{15}$N analysis. An external standard was used to generate a calibration series for quantitation of THAA nitrogen with the GC/MS. The external standard was a mixture of 16 common protein amino acids, each with known concentration and $\delta^{15}$N composition, was used as a calibration series for GC/MS quantitation of THAA nitrogen and for calibration of individual AA $\delta^{15}$N values. For $\delta^{15}$N analysis, each sample was injected and analyzed in quadruplicate with an average standard deviation of ±1.1‰ for each AA based on a minimum of three injections. Detailed explanations of both GC/MS and GC/IRMS protocols can be found in Batista et al. (2014).
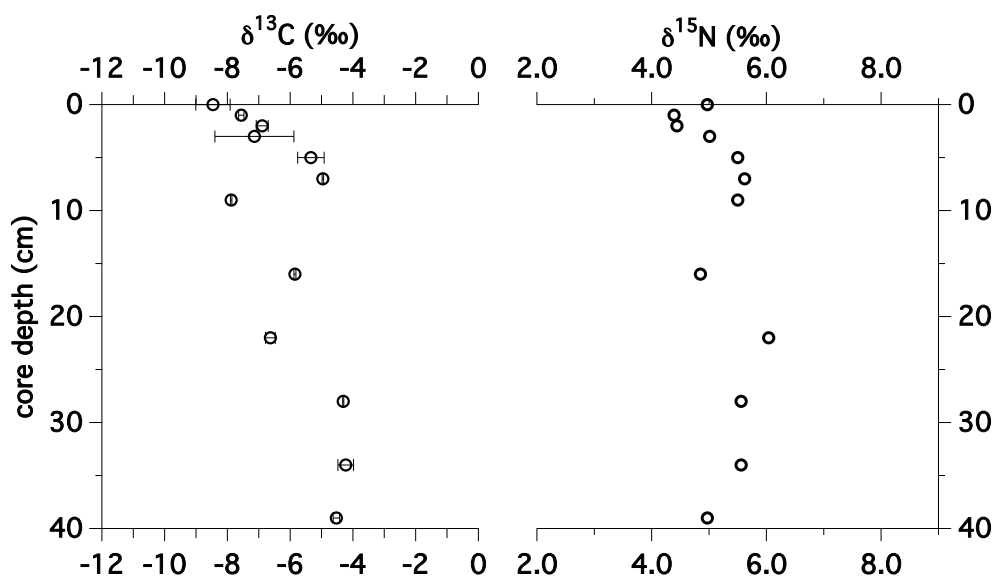
**Figure EA 2-1. Stable carbon and nitrogen isotopic composition of the Bound fraction determined in sediment intervals.**
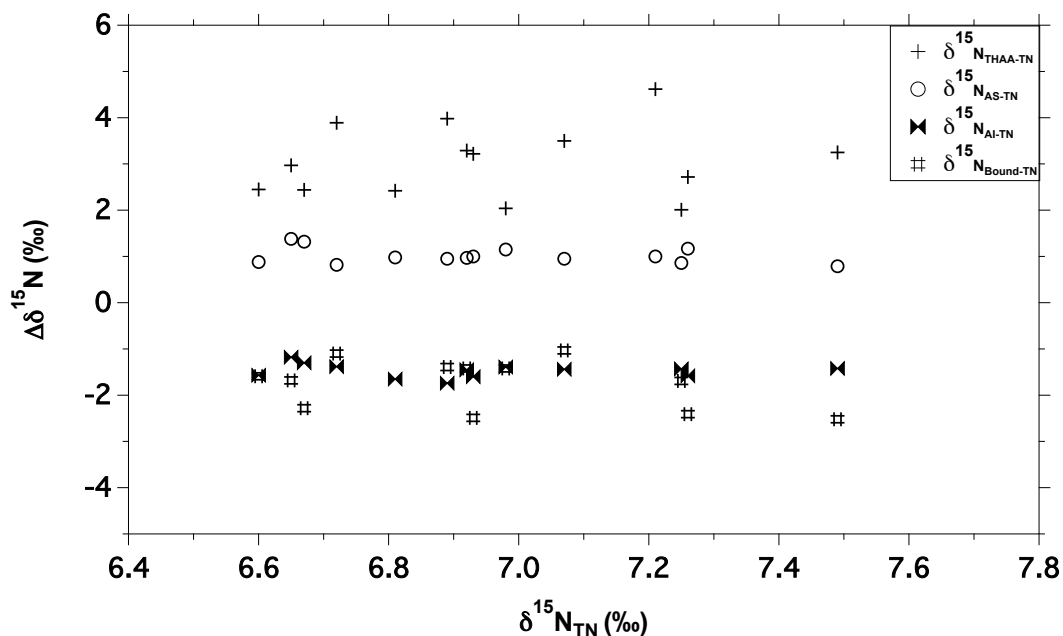


**Figure EA 2-2.  $\delta^{15}N_{TN}$ vs. $\Delta\delta^{15}N$ for each operational organic fraction.** $\delta^{15}N$ of total nitrogen (TN) versus $\delta^{15}N$ offsets ($\Delta\delta^{15}N$) between sedimentary fractions of total hydrolysable amino acid (THAA; $\Delta\delta^{15}N_{THAA—TN}$; plus), acid-soluble (AS; $\Delta\delta^{15}N_{AS—TN}$; circle), acid-insoluble (AI; $\Delta\delta^{15}N_{AI—TN}$; double diamond), bound ($\Delta\delta^{15}N_{Bound—TN}$; #) nitrogen relative to TN.

146

**Table EA 2-1. Elemental composition for isolated fractions reported***

| Sample | Weight percent carbon | | | | | | | Weight percent nitrogen | | | | |
|---|---|---|---|---|---|---|---|---|---|---|---|---|
| | Bulk | TOC | Lipids | Acid Soluble | THAA[a] | Acid Insoluble | Bound | Bulk | Acid Soluble | THAA | Acid Insoluble | Bound |
| Plankton tow | n.d. | 7.56 | n.d. | 1.93 | 1.61 | n.d. | n.d. | 1.38 | 0.44 | 0.44 | n.d. | n.d. |
| Sediment trap | n.d. | 3.70 | n.d. | 1.11[b] | 0.24 | 2.41[b] | n.d. | 0.53 | 0.28[b] | 0.06 | 0.25[b] | n.d. |
| MC 0 cm | 3.01 | 2.42 | 0.05 | 0.51 | 0.21 | 1.91 | 0.59 | 0.33 | 0.14 | 0.05 | 0.23 | 0.05 |
| MC 1 cm | 3.39 | 2.59 | 0.04 | 0.54 | 0.16 | 2.05 | 0.80 | 0.35 | 0.15 | 0.04 | 0.22 | 0.04 |
| MC 2cm | 3.49 | 2.63 | 0.05 | 0.56 | 0.12 | 2.07 | 0.86 | 0.37 | 0.15 | 0.03 | 0.24 | 0.05 |
| MC 3 cm | 3.79 | 2.78 | 0.05 | 0.53 | 0.06 | 2.25 | 1.01 | 0.37 | 0.15 | 0.02 | 0.25 | 0.04 |
| MC 5 cm | 3.93 | 2.89 | 0.04 | 0.48 | 0.09 | 2.41 | 1.04 | 0.37 | 0.14 | 0.02 | 0.23 | 0.05 |
| MC 7 cm | 4.11 | 2.91 | 0.07 | 0.49 | 0.11 | 2.42 | 1.20 | 0.38 | 0.14 | 0.03 | 0.24 | 0.05 |
| MC 9 cm | 3.52 | 2.53 | 0.05 | 0.41 | 0.07 | 2.12 | 0.99 | 0.32 | 0.12 | 0.02 | 0.19 | 0.04 |
| MC 11 cm | 3.90 | 2.72 | 0.06 | 0.47 | 0.13 | 2.25 | 1.18 | 0.36 | 0.13 | 0.03 | 0.22 | 0.05 |
| MC 16 cm | 4.41 | 2.86 | 0.05 | 0.47 | 0.07 | 2.39 | 1.55 | 0.41 | 0.14 | 0.02 | 0.23 | 0.04 |
| MC 22 cm | 3.63 | 2.38 | 0.04 | 0.33 | 0.06 | 2.05 | 1.25 | 0.33 | 0.10 | 0.01 | 0.20 | 0.05 |
| MC 28 cm | 3.74 | 2.46 | 0.04 | 0.45 | 0.06 | 2.01 | 1.28 | 0.34 | 0.13 | 0.02 | 0.20 | 0.05 |
| MC 34 cm | 3.91 | 2.64 | 0.04 | 0.40 | 0.04 | 2.24 | 1.27 | 0.37 | 0.12 | 0.01 | 0.21 | 0.05 |
| MC 39 cm | 3.84 | 2.73 | 0.04 | 0.35 | 0.05 | 2.38 | 1.11 | 0.34 | 0.10 | 0.01 | 0.21 | 0.05 |
| Avg. multicore | 3.74 | 2.66 | 0.05 | 0.46 | 0.10 | 2.20 | 1.09 | 0.35 | 0.13 | 0.02 | 0.22 | 0.05 |
| 1σ | 0.35 | 0.18 | 0.01 | 0.07 | 0.05 | 0.17 | 0.25 | 0.02 | 0.02 | 0.01 | 0.02 | 0.00 |

Abbreviations as defined previously. n.d. = no data.
*Values reported on dry, post-treatment mass of material, not salt corrected.
[a]THAA wt% C values based on wt% N yields for THAA fraction and mean C/N values for amino acids.
[b]Wt % C and N for the AS and AI fractions (L. A. Roland, unpublished data) from the same SBB sediment trap material used in this study.

# Global and regional implications of foraminifera-bound $\delta^{15}$N records from the Western Pacific

Fabian C. Batista[1], Haojia Ren[2,3], Matthew D. McCarthy[1], A. Christina Ravelo[1]

[1]Ocean Sciences Department, University of California, Santa Cruz

[2]Lamont-Doherty Earth Observatory, Columbia University

[3]Research Center for Environmental Changes, Academia Sinica

*If you look at the ecological circuitry of this planet, the ways in which materials like carbon or sulfur or phosphorous or nitrogen get cycled in ways that makes them available for our biology, the organisms that do the heavy lifting are bacteria.*
                                                                                -Andrew H. Knoll

ABSTRACT

The long-term cooling trend, from the warm Pliocene to the Pleistocene, was accompanied by decreasing atmospheric $CO_2$. Fluctuations in the global inventory of fixed nitrogen (N), a critical nutrient for marine primary productivity, could have generated changes in the strength of the biological pump driving variations in atmospheric $CO_2$. Stable nitrogen isotopic compositions of sedimentary N have been used to study the marine N cycle, to assess past utilization changes of nitrate in the surface ocean, to infer regional changes in the relative balance of denitrification to $N_2$ fixation, and/or changes in the $\delta^{15}N$ value of preformed nitrate. Sedimentary $\delta^{15}N$ records in the major low-latitude oxygen minimum zones (OMZs) show a marked, albeit a time-transgressive positive increase in sedimentary $\delta^{15}N$ of approximately 2‰ from 2.1 to 1.6 Ma. This increase in $\delta^{15}N$ has been interpreted to represent (1) a regional ventilation-driven expansion of the OMZs and subsequent expansion of denitrification; and (2) an increase in the mean deep ocean nitrate $\delta^{15}N$ value. Current data cannot reconcile these explanations due to insufficient geographic distribution of $\delta^{15}N$ records predominantly from regions within or proximal to the OMZs. To address this issue, reported here are two new $\delta^{15}N$ records of well-preserved marine derived organic nitrogen based on foraminifera-bound $\delta^{15}N$ (FB-$\delta^{15}N$) measurements. One of these new FB-$\delta^{15}N$ records is from a region affected by denitrification and the other from an $N_2$ fixation region away from the direct influence of OMZ denitrification. At ODP Site 806 in the western equatorial Pacific, FB-$\delta^{15}N$ values increase from 5‰ to 8‰ over the last 5 Ma, similar to the magnitude

149

and approximate timing of existing $\delta^{15}N$ records from the OMZs, and is consistent with the well-characterized westerly transport of $\delta^{15}N$ signatures across the equatorial Pacific that are influenced by the OMZ.  In contrast, the FB-$\delta^{15}N$ record at DSDP Site 451, in the western subtropical north Pacific, shows no such secular trend for the last 5 Ma, and may indicate that $\delta^{15}N$ increase is confined to the OMZ and regions affected by the OMZs.  These new data suggest that mean ocean nitrate $\delta^{15}N$ is steady over these long timescales due to tight coupling between the major source and sink processes of oceanic fixed N, and also imply both that main fractionations and relative ratio of pelagic to benthic denitrification must have remained steady over the last 5 Ma.  Additional $\delta^{15}N$ records distributed through other oligotrophic regions are needed to confirm this observation.

**Introduction**

Oceanic fixed nitrogen (N), including all forms except $N_2$, is an essential limiting

nutrient of marine primary production and carbon fixation [Eppley and Peterson,

1979]. The residence time of oceanic fixed N is relatively short, on the order of 3000

years [Gruber and Sarmiento, 1997; Brandes and Devol, 2002]. As a consequence,

small imbalances in the major source and sink terms, if maintained for even several

hundred years, could have potential impacts on marine primary production and

subsequently atmospheric $CO_2$ [Devol, 2002]. A better understanding of pre-

anthropogenic changes in the oceanic N inventory is essential, given this potential

important linkage between the oceanic N cycle and global C cycle. Particularly in the

broader context of future change given the global N cycle is strongly being altered

with an estimated doubling of the natural flux of fixed N to the oceans from land from

the production and distribution of artificial N fertilizers [Gruber and Galloway, 2008].

It has been posited that over glacial-interglacial timescales, the fixed N inventory

exhibits variations on the order of 10 to 50%. Specifically, during warm periods,

denitrification is thought to increase removal of fixed N due to expanded suboxic

conditions, and conversely cool periods are thought to be characterized by a reduction

in denitrification and/or an increase in $N_2$ fixation increasing the fixed N inventory,

thus contributing to atmospheric $CO_2$ sequestration through marine primary

production [McElroy, 1983; Michaels et al., 1996; Falkowski, 1997; Gruber and

Sarmiento, 1997; Broecker and Henderson, 1998; Ganeshram et al., 2000; Brandes

and Devol, 2002; Altabet et al., 2002; Karl et al., 2002 Deutsch et al., 2004; Eugster

et al., 2013]. In stark contrast to the glacial-interglacial paradigm for fixed N, during the long-term, multi-million year global cooling trend from the Pliocene to Pleistocene, when oxygen solubility was increasing, there is a broadly observed increased denitrification due to expanding suboxia within the major oxygen minimum zones (OMZs), which is thought to be driven by changes in mode water circulation [Liu et al., 2005, Liu et al., 2008; Etourneau et al., 2013; Robinson et al., 2014].

The $\delta^{15}N$ composition of oceanic fixed nitrate and by extension, the $\delta^{15}N$ composition of total sedimentary N ($\delta^{15}N_{TN}$), provide powerful constraints for evaluating the relative importance of the primary source, $N_2$ fixation, and sink, denitrification, which act to set the oceanic N inventory [Brandes and Devol, 2002]. Internal cycling of fixed N, such as the changes in the extent of N utilization by phytoplankton, has also been evaluated by evaluated with $\delta^{15}N$ measurements of nitrate and sedimentary $\delta^{15}N_{TN}$ [Altabet and Francois, 1994]. The basis for using nitrate $\delta^{15}N$ measurements to infer details about the marine N cycle is founded on the principal that each of the transformations of marine N, particularly the addition and removal of nitrogen through $N_2$ fixation and denitrification, respectively, impart a distinct imprint on the $\delta^{15}N$ composition of nitrate with unique kinetic isotopic fractionations [Cline and Kaplan, 1975; Sigman et al, 2009a].

In the modern ocean, nitrate is the most abundant form of fixed N with a mean deep ocean $\delta^{15}N$ value of 5±0.5‰ [Sigman et al., 2000; Galbraith 2008]. $N_2$ fixation adds fixed N with a $\delta^{15}N$ close to that of atmospheric $N_2$, ca. -2 to 0‰, with its negligible kinetic isotopic effect ($\varepsilon = \delta^{15}N_{reactant} - \delta^{15}N_{instaneous}$) [Wada and Hattori,

1976], which acts to decrease the local thermocline nitrate $\delta^{15}N$ [Dore et al., 2002; Casciotti et al., 2008; Knapp et al., 2005].  In contrast, denitrification enriches the $\delta^{15}N$ of residual nitrate, but the degree of isotopic enrichment is dependent upon the fraction of unreacted local fixed N [Mariotti et al., 1981; Altabet, 2005].  Benthic denitrification (BD) removes fixed N from sedimentary pore-waters to near completion, resulting in a minor kinetic isotopic effect with an $\varepsilon_{BD}$ value of ca. ~0 to 3‰ [Brandes and Devol, 2002; Lehmann et al., 2004], but recent estimates suggest that $\varepsilon_{BD}$ values are slightly higher at 4 to 8‰ [Lehmann et al., 2007; Granger et al., 2011; Alkhatib et al., 2012; Somes et al., 2013].  Pelagic denitrification (PD) exhibits a kinetic isotope effect with an $\varepsilon_{PD}$ value on the order of 20 to 30‰ [Somes et al., 2013].  At steady state, the net effect of all the kinetic isotopic fractionations during $N_2$ fixation, benthic and pelagic denitrification, and the relative ratio of PD:BD, with their accompanying $\varepsilon$ values, sets the whole ocean $\delta^{15}N$ of fixed N [Brandes and Devol, 2002; Altabet 2007].   However, if it can be assumed that the kinetic fractionation effects, which are determined by microbial processes, are unchanging, and the $\delta^{15}N$ of atmospheric N is not varying [Galbraith et al., 2008], then the relative ratio of PD:BD is what determines the whole ocean $\delta^{15}N$ value of fixed N.

Modern studies do not have long enough time series to capture how the N cycle balances itself on a global basis over long timescales approaching the residence time of oceanic fixed N (ca. 3 kyr) and longer.  For several decades now, paleoceanographic studies of the N cycle have applied sedimentary $\delta^{15}N_{TN}$ records as a proxy for sinking particulate $\delta^{15}N$ and by extension, the $\delta^{15}N$ value of surface ocean

nitrate [Altabet and Francois, 1994; Altabet et al., 1999; Altabet et al., 2006] . In any given location, $\delta^{15}N_{TN}$ values can be used to infer local and regional processes overprinted on a global baseline of whole ocean nitrate $\delta^{15}N$. For instance, $\delta^{15}N_{TN}$ have been used to infer (1) changes in the $\delta^{15}N$ of preformed nitrate, (2) regional nitrate $\delta^{15}N$ changes through adjustment of the relative ratio of pelagic to benthic denitrification (PD:BD) or $N_2$ fixation relative to the whole ocean, (3) and relative changes in the extent of nitrate utilization by marine autotrophs during primary production [Altabet 2006; Galbraith et al., 2008]. Compiling spatially distributed $\delta^{15}N$ records has therefore been invaluable for examining temporal trends and spatial coupling of N cycle processes.

A recent multi-site compilation of new and existing $\delta^{15}N_{TN}$ records from the eastern tropical Pacific, North Pacific and the Arabian Sea was presented for the Pliocene and Pleistocene [Robinson et al., 2014]. These records showed a broadly consistent, albeit time-transgressive increase in sedimentary $\delta^{15}N_{TN}$ values in the major OMZs between 2.1 and 1.5 Ma, which occurred during a long-term global cooling trend, and was interpreted reduced pelagic denitrification in the Pliocene warm period which increased in the colder Pleistocene due to expansion of suboxia and the OMZs after 2.1 Ma. This result is in stark contrast to predicted mean trends observed over glacial-interglacial timescales, which anticipates that global cooling would lead to a decreasing trend in sedimentary $\delta^{15}N_{TN}$ values as a result of either increased $N_2$ fixation linked to aridity-driven Fe-fertilization from dust, low $NO_3^-$ :$PO_4^{3-}$ ratios from enhanced denitrification in warmer periods, and/or a denitrification

154

decrease driven by increased ventilation of intermediate and mode waters [Robinson et al., 2014]. Ten of the twelve sedimentary $\delta^{15}N_{TN}$ records compiled by Robinson and co-authors [2014] displayed the increasing $\delta^{15}N_{TN}$ trend. The same records that exhibited the increasing $\delta^{15}N_{TN}$ trend were also located within or downstream from the major OMZs. Thus the extremely limited spatial distribution of these records and bias towards sampling within the OMZ makes it difficult to study global scale aspects of the linkages and coupling between the source and sink processes of fixed N over long million-year timescales.

Several studies have posited that ocean circulation changes which likely brought about the expansion in pelagic denitrification after 2.1 Ma in low latitude OMZs resulted in an increase in the global mean ocean nitrate $\delta^{15}N$ at that time [Liu et al., 2008; Etourneau et al., 2009] and/or a net loss of N from the global ocean [Filippelli and Flores, 2009]. However, to accurately infer secular shifts in the global mean $\delta^{15}N$ value of oceanic nitrate or the ocean fixed N inventory, appropriate spatial coverage with well-preserved $\delta^{15}N_{TN}$ records are required from regions that represent both the main sources and sinks of fixed N. The bias towards reconstructing sedimentary $\delta^{15}N_{TN}$ records within regions of high deposition and high preservation, often overlap the major OMZs, and results in poor global spatial coverage of $\delta^{15}N_{TN}$ records [Tesdal et al., 2013]. An indirect consequence is that the oligotrophic ocean is grossly under sampled due to the inherent low export production in these regions. Low export production in these regions result in low deposition rates of sedimentary organic matter, thus enhancing the demand for the limited nitrogen reaching the

seafloor. As a consequence, primary signals of surface N dynamics are marred by alteration of sedimentary organic N thus leading to unreliable $\delta^{15}N_{TN}$ records in oligotrophic regions [Robinson et al. 2012]. Exacerbating this issue is the low organic N content of sediments in the oligotrophic ocean, such that any residual surface derived N is likely easily contaminated by allocthonous sources of combustible N. Thus there are exceptionally few $\delta^{15}N_{TN}$ records from open-ocean, oligotrophic regions which are characterized by surface ocean dwelling organism that engage in $N_2$ fixation, the key process for balancing denitrification, but more important for this work is that these regions most likely represent the $\delta^{15}N$ of the thermocline water and thus are more representative of whole ocean $\delta^{15}N$ changes. However, recent development of a new proxy has made it easier to study $\delta^{15}N$ dynamics in oligotrophic ocean sediments.

Ren and co-authors [2009] developed novel methodology to analyze the $\delta^{15}N$ of foraminifera-bound organic N (FB-$\delta^{15}N$). These measurements access a sedimentary archive of organic N, which approximates the $\delta^{15}N$ value of subsurface nitrate [Ren et al., 2008], is physically protected from pre- and post- burial isotopic alteration and is free of contamination by allocthonous N sources. FB-$\delta^{15}N$ measurements of euphotic zone dwelling, symbiotic, spinose species from modern surface sediments have been shown to integrate the $\delta^{15}N$ of new N supply, which is dominated by the $\delta^{15}N$ of thermocline nitrate relative to the supply of depleted $\delta^{15}N$ by $N_2$ fixation in oligotrophic regions [Altabet, 1988; Karl et al., 1997; Knapp et al., 2005; Casciotti et al., 2008].

Here we present two new low-resolution FB-$\delta^{15}$N records from 5 Ma to present.

One in the western equatorial Pacific (WEP) at ODP site 806 bathed in waters

exported from the major OMZs located in the eastern equatorial Pacific (EEP) and

one in the western subtropical north Pacific (WSNP) at DSDP Site 451 characterized

by oligotrophic, nutrient starved waters. These new records are used to infer if the

mean global ocean nitrate $\delta^{15}$N value is stable over the last 5 Ma, specifically to

discern if there is evidence for an increase in the mean ocean nitrate $\delta^{15}$N value on the

order of 2‰, concomitant with the strong evidence for expanded denitrification after

2.1 Ma in the major OMZs. We compare our FB-$\delta^{15}$N record to existing $\delta^{15}$N$_{TN}$ data

at ODP 806 to confirm that FB-$\delta^{15}$N values accurately track the previously observed

$\delta^{15}$N$_{TN}$ trend [Rafter and Charles, 2012]. We then present and discuss the possible

scenarios which might explain our FB-$\delta^{15}$N record at DSDP 451, and consider the

long-term N cycle response in regions characterized by N$_2$ fixation and the

background $\delta^{15}$N value of mean oceanic nitrate.

**Materials & Methods**

**Samples and Age Models**

Sediment samples were obtained from sediment cores from the Ontong Java

Plateau in the WEP at Ocean Drilling Program (ODP) Site 806 (3° N, 156° E, 2.52

km) and from the Western Mariana Ridge in the WSNP at Deep Sea Drilling Project

(DSDP) Site 451 (18° N, 143° E, 2.06 km), Table 1. Sites were selected for

preserved calcareous rich oozes content and for proximity to and influence by the

processes, pelagic denitrification and pelagic N$_2$ fixation, as determined by subsurface

maps (Figure 3.1) of dissolved $O_2$ and N*, where N* is a measure of N excess or deficit [Gruber and Sarmiento, 1997]. ODP Site 806 located in the WEP was particularly well suited for a new FB-$\delta^{15}$N record due to its incorporation of nitrate $\delta^{15}$N signatures influenced by denitrification occurring in the eastern Pacific (Figure 3.1A) [Rafter and Charles, 2012; Rafter et al., 2012]. This WEP record also serves as a reference site in the DSDP Site 451 located in the WSNP, which was specifically selected for its low N* value (Figure 3.1B) and thus its propensity to host pelagic $N_2$ fixation, but also represent $\delta^{15}$N values of the mean ocean nitrate.

The age model for ODP Site 806 was based on that of Wara et al. [2005]. Accumulation rates for DSDP Site 451, are based on biostratigraphic zonal boundaries following Schlanger et al. [1976] and nannofossil zones after Martini and Worsley [1970], which were used to linearly interpolate ages for each sample interval. Cores from ODP Site 806 and DSDP Site 451 were sampled at intervals, yielding an average sampling frequency of 1 sample per ~100 kyr.

**Foraminifera-Bound Stable Nitrogen Isotopes (FB-$\delta^{15}$N)**

FB-$\delta^{15}$N measurements of fossil shells of the three common planktonic foraminifera species, Globogerinoides sacculifer (without final sacc-like chamber, >325 μm fraction) and Globogerinoides ruber or Globigerinoides obliquus extremus (>250 μm fraction) for the last 5-0 Ma at ODP Site 806 and DSDP Site 451. Note that G. ruber and G. obliquus extremus shells were combined for FB-$\delta^{15}$N analysis at DSDP Site 451, but were not included in the G. ruber FB-$\delta^{15}$N data at ODP Site 806. The protocol for measuring FB-$\delta^{15}$N is based on that established by Ren and

colleagues [2009] which includes (1) crushing foram shells (Figure EA 3-1) followed by mechanical cleaning by sonicating for 5 mins at pH 8 in 2% sodium hexametaphosphate, followed by DI rinses; (2) reductive cleaning with sodium bicarbonate buffered dithionite-citrate reagent to remove organo-metal complexes [Leite et al., 2000], then chemical oxidation with sodium hypochlorite to remove external N contamination, followed by 6N HCl dissolution of the cleaned shells; (3) conversion of dissolved organic nitrogen in solution to nitrate via persulfate oxidation; (4) quantitation of nitrate concentration by chemiluminescence [Braman and Hendrix, 1989]; and (5) denitrifier method for conversion of nitrate to nitrous oxide followed by $\delta^{15}N$ analysis of the nitrous oxide by automated extraction and gas-chromatography-isotope ratio mass spectrometry [Casciotti et al., 2002].

FB-$\delta^{15}N$ analysis typically requires a minimum of 5 mg of foraminifera shells before cleaning, then splitting the samples after cleaning, prior to shell dissolution to allow for duplicate or triplicate isotopic analysis. For approximately 75% of samples from ODP Site 806, we had sufficient mass of cleaned shells to generate persulfate oxidation replicates, and for approximately 75% of samples, we generated sufficient nitrate for duplicate FB-$\delta^{15}N$ measurements. For DSDP Site 451, there was insufficient mass of cleaned shells for replicate persulfate oxidation of samples, and 25% of samples had duplicate FB-$\delta^{15}N$ analysis. FB-$\delta^{15}N$ measurements achieved a standard deviation (1 sigma) generally better than 0.18‰.

## Results

### FB-$\delta^{15}$N at ODP Site 806

New FB-$\delta^{15}$N records generated for this work are shown in Figure 3.2 with the global stack of benthic foraminifer $\delta^{18}$O [Lisiecki and Raymo, 2005] for context along with previously published $\delta^{15}$N$_{TN}$ records that extend from the Pliocene to present. FB-$\delta^{15}$N results for two euphotic zone dwellers, G. ruber (n=26) and G. sacculifer (n=9) at ODP Site 806 in the WEP exhibit similar trends throughout the record. Differences in the individual FB-$\delta^{15}$N values of coeval G. ruber and G. sacculifer at ODP Site 806 (Figure 3.2B, Table 2) are typically less than 1‰, similar to previous observations by Ren and colleagues [2009]. FB-$\delta^{15}$N values for G. ruber and G. sacculifer range from 4.2‰ to 10‰ with an average of ~6‰ during the early Pliocene then increase to ~8‰ in the early Pleistocene after ca. 2.1 Ma. The overall trend and 2‰ increase in FB-$\delta^{15}$N at ODP Site 806 is similar to the 4 Myr long trend in $\delta^{15}$N$_{TN}$ at ODP 1012 in the eastern North Pacific (ENP), and is similar to the existing 1 Myr long $\delta^{15}$$_{TN}$ record at ODP Site 806 (Figure 3.2B).

### FB-$\delta^{15}$N at DSDP Site 451

In stark contrast to the increasing trend in FB-$\delta^{15}$N values at ODP Site,806, FB-$\delta^{15}$N values of G. ruber and G. obliquus extremus at DSDP Site 451 in the WSNP but do not exhibit a secular trend, though values range from 0.7 to 5.4‰, (Figure 3.2C, Table 3). For the past 4.5 Myr, average FB-$\delta^{15}$N values of G. ruber and G. obliquus extremus at DSDP Site 451 are 2.9 ± 0.9‰ (n= 45). FB-$\delta^{15}$N measurements of G. sacculifer (n=6) were distributed randomly throughout the DSDP 451 record with an

average $3.2 \pm 0.3$‰. Discrete individual FB-$\delta^{15}$N values of coeval G. ruber and G. obliquus extremus are within 0.4‰, similar to previous observations by Ren and colleagues [2009]. The regional and global context of these new FB-$\delta^{15}$N records are now considered with respect to existing $\delta^{15}$N$_{TN}$ records and the oceanographic mechanisms which have been proposed to reconcile them.

**Discussion**

**ODP Site 806: A Record of EEP Nutrient Dynamics**

Comparison of FB-$\delta^{15}$N values (n=8) and the previously published high-resolution $\delta^{15}$N$_{TN}$ record at ODP Site 806 [Rafter et al., 2012] indicates good similarity in the general trend for the last 1.2 Ma. The FB-$\delta^{15}$N record at ODP Site 806 extends to 5.5 Ma, well beyond available local comparable $\delta^{15}$N$_{TN}$ data. However, several high-resolution $\delta^{15}$N$_{TN}$ records that extend to the Pliocene are available elsewhere in the Pacific to which this new record can be compared. Liu et al. [2005, 2008] generated a 4 Ma long $\delta^{15}$N$_{TN}$ record in the eastern North Pacific (ENP) at ODP Site 1012, which shows a strong increase of ca. 2‰ at about 2.1 Ma. Discrete FB-$\delta^{15}$N values at Site 806 overlap $\delta^{15}$N$_{TN}$ values from Site 1012 and the long-term trends in the WEP and ENP trends are remarkably similar. In fact, the trend in the FB-$\delta^{15}$N record for Site 806 matches the general trend in other long, high-resolution $\delta^{15}$N$_{TN}$ records at ODP Sites 1239 and 849 in the EEP [Etourneau et al., 2010; Rafter and Charles, 2012], and the Benguella Upwelling System (BUS) in the Southeastern Atlantic at ODP Site 1082 [Robinson et al., 2002; Etourneau 2013]. Despite the similarity in overall $\delta^{15}$N trends for the records of the WEP, EEP and

BUS, there is an offset in the absolutes $\delta^{15}N$ values, where the EEP and BUS $\delta^{15}N$ records are consistently offset towards lower $\delta^{15}N_{TN}$ values by approximately 2 to 4‰ (Figure 3.3C).

The observed $\delta^{15}N$ offset between EEP and WEP records with lower $\delta^{15}N$ values in the EEP at ODP Sites 1239 and 849 is at least consistent with well characterized surface ocean nitrate utilization gradient in the equatorial Pacific [Rafter and Charles, 2012; Rafter et al., 2012]. Rafter and co-authors [2012] describe a homogenous subsurface nitrate $\delta^{15}N$ value across the entire equatorial Pacific, but zonal asymmetry in the supply of nutrients (higher surface nitrate supply in the EEP) is a major driver of lower nitrate utilization in the EEP. Lower sedimentary $\delta^{15}N$ values in the EEP relative to the WEP reflects the differences in surface nitrate utilization, where it is typically more complete in the WEP, and less so in the EEP due to replete nutrient conditions there [Rafter and Charles, 2012]. Elevated $\delta^{15}N$ values of residual surface nitrate are then rapidly carried through westward surface advection in the equatorial Pacific from the EEP to the WEP, is subsequently utilized to completion and transferred to sediments in the WEP, contributing further to the sedimentary $\delta^{15}N_{TN}$ gradients across the equatorial Pacific [Rafter et al. 2012; Jia et al., 2011; Yoshikawa et al., 2006].

That the ODP 806 FB-$\delta^{15}N$ record matches both the trend and magnitude of $\delta^{15}N_{TN}$ values in the ODP 1012 record suggests a similar utilization difference of the surface nitrate reservoir in the ENP relative to the EEP. Subsurface nitrate in the ENP has a value of ~8‰ [Sigman et al., 2003; Sigman et al., 2005], same as the

equatorial Pacific nitrate $\delta^{15}N$ value, but differences in the surface nitrate utilization in the ENP relative to the EEP, similar to the WEP and EEP, likely explain the similarity in the absolute $\delta^{15}N$ values of the WEP and ENP $\delta^{15}N_{TN}$ and FB-$\delta^{15}N$ records, with an offset towards higher $\delta^{15}N$ values relative to the EEP $\delta^{15}N_{TN}$ records. An overall similar trend in $\delta^{15}N$ records at ODP Site 806 and ODP Site 1082 with an consistent offset in $\delta^{15}N$ values for the records in the WEP relative to the BUS, suggests a similar mean ocean $\delta^{15}N$ value, but a similar nutrient utilization difference between these distal settings.

Our new FB-$\delta^{15}N$ record at ODP Site 806 therefore conforms to the widely observed, albeit time-transgressive, positive 2‰ $\delta^{15}N$ shift featured throughout the major OMZs after 2.1 Ma. The $\delta^{15}N$ shift in the ENP (2.1 Ma), the EEP, WEP and BUS indicates an expansion in the volume of suboxic zones and pelagic denitrification [Robinson et al., 2014]. The primary driver of this OMZ expansion is likely due to changes in intermediate and mode water ventilation, either due to global cooling related stratification of high latitude locations where intermediate ventilation occurs [de Boer et al., 2007], or a shift in the distribution of water masses.

Robinson and co-authors [2014] specifically attribute the time-transgressive $\delta^{15}N_{TN}$ increase to regional differences in timing of water mass ventilation changes. Regardless of the mechanism, Robinson and co-authors [2014] provide substantial evidence for expansion of the major OMZs and subsequent intensification of pelagic denitrification in low latitudes after 2.1 Ma. However, it is important to acknowledge that while ten of the twelve $\delta^{15}N_{TN}$ records compared in the study show the positive

shift in $\delta^{15}N$, these same ten sites were also within, or downstream from the major OMZs. Thus, it remains unclear if these $\delta^{15}N$ changes impacted the global mean ocean nitrate $\delta^{15}N$ value. With the lack of $\delta^{15}N$ records in regions characterized by $N_2$ fixation, there is insufficient information to test whether the secular $\delta^{15}N$ positive shift in the major OMZs is representative of a global increase in mean oceanic nitrate $\delta^{15}N$ or indicative of regional changes only.

As a thought experiment, if the FB-$\delta^{15}N$ record at ODP Site 806 (and the other $\delta^{15}N_{TN}$ records that exhibit the increasing $\delta^{15}N$ shift after 2.1 Ma) in fact represent a global increase in mean ocean nitrate $\delta^{15}N$ on the order of 2‰, then the relative ratio ratio of PD:BD must have changed. This is assumes that at a steady state $\delta^{15}N$ budget of fixed N in the ocean, the major source and sinks, will set the whole ocean $\delta^{15}N$ value of fixed N and the kinetic fractionation effects for $N_2$ fixation, benthic and pelagic denitrification, which are determined by microbial processes, are constant. If so, then at steady state the relative ratio of PD:BD determines the whole ocean $\delta^{15}N$ value of fixed N. However, if the broadly observed trends towards increasing $\delta^{15}N$ values were only regional features of marine N dynamics localized to the major OMZs such denitrification rates increased without a direct change in the ratio of PD:BD, steady state isotopic mass balance would then require that $N_2$ fixation rates would have increased to balance the increasing $\delta^{15}N$ value of fixed N in the OMZs to maintain a balanced mean ocean nitrate $\delta^{15}N$ budget, and preclude a global increasing trend in mean ocean nitrate $\delta^{15}N$. To test these scenarios, the new FB-$\delta^{15}N$ record at DSDP Site 451 in the WSNP is considered next, and used to assess the evolution of

mean deep ocean nitrate $\delta^{15}N$ values across the Pliocene - Pleistocene transition, to track the response of mean ocean $\delta^{15}N$ values as a result of the observed sedimentary $\delta^{15}N$ increases throughout the major OMZ, and at sites downstream [Robinson et al., 2014].

## DSDP Site 451: Evaluating a Mean Ocean $\delta^{15}N$ Shift

The surface N budget that supports new production in the oligotrophic ocean, like that of the WSNP, is a combination of newly added N from $N_2$ fixation and nitrate diffusing upward from the subsurface global thermocline [Casciotti et al., 2008; Shiozaki et al., 2009, 2010]. It is likely that the mean FB-$\delta^{15}N$ values of the WSNP DSDP 451 record most directly suggests that there was no secular trend in the global mean ocean nitrate $\delta^{15}N$ for the last 5 Ma (Figure 3.2C). This inference is based on the isotopic end-members for the two primary sources, $N_2$ fixation and subsurface nitrate, that comprise the surface N budget for this region. $N_2$ fixation adds organic N to the surface ocean with a $\delta^{15}N$ value of ~-1‰ and mean ocean subsurface nitrate has a $\delta^{15}N$ value of 6‰ at 150 m water depth in the oligotrophic western equatorial Pacific [Yoshikawa et al., 2006] and 300 m water depth in the oligotrophic North Pacific Subtropical Gyre [Casciotti et al., 2008]. This conclusion would then also require the assumption that for the last 5 Ma the relative ratio of $N_2$ fixation relative to thermocline nitrate ($N_{fix}:N_{therm}$) comprising the surface N budget has remained unchanged, as well as the isotopic end-members value for these two primary N sources. While the past relative ratio of new production contributed by

165

thermocline N and $N_2$ fixation cannot be determined, modern estimates from the oligotrophic subtropical North Pacific provide some constraint.

In the modern ocean, several estimates of the $N_{fix}$:$N_{therm}$ ratio exist for the oligotrophic North Pacific surface N budget. The contribution of $N_2$ fixation has been shown to vary widely in the contribution to the surface N budget of the oligotrophic ocean; however, each study summarized below indicates that subsurface nitrate is most likely the dominant N contribution. We therefore use the new FB-$\delta^{15}$N record at DSDP 451 in the WSNP to represent thermocline nitrate $\delta^{15}$N. This hypothesis is supported by several observations for the oligotrophic ocean. For instance, at Station ALOHA, in the North Pacific Subtropical Gyre the average contribution of $N_2$ fixation to new production, has been estimated from decadal time series data, to represent ca. 50% [Karl et al., 1997; Dore et al., 2002]; however, end-member $\delta^{15}$N values of subsurface nitrate used in this isotopic budget for these estimates were recently refined further, with highly resolved nitrate $\delta^{15}$N measurements over a few weeks in boreal summer, resulting in a revised calculation that indicates that $N_2$ fixation accounts for only ~19% of new production [Casciotti et al., 2008]. Shiozaki et al. [2009, 2010] quantified in-situ rates of $N_2$ fixation during boreal spring in the western North Pacific along 155° E and found that $N_2$ fixation contributed 2 – 37% of new production between from 0° to 28° N. This data set indicates that $N_2$ fixation contributions near DSDP Site 451 (18° N, 143° E) between 16° and 20° N comprise 10 – 20% of new production, which is consistent with updated estimates for the North Pacific Subtropical Gyre at station ALOHA [Casciotti et al., 2008], which together

suggest that thermocline nitrate is the dominant N source supporting new production in the oligotrophic ocean.

If these latter estimates of the surface N budget by Casciotti et al. [2008] and Shiozaki et al [2009, 2010] are accurate, and the surface N supply is dominated by thermocline N, then $\delta^{15}N$ records from an oligotrophic region of the North Pacific would thus reflect changes in the mean $\delta^{15}N$ value of thermocline nitrate, acting as a proxy for the global mean oceanic nitrate $\delta^{15}N$ value. Therefore the DSDP Site 451 FB-$\delta^{15}N$ record represents a viable candidate for a site recording past variability in mean ocean nitrate $\delta^{15}N$. If this inference for the DSDP 451 surface nitrate $\delta^{15}N$ value is correct, then our FB-$\delta^{15}N$ record at this site indicates that the whole ocean $\delta^{15}N$ value is nearly constant over the past ~5 Ma (Figure 3.2C). However, since the past relative ratio of new production contributed by thermocline N and $N_2$ fixation cannot be clearly determined, we must explore several scenarios to explain our FB-$\delta^{15}N$ record at Site 451. First, we consider the possibility that the $N_{fix}:N_{therm}$ ratio has remained similar to the average modern ratio 0.3:0.7 throughout the core of the oligotrophic subtropical North Pacific, and then an alternate possibility that $N_2$ fixation was a larger portion of the surface N supply for the FB-$\delta^{15}N$ record than it is today.

We first consider a scenario in which our FB-$\delta^{15}N$ record at DSDP Site 451 is dominated by thermocline nitrate source, as supported by modern estimates from the oligotrophic North Pacific described above [Casciotti et al., 2008; Shiozaki et al., 2009, 2010]. If the positive 2‰ $\delta^{15}N$ increase in OMZ $\delta^{15}N_{TN}$ records at several mid

167

to low latitude sites (e.g., sites 1012, 1239, 849) represent a shift in the baseline value of mean deep ocean nitrate $\delta^{15}N$, then FB-$\delta^{15}N$ data at DSDP Site 451 in the WSNP should also reflect this change. In contrast to the FB-$\delta^{15}N$ and $\delta^{15}N_{TN}$ records at ODP Site 806 and OMZ $\delta^{15}N_{TN}$ records (Figure 3.2B & 3.3C), there is no secular trend in FB-$\delta^{15}N$ record at 451 (Figure 3.2C). This would suggest that there was no change in the mean ocean nitrate $\delta^{15}N$, and so supports the idea of OMZ intensity as driving the change in the other records.

An alternate scenario could be that local processes in the WSNP conceal an actual positive shift in mean ocean nitrate $\delta^{15}N$. There are two possible ways that the FB-$\delta^{15}N$ at DSDP Site 451 could conceal a whole ocean $\delta^{15}N$ increase of 2‰. First, if the $N_{fix}:N_{therm}$ changed so precisely that newly fixed N gradually increased to be a higher proportion of the surface N budget at DSDP 451, then perhaps the change in the local surface $\delta^{15}N$ budget may have exactly balanced the $^{15}N$ enrichment in whole ocean nitrate $\delta^{15}N$, thus concealing the 2‰ increase. Modeling efforts would be required to test the feasibility of this scenario, but it seems unlikely. Specifically, evaluating this scenario with a fully coupled biogeochemical model could be used to test the relative potential for local oligotrophic surface $\delta^{15}N$ budgets to mask a whole ocean $\delta^{15}N$ increase. Somes and co-authors [2010] have described a nitrogen isotope model incorporated into a three-dimensional ocean component of a global Earth system climate model [Somes et al., 2010] that could be parameterized with the data generated here to account for ocean circulation, primary production, sediment

168

deposition, and all the kinetic isotopic fractionations associated with key nitrogen transformations necessary to test this scenario.

A second alternate scenario that would also satisfy a masking of a mean ocean nitrate $\delta^{15}N$ increase could be a fixed $N_{fix}:N_{therm}$ ratio, with a dominant $N_2$ fixation contribution to the local surface N budget supporting new production. If $N_2$ fixation was the dominant surface N source, it would also dominate the surface $\delta^{15}N$ budget, and could contribute to concealing a 2‰ increase in mean whole ocean nitrate. A simple isotopic mass balance can be used to test the $N_{fix}:N_{therm}$ ratio in the oligotrophic ocean required to mask a 2‰ increase in whole ocean nitrate, Given that the uncertainty in FB-$\delta^{15}N$ values is <0.2‰, a change in the surface $\delta^{15}N$ budget must exceed this uncertainty. However, to mask a whole ocean increase of 2‰, the surface $\delta^{15}N$ budget, as driven by a fixed unknown $N_{fix}:N_{therm}$ ratio, must conceal this change. Put another way, for the $\delta^{15}N$ budget of the surface oligotrophic ocean to conceal a whole ocean 2‰ increase, the difference between the $\delta^{15}N$ budget of the surface oligotrophic ocean before and after the whole ocean change, must be less than or equal to 0.2‰, the analytical uncertainty of FB-$\delta^{15}N$ measurements. If we take the $\delta^{15}N$ contribution of $N_2$ fixation to add fixed N with a $\delta^{15}N$ value of -1‰, and assume that today's oligotrophic $\delta^{15}N$ nitrate value of 6‰ at 150-300 m [Yoshikawa et al., 2006; Casciotti et al., 2008] is representative of the Pleistocene whole ocean nitrate $\delta^{15}N$ value and is 2‰ higher than the Pliocene whole ocean nitrate $\delta^{15}N$ of 4‰, then a fixed $N_{fix}:N_{therm}$ ratio of 0.9:0.1 is required to conceal the $\delta^{15}N$ increase in whole ocean nitrate $\delta^{15}N$. This $N_{fix}:N_{therm}$ ratio requirement of at least 0.9:0.1 is an unlikely

partitioning of the surface N budget, provided the modern oligotrophic North Pacific is already greatly stratified, and yet modern estimates of the $N_{fix}:N_{therm}$ average only 0.2:0.8 in the WSNP [Shiozaki et al., 2009] and the North Pacific Subtropical Gyre at Station ALOHA [Casciotti et al., 2008], with a maximum observed $N_{fix}:N_{therm}$ ratio of 0.5:0.5 at Station ALOHA [Karl et al., 1997; Dore et al., 2002; Karl et al., 2002], the core of the subtropical gyre.

Overall, we cannot suggest a justifiable mechanism that would satisfy the possibility that local changes in the ratio of surface N sources at Site 451 masked a global change in mean ocean nitrate $\delta^{15}N$ of 2‰. Thus, we suggest that the most likely interpretation of the FB-$\delta^{15}N$ record at DSDP Site 451 is a representation of mean ocean nitrate $\delta^{15}N$, and the monotonic nature of the FB-$\delta^{15}N$ record indicates strong coupling of the fixed N sources and a long-term steady state balance of the $\delta^{15}N$ budget throughout the last 5 Ma.

**Conclusion**

Our new FB-$\delta^{15}N$ data in the WEP at ODP 806 and in the WSNP at DSDP 451 add to a global view of the N dynamics over the last 5 Ma. The major OMZs clearly experienced an $\delta^{15}N_{TN}$ excursion after 2.1 Ma on the order of a ~2‰ increase, likely due to decreased ventilation and reduced oxygenation of intermediate and mode waters supplying the low latitude OMZ, in the cooler Pleistocene relative to the warm Pliocene [de Boer et al., 2007; Robinson et al., 2014]. This widely observed ~2‰ increase in $\delta^{15}N_{TN}$ records was also detected away from the core of major OMZs, as far afield as the WEP, as indicated by the similarity in the FB-$\delta^{15}N$ trend at ODP 806,

which is consistent with zonal gradients in surface nitrate utilization across the equatorial Pacific [Rafter et al., 2012]. However, we find that these broadly consistent $\delta^{15}N$ trends are confined to the major OMZs or locations directly downstream, and due a combination of the dilution effect and tight coupling of the pelagic $N_2$ fixation, pelagic and benthic denitrification, these data do not appear to represent changes throughout the global ocean.

We find that the non-secular trend in FB-$\delta^{15}N$ record at DSDP Site 451 in the WSNP is evidence for tight coupling between the main sources and sinks of fixed N over the last 5 Ma, which contributed to a steady mean ocean nitrate $\delta^{15}N$. This result implies that the kinetic fractionations for the major sources and sinks of fixed N, and the relative ratio of PD:BD did not change, in spite of the major global changes during the Plio-Pleistocene transition, which include sea level, volume of the OMZs, and shelf area. However, additional broadly distributed $\delta^{15}N$ records are needed throughout oligotrophic regions to confirm this observation. Fully coupled ocean models featuring stable isotope biogeochemistry such as that of Somes et al. [2010] could be used to test this hypothesis that the mean ocean nitrate $\delta^{15}N$ value did not change and particularly whether the observed stable $\delta^{15}N$ budget for whole ocean nitrate over the last 5 Ma also represents a stable inventory of oceanic fixed N.

**Acknowledgements**

## References

Alkhatib, M., Lehmann, M.F. and del Giorgio, P.A. (2012) The nitrogen isotope effect of benthic remineralization-nitrification-denitrification coupling in an estuarine environment. Biogeosciences 9, 1633-1646.

Altabet, M. (2006a) Constraints on oceanic N balance/imbalance from sedimentary 15 N records. Biogeosciences Discussions 3, 1121-1155.

Altabet, M. and Francois, R. (1994) Sedimentary nitrogen isotopic ratio as a recorder for surface ocean nitrate utilization. Global Biogeochemical Cycles, 103-116.

Altabet, M., Pilskaln, C., Thunell, R., Pride, C., Sigman, D., Chavez, F. and Francois, R. (1999) The nitrogen isotope biogeochemistry of sinking particles from the margin of the Eastern North Pacific. Deep-Sea Research Part I-Oceanographic Research Papers, 655-679.

Altabet, M.A. (1988) Varitiations in nitrogen isotopic composition between sinking and suspended particles - implications for nitrogen cycling and particle transformation in the open ocean. Deep-Sea Research Part a-Oceanographic Research Papers 35, 535-554.

Altabet, M.A. (2006b) Isotopic tracers of the marine nitrogen cycle: Present and past, Marine organic matter: biomarkers, isotopes and DNA. Springer, pp. 251-293.

Altabet, M.A. (2007) Constraints on oceanic N balance/imbalance from sedimentary N-15 records. Biogeosciences 4, 75-86.

Altabet, M.A., Higginson, M.J. and Murray, D.W. (2002) The effect of millennial-scale changes in Arabian Sea denitrification on atmospheric CO2. Nature 415, 159-162.

Braman, R.S. and Hendrix, S.A. (1989) Nanogram nitrite and nitrate determination in environmental and biological materials by vanadium(III) reductino with chemiluminescence detection. Analytical Chemistry 61, 2715-2718.

Brandes, J.A. and Devol, A.H. (2002) A global marine-fixed nitrogen isotopic budget: Implications for Holocene nitrogen cycling. Global Biogeochemical Cycles 16, 14.

Broecker, W.S. and Henderson, G.M. (1998) The sequence of events surrounding Termination II and their implications for the cause of glacial-interglacial CO2 changes. Paleoceanography 13, 352-364.

Casciotti, K.L., Sigman, D.M., Hastings, M.G., Bohlke, J.K. and Hilkert, A. (2002) Measurement of the oxygen isotopic composition of nitrate in seawater and freshwater using the denitrifier method. Analytical Chemistry 74, 4905-4912.

Casciotti, K.L., Trull, T.W., Glover, D.M. and Davies, D. (2008) Constraints on nitrogen cycling at the subtropical North Pacific Station ALOHA from isotopic measurements of nitrate and particulate nitrogen. Deep-Sea Research Part Ii-Topical Studies in Oceanography 55, 1661-1672.

Cline, J.D. and Kaplan, I.R. (1975) Isotopic fractionation of dissolved nitrate during denitrification in the eastern tropical north pacific ocean. Marine Chemistry 3, 271-299.

de Boer, A.M., Sigman, D.M., Toggweiler, J.R. and Russell, J.L. (2007) Effect of global ocean temperature change on deep ocean ventilation. Paleoceanography 22.

Deutsch, C., Sigman, D.M., Thunell, R.C., Meckler, A.N. and Haug, G.H. (2004) Isotopic constraints on glacial/interglacial changes in the oceanic nitrogen budget. Global Biogeochemical Cycles 18.

Devol, A.H. (2002) Global change - Getting cool with nitrogen. Nature 415, 131-132.

Dore, J.E., Brum, J.R., Tupas, L.M. and Karl, D.M. (2002) Seasonal and interannual variability in sources of nitrogen supporting export in the oligotrophic subtropical North Pacific Ocean. Limnology and Oceanography 47, 1595-1607.

Eppley, R.W. and Peterson, B.J. (1979) Particulate organic-matter flux and planktonic new production in the deep ocean. Nature 282, 677-680.

Etourneau, J., Martinez, P., Blanz, T. and Schneider, R. (2009) Pliocene-Pleistocene variability of upwelling activity, productivity, and nutrient cycling in the Benguela region. Geology 37, 871-874.

Etourneau, J., Robinson, R.S., Martinez, P. and Schneider, R. (2013) Equatorial Pacific peak in biological production regulated by nutrient and upwelling

during the late Pliocene/early Pleistocene cooling. Biogeosciences 10, 5663-5670.

Eugster, O., Gruber, N., Deutsch, C., Jaccard, S.L. and Payne, M.R. (2013) The dynamics of the marine nitrogen cycle across the last deglaciation. Paleoceanography 28.

Falkowski, P.G. (1997) Evolution of the nitrogen cycle and its influence on the biological sequestration of CO2 in the ocean. Nature 387, 272-275.

Filippelli, G.M. and Flores, J.A. (2009) From the warm Pliocene to the cold Pleistocene: A tale of two oceans. Geology 37, 959-960.

Galbraith, E.D., Sigman, D.M., Robinson, R.S. and Pedersen, T.F. (2008) Nitrogen in past marine environments.

Ganeshram, R.S., Pedersen, T.F., Calvert, S.E., McNeill, G.W. and Fontugne, M.R. (2000) Glacial-interglacial variability in denitrification in the world's oceans: Causes and consequences. Paleoceanography 15, 361-376.

Garcia, H.E., R. A. Locarini, T. P. Boyer, J. I. Antonov, M. M. Zweng, O. K. Baranova, and D. R. Johnson (2010a) World Ocean Atlas 2009, Volume 4: Nutrients (phosphate, nitrate, and silicate), in: Levitus, S. (Ed.), NOAA Atlas NESDIS 71, Washington, D.C., p. 398.

Garcia, H.E., R. A. Locarini, T. P. Boyer, J. I. Antonov, O. K. Baranova, M. M. Zweng, and D. R. Johnson (2010b) World Ocean Atlas 2009, Volume 3: Dissolved Oxygen, Apparent Oxygen Utilization, and Oxygen Saturation, in: Levitus, S. (Ed.), NOAA Atlast NESDIS 70, Washington, D.C., p. 344.

Gruber, N. and Galloway, J.N. (2008) An Earth-system perspective of the global nitrogen cycle. Nature 451, 293-296.

Gruber, N. and Sarmiento, J.L. (1997) Global patterns of marine nitrogen fixation and denitrification. Global Biogeochemical Cycles 11, 235-266.

Karl, D., Letelier, R., Tupas, L., Dore, J., Christian, J. and Hebel, D. (1997) The role of nitrogen fixation in biogeochemical cycling in the subtropical North Pacific Ocean. Nature 388, 533-538.

Karl, D., Michaels, A., Bergman, B., Capone, D., Carpenter, E., Letelier, R., Lipschultz, F., Paerl, H., Sigman, D. and Stal, L. (2002) Dinitrogen fixation in the world's oceans. Biogeochemistry 57, 47-+.

Knapp, A.N., Sigman, D.M. and Lipschultz, F. (2005) N isotopic composition of dissolved organic nitrogen and nitrate at the Bermuda Atlantic time-series study site. Global Biogeochemical Cycles 19.

Lehmann, M.F., Sigman, D.M. and Berelson, W.M. (2004) Coupling the N-15/N-14 and O-18/O-16 of nitrate as a constraint on benthic nitrogen cycling. Marine Chemistry 88, 1-20.

Lehmann, M.F., Sigman, D.M., McCorkle, D.C., Granger, J., Hoffmann, S., Cane, G. and Brunelle, B.G. (2007) The distribution of nitrate N-15/N-14 in marine sediments and the impact of benthic nitrogen loss on the isotopic composition of oceanic nitrate. Geochimica Et Cosmochimica Acta 71, 5384-5404.

Leite, S.Q.M., Colodete, C.H.A., Dieguez, L.C. and San Gil, R.A.S. (2000) Iron extraction from Brazilian smectite by dithionite-citrate-bicarbonate method. Quimica Nova 23, 297-302.

Lisiecki, L.E. and Raymo, M.E. (2005) A Pliocene-Pleistocene stack of 57 globally distributed benthic delta O-18 records (vol 20, art no PA1003, 2005). Paleoceanography 20.

Liu, Z.H., Altabet, M.A. and Herbert, T.D. (2005) Glacial-interglacial modulation of eastern tropical North Pacific denitrification over the last 1.8-Myr. Geophys. Res. Lett. 32.

Liu, Z.H., Altabet, M.A. and Herbert, T.D. (2008) Plio-Pleistocene denitrification in the eastern tropical North Pacific: Intensification at 2.1 Ma. Geochem. Geophys. Geosyst. 9.

Mariotti, A., Germon, J.C., Hubert, P., Kaiser, P., Letolle, R., Tardieux, A. and Tardieux, P. (1981) Experimental-determination of nitrogen kinetic isotope fractionation - some principals - illustration for the denitrification and nitrification processes. Plant and Soil 62, 413-430.

Martini, E. and Worsley, T. (1970) Standard Neogene calcareous nannoplankton zonation. Nature 225, 289-&.

McElroy, M.B. (1983) Marine biological-controls on atmospheric CO2 and climate. Nature 302, 328-329.

Rafter, P.A. and Charles, C.D. (2012) Pleistocene equatorial Pacific dynamics inferred from the zonal asymmetry in sedimentary nitrogen isotopes. Paleoceanography 27, 8.

Rafter, P.A., Sigman, D.M., Charles, C.D., Kaiser, J. and Haug, G.H. (2012) Subsurface tropical Pacific nitrogen isotopic composition of nitrate: Biogeochemical signals and their transport. Global Biogeochemical Cycles 26.

Ren, H., Sigman, D.M., Meckler, A.N., Plessen, B., Robinson, R.S., Rosenthal, Y. and Haug, G.H. (2009) Foraminiferal Isotope Evidence of Reduced Nitrogen Fixation in the Ice Age Atlantic Ocean. Science 323, 244-248.

Robinson, R.S., Etourneau, J., Martinez, P.M. and Schneider, R. (2014) Expansion of pelagic denitrification during early Pleistocene cooling. Earth Planet. Sci. Lett. 389, 52-61.

Robinson, R.S., Kienast, M., Albuquerque, A.L., Altabet, M., Contreras, S., Holz, R.D., Dubois, N., Francois, R., Galbraith, E., Hsu, T.C., Ivanochko, T., Jaccard, S., Kao, S.J., Kiefer, T., Kienast, S., Lehmann, M., Martinez, P., McCarthy, M., Mobius, J., Pedersen, T., Quan, T.M., Ryabenko, E., Schmittner, A., Schneider, R., Schneider-Mor, A., Shigemitsu, M., Sinclair, D., Somes, C., Studer, A., Thunell, R. and Yang, J.Y. (2012) A review of nitrogen isotopic alteration in marine sediments. Paleoceanography 27, 13.

Schlanger, S.O.J., E. D. (1976) Initial Reports. DSDP. U.S. Govt. Printing Office, Washington.

Schlitzer, R. (2002) Interactive analysis and visualization of geoscience data with Ocean Data View. Computers & Geosciences 28, 1211-1218.

Sigman, D., Karsh, K. and Casciotti, K. (2009) Ocean process tracers: nitrogen isotopes in the ocean. Encyclopedia of ocean science, 2nd edn. Elsevier, Amsterdam.

Somes, C.J., Oschlies, A. and Schmittner, A. (2013) Isotopic constraints on the pre-industrial oceanic nitrogen budget. Biogeosciences 10, 5889-5910.

Somes, C.J., Schmittner, A., Galbraith, E.D., Lehmann, M.F., Altabet, M.A., Montoya, J.P., Letelier, R.M., Mix, A.C., Bourbonnais, A. and Eby, M. (2010) Simulating the global distribution of nitrogen isotopes in the ocean. Global Biogeochemical Cycles 24.

Tesdal, J.E., Galbraith, E.D. and Kienast, M. (2013) Nitrogen isotopes in bulk marine sediment: linking seafloor observations with subseafloor records. Biogeosciences 10, 101-118.

Wada, E. and Hattori, A. (1976) Natural abundance of N-15 in particulate organic-matter in North Pacific Ocean. Geochimica Et Cosmochimica Acta 40, 249-251.

Wara, M.W., Ravelo, A.C. and Delaney, M.L. (2005) Permanent El Nino-like conditions during the Pliocene warm period. Science 309, 758-761.

Yoshikawa, C., Yamanaka, Y. and Nakatsuka, T. (2006) Nitrate-nitrogen isotopic patterns in surface waters of the western and central equatorial Pacific. Journal of Oceanography 62, 511-525.

**Dissolved Oxygen [mL/L] at 250 m water depth**

A.

60°N

30°N — ENP 1012
WSNP 451

EQ — EEP 849
WEP 806 — EEP 1239

30°S — BUS 1082

60°S

Ocean Data View

90°E    180°W    90°W    0°

8  6  4  2  0

**N\* [µmol/kg] at 250 m water depth**

B.

60°N

30°N — ENP 1012
WSNP 451

EQ — EEP 849
WEP 806 — EEP 1239

30°S — BUS 1082

60°S

Ocean Data View

90°E    180°W    90°W    0°

7.5  5  2.5  0  -2.5  -5  -7.5
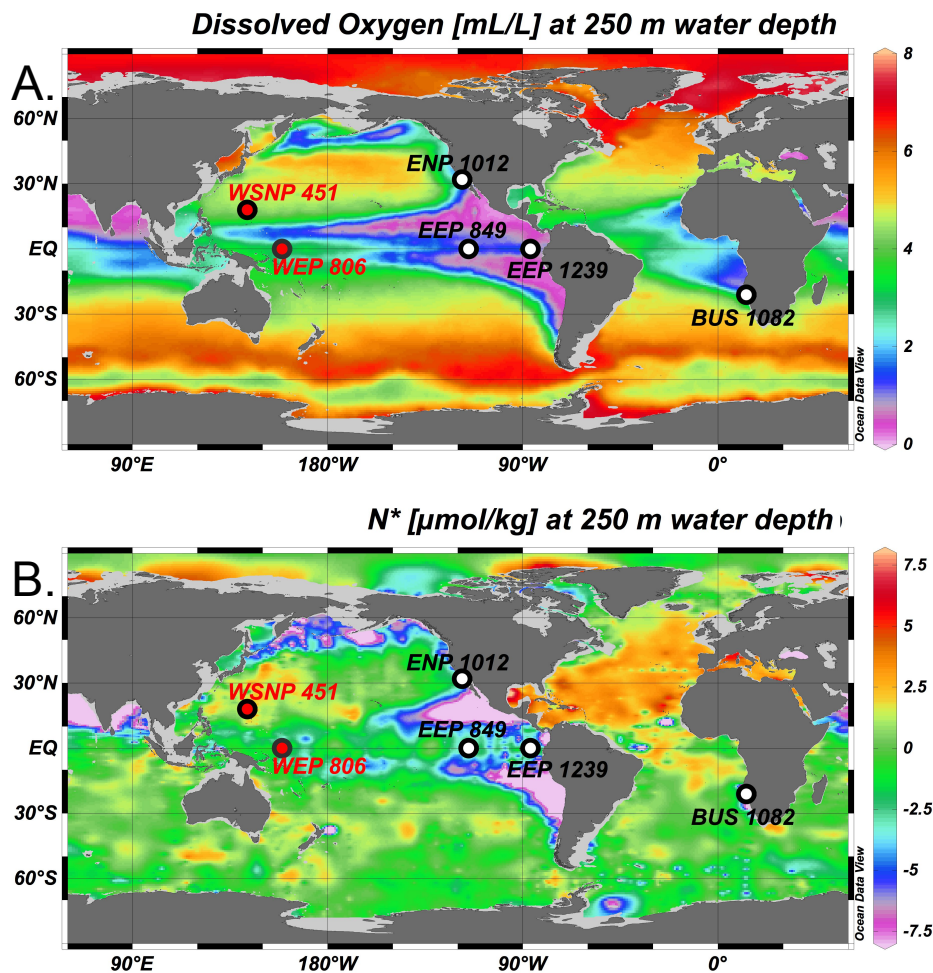
**Figure 3.1. Site locations overlain on global maps of dissolved [O$_2$] (mL L$^{-1}$) and N\* (µmol kg$^{-1}$) at 250 m water depth.**

Four of the sites existing $\delta^{15}$N records from regions of pelagic denitrification that feature the ca. 2‰ positive shift between 2.1- 1.6 Ma [Robinson et al., 2014] are shown with white circles, as detailed in in Table 1.  New FB-$\delta^{15}$N records generated in this study in the WSNP at DSDP Site 451 and in the WEP at ODP Site 806 shown are shown with red circles.  Maps were generated with Ocean Data View (ODV) [Schlitzer, 2002] with data from the World Ocean Atlas 2009 [Garcia, 2010a, b].  (A) dissolved [O$_2$] (ml L$^{-1}$) with values below 5 ml L$^{-1}$ defining the major oxygen minimum zones (OMZs) where pelagic denitrification significantly impacts the stoichiometric ratio of NO$_3^-$:PO$_4^{3-}$.  (B) N\* shown is a measure of deviations from the stoichiometric Redfield ratio of NO$_3^-$:PO$_4^{3-}$ of 16:1, where N\* = [NO$_3^-$] – 16 x [PO$_4^{3-}$] + 2.9 µmol kg$^{-1}$ after Gruber and Sarmiento [1997], whereby a nitrate excess (deficit) are determined by positive (negative) N\* values are sensitive to dissolved [O$_2$]. Nitrate deficits typically occur in the major oxygen minimum zones below 5 ml L$^{-1}$ and nitrate excesses are typical in the oligotrophic open oceans.
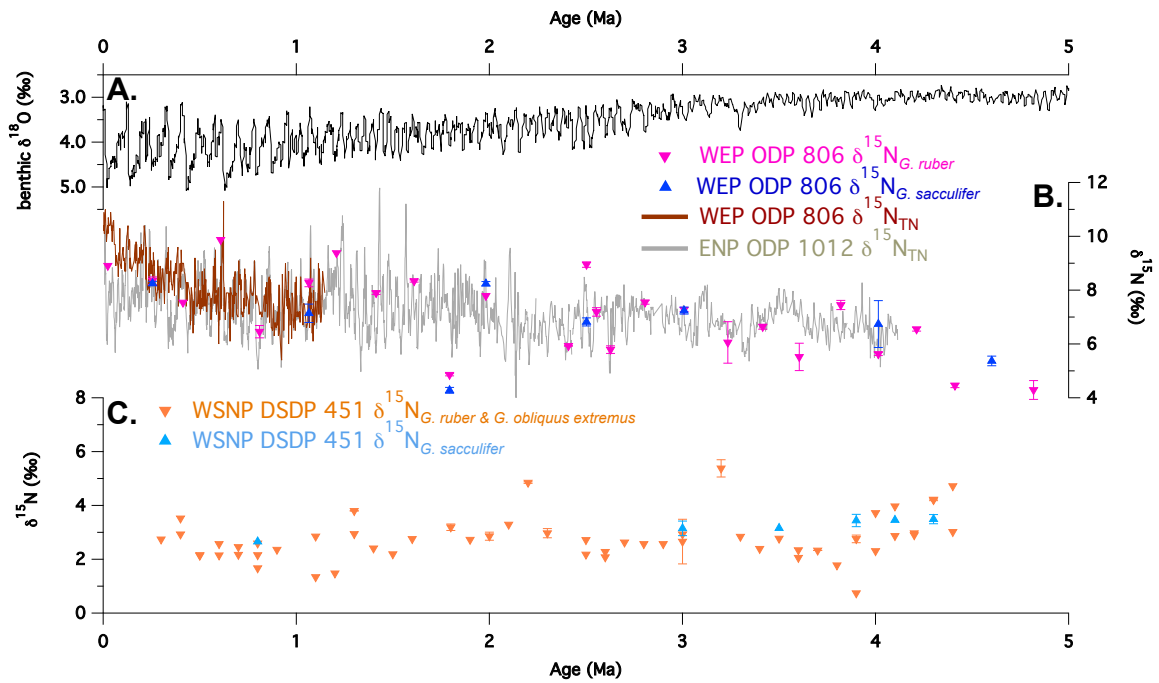
**Figure 3.2. Benthic $\delta^{18}$O stack and comparison of FB-$\delta^{15}$N and global compilation of $\delta^{15}N_{TN}$ records throughout the Pliocene-Pleistocene.**
(A) LR04 benthic $\delta^{18}$O stack [Lisiecki & Raymo, 2005]; (B) $\delta^{15}N_{TN}$ records from the Eastern North Pacific (ENP) at ODP Sites 1012 [Liu et al., 2005, 2008], and the Western Equatorial Pacific (WEP) at ODP Site 806 [Rafter and Charles., 2012] as well as FB-$\delta^{15}$N records of G. sacculifer and G. ruber at ODP site 806 [this study]; (C) FB-$\delta^{15}$N records of G. sacculifer, G. ruber and G. obliquus extremus in the western subtropical North Pacific (WSNP) at DSDP Site 451 [this study].
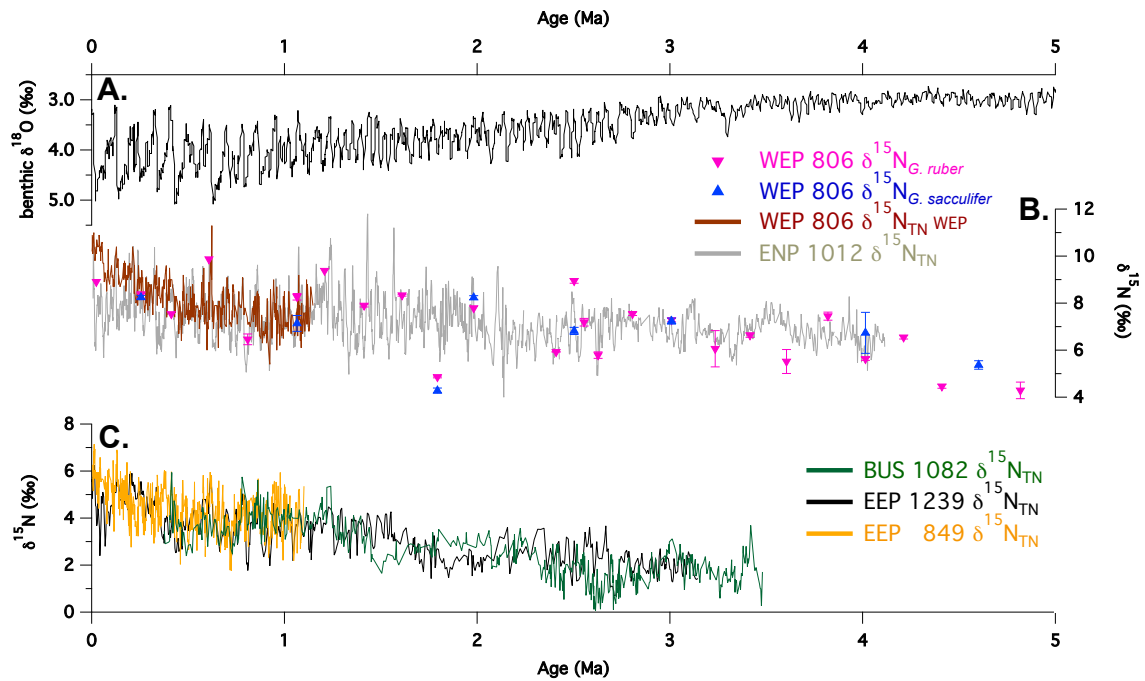
**Figure 3.3 Benthic $\delta^{18}$O stack and comparison of FB-$\delta^{15}$N and $\delta^{15}$N$_{TN}$ records from regions exhibiting pelagic denitrification increase from the Pliocene to the Pleistocene.**
(A) LR04 benthic $\delta^{18}$O stack [Lisiecki & Raymo, 2005]; (B) $\delta^{15}$N$_{TN}$ records from the Eastern North Pacific (ENP) at ODP Sites 1012 [Liu et al., 2005, 2008], and the Western Equatorial Pacific (WEP) at ODP Site 806 [Rafter and Charles., 2012] as well as FB-$\delta^{15}$N records of G. sacculifer and G. ruber at ODP Site 806 [this study]; (C) $\delta^{15}$N$_{TN}$ records from ODP Site 1082 in the Benguela Upwelling System (BUS) in the southeastern Atlantic [Robinson et al, 2002; Etourneau et al., 2009], and ODP Sites 1239 [Etourneau et al., 2013] and 849 [Rafter and Charles, 2012] from the Eastern Equatorial Pacific (EEP).

**Table 3.1 Site locations for $\delta^{15}N_{TN}$ and FB-$\delta^{15}N$ records in Fig. 3.1 to 3.3**

| Location | Site | Latitude, longitude | Original reference |
|---|---|---|---|
| Western Subtropical North Pacific | DSDP 451 | 18° 0' N, 143° 16' E | This study |
| Western Equatorial Pacific | ODP 806 | 0° 11' N, 159° 22' W | This study |
| | | | Rafter and Charles [2012] |
| Eastern North Pacific | ODP 1012 | 32° 17' N, 118° 24' W | Liu et al. [2008] |
| Eastern Equatorial Pacific | ODP 849 | 0° 11' N, 110° 30' W | Rafter and Charles [2012] |
| Eastern Equatorial Pacific | ODP 1239 | 0° 40' S, 82° 5' W | Etourneau et al. [2013] |
| Eastern South Atlantic | ODP 1082 | 21° 6' S, 11° 49' E | Robinson et al. [2002]; |
| | | | Etourneau et al., [2009] |

**Table 3.2 Foram-bound δ<sup>15</sup>N compositions from the western subtropical North Pacific at DSDP Site 451**

| HOLE | CORE | SECTION | HALF | INVTERVAL [cm] | Age [Ma] | $\delta^{15}N_{G. Ruber}$ | $\delta^{15}N_{G. Sacculifer}$ |
|------|------|---------|------|----------------|----------|---------|-----------|
| U0451Z | 1R | 2 | W | 23-26 | 0.14 | 3.52 | |
| U0451Z | 1R | 2 | W | 100-104 | 0.43 | 2.14 | |
| U0451Z | 1R | 2 | W | 134-137 | 0.57 | 2.15 | |
| U0451Z | 1R | 3 | W | 16-19 | 0.71 | 2.17 | |
| U0451Z | 1R | 3 | W | 43-47 | 0.86 | 2.59 | 2.66 |
| U0451Z | 1R | 3 | W | 70-73 | 1.00 | 1.67 | |
| U0451Z | 2R | 1 | W | 22-25 | 1.19 | 2.85 | |
| U0451Z | 2R | 1 | W | 97-100 | 1.38 | 3.80 | |
| U0451Z | 2R | 2 | W | 22.5-25.5 | 1.57 | 2.19 | |
| U0451Z | 2R | 2 | W | 91.5-94.5 | 1.76 | 2.76 | |
| U0451Z | 2R | 3 | W | 22-25 | 1.95 | 3.19 | |
| U0451Z | 2R | 3 | W | 86-89 | 2.14 | 2.73 | |
| U0451Z | 2R | 4 | W | 23-27 | 2.33 | 2.86 | |
| U0451Z | 2R | 5 | W | 23-26 | 2.52 | 3.29 | |
| U0451Z | 2R | 5 | W | 92-95 | 2.62 | 4.85 | |
| U0451Z | 2R | 6 | W | 57-60 | 2.71 | 2.97 | |
| U0451Z | 3R | 1 | W | 23-25 | 2.78 | 2.72 | |
| U0451Z | 3R | 1 | W | 100-103 | 2.85 | 2.18 | |
| U0451Z | 3R | 1 | W | 139-142 | 2.91 | 2.08 | |
| U0451Z | 3R | 2 | W | 48-51 | 2.98 | 2.28 | |
| U0451Z | 3R | 2 | W | 122-125 | 3.12 | 2.63 | |
| U0451Z | 3R | 3 | W | 52.5-55.5 | 3.19 | 2.57 | |
| U0451Z | 3R | 3 | W | 137-140 | 3.25 | 2.57 | |
| U0451Z | 3R | 4 | W | 60-63 | 3.32 | 2.93 | |
| U0451Z | 3R | 4 | W | 125-128 | 3.39 | 3.14 | 3.15 |
| U0451Z | 3R | 5 | W | 54-57 | 3.46 | 5.38 | |
| U0451Z | 3R | 5 | W | 136-139 | 3.52 | 2.84 | |
| U0451Z | 3R | 6 | W | 54-57 | 3.59 | 2.39 | |
| U0451Z | 3R | 6 | W | 139-142 | 3.66 | 2.77 | 3.16 |
| U0451Z | 4R | 1 | W | 15-18 | 3.70 | 2.34 | |
| U0451Z | 4R | 1 | W | 65-68 | 3.74 | 2.06 | |
| U0451Z | 4R | 1 | W | 115-118 | 3.79 | 2.33 | |
| U0451Z | 4R | 2 | W | 15-18 | 3.83 | 1.78 | |
| U0451Z | 4R | 2 | W | 65-68 | 3.87 | 0.74 | |
| U0451Z | 4R | 2 | W | 115-118 | 3.91 | 2.76 | 3.44 |
| U0451Z | 4R | 3 | W | 14-18 | 3.95 | 2.31 | |
| U0451Z | 4R | 3 | W | 65-68 | 3.99 | 3.72 | |
| U0451Z | 4R | 3 | W | 143-146 | 4.04 | 2.87 | |
| U0451Z | 4R | 4 | W | 17-20 | 4.12 | 3.97 | 3.46 |
| U0451Z | 4R | 4 | W | 67-70 | 4.20 | 2.90 | |
| U0451Z | 4R | 4 | W | 115-119 | 4.28 | 2.97 | |
| U0451Z | 4R | 5 | W | 40-43 | 4.36 | 4.22 | |

**Table 3.3 Foram-bound $\delta^{15}$N compositions from the Western Equatorial Pacific at ODP Site 806**

| HOLE | CORE | SECTION | HALF | INTERVAL [cm] | Age [Ma] | $\delta^{15}N_{G.\ Ruber}$ | $\delta^{15}N_{G.\ Sacculifer}$ |
|------|------|---------|------|---------------|----------|---------------------------|----------------------------------|
| 806A | 1 | H | 1 | 14-16 | 0.02 | 8.91 | |
| 806A | 1 | H | 4 | 6-8 | 0.26 | 8.35 | 8.25 |
| 806A | 1 | H | 6 | 6-8 | 0.41 | 7.54 | |
| 806A | 2 | H | 3 | 105-107 | 0.61 | 9.87 | |
| 806A | 2 | H | 6 | 105-107 | 0.81 | 6.46 | |
| 806A | 3 | H | 3 | 145-147 | 1.07 | 8.27 | 7.14 |
| 806A | 3 | H | 6 | 15-17 | 1.21 | 9.38 | |
| 806A | 4 | H | 3 | 25-27 | 1.41 | 7.90 | |
| 806A | 4 | H | 6 | 15-17 | 1.61 | 8.34 | |
| 806A | 5 | H | 3 | 65-67 | 1.79 | 4.86 | 4.28 |
| 806A | 5 | H | 6 | 105-107 | 1.98 | 7.79 | 8.24 |
| 806A | 6 | H | 5 | 45-47 | 2.41 | 5.93 | |
| 806A | 6 | H | 6 | 83-85 | 2.50 | 8.95 | 6.82 |
| 806B | 7 | H | 2 | 2-4 | 2.55 | 7.19 | |
| 806B | 7 | H | 3 | 62-64 | 2.63 | 5.79 | |
| 806B | 7 | H | 6 | 82-84 | 2.81 | 7.55 | |
| 806B | 8 | H | 4 | 42-44 | 3.01 | 7.28 | 7.24 |
| 806B | 9 | H | 3 | 42-44 | 3.23 | 6.06 | |
| 806B | 10 | H | 1 | 82-84 | 3.42 | 6.64 | |
| 806B | 10 | H | 6 | 122-124 | 3.60 | 5.52 | |
| 806B | 11 | H | 5 | 92-94 | 3.82 | 7.45 | |
| 806B | 12 | H | 5 | 92-94 | 4.01 | 5.63 | 6.74 |
| 806B | 13 | H | 5 | 2-4 | 4.21 | 6.55 | |
| 806B | 14 | H | 5 | 42-44 | 4.41 | 4.46 | |
| 806B | 15 | H | 5 | 42-44 | 4.60 | | 5.37 |
| 806B | 16 | H | 6 | 122-124 | 4.82 | 4.29 | |
| 806B | 17 | H | 4 | 32-34 | 5.02 | 5.68 | 5.34 |
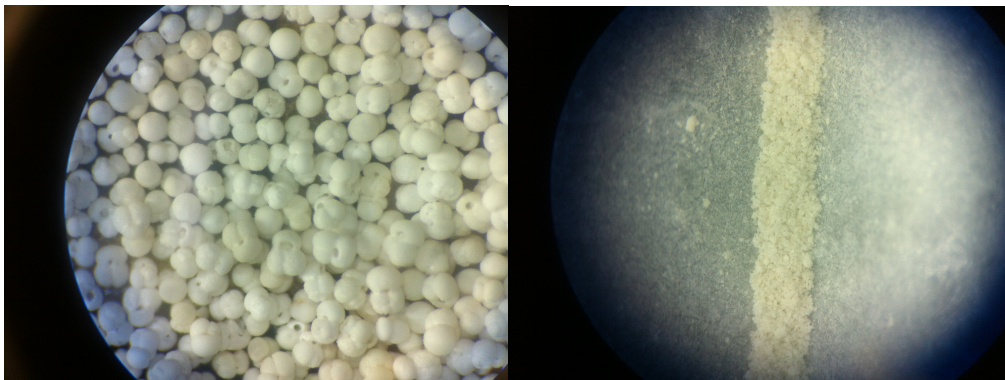
**Figure EA 3-1 Images of G. ruber shells (>250 μm fraction) isolated for FB-$\delta^{15}$N-G. ruber measurements.**
Several hundred uncrushed (left) and crushed (right) G. ruber shells in prior to cleaning protocols described in Materials and Methods.

# Appendix A: $\delta^{15}N_{AA}$ methodology and preliminary results from deep-sea Bamboo coral from the California Current System

Fabian C. Batista[1], Tessa M. Hill[2,3], Thomas P. Guilderson[1,4], A. Christina Ravelo[1], Matthew D. McCarthy[1]

[1]Ocean Sciences Department, University of California, Santa Cruz

[2]Department of Earth & Planetary Sciences, University of California, Davis

[3]Bodega Marine Laboratory, University of California

[4]Center for Accelerator Mass Spectrometry, Lawrence Livermore National Laboratory

*One of the most striking observations of marine biology is the fact that some parts of the ocean are fertile while other parts are quite barren. There must be chemical factors, which determine fertility, and an explanation of this was perhaps the first serious question which oceanographers asked the chemist. In the year 1930 there were probably no more than a dozen professional chemists in the world who were actively interested in the ocean, and practically every one of them was trying to answer this question.*

-Norris Rakestraw

## Materials and Methods

### Coral samples and sectioning

The sampling approach for collecting deep-sea Bamboo coral specimen for this work was previously described (Hill et al., 2014). Briefly specimens of bamboo corals utilized in this study were collected as part of two expeditions on the Monterey Bay Aquarium Research Institute (MBARI) vessel R/V Western Flyer utilizing the ROV Tiburon along the California margin, including the Pioneer Seamount and Monterey Canyon in 2004 and 2007. The two corals used in this study were collected live at the Pioneer Seamount (T1100 A4) recovered from 1285 meters water depth (mwd) at 37.359 latitude, -123.394 longitude, and the Monterey Canyon (T1104 A7) recovered from 870 mwd at 36.744 latitude, -122.037 longitude.

Organic nodes from the basal section (that nearest the attachment to substrate) of the coral were selected for subsequent analyses. Separation of the organic nodes from the calcite internodes (Fig. 4.2) was accomplished by cutting the calcite above and below the node with a diamond saw and subsequent immersion of the node in 0.5 N HCl to remove the remaining calcite interspersed throughout the node. Once the calcite was removed, the nodes were stored in deionized water prior to subsampling for elemental and isotopic analyses. Individual nodes were sampled at ~1mm intervals using forceps and scalpel under a stereomicroscope with an attached digital camera. Images taken prior to and during peeling are shown in Appendix B. These samples were then dried overnight at 50° C and stored in polyethylene vials in desiccators at room temperature.

## Analyses

### Radiocarbon ($\Delta^{14}C$) analysis

$\Delta^{14}C$ analysis was performed on approximately 600 to 900 mg of gorgonin tissue at the Center for Accelerator Mass Spectrometry, Lawrence Livermore National Laboratory. Samples were converted to $CO_2$ and then reduced to graphite in the presence of iron catalysts under ~1 atm of $H_2$ and high temperature. Results include a $^{14}C$-free background correction, and a $\delta^{13}C$-normalization. Results are reported as conventional (non-reservoir corrected) radiocarbon $\Delta^{14}C$ (‰) values, as per international convention (Stuiver and Polach, 1977).

### Bulk elemental and stable isotopic analysis

Approximately 0.4 to 1.5 mg gorgonin tissue was used for elemental composition (wt% C, wt% N), elemental C/N ratios, and $\delta^{13}C_{org}$ and $\delta^{15}N_{bulk}$ composition. Samples were analyzed at the Stable Isotope Laboratory at the University of California, Santa Cruz with an Carlo Erba EA1108 CHNS/O elemental analyzer interfaced to a Thermo Finnigan Conflo II and Delta$^{Plus}$ XP isotope ratio mass spectrometer (Thermo Finninagan, USA). Bulk elemental and stable isotopic compositions were analyzed in duplicate for greater than 15% of samples to verify expected precision. Internal and international reference materials (acetanilide from Indiana University) were for isotopic corrections and instrument drift; analytical reproducibility for both $\delta^{13}C$ and $\delta^{15}N$ measurements was better than ±0.2‰.

**Compound specific isotopic analysis and mol% AA**

Approximately 1.5 to 8 mg of organic node tissue was used for $\delta^{15}N_{AA}$ and mol% AA compositions. Samples were hydrolyzed in ~5 mL of 6 N HCl for 20 hr, and spiked with norleucine internal standard ($\delta^{15}N=7.9$‰). Hydrolysates were evaporated to dryness under a stream of $N_2$ and stored in a dessicator overnight, followed by formation of trifluoroacetyl/isopropyl ester derivatives (McCarthy et al., 2007). Amino-acid molar composition was determined with an Agilent 7890A gas chromatograph fitted with a SGE BPX-5 column (60 m x 0.32 mm internal diameter, 1 μm film thickness). Response factors were determined with a dilution series of external amino-acid mixture of 16 common protein amino acids. Reproducibility, as measured by the standard deviation of analytical replicates, averaged <5 mol%.

Compound specific $\delta^{15}N$ amino acid analysis ($\delta^{15}N_{AA}$) was determined on amino-acid derivatives using previously published procedures (McCarthy et al., 2007; Batista et al., 2014). Derivatives were analyzed on a Thermo Trace Ultra gas chromatographic, fitted with a SGE BPX-5 capillary (60 m x 0.32 mm internal diameter, 1 μm film thickness), in line with the oxidation and reduction furnaces of an Thermo GC/C III unit, interfaced to a ThermoFinnigan Delta[Plus] XP isotope ratio mass spectrometer. Samples were analyzed in quadruplicate at minimum. Analytical accuracy was monitored by analysis of norleucine internal standard and co-derivatized amino acid external standards for which authentic $\delta^{15}N$ values of each amion acid were determined offline. Reproducibility for individual $\delta^{15}N$ values of each amino acid were typically better than 2‰.

## $\delta^{15}N_{AA}$ parameters and nomenclature

The paradigm of $\delta^{15}N_{AA}$ conventions is summarized in Chapter 2, but briefly, protein AAs are divided into two main groupings based on current literature conventions (e.g., Popp et al., 2007; McCarthy et al., 2007). The Trophic AA (Tr AA; Ala, Asx, Glx, Ile, Leu, Pro, Val) are those generally exhibiting more enriched $\delta^{15}N$ values, du to assumed larger $^{15}N$ enrichment with trophic transfer. The Source AA (Src AA; Gly, Lys, Phe, Ser, Tyr) are those with typically lower $\delta^{15}N$ values, based on the assumption of little to no $\delta^{15}N$ change with trophic transfer. We note that Thr was originally grouped with source AA (McClelland and Montoya, 2002; Chikaraishi et al, 2009), however has now been shown to in fact have "inverse" N isotopic fractionation with trophic transfer that is unique among commonly measured AA (Germain et al., 2013). Following the convention of previous authors (e.g., McCarthy et al., 2013) $\delta^{15}N_{AA}$ data are organized for coral gorgonin samples by Tr and Src AA groupings, and then in alphabetical order.

Trophic positions were calculated from $\delta^{15}N_{AA}$ values of Glu and Phe, following the most widely applied current formulation from Chikaraishi et al. (2009). This approach is based on a calibrated difference in $\delta^{15}N_{Glx}$ and $\delta^{15}N_{Phe}$ defined as:

$$TP = \frac{(\delta^{15}N_{Glx} - \delta^{15}N_{Phe} - 3.4\text{‰})}{7.6\text{‰}} + 1$$

where 3.4‰ is the empirical difference between $\delta^{15}N_{Glu}$ and $\delta^{15}N_{Phe}$ in aquatic marine autotrophs and 7.6‰ is the N isotopic trophic enrichment factor (TEF) of $\delta^{15}N_{Glx}$ relative to $\delta^{15}N_{Phe}$ per trophic transfer.

Finally, $\Sigma V$ is commonly applied as a test of the extent of preservation of $\delta^{15}N_{AA}$ data, the fidelity of primary signals and validity in interpretation of $\delta^{15}N_{AA}$ based proxies. It is used as a measure of total heterotrophic AA resynthesis, originally proposed by McCarthy and co-authors (2007), and is based on the average deviation of individual $\delta^{15}N$ values of Tr AA (Ala, Val, Leu, Ile, Pro, Asx, Glx) from the $\delta^{15}N_{Tr}$ (the mean $\delta^{15}N$ of Tr AA). $\Sigma V$ is defined as:

$$\Sigma V = \frac{1}{n} \Sigma |\chi_i|$$

where $\chi_i$, is the offset in $\delta^{15}N$ of each AA from the average $= [\delta^{15}N_i - \text{Average } \delta^{15}N_i]$, and $n$ is the number of AA used in the calculation.

**Preliminary results**
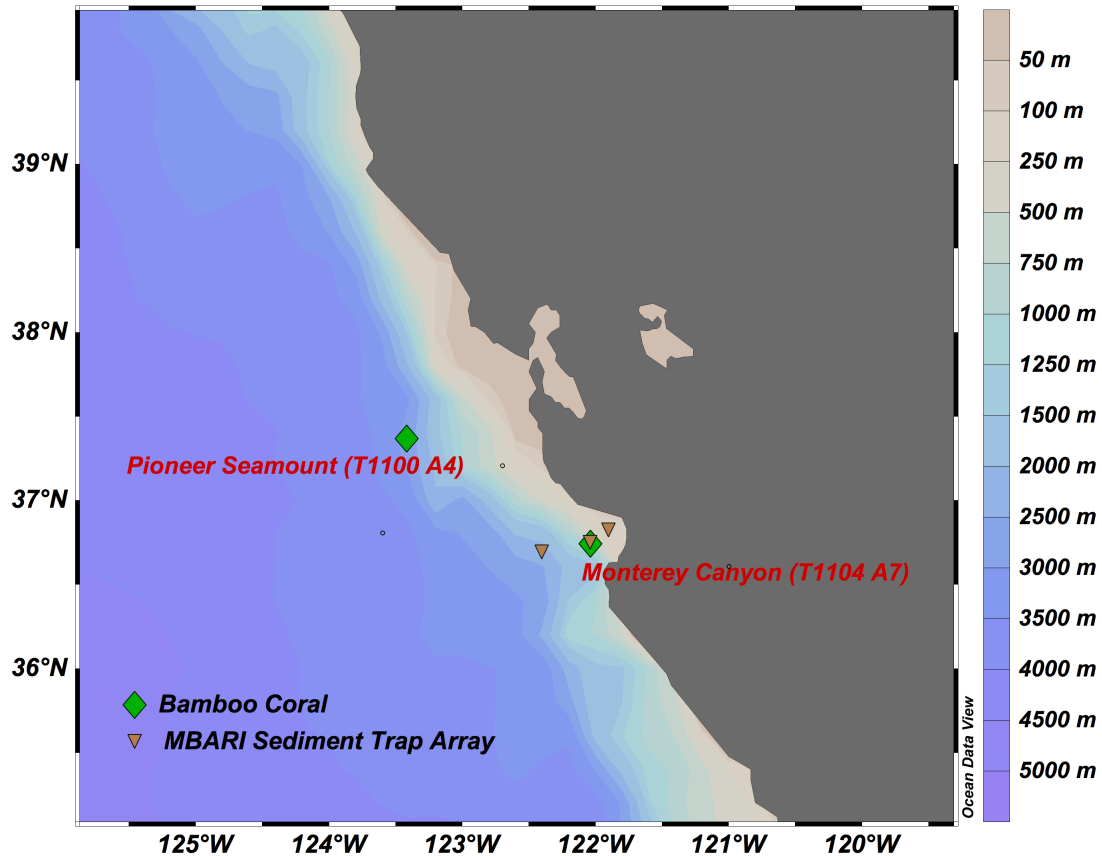


**Figure 4.1 Map of sample sites located on the central California coast.**
Sample site locations overlain on a bathymetric map with depth scale on right side of map. Green diamonds indicate locations where Bamboo coral specimen were hand selected by an manned submersible vehicle in Monterey Canyon at 870 m water depth (mwd) and from the Pioneer Seamount at 1285 mwd. Note that the bathymetry in this map does not resolve the Pioneer Seamount. Inverted brown triangles indicate locations of MBARI sediment trap arrays in Monterey Bay. This map was generated with Ocean Data View (Schlitzer, 2002).
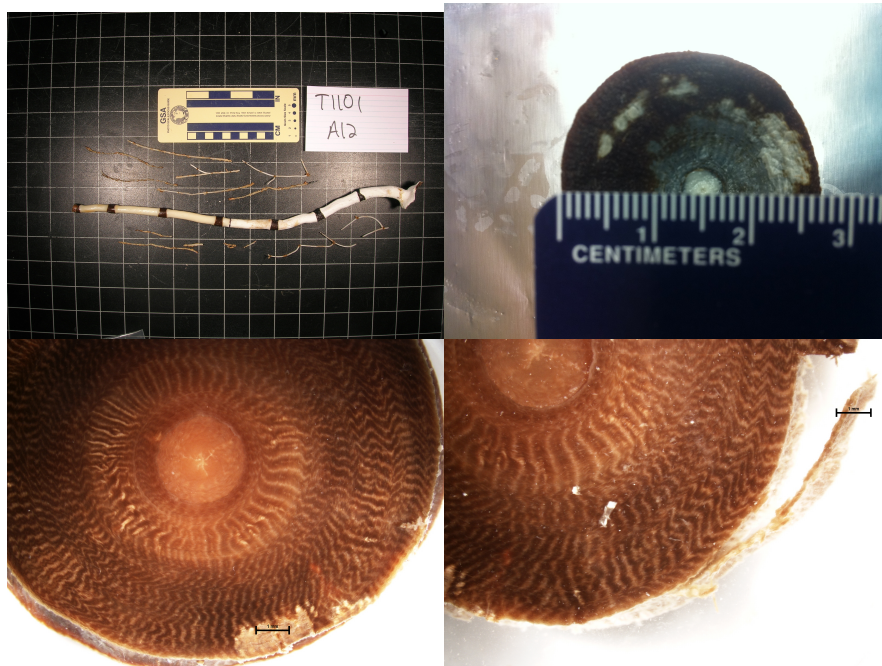
**Figure 4.2 Photographs of a bamboo coral skeleton and cross section of an organic skeletal node from a Pioneer Seamount coral specimen T1100 A4.**
Example of bamboo coral skeleton showing the dark organic nodes and white calcitic internodes (top left). A cross section of an ca. 26 cm diameter organic node isolated from bamboo coral skeletal specimen (T1100 A4) collected at the Pioneer Seamount (top right). Cross section of the polished organic node after carbonate removal prior to peeling growth layers (bottom left) and during peeling with forceps (bottom right). In the bottom two images, the black scale bar, represents 2 mm.
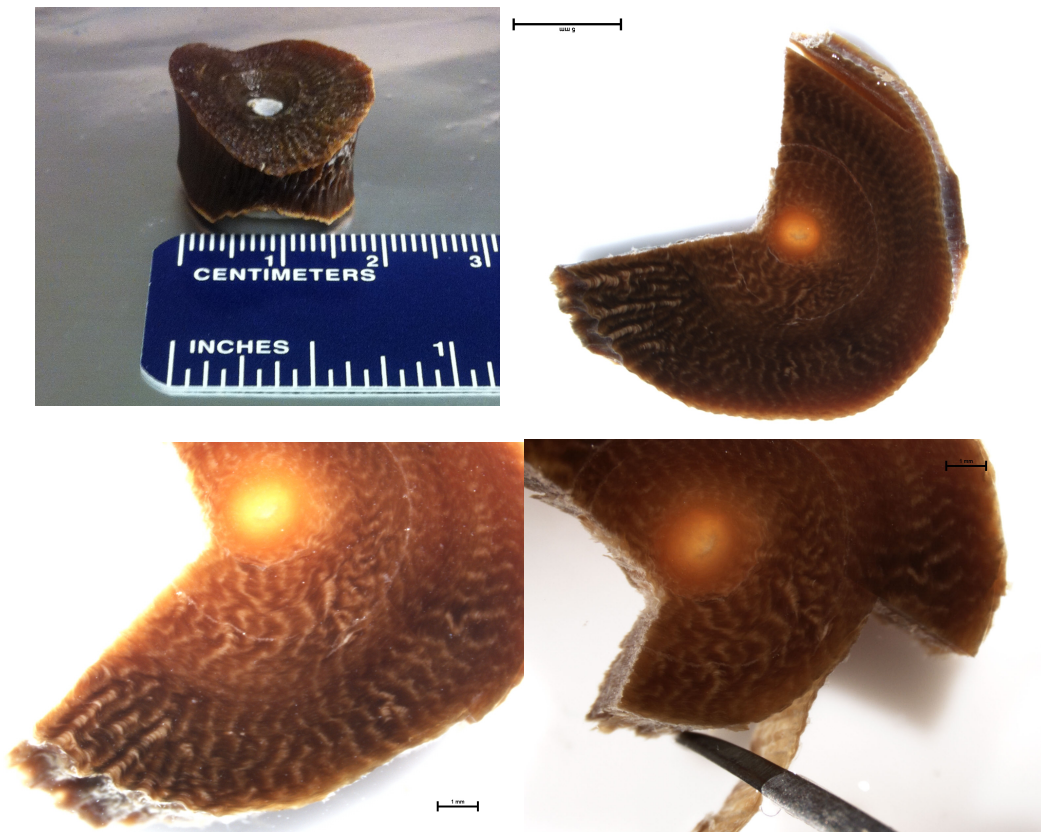
**Figure 4.3 Cross sectional photographs of an organic skeletal node isolated from the Pioneer Seamount coral specimen T1104 A7.**
A cross section of an ca. 13 cm diameter organic node isolated from bamboo coral skeletal specimen (T1104 A7) collected in Monterey Canyon (top left). Cross sections of the polished organic node after carbonate removal prior to peeling growth layers used in this study (top right) and during peeling with forceps (bottom left and right). In the images with polished cross sections, the black scale bar represents 2 mm. Note that approximately one quarter wedge of the organic node was removed for another study.
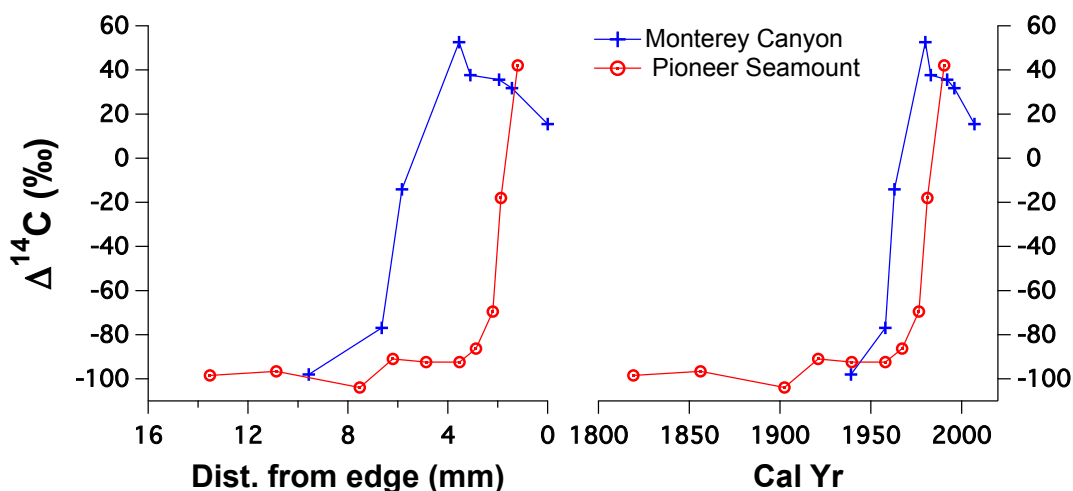
**Figure 4.4 Radiocarbon age models for Bamboo coral from Monterey Canyon and Pioneer Seamount.**

Gorgonin $\Delta^{14}$C values from the coral specimens investigated here exhibit pre-anthropogenic $\Delta^{14}$C values of approximately -100‰ in the interior portion of the skeleton. Both specimen exhibit similar enrichment in $^{14}$C indicative of post-bomb (post-1957) values near the outer edge of the node (0-4 mm), with $\Delta^{14}$C values ranging from +20 to +58‰ (Table 4.1 & 4.2, Figure 4.2). Linear extension rates were determined to be 0.07 and 0.13 mm yr$^{-1}$ for Pioneer Seamount and Monterey Canyon coral specimen, respectively. Elevated $\Delta^{14}$C signal observed in both corals is consistent with increased $^{14}$C in the atmosphere and surface waters due to atmospheric nuclear weapons testing during the 1950s and early 1960s (bomb radiocarbon; Broecker et al., 1985). Evidence of bomb carbon spike or local $\Delta^{14}$C maxima resulted from curtailment in weapons testing and has been observed previously in deep-sea coral investigations (e.g., Roark et al., 2005; Sherwood et al., 2006; Sherwood et al., 2009). The observed $\Delta^{14}$C spike in both coral specimens is interpreted here as an indication that a surface derived food source is influencing the organic node geochemistry. Thus, time-series isotopic and elemental analysis of gorgonin material has the potential to record surface ocean biogeochemistry.
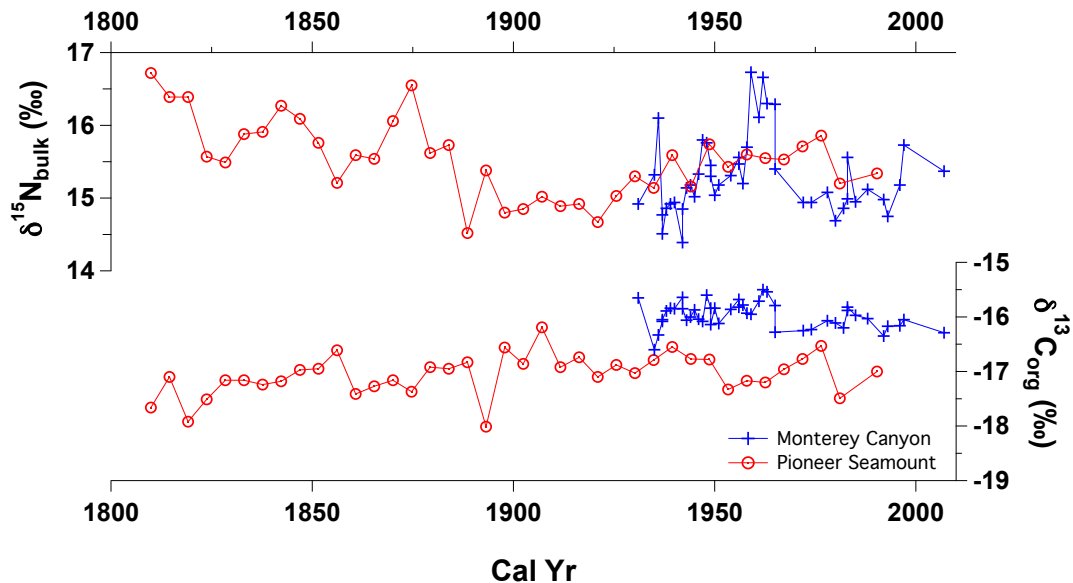
**Figure 4.5 Comparison of centennial-length time-series data for Pioneer Seamount and Monterey Bay Bamboo coral specimens.**
(a) $\delta^{15}N_{bulk}$ and (b) $\delta^{13}C_{org}$ records for the Monterey Canyon (blue) and Pioneer Seamount (red) Bamboo coral specimens. Despite the proximity of the sample location for these specimens, the overlap in $\delta^{15}N$ values and the consistent 1‰ offset in $\delta^{13}C_{org}$ highlights a decoupling of the processes, which control $\delta^{13}C_{org}$ and $\delta^{15}N_{bulk}$ variables within deep-sea Bamboo coral from the California Current System. This is consistent with productivity gradients driving the offset in $\delta^{13}C_{org}$ records, and the lack of an offset in $\delta^{15}N_{bulk}$ suggests no strong difference in surface nitrate utilization between the offshore and inshore coral specimens, as well as no zonal gradient in nitrate $\delta^{15}N$, which is consistent with a uniform subsurface nitrate $\delta^{15}N$ value of ca. 8‰ for this region (Wankel et al., 2007).
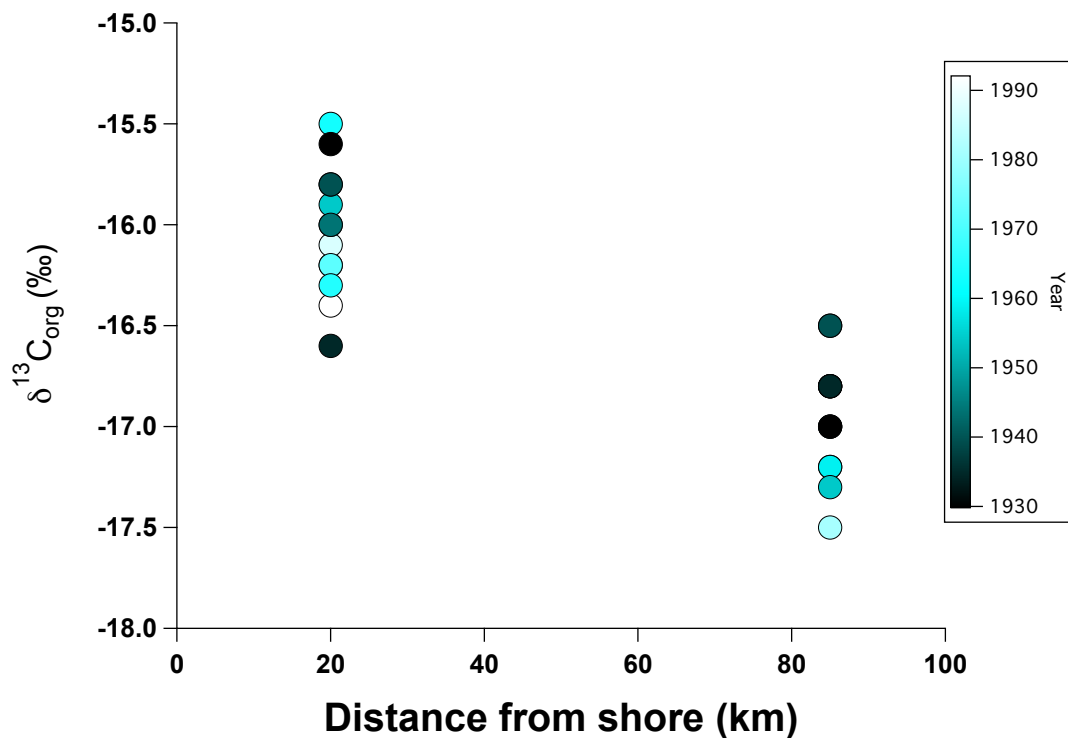
**Figure 4.6 Relationship between $\delta^{13}C_{org}$ of Bamboo coral gorgonin node and distance from shore.**

A significant negative correlation exists between Bamboo coral organic node $\delta^{13}C_{org}$ values and distance from shore. This relationship has been previously noted in zooplankton and nekton up to 50 km offshore in the northern California Current ecosystem (Miller et al, 2008) and in particulate organic matter in the Santa Barbara Channel of southern California Current System (Miller et al., 2013). The $\delta^{13}C_{org}$ values for the Monterey Canyon coral specimen at 20 km distance and Pioneer Seamount coral specimen at 85 km are statistically unique resulting from a strong cross-shelf productivity gradient, where the near shore Monterey Canyon coral exhibits higher productivity vs. lower productivity in the offshore Pioneer Seamount coral and supports previous evidence from the region for non-diffusive inorganic carbon uptake resulting from various factors particularly including cell size and growth rate (Rau et al., 2001). This cross-shelf gradient in $\delta^{13}C_{org}$ values is a widely observed phenomenon in high productivity, eastern margins settings, and has specifically been observed in phytoplankton, zooplankton, nekton and POM throughout the California Current System (Miller et al., 2008; Miller et al., 2013). Overall, that the coral $\delta^{13}C_{org}$ results presented here match previous observations of living OM and recently exported POM is consistent with the $\Delta^{14}C$ data discussed above and the notion that gorgonin nodes in long-lived deep-sea coral skeleton are robust archives with potential for high-temporal paleoenvironmental reconstructions reflective of surface ocean biogeochemical dynamics.
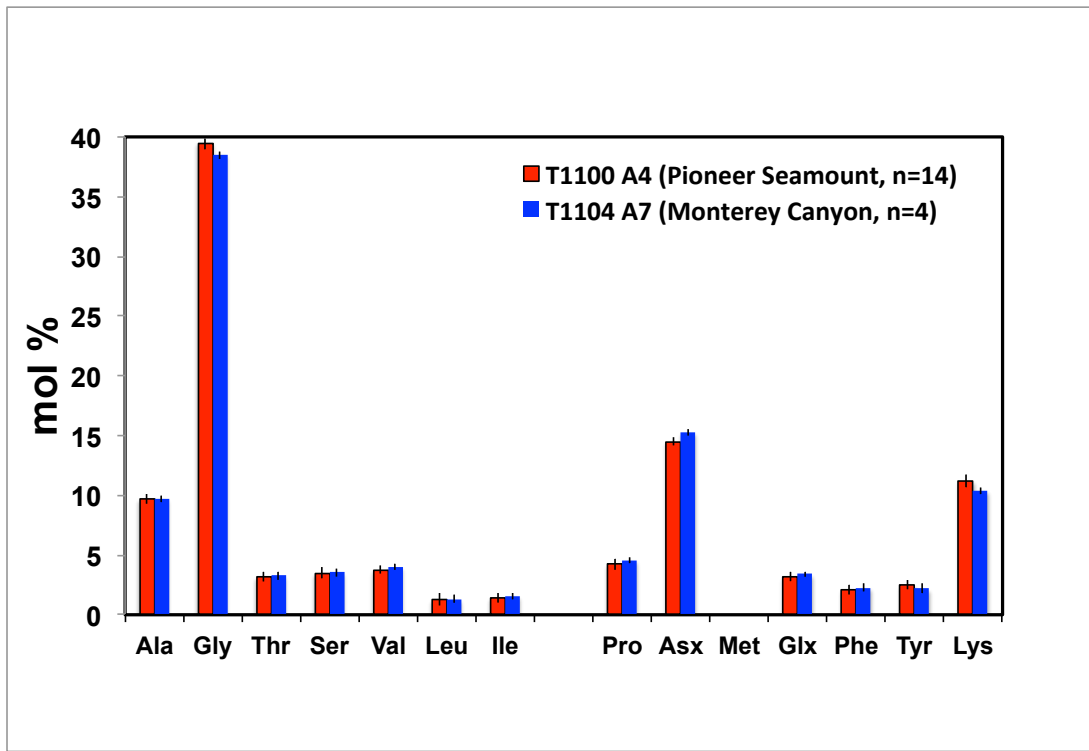
**Figure 4.7 Histogram of amino acid composition in organic nodes from deep-sea Bamboo coral.**
Comparison of mol% AA composition in the Pioneer Seamount (red) and Monterey Canyon (blue) Bamboo coral specimen shows excellent intra- and inter-specimen reproducibility, therefore suggesting preservation of the organic proteinaceous nodes used for the time-series reconstructions in this study. Note the peculiar AA composition with an abundance of Glycine (Gly), which is particularly unique from most living terrestrial and marine organisms (Cowie and Hedges, 1992). The Gly mol% of ca. 40% is much higher than is seen elsewhere in living organisms (Cowie and Hedges, 1992), except in other gorgonian corals, where Lepidisis, Keratoisis, and Gerardia have also been found to have a high mol% abundance of Glycine of approximately 30-40% (Sherwood et al., 2014; K. Strzepek, personal communication). The invariant amino acid distribution throughout the lifespan of both corals specimens (100-200 y) is interpreted as supporting evidence that these gorgonin nodes are unaltered archives appropriate for paleoenvironmental reconstruction and exploration of CSIA $\delta^{15}N_{AA}$ data and associated parameters: $\delta^{15}N_{AvgTr}$, $\delta^{15}N_{AvgSrc}$ and $TP_{Glu/Phe}$.
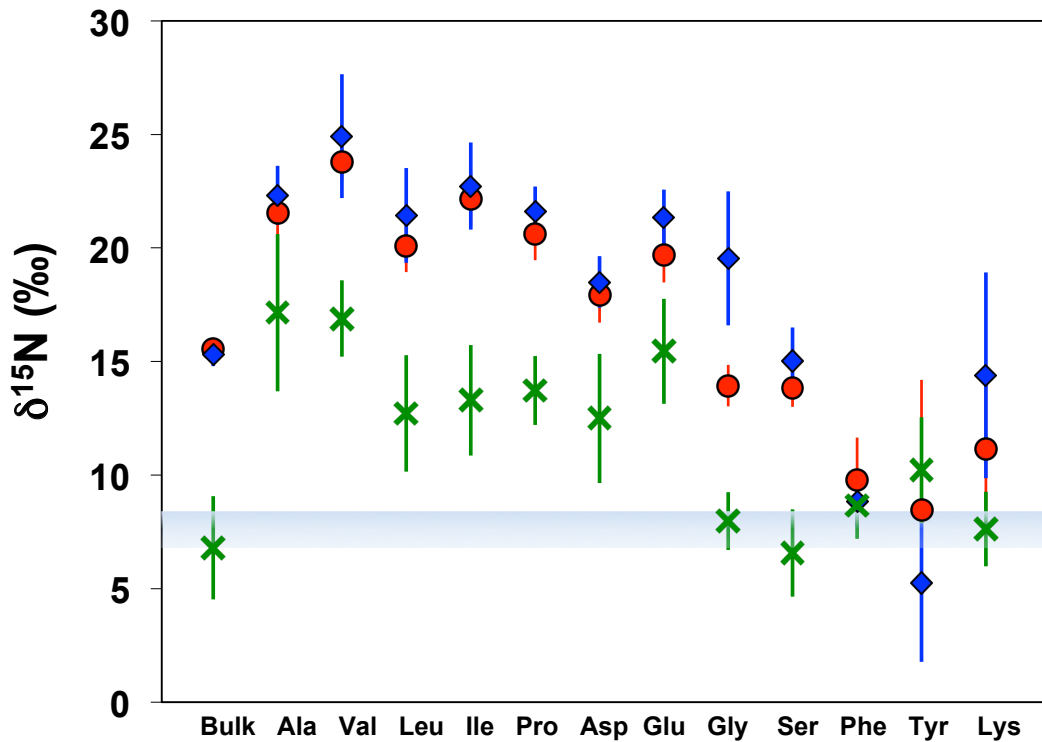
**Figure 4.8 Comparison of mean $\delta^{15}N_{bulk}$ and $\delta^{15}N_{AA}$ results for Bamboo coral specimen and sinking particles from the region.**

$\delta^{15}N_{bulk}$ and $\delta^{15}N_{AA}$ results in Bamboo coral from Monterey Canyon (blue, n=80) and Pioneer Seamount (red, n=56) compared with those in sinking particles from MBARI sediment trap arrays (green, n=30; O. Sherwood, personal communication). Error bars represent $\pm 1\sigma$ for each sample type. For reference, the mean subsurface nitrate $\delta^{15}N$ value (n=20; Wankel et al., 2007), sampled seasonally between 2002 and 2004 at the MBARI sediment trap arrays in Monterey Bay, California is shown as a shaded blue bar (width represents $\pm 1\sigma$). The relative offset in $\delta^{15}N_{bulk}$ values between the sediment trap and two coral samples is a trophic enrichment effect, where expectation prescribes a $\delta^{15}N$ fractionation in the trophic AA (TrAA; see x-axis: Ala to Glu) that drive net increases in $\delta^{15}N_{bulk}$ values through trophic transfer, while source AA $\delta^{15}N$ values (SrcAA; see x-axis: Gly to Lys) should reflect variations in baseline source nitrate $\delta^{15}N$ only. Non-conservative behavior in $\delta^{15}N$ values of specific Src AA (i.e., Gly, Ser, Tyr, and Lys) in Bamboo coral relative to sinking particles suggests that this paradigm requires revision. However, note the stability in $\delta^{15}N_{Phe}$ values of all sample types as indicated by small $1\sigma$ and the similarity to the mean nitrate $\delta^{15}N$ value in Monterey Bay (7.6‰).
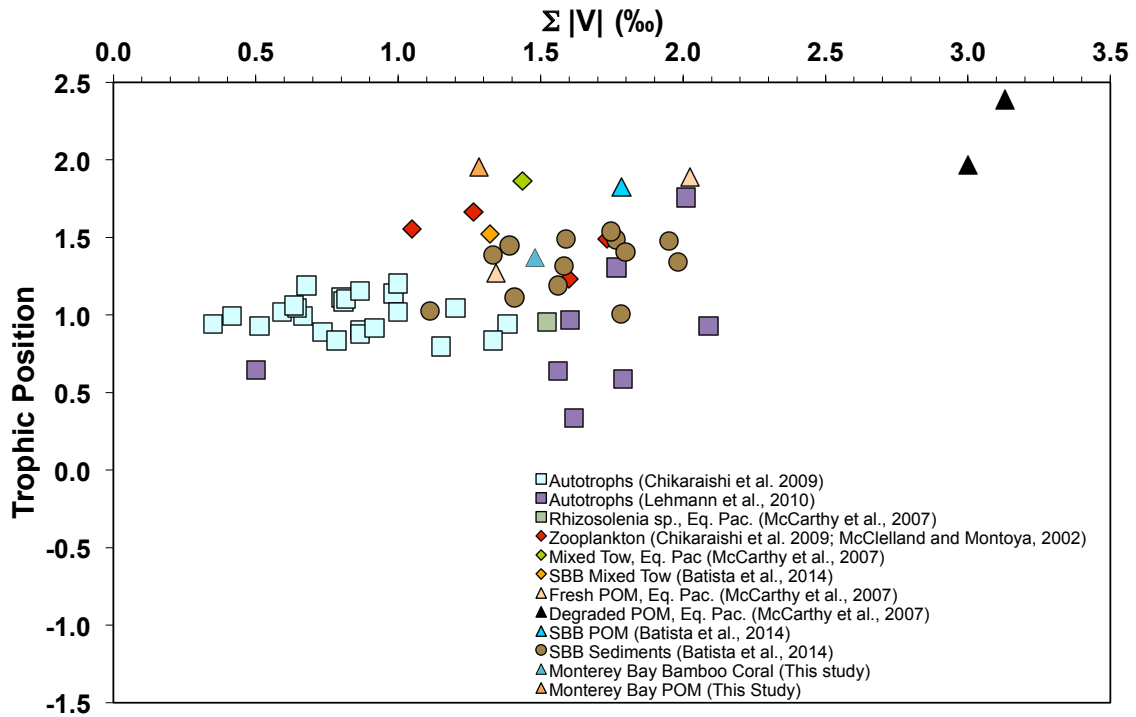
**Figure 4.9 Scatterplot compilation of ΣV vs. Trophic Position for various oceanographic materials.**

Samples plotted here include cultured autotrophs, zooplankton and field samples including a mixed plankton tow, fresh and degraded POM, surface sediments and Bamboo coral. The $TP_{Glu/Phe}$ and ΣV values for the Bamboo coral samples support the notion that these organisms primarily rely on freshly exported POM, as inferred from $\Delta^{14}C$ data.
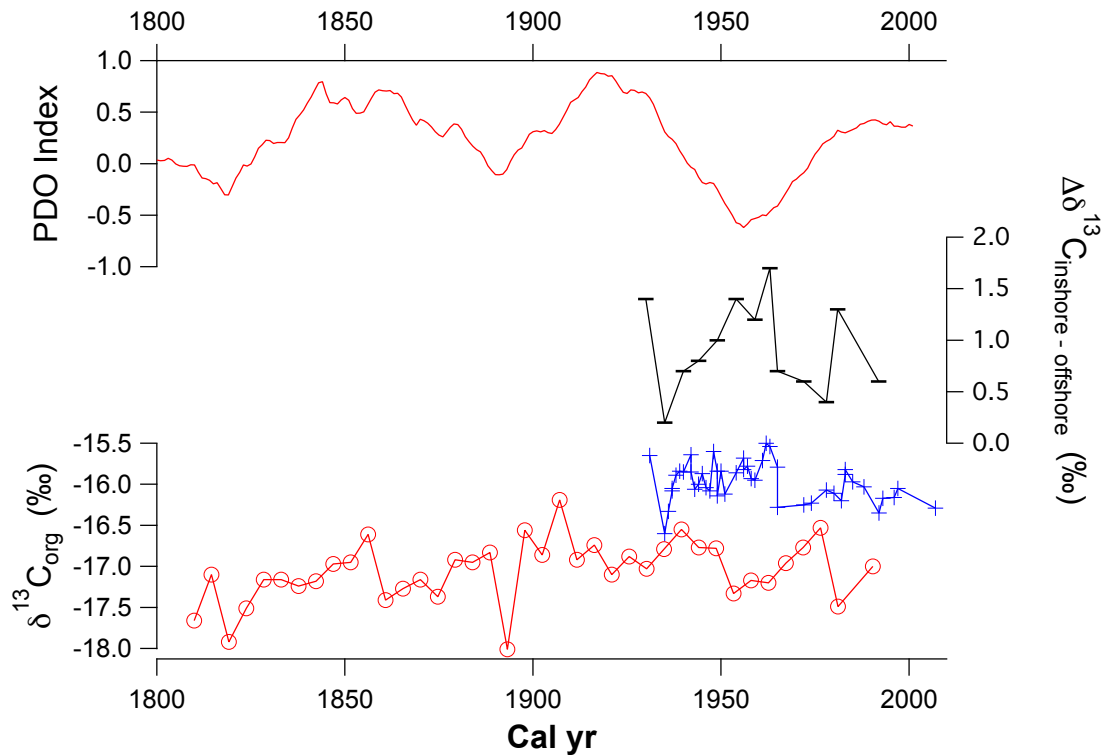
**Figure 4.10 Comparison of the PDO Index (25-y smoothed) with $\Delta\delta^{13}C_{inshore-offshore}$ and the $\delta^{13}C_{org}$ time-series data.**

The $\delta^{13}C_{org}$ offset ($\Delta\delta^{13}C_{inshore-offshore}$) between the inshore Monterey Canyon (blue) and offshore Pioneer Seamount (red) $\delta^{13}C_{org}$ records is a measure of the cross-shelf productivity gradient where (+/-) $\Delta\delta^{13}C_{inshore-offshore}$ values indicate (higher/lower) cross-shelf gradient in productivity. The smoothed PDO Index (Mantua et al., 1997; MacDonald and Case, 2005) is significantly negatively correlated to the Monterey Canyon $\delta^{13}C_{org}$ record, where the cool PDO phase (negative PDO Index values) corresponds with increased $\delta^{13}C_{org}$ values due to higher local productivity over the Monterey Canyon. However, the PDO Index is not correlated with either the Pioneer Seamount $\delta^{13}C_{org}$ record or the $\Delta\delta^{13}C_{inshore-offshore}$, which indicates a decoupling of the processes which drive productivity at these proximal locations. The strong relationships of $\delta^{13}C_{org}$ and $\Delta\delta^{13}C_{inshore-offshore}$ values with the PDO Index are consistent with previous findings that productivity in the eastern Pacific is also strongly correlated to this climate index (Chavez et al., 2003a, b).
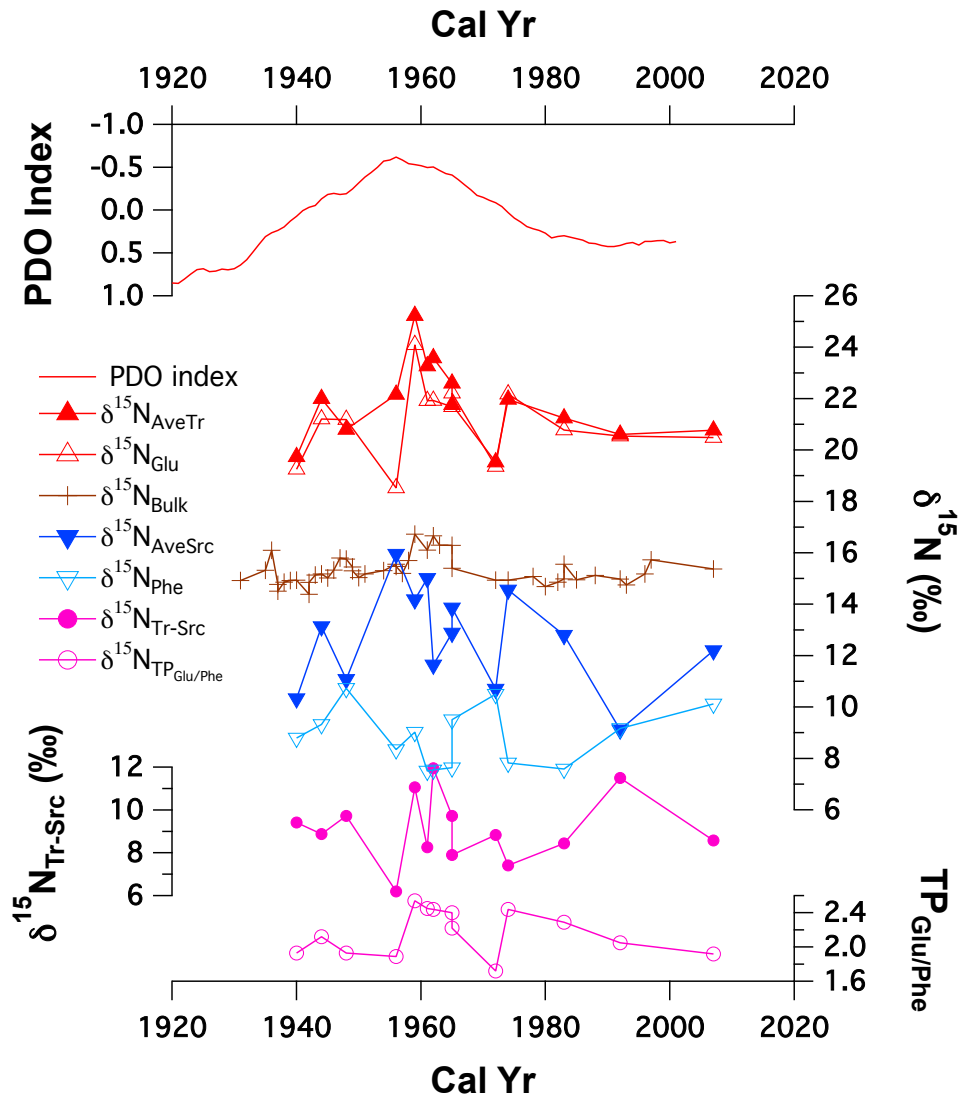
**Figure 4.11 Comparison of time-series data of Monterey Canyon (T1104 A7) Bamboo coral to the PDO Index (25-y smoothed).**
The 25-y smoothed PDO Index is significantly negatively correlated with $\delta^{15}N_{bulk}$, $\delta^{15}N_{AvgTr}$, and $\delta^{15}N_{AvgSrc}$, while the $\delta^{15}N_{bulk}$ record at Monterey Canyon is significantly positively correlated with $TP_{Glu/Phe}$, $\delta^{15}N_{AvgTr}$, $\delta^{15}N_{Glu}$, it is not correlated with other parameters ($\delta^{15}N_{Tr-Src}$, $\delta^{15}N_{Phe}$) shown here. The cool PDO phase (negative PDO Index values) is associated with increased inshore upwelling that drives higher inshore productivity, and the cross-shelf $\delta^{13}C$ gradients, shown above in Figure 4.10 and corresponds to net increases in the $\delta^{15}N_{AvgTr}$, $\delta^{15}N_{AvgSrc}$ and $\delta^{15}N_{bulk}$ gorgonin values for the inshore Monterey Canyon coral specimen. Increases in these $\delta^{15}N_{AA}$ parameters may result from either an increase in the nitrate demand to supply ratio or in the supply of $^{15}N$ enriched nitrate. The former nutrient utilization change seems less likely, given intensified upwelling during the cool PDO phase.
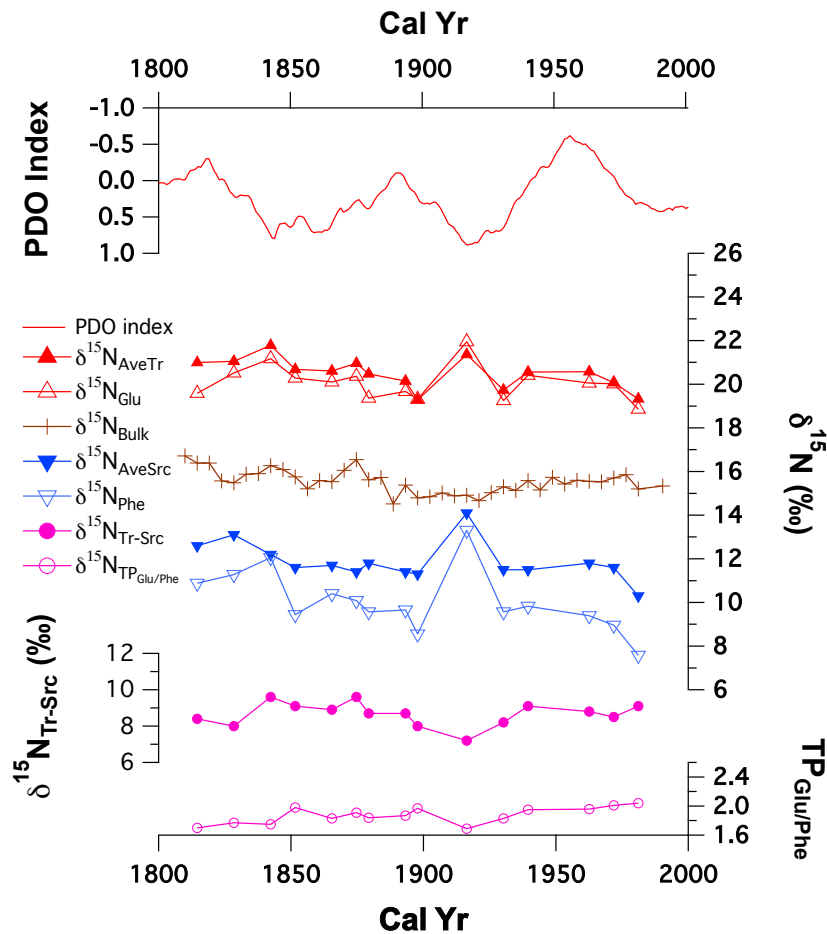
**Figure 4.12 Comparison of time-series data of Pioneer Seamount (T1100 A4) Bamboo coral to the PDO Index (25-y smoothed).**

The 25-y smoothed PDO Index does not correlate with $\delta^{15}N_{bulk}$ or any of the $\delta^{15}N_{AA}$ based parameters shown here, while the $\delta^{15}N_{bulk}$ record is, however, significantly positively correlated with $\delta^{15}N_{AvgTr}$ and $\delta^{15}N_{Tr-Src}$, but none of the other parameters shown here. $\delta^{15}N_{bulk}$, $\delta^{15}N_{AvgTr}$ and $\delta^{15}N_{AvgSrc}$ parameters are not significantly correlated with the PDO Index. The lack of a relationship between these particular $\delta^{15}N_{AA}$ parameters and the PDO Index may be attributable to circulation dynamics in the California Current System. During the cool PDO phase, the southward flowing California Current jet strengthens, and separates the eutrophic coastal region from the more oligotrophic waters of the CC (Collins et al., 2003) where the Pioneer Seamount is located, and where curl-driven upwelling with slower vertical velocities is much more important, relative to inshore sites (Rykaczewski and Checkley, 2008; Checkley and Barth, 2009). These aspects of CCS circulation dynamics are consistent with increased productivity gradients and $\Delta\delta^{13}C_{inshore-offshore}$ values during the cool PDO phase (negative PDO Index values), as noted above. Overall, these records of $\delta^{15}N_{AA}$ and $\delta^{15}N_{bulk}$ at the Pioneer Seamount indicate a long-term stability in nitrate $\delta^{15}N$ throughout the California Current System through the past two centuries.

203

**Table 4.1 Elemental composition, $\Delta^{14}C$, and $\delta^{13}C$ and $\delta^{15}N$ in Monterey Canyon Bamboo coral T1104 A7 organic node**

| mm from edge | Cal Yr | $\Delta^{14}C$ (‰) | $\delta^{13}C_{org}$ (‰) | $\delta^{15}N_{bulk}$ (‰) | wt% C | wt% N | C/N |
|---|---|---|---|---|---|---|---|
| 0.00 | 2007.0 | 15.5 | -16.3 | 15.4 | 44.8 | 16.5 | 3.2 |
| 1.29 | 1997.0 | | -16.0 | 15.7 | 38.5 | 14.0 | 3.2 |
| 1.43 | 1996.0 | 31.8 | -16.2 | 15.2 | 43.2 | 15.6 | 3.2 |
| 1.86 | 1992.6 | | -16.2 | 14.8 | 39.3 | 14.3 | 3.2 |
| 1.95 | 1991.9 | 35.6 | -16.4 | 15.0 | 46.4 | 17.1 | 3.2 |
| 2.47 | 1987.9 | | -16.0 | 15.1 | 41.9 | 15.3 | 3.2 |
| 2.79 | 1985.4 | | -16.0 | 15.0 | 43.5 | 16.0 | 3.2 |
| 3.08 | 1983.2 | | -15.8 | 15.6 | 43.0 | 15.6 | 3.2 |
| 3.10 | 1983.0 | 37.7 | -15.9 | 15.0 | 43.0 | 15.7 | 3.2 |
| 3.27 | 1981.7 | | -16.2 | 14.9 | 43.4 | 15.9 | 3.2 |
| 3.55 | 1979.6 | 52.6 | -16.1 | 14.7 | 42.9 | 15.6 | 3.2 |
| 3.70 | 1978.4 | | -16.1 | 15.1 | 43.7 | 16.0 | 3.2 |
| 4.26 | 1974.1 | | -16.2 | 14.9 | 41.7 | 15.3 | 3.2 |
| 4.53 | 1972.0 | | -16.2 | 14.9 | 46.1 | 16.9 | 3.2 |
| 5.53 | 1965.4 | | -16.3 | 15.4 | 43.3 | 15.9 | 3.2 |
| 5.66 | 1964.5 | | -15.8 | 16.3 | 42.7 | 15.8 | 3.2 |
| 5.84 | 1963.3 | -14.1 | -15.5 | 16.3 | 43.0 | 15.8 | 3.2 |
| 6.08 | 1961.8 | | -15.5 | 16.7 | 46.2 | 17.1 | 3.1 |
| 6.26 | 1960.6 | | -15.7 | 16.1 | 47.9 | 17.7 | 3.2 |
| 6.52 | 1958.9 | | -16.0 | 16.7 | 39.0 | 14.4 | 3.2 |
| 6.65 | 1958.0 | -76.9 | -15.9 | 15.7 | 40.6 | 15.0 | 3.2 |
| 6.79 | 1957.1 | | -15.8 | 15.2 | 42.3 | 15.6 | 3.2 |
| 6.92 | 1956.2 | | -15.8 | 15.5 | 41.9 | 15.5 | 3.2 |
| 7.00 | 1955.7 | | -15.7 | 15.6 | 40.9 | 15.1 | 3.2 |
| 7.28 | 1953.8 | | -15.9 | 15.3 | 44.3 | 16.3 | 3.2 |
| 7.66 | 1951.3 | | -16.1 | 15.2 | 43.7 | 16.1 | 3.2 |
| 7.84 | 1950.1 | | -15.8 | 15.0 | 43.7 | 16.2 | 3.1 |
| 8.01 | 1949.0 | | -16.1 | 15.3 | 44.0 | 16.1 | 3.2 |
| 8.03 | 1948.9 | | -15.8 | 15.5 | 38.2 | 14.1 | 3.2 |
| 8.12 | 1948.3 | | -15.6 | 15.8 | 41.1 | 15.1 | 3.2 |
| 8.27 | 1947.3 | | -16.1 | 15.8 | 44.5 | 16.3 | 3.2 |
| 8.50 | 1945.8 | | -16.0 | 15.3 | 38.8 | 14.3 | 3.2 |
| 8.62 | 1945.0 | | -15.9 | 15.0 | 40.5 | 14.9 | 3.2 |
| 8.76 | 1944.1 | | -16.0 | 15.2 | 39.4 | 14.5 | 3.2 |
| 8.92 | 1943.0 | | -16.1 | 15.1 | 42.9 | 15.9 | 3.1 |
| 9.03 | 1942.3 | | -15.9 | 14.9 | 42.0 | 15.6 | 3.1 |
| 9.12 | 1941.7 | | -15.6 | 14.4 | 48.8 | 17.9 | 3.2 |
| 9.40 | 1939.8 | | -15.8 | 14.9 | 42.1 | 15.6 | 3.1 |
| 9.57 | 1938.7 | -98.0 | -15.8 | 14.9 | 40.2 | 15.2 | 3.1 |
| 9.72 | 1937.7 | | -15.9 | 14.9 | 45.6 | 16.9 | 3.1 |

**Table 4.1 (continued) Elemental composition, $\Delta^{14}$C, and $\delta^{13}$C and $\delta^{15}$N in Monterey Canyon Bamboo coral T1104 A7 organic node**

| mm from edge | Cal Yr | $\Delta^{14}$C (‰) | $\delta^{13}C_{org}$ (‰) | $\delta^{15}N_{bulk}$ (‰) | wt% C | wt% N | C/N |
|---|---|---|---|---|---|---|---|
| 9.79 | 1937.3 | | -16.1 | 14.5 | 41.5 | 15.6 | 3.1 |
| 9.85 | 1936.9 | | -16.1 | 14.8 | 42.9 | 16.1 | 3.1 |
| 9.97 | 1936.1 | | -16.3 | 16.1 | 40.4 | 15.1 | 3.1 |
| 10.06 | 1935.5 | | -16.6 | 15.3 | 42.6 | 16.0 | 3.1 |
| 10.76 | 1930.9 | 15.5 | -15.6 | 14.9 | 33.8 | 11.6 | 3.4 |

**Table 4.2 Elemental composition, $\Delta^{14}$C, and $\delta^{13}$C and $\delta^{15}$N in Pioneer Seamount Bamboo coral T1100 A4 organic node**

| mm from edge | Cal Yr | $\Delta^{14}$C (‰) | $\delta^{13}C_{org}$ (‰) | $\delta^{15}N_{bulk}$ (‰) | wt% C | wt% N | C/N |
|---|---|---|---|---|---|---|---|
| 1.20 | 1990.3 | 42.09 | -17.0 | 15.3 | 46.0 | 16.8 | 3.2 |
| 1.87 | 1981.1 | -17.98 | -17.5 | 15.2 | 43.1 | 15.8 | 3.2 |
| 2.20 | 1976.5 | -69.49 | -16.5 | 15.9 | 42.4 | 15.6 | 3.2 |
| 2.53 | 1971.8 | | -16.8 | 15.7 | 43.8 | 16.2 | 3.2 |
| 2.87 | 1967.2 | -86.24 | -17.0 | 15.5 | 42.7 | 15.8 | 3.2 |
| 3.20 | 1962.6 | | -17.2 | 15.6 | 42.9 | 15.9 | 3.1 |
| 3.53 | 1958.0 | -92.38 | -17.2 | 15.6 | 43.9 | 16.3 | 3.2 |
| 3.87 | 1953.3 | | -17.3 | 15.4 | 45.2 | 16.5 | 3.2 |
| 4.20 | 1948.7 | | -16.8 | 15.7 | 43.9 | 16.0 | 3.2 |
| 4.53 | 1944.1 | | -16.8 | 15.2 | 45.4 | 16.8 | 3.2 |
| 4.87 | 1939.4 | -92.38 | -16.6 | 15.6 | 43.4 | 16.0 | 3.2 |
| 5.20 | 1934.8 | | -16.8 | 15.1 | 45.5 | 16.9 | 3.1 |
| 5.53 | 1930.2 | | -17.0 | 15.3 | 43.9 | 16.4 | 3.1 |
| 5.87 | 1925.6 | | -16.9 | 15.0 | 41.8 | 15.5 | 3.1 |
| 6.20 | 1920.9 | -90.94 | -17.1 | 14.7 | 43.9 | 16.3 | 3.1 |
| 6.53 | 1916.3 | | -16.7 | 14.9 | 44.0 | 16.4 | 3.1 |
| 6.87 | 1911.7 | | -16.9 | 14.9 | 44.1 | 16.5 | 3.1 |
| 7.20 | 1907.1 | | -16.2 | 15.0 | 42.1 | 15.7 | 3.1 |
| 7.53 | 1902.4 | -103.86 | -16.9 | 14.8 | 42.7 | 15.9 | 3.1 |
| 7.87 | 1897.8 | | -16.6 | 14.8 | 44.2 | 16.5 | 3.1 |
| 8.20 | 1893.2 | | -18.0 | 15.4 | 46.6 | 17.4 | 3.1 |
| 8.53 | 1888.5 | | -16.8 | 14.5 | 45.6 | 17.0 | 3.1 |
| 8.87 | 1883.9 | | -16.9 | 15.7 | 44.0 | 16.5 | 3.1 |
| 9.20 | 1879.3 | | -16.9 | 15.6 | 44.0 | 16.5 | 3.1 |
| 9.53 | 1874.7 | | -17.4 | 16.5 | 43.8 | 16.4 | 3.1 |
| 9.87 | 1870.0 | | -17.2 | 16.1 | 43.7 | 16.3 | 3.1 |
| 10.20 | 1865.4 | | -17.3 | 15.5 | 43.2 | 16.2 | 3.1 |
| 10.53 | 1860.8 | | -17.4 | 15.6 | 44.0 | 16.4 | 3.1 |
| 10.87 | 1856.2 | -96.55 | -16.6 | 15.2 | 48.4 | 18.1 | 3.1 |
| 11.20 | 1851.5 | | -17.0 | 15.8 | 44.0 | 16.5 | 3.1 |
| 11.53 | 1846.9 | | -17.0 | 16.1 | 45.8 | 17.1 | 3.1 |
| 11.87 | 1842.3 | | -17.2 | 16.3 | 46.2 | 17.3 | 3.1 |
| 12.20 | 1837.7 | | -17.2 | 15.9 | 42.6 | 15.9 | 3.1 |
| 12.53 | 1833.0 | | -17.2 | 15.9 | 40.5 | 15.2 | 3.1 |
| 12.87 | 1828.4 | | -17.2 | 15.5 | 41.3 | 15.5 | 3.1 |
| 13.20 | 1823.8 | | -17.5 | 15.6 | 43.8 | 16.4 | 3.1 |
| 13.53 | 1819.1 | -98.44 | -17.9 | 16.4 | 43.4 | 16.3 | 3.1 |
| 13.87 | 1814.5 | | -17.1 | 16.4 | 43.8 | 16.4 | 3.1 |
| 14.20 | 1809.9 | | -17.7 | 16.7 | 42.6 | 16.0 | 3.1 |

**Table 4.3 $\delta^{15}N_{AA}$ (‰) data for organic node from Monterey Canyon Bamboo coral specimen T1104 A7**

| mm from edge | Cal Yr | ALA | ASP | GLU | ILE | LEU | PRO | VAL | GLY | LYS | PHE | SER | TYR | THR |
|---|---|---|---|---|---|---|---|---|---|---|---|---|---|---|
| 0 | 2007 | 21.8 | 17.9 | 20.5 | 21.4 | 20.1 | 21.2 | 22.4 | 16.5 | 11.8 | 10.1 | 13.6 | 9.0 | -10.9 |
| 1.95 | 1992 | 21.9 | 17.6 | 20.5 | 20.8 | 20.6 | 21.1 | 21.7 | 16.2 | 3.3 | 9.2 | 13.6 | 3.3 | -12.1 |
| 3.10 | 1983 | 20.9 | 18.0 | 20.8 | 21.9 | 20.9 | 21.0 | 25.2 | 20.7 | 13.8 | 7.6 | 14.9 | 7.0 | -11.5 |
| 4.26 | 1974 | 22.0 | 18.6 | 22.2 | 22.7 | 21.2 | 21.6 | 25.5 | 21.3 | 14.7 | 7.8 | 15.1 | 13.8 | -9.3 |
| 4.53 | 1972 | 20.1 | 16.8 | 19.4 | 20.7 | 18.6 | 19.9 | 21.3 | 15.4 | 11.3 | 10.5 | 12.7 | 3.7 | -10.2 |
| 5.53 | 1965 | 21.7 | 17.4 | 22.2 | 23.3 | 21.0 | 21.3 | 25.4 | 21.6 | 17.2 | 9.5 | 15.7 | 5.3 | -10.7 |
| 5.66 | 1964 | 22.7 | 19.0 | 21.7 | 23.9 | 22.5 | 21.6 | 26.8 | 22.4 | 15.0 | 7.6 | 16.4 | 3.0 | -13.7 |
| 6.08 | 1962 | 23.3 | 20.0 | 21.9 | 25.3 | 23.3 | 23.2 | 28.0 | 22.3 | 8.1 | 7.6 | 17.0 | 3.3 | -14.3 |
| 6.26 | 1961 | 23.6 | 19.4 | 21.9 | 24.6 | 23.6 | 22.3 | 27.4 | 21.9 | 14.5 | 7.5 | 16.2 |  | -12.7 |
| 6.52 | 1959 | 25.3 | 21.1 | 24.1 | 26.4 | 26.1 | 24.3 | 29.4 | 23.1 | 17.1 | 9.0 | 17.1 | 4.6 | -13.6 |
| 6.92 | 1956 | 23.1 | 18.8 | 18.5 | 23.8 | 22.5 | 21.8 | 26.5 | 21.4 | 18.3 | 8.3 | 15.8 |  | -11.5 |
| 8.12 | 1948 | 22.2 | 18.5 | 21.2 | 20.9 | 19.1 | 21.3 | 22.4 | 16.2 | 12.7 | 10.7 | 14.6 | 1.2 | -9.7 |
| 8.76 | 1944 | 22.7 | 18.5 | 21.2 | 22.6 | 21.9 | 21.1 | 25.9 | 19.7 | 14.5 | 9.3 | 15.3 | 6.9 | -12.6 |
| 9.40 | 1940 | 21.1 | 17.4 | 19.3 | 20.0 | 18.6 | 21.0 | 20.9 | 15.2 | 11.0 | 8.8 | 12.5 | 4.1 | -8.8 |
| **Average** | | **22.3** | **18.5** | **21.1** | **22.7** | **21.4** | **21.6** | **24.9** | **19.5** | **13.1** | **8.8** | **15.0** | **5.4** | **-11.5** |
| **1σ** | | **1.3** | **1.1** | **1.4** | **1.9** | **2.1** | **1.1** | **2.7** | **3.0** | **3.9** | **1.1** | **1.5** | **3.4** | **1.7** |

**Table 4.4 $\delta^{15}N_{AA}$ (‰) data for organic node from Pioneer Seamount Bamboo coral specimen T1100 A4**

| mm from edge | Cal Yr | ALA | ASP | GLU | ILE | LEU | PRO | VAL | GLY | LYS | PHE | SER | TYR | THR |
|---|---|---|---|---|---|---|---|---|---|---|---|---|---|---|
| 1.87 | 1981 | 19.7 | 15.3 | 18.9 | 20.4 | 19.2 | 19.7 | 22.1 | 14.6 | 11.4 | 7.6 | 13.6 | 6.9 | -12.9 |
| 2.53 | 1972 | 20.5 | 16.4 | 20.0 | 20.8 | 19.9 | 20.4 | 22.5 | 15.1 | 12.7 | 9.0 | 14.1 | 9.7 | -11.8 |
| 3.20 | 1963 | 20.9 | 17.1 | 20.1 | 22.2 | 20.3 | 20.8 | 22.7 | 15.6 | 12.9 | 9.4 | 14.3 | 9.2 | -10.3 |
| 4.87 | 1939 | 21.1 | 16.6 | 20.4 | 21.7 | 20.7 | 20.8 | 22.6 | 16.3 | 12.5 | 9.8 | 14.3 | 6.1 | -10.2 |
| 5.53 | 1930 | 20.0 | 16.0 | 19.2 | 21.1 | 19.4 | 20.2 | 22.3 | 14.8 | 12.1 | 9.6 | 13.9 | 9.1 | -11.9 |
| 6.53 | 1916 | 20.8 | 18.9 | 21.9 | 21.9 | 20.5 | 22.1 | 23.5 | 17.5 |  | 13.3 | 14.7 | 11.9 | -10.6 |
| 7.87 | 1898 | 19.7 | 16.0 | 19.3 | 20.0 | 18.9 | 19.7 | 21.4 | 15.3 | 12.8 | 8.6 | 13.6 | 8.9 | -11.1 |
| 8.20 | 1893 | 20.4 | 16.9 | 19.7 | 21.0 | 19.7 | 20.5 | 22.7 | 16.2 | 12.5 | 9.7 | 14.2 | 6.3 | -11.0 |
| 9.20 | 1879 | 21.4 | 16.8 | 19.4 | 20.9 | 21.0 | 21.2 | 22.8 | 16.3 | 12.3 | 9.6 | 14.6 | 8.4 | -9.7 |
| 9.53 | 1875 | 21.9 | 17.5 | 20.4 | 21.9 | 20.3 | 21.8 | 23.0 | 16.5 | 12.7 | 10.1 | 15.2 | 3.8 | -11.1 |
| 10.20 | 1865 | 21.3 | 17.4 | 20.1 | 20.9 | 20.3 | 21.5 | 22.7 | 16.3 | 13.2 | 10.4 | 15.2 | 4.9 | -8.8 |
| 11.20 | 1852 | 20.8 | 17.2 | 20.3 | 21.5 | 20.0 | 21.7 | 23.2 | 15.1 | 12.5 | 9.4 | 14.2 | 8.9 | -10.7 |
| 11.87 | 1842 | 22.6 | 18.6 | 21.2 | 23.1 | 21.0 | 22.8 | 23.2 | 16.9 | 12.2 | 12.1 | 15.2 | 4.7 | -8.0 |
| 12.87 | 1828 | 21.7 | 17.9 | 20.5 | 21.2 | 20.9 | 21.9 | 23.4 | 16.4 | 11.5 | 11.3 | 14.5 | 13.3 | -10.5 |
| 13.87 | 1815 | 22.6 | 18.7 | 19.6 | 21.6 | 19.7 | 22.7 | 22.2 | 17.0 | 11.2 | 10.9 | 14.1 | 11.4 | -10.2 |
| **Average** |  | **21.0** | **17.1** | **20.1** | **21.3** | **20.1** | **21.2** | **22.7** | **16.0** | **12.3** | **10.0** | **14.4** | **8.2** | **-10.6** |
| **1σ** |  | **0.9** | **1.0** | **0.8** | **0.8** | **0.7** | **1.0** | **0.5** | **0.9** | **0.6** | **1.4** | **0.5** | **2.8** | **1.2** |

**Table 4.5 Derived parameters based on δ$^{15}$N$_{AA}$ results for Monterey Canyon Bamboo coral specimen T1104 A7**

| mm from edge | Cal Yr | Avg. Tr. | Avg. Src. | TP$_{Glu/Phe}$ | ΣV |
|---|---|---|---|---|---|
| 0.00 | 2007.0 | 20.8 | 12.2 | 1.9 | 1.1 |
| 1.95 | 1991.9 | 20.6 | 9.1 | 2.0 | 0.9 |
| 3.10 | 1983.0 | 21.2 | 12.8 | 2.3 | 1.3 |
| 4.26 | 1974.1 | 22.0 | 14.6 | 2.4 | 1.3 |
| 4.53 | 1972.0 | 19.5 | 10.7 | 1.7 | 1.1 |
| 5.53 | 1965.4 | 21.8 | 13.9 | 2.2 | 1.6 |
| 5.66 | 1964.5 | 22.6 | 12.9 | 2.4 | 1.6 |
| 6.08 | 1961.8 | 23.6 | 11.6 | 2.4 | 1.8 |
| 6.26 | 1960.6 | 23.3 | 15.0 | 2.4 | 1.8 |
| 6.52 | 1958.9 | 25.2 | 14.2 | 2.5 | 1.8 |
| 6.92 | 1956.2 | 22.2 | 16.0 | 1.9 | 1.7 |
| 8.12 | 1948.3 | 20.8 | 11.1 | 1.9 | 1.1 |
| 8.76 | 1944.1 | 22.0 | 13.1 | 2.1 | 1.5 |
| 9.40 | 1939.8 | 19.7 | 10.3 | 1.9 | 1.1 |

**Table 4.6 Derived parameters based on δ$^{15}$N$_{AA}$ results for Pioneer Seamount Bamboo coral specimen T1100 A4**

| mm from edge | Cal Yr | Avg. Tr. | Avg. Src. | TP$_{Glu/Phe}$ | ΣV |
|---|---|---|---|---|---|
| 1.87 | 1981.1 | 19.3 | 10.3 | 2.0 | 1.3 |
| 2.53 | 1971.8 | 20.1 | 11.6 | 2.0 | 1.1 |
| 3.20 | 1962.6 | 20.6 | 11.8 | 2.0 | 1.2 |
| 4.87 | 1939.4 | 20.6 | 11.5 | 1.9 | 1.2 |
| 5.53 | 1930.2 | 19.7 | 11.5 | 1.8 | 1.3 |
| 6.53 | 1916.3 | 21.4 | 14.1 | 1.7 | 1.1 |
| 7.87 | 1897.8 | 19.3 | 11.3 | 2.0 | 1.1 |
| 8.20 | 1893.2 | 20.1 | 11.4 | 1.9 | 1.2 |
| 9.20 | 1879.3 | 20.5 | 11.8 | 1.8 | 1.4 |
| 9.53 | 1874.7 | 21.0 | 11.4 | 1.9 | 1.4 |
| 10.20 | 1865.4 | 20.6 | 11.7 | 1.8 | 1.1 |
| 11.20 | 1851.5 | 20.7 | 11.6 | 2.0 | 1.3 |
| 11.87 | 1842.3 | 21.8 | 12.2 | 1.8 | 1.3 |
| 12.87 | 1828.4 | 21.1 | 13.1 | 1.8 | 1.1 |
| 13.87 | 1814.5 | 21.0 | 12.6 | 1.7 | 1.5 |

**Table 4.7 Pearson correlation coefficients: PDO (25-y smoothed) vs. $\delta^{15}N$ & $\delta^{13}C$**

| PDO vs. | Pioneer Seamount[a] | Monterey Canyon[a] |
|---|---|---|
| $\delta^{13}C_{org}$ | 0.22, n=39 | **-0.52, n=44, *p<0.01*** |
| $\delta^{15}N_{bulk}$ | -0.24, n=39 | **-0.42, n=44, *p<0.01*** |
| $\delta^{15}N_{AvgTr}$ | 0.24, n=15 | **-0.66, n=13, *p<0.02*** |
| $\delta^{15}N_{AvgSrc}$ | 0.23, n=15 | **-0.63, n=13, *p<0.05*** |
| $TP_{Glu/Phe}$ | -0.34, n=15 | -0.29, n=13 |

[a]Pearson correlation coefficients, n = number of pairs in the correlation, *P*-value listed for significant linear relationships between $\delta^{15}N_{bulk}$ and the listed parameter. The Pearson correlation coefficient is a measure of the strength of a linear relationship between two variable arrays, values range from -1 to 0 for inverse relationships and 0 to +1 for positive linear relationships.

**Table 4.8 Pearson correlation coefficient for $\delta^{15}N_{bulk}$ vs. $\delta^{15}N_{AA}$ parameters, $\delta^{13}C$, and C/N**

| $\delta^{15}N_{bulk}$ vs. | Pioneer Seamount[a] | Monterey Canyon[a] |
|---|---|---|
| $TP_{Glu/Phe}$ | -0.19, n=15 | **0.61, n=14, *p<0.005*** |
| $\delta^{15}N_{AvgTr}$ | **0.56, n=15, *p<0.05*** | **0.83, n=14, *p<0.0005*** |
| $\delta^{15}N_{Glu}$ | 0.10, n=15 | **0.62, n=14, *p<0.01*** |
| $\delta^{15}N_{AvgSrc}$ | -0.02, n=15 | 0.28, n=14 |
| $\delta^{15}N_{Phe}$ | 0.14, n=15 | 0.27, n=14 |
| $\delta^{13}C$ | **-0.44, n=39, *p<0.01*** | -0.09, n=45 |

[a]Pearson correlation coefficients, n = number of pairs in the correlation, *P*-value listed for significant linear relationships between $\delta^{15}N_{bulk}$ and the listed parameter. The Pearson correlation coefficient is a measure of the strength of a linear relationship between two variable arrays, values range from -1 to 0 for inverse relationships and 0 to +1 for positive linear relationships.

**Summary and Conclusions**

These new paleoenvironmental records from bamboo coral gorgonin skeletal nodes from Monterey Canyon and Pioneer Seamount specimens provide robust archives of surface ocean biogeochemistry for the central California Current System. Excellent preservation of the gorgonin nodes as suggested from invariant elemental compositions of C and N, C/N ratios, amino acid compositions and $\Sigma V$ results through out the lifespan of both coral specimens. $\Delta^{14}C$ data support the notion that these deep-sea coral rely on a diet of freshly exported POM from the surface ocean. This interpretation is further supported by low $\Sigma V$ values, and the relative offsets in $\delta^{15}N_{bulk}$ and $\delta^{15}N_{AA}$ patterns between coral gorgonin and sinking particles, which indicates a trophic transfer from sinking particles to corals and thus strong coupling of benthic-pelagic food webs.

The cross-shelf productivity-driven $\delta^{13}C$ gradient captured by the Monterey Canyon and Pioneer Seamount $\delta^{13}C_{org}$ records indicate these gradients have been stable since 1930. However, the relative geographic locations of these coral specimens do not capture the larger scale north to south $\delta^{15}N$ gradients inherent in nitrate $\delta^{15}N$ along the California Margin and eastern north Pacific. Still, there appears to be a decoupling of the nitrogen dynamics, which control the $\delta^{15}N_{bulk}$ records at the Monterey Canyon and Pioneer Seamount. Increases in upwelling strength and nutrient supply, appear to change the nutrient utilization (demand to supply ratio) and govern the inshore $\delta^{15}N_{bulk}$ gorgonin record for the Monterey Canyon specimen. While the Pioneer Seamount coral is not as sensitive to these inshore upwelling

dynamics, but rather the more stable curl-driven upwelling.  Overall, the $\delta^{15}N_{bulk}$, $\delta^{15}N_{AvgTr}$, $\delta^{15}N_{AvgSrc}$, $\delta^{15}N_{Phe}$ and $TP_{Glu/Phe}$ records for these gorgonin coral, suggest that trophic structure and nutrient dynamics, while punctuated by minor interannual and decadal perturbations, are remarkably stable throughout the last two centuries.

Future applications of $\delta^{15}N_{AA}$ based investigations $\delta^{15}N_{bulk}$ records in deep-sea coral gorgonin archives along the California Margin could benefit from (1) higher resolution sampling, to better capture secular trends in interannual variations, (2) attempt to extend the temporal reconstructions with coral gorgonin by combining tying together living and dead coral records, and (3) select corals that are spatially distributed north to south along the California Margin, to resolve variability in nitrate $\delta^{15}N$ gradients over the lifespan of new coral records.

## Acknowledgements

# References

Batista, F.C., Ravelo, A.C., Crusius, J., Casso, M.A. and McCarthy, M.D. (2014) Compound specific amino acid delta N-15 in marine sediments: A new approach for studies of the marine nitrogen cycle. Geochimica Et Cosmochimica Acta 142, 553-569.

Broecker, W.S., Peng, T.H., Ostlund, G. and Stuiver, M. (1985) THE DISTRIBUTION OF BOMB RADIOCARBON IN THE OCEAN. Journal of Geophysical Research-Oceans 90, 6953-6970.

Chavez, F.P., Ryan, J., Lluch-Cota, S.E. and Niquen, M. (2003a) From anchovies to sardines and back: Multidecadal change in the Pacific Ocean. Science 299, 217-221.

Chavez, F.P., Ryan, J., Lluch-Cota, S.E. and Niquen, M. (2003b) Sardine fishing in the early 20th century - Response. Science 300, 2033-2033.

Checkley, D.M. and Barth, J.A. (2009) Patterns and processes in the California Current System. Progress in Oceanography 83, 49-64.

Chikaraishi, Y., Ogawa, N., Kashiyama, Y., Takano, Y., Suga, H., Tomitani, A., Miyashita, H., Kitazato, H. and Ohkouchi, N. (2009) Determination of aquatic food-web structure based on compound-specific nitrogen isotopic composition of amino acids. LIMNOLOGY AND OCEANOGRAPHY-METHODS, 740-750.

Collins, C.A., Pennington, J.T., Castro, C.G., Rago, T.A. and Chavez, F.P. (2003) The California Current system off Monterey, California: physical and biological coupling. Deep-Sea Research Part Ii-Topical Studies in Oceanography 50, 2389-2404.

Cowie, G.L. and Hedges, J.I. (1992) SOURCES AND REACTIVITIES OF AMINO-ACIDS IN A COASTAL MARINE-ENVIRONMENT. Limnology and Oceanography 37.

Germain, L.R., Koch, P.L., Harvey, J. and McCarthy, M.D. (2013) Nitrogen isotope fractionation in amino acids from harbor seals: implications for compound-specific trophic position calculations. Marine Ecology Progress Series 482, 265-+.

Hill, T.M., Myrvold, C.R., Spero, H.J. and Guilderson, T.P. (2014) Evidence for benthic-pelagic food web coupling and carbon export from California margin bamboo coral archives. Biogeosciences 11, 3845-3854.

Mantua, N.J., Hare, S.R., Zhang, Y., Wallace, J.M. and Francis, R.C. (1997) A Pacific interdecadal climate oscillation with impacts on salmon production. Bulletin of the American Meteorological Society 78, 1069-1079.

McCarthy, M.D., Benner, R., Lee, C. and Fogel, M.L. (2007) Amino acid nitrogen isotopic fractionation patterns as indicators of heterotrophy in plankton, particulate, and dissolved organic matter. Geochimica Et Cosmochimica Acta 71, 4727-4744.

McClelland, J.W. and Montoya, J.P. (2002) Trophic relationships and the nitrogen isotopic composition of amino acids in plankton. Ecology 83, 2173-2180.

Miller, R.J., Page, H.M. and Brzezinski, M.A. (2013) delta C-13 and delta N-15 of particulate organic matter in the Santa Barbara Channel: drivers and implications for trophic inference. Marine Ecology Progress Series 474, 53-66.

Miller, T.W., Brodeur, R.D. and Rau, G.H. (2008) Carbon stable isotopes reveal relative contribution of shelf-slope production to the northern California Current pelagic community. Limnology and Oceanography 53, 1493-1503.

Rau, G.H., Chavez, F.P. and Friederich, G.E. (2001) Plankton C-13/C-12 variations in Monterey Bay, California: evidence of non-diffusive inorganic carbon uptake by phytoplankton in an upwelling environment. Deep-Sea Research Part I-Oceanographic Research Papers 48, 79-94.

Roark, E.B., Guilderson, T.P., Flood-Page, S., Dunbar, R.B., Ingram, B.L., Fallon, S.J. and McCulloch, M. (2005) Radiocarbon-based ages and growth rates of bamboo corals from the Gulf of Alaska. Geophys. Res. Lett. 32.

Rykaczewski, R.R. and Checkley, D.M. (2008) Influence of ocean winds on the pelagic ecosystem in upwelling regions. Proc. Natl. Acad. Sci. U. S. A. 105, 1965-1970.

Schlitzer, R. (2002) Interactive analysis and visualization of geoscience data with Ocean Data View. Computers & Geosciences 28, 1211-1218.

Sherwood, O.A., Guilderson, T.P., Batista, F.C., Schiff, J.T. and McCarthy, M.D. (2014) Increasing subtropical North Pacific Ocean nitrogen fixation since the Little Ice Age. Nature 505, 78.

Sherwood, O.A., Scott, D.B. and Risk, M.J. (2006) Late Holocene radiocarbon and aspartic acid racernization dating of deep-sea octocorals. Geochimica Et Cosmochimica Acta 70, 2806-2814.

Sherwood, O.A., Thresher, R.E., Fallon, S.J., Davies, D.M. and Trull, T.W. (2009) Multi-century time-series of N-15 and C-14 in bamboo corals from deep Tasmanian seamounts: evidence for stable oceanographic conditions. Marine Ecology-Progress Series 397, 209-218.

Stuiver, M. and Polach, H.A. (1977) REPORTING OF C-14 DATA - DISCUSSION. Radiocarbon 19, 355-363.

Wankel, S.D., Kendall, C., Pennington, J.T., Chavez, F.P. and Paytan, A. (2007) Nitrification in the euphotic zone as evidenced by nitrate dual isotopic composition: Observations from Monterey Bay, California. Global Biogeochemical Cycles 21.